THE

LONDON, EDINBURGH, AND DUBLIN

PHILOSOPHICAL MAGAZINE

AND

JOURNAL OF SCIENCE.

[SEVENTH SERIES.]

JULY 1934.

I. *Photographic Intermittency Effect and the Discrete Structure of Light.* *By* L. SILBERSTEIN *and* J. H. WEBB. (Communication No. 526 from the Kodak Research Laboratories *.)

IT is well known that an intermittent exposure, consisting of a number of flashes separated by dark intervals, does not, in general, produce the same photographic effect as a continuous exposure of equal overall duration and equal total energy. This is commonly called the intermittency effect. This effect has been observed by numerous experimenters, to wit, with visible and ultra-violet light, but—as may be well stated at the outset—not with X-rays. It has been found experimentally that when, under certain intensity conditions, the frequency of the flashes is steadily increased, a point is reached at which the intermittency effect disappears. The frequency thus specified may be referred to as the fusion frequency. Extensive experimental investigations on the latter have been recently made by one of us †. The main result of these experiments was that the fusion frequency is roughly proportional to the intensity of light. As to the theoretical explanation of this and the allied properties of the intermittency effect only vague qualitative

* Communicated by The Eastman Kodak Co.

† J. H. Webb, J. Opt. Soc. Amer. xxiii. no. 5, pp. 157–169 (May 1933).

considerations were at that time given, which were based on the concept of light-quanta and on a first-sight impression that the intermittency effects should disappear just when the frequency of flash becomes equal to the frequency of quantum hits of a grain. A thorough analysis of the problem, however, which has since been undertaken has disclosed a number of subtle intricacies and enabled us to place the theory of these phenomena on a sound basis. This has not only accounted for the rough proportionality of the fusion frequency to the intensity of light, but has also yielded the value of the proportionality factor in its dependence on the size of the grain and on the ratio of the dark gaps to the duration of the light-flashes in the intermittent exposure.

It is the purpose of this paper, first, to expound this theory and, in the next place, to show its agreement with the experimental findings. Its subject has seemed to deserve the interest of the general physicist since it gives additional evidence of the discrete structure of light, in so far as the consequences of the assumption of such a structure are in good harmony with the observed facts.

Theoretical Part.

The problem in hand amounts to a comparison of a continuous with an intermittent exposure and to finding out under what conditions they can be expected to give the same photographic effects. From the standpoint of the light-quantum theory both the "continuous" and the intermittent exposure consist in a bombardment of the photographic plate by a shower of discrete energy parcels or quanta, the hits sustained by any silver halide grain being separated by finite time intervals. Microscopically, then, both kinds of exposure are intermittent, and their effects can differ from each other only through the spacing of the quantum hits, the intervals between successive hits of any grain and their probable distribution in time. The problem is thus reduced to a determination of the probable interval between successive quantum hits of a grain and of the probable deviations (standard deviations) of all possible intervals from this probable value for the continuous and for the (macroscopically) intermittent exposures and to a comparison of the two sets of results.

Let us first consider the relations for a continuous exposure. The photographic plate is in this case illuminated by monochromatic light of constant intensity. The wave-length of the light and therefore the energy ($h\nu$) carried by each quantum being fixed, the intensity can be directly expressed by the number of quanta thrown upon the plate per unit area and unit time. Let this number be n, a constant throughout the duration of the exposure. Let S be the area of a portion of the plate just large enough to ensure statistical regularity, *i. e.*, such that the number of quanta striking it actually within the time t is nSt. (In view of the microscopic haphazardness of the shower of quanta an area S, of these properties, cannot, of course, be pushed below a certain limit.)

Consider one of the silver halide grains spread over S. Let its size (effective area) be a. Then the probability that the grain shall be hit by a single light-quantum thrown upon S is $p=a/S$. We will assume that this is a small fraction. (If S is, say, a square mm., then, since the linear dimensions of the grains are of the order of a micron, p would be of the order of 10^{-6}.) The grain will be hit irregularly, now in shorter and now in longer intervals. Let t be any one of these intervals between two successive hits. Suppose that the grain has just been hit by a quantum. The probability that it will be missed by the next m quanta thrown upon S and hit by the $(m+1)$st quantum is $q^m p$, where $q=1-p$. But the interval thus arising is $(m+1)/nS$. Hence, the probability of a hitless interval t is

$$P(t)=pq^n, \quad \text{where } t=(m+1)/nS. \quad . \quad . \quad . \quad (1)$$

This gives the frequency distribution of the intervals. The probable interval, which we will denote by (t) or τ, is the sum of the products of all possible t into their probabilities, and since the total number of quanta thrown upon S during the whole exposure can be supposed to be very great, the summation can safely be extended up to $m=\infty$. Thus

$$\tau=(t)=\frac{p}{nS}\sum_{m=0}^{\infty}[m+1]q^m,$$

The sum can be written

$$\frac{d}{dq}\sum_{0}^{\infty}q^{m+1}=\frac{d}{dq}\left(\frac{q}{1-q}\right)=\frac{1}{(1-q)^2}=\frac{1}{p^2}.$$

Hence, $(t)=1/nSp$ or

$$(t)=\tau=\frac{1}{na}. \quad . \quad . \quad . \quad . \quad . \quad . \quad . \quad (2)$$

Thus, the probable interval is inversely proportional to the intensity of light and to the size of the grain. (This result would follow also directly by disregarding the chance element and saying that the grain is hit na times per second.) If the number of hits actually sustained by the grain is large, and such in fact is the number of hits by quanta of visible light required to make a grain developable *, the probable interval (2) is at the same time the average (arithmetical mean) of the actual intervals.

A haphazard succession of events, here hits, is not, of course, sufficiently characterized by their probable or average spacing alone. To characterize it more closely, let us determine the standard deviation, Δ, of the intervals. It is true that the whole set is completely specified by the distribution law (1), but, as will be realized in the sequel, this law cannot be feasibly compared with the corresponding law for the intermittent exposure, and this forces us to use instead the standard deviation as a derivate attribute of this distribution. Now, the standard deviation, which is originally defined as the square root of the probable value of the squared deviation from the average, is known to be given by

$$\Delta^2=(t^2)-(t)^2, \quad . \quad . \quad . \quad . \quad . \quad . \quad (3)$$

where (t^2) is the probable value of t^2. Now, by (1),

$$(t^2)=\frac{p}{n^2S^2}\sum_{m=0}^{\infty}[m+1]^2q^m.$$

The sum on the right hand can be evaluated as follows:

$$\Sigma=1+2^2q+3^2q^2+\ldots,$$

$$q\Sigma=\quad q+2^2q^2+3^2q^3+\ldots,$$

whence

$$p\Sigma=1+3q+5q^2+7q^3+\ldots,$$

$$qp\Sigma=\quad q+3q^2+5q^3+\ldots;$$

$$p^2\Sigma=1+2q+2q^2+\ldots=\frac{1+q}{1-q}.$$

* According to Eggert and Noddack's estimates this number runs into hundreds.

Thus

$$\sum_{m=0}^{\infty}[m+1]^2q^m=\frac{1+q}{p^3},$$

Hence,

$$(t^2)=\frac{1+q}{n^2S^2p^2}=\frac{1+q}{n^2a^2}.$$

and, by (2) and (3),

$$\Delta^2=\frac{q}{n^2a^2}=q\tau^2.$$

Ultimately, therefore, the standard deviation of the intervals between successive hits of a grain in the continuous exposure becomes

$$\Delta=\sqrt{q}\tau, \quad . \quad . \quad . \quad . \quad . \quad . \quad . \quad (4a)$$

or, since to all purposes

$$\sqrt{q}\doteq 1-\frac{1a}{2S}\doteq 1,$$

simply

$$\Delta=\tau=\frac{1}{na}. \quad . \quad . \quad . \quad . \quad . \quad . \quad . \quad (4)$$

The standard deviation of the intervals is thus comparatively large, viz., practically equal to the probable or average interval itself.

Let us now turn to consider an intermittent exposure, that is to say, a regular succession of monochromatic light-flashes (of the same wave-length as before), each of duration T, separated by gaps or dark intervals θ. Let n' be the constant light intensity within each flash, again in quanta per unit area and unit time.

Owing to the presence of the dark gaps, the frequency distribution of the intervals t' between the successive quantum hits of a given grain of size a will now be much more complicated than in the case of the continuous exposure.

In fact, let N be the number of quanta falling upon the whole area S during each flash, *i. e.*,

$$N=n'ST. \quad . \quad . \quad . \quad . \quad . \quad (5)$$

Imagine each flash time T divided by equidistant instants, including end-points of the flash, to be marked by K=0, 1, 2, ... N−1. The totality of possible hitless

intervals t' will then consist of N classes, viz., intervals t_0' starting at the beginning of a flash, intervals t_1', t_2', etc., generally t_K', starting at an instant marked 1 or 2, etc., generally K. The probabilities of intervals of equal length but belonging to different classes will manifestly be different. The total probability $P(t')$ of an interval of given length t' is the sum of its partial probabilities as interval of any of the N classes. The expression thus obtained for $P(t')$ changes abruptly its form when t' passes through the values θ, T, $T+\theta$, $2T+\theta$, and so on *. Such being the case, the distribution law, which is to take over the rôle of (1), is found to consist of an unwieldy set of formulæ not serviceable for the desired comparison of an intermittent with a continuous exposure and for setting up the criteria of their photographic indiscernibility. Moreover, there are only two parameters at our disposal, the ratio of intensities $n' : n$ and the duration T of a flash (while θ/T is to be left free), and these are insufficient for bringing into coincidence the whole distribution laws as expressed by $P(t)$ and $P(t')$. Under these circumstances we shall compare, instead of the distribution laws themselves, their two most characteristic attributes, that is, the probable intervals and the standard deviations of the intervals. Their comparison will just absorb the two parameters at our disposal. We proceed, therefore, to determine these two attributes for the intermittent exposure.

Let (t') be the probable value of the interval of the K-th class. Then, since all the N starting-points of the intervals are equally probable, the resultant probable interval (t'), based on all classes, will be

$$(t') = \frac{1}{N} \sum_{K=0}^{N-1} (t_K'). \quad . \quad . \quad . \quad . \quad . \quad . \quad (6)$$

It remains to determine (t_K') for any of the assigned K's.

* Thus, for instance, in the simplest case of $\theta = T$, one finds with $1/n'$S as unit of time and denoting by r an integer smaller than N,

$$P(r) = \frac{N-r}{N} pq^{r-1},$$

while

$$P(N) = \frac{p}{N}(q^{N-1}+1), \quad P(N+r) = \frac{r+1}{N} pq^r,$$

$$P(2N+r) = \frac{N-r}{N} pq^{N+r},$$

and so on.

Now, the probability that the contemplated grain will be missed by m quanta thrown upon S and hit by the $(m+1)$st quantum is, as before, pq^m, with the essential difference, however, that when $m=\mathrm{N}-1-\mathrm{K}$, the end of a flash is reached, so that for the next higher value of m the gap θ is inserted. Similarly, when m exceeds $2\mathrm{N}-1-\mathrm{K}$, one more gap θ is added to the hitless interval, and so on. In fine pq^m is the probability of

$$t'_{\mathrm{K}}=\frac{m+1}{n'\mathrm{S}} \qquad \text{for} \qquad 0\leq m\leq \mathrm{N}-1-\mathrm{K},$$

$$t'_{\mathrm{K}}=\frac{m+1}{n'\mathrm{S}}+\theta \qquad \text{for} \qquad \mathrm{N}-1-\mathrm{K}\leqq m\leq 2\mathrm{N}-1-\mathrm{K},$$

$$t'_{\mathrm{K}}=\frac{m+1}{n'\mathrm{S}}+2\theta \qquad \text{for} \qquad 2\mathrm{N}-1-\mathrm{K}\leq m\leq 3\mathrm{N}-1-\mathrm{K},$$

and so on. Consequently,

$$(t'_{\mathrm{K}})=\frac{p}{n'\mathrm{S}}\sum_{m=0}^{\infty}[m+1]q^m$$

$$+p\theta\left\{\sum_{\mathrm{N}-\mathrm{K}}^{2\mathrm{N}-1-\mathrm{K}}q^m+2\sum_{2\mathrm{N}-\mathrm{K}}^{3\mathrm{N}-1-\mathrm{K}}q^m+3\sum_{3\mathrm{N}-\mathrm{K}}^{4\mathrm{N}-1-\mathrm{K}}q^m+\dots\right\}.$$

The first term is as before, only with n replaced by n', *i.e.*, $1/n'a$, which we will denote by τ'. The bracketed coefficient of $p\theta$ can be written

$$q^{-\mathrm{K}}[q^{\mathrm{N}}+2q^{2\mathrm{N}}+3q^{3\mathrm{N}}+\dots]\sum_{0}^{\mathrm{N}-1}q^m$$

$$=\frac{q^{\mathrm{N}-\mathrm{K}}}{(1-q^{\mathrm{N}})^2}\cdot\frac{1-q^{\mathrm{N}}}{1-q}=\frac{q^{\mathrm{N}-\mathrm{K}}}{p(1-q^{\mathrm{N}})},$$

so that

$$(t'_{\mathrm{K}})=\tau'+\theta\frac{q^{\mathrm{N}}}{1-q^{\mathrm{N}}}\cdot q^{-\mathrm{K}}.$$

This has to be summed over K, as in (6), and since

$$\sum_{0}^{\mathrm{N}-1}q^{-\mathrm{K}}=\frac{1-q^{\mathrm{N}}}{pq^{\mathrm{N}-1}},$$

we have

$$(t')=\tau'+\frac{q\theta}{\mathrm{N}p}=\tau'+\frac{q\theta}{n'a\mathrm{T}}.$$

Ultimately, therefore, the probable interval between successive hits of a grain in the intermittent exposure is, rigorously,

$$(t')=\tau'\left[1+\frac{q\theta}{\mathrm{T}}\right], \quad . \quad . \quad . \quad . \quad . \quad (7a)$$

or, since $q=1-\frac{a}{\mathrm{S}}\doteq 1$, to all purposes,

$$(t')=\tau'\left[1+\frac{\theta}{\mathrm{T}}\right], \quad . \quad . \quad . \quad . \quad . \quad . \quad (7)$$

where $\tau'=1/n'a$. For every grain that has been made developable this is also the average of the actual intervals, since such a grain must have actually been hit a great many times *.

The same reasoning can be applied for determining the standard deviation of the intervals, Δ'. Since this is given by $\Delta'^2=(t'^2)-(t')^2$, we have only to find (t'^2), the probable value of the squared interval. Similarly to (6) we shall have

$$(t'^2)=\frac{1}{\mathrm{N}}\sum_{\mathrm{K}=0}^{\mathrm{N}-1}(t'^2_{\mathrm{K}}). \quad . \quad . \quad . \quad . \quad . \quad . \quad (8)$$

Now,

$$(t'^2_{\mathrm{K}})=p\sum_{0}^{\mathrm{N}-1-\mathrm{K}}\left[\frac{m+1}{n'\mathrm{S}}\right]^2 q^m+p\sum_{\mathrm{N}-\mathrm{K}}^{2\mathrm{N}-1-\mathrm{K}}\left[\frac{m+1}{n'\mathrm{S}}+\theta\right]^2 q^m$$
$$+p\sum_{2\mathrm{N}-\mathrm{K}}^{3\mathrm{N}-1-\mathrm{K}}\left[\frac{m+1}{n'\mathrm{S}}+2\theta\right]^2 q^m+\ldots$$

or

$$(t'^2_{\mathrm{K}})=\frac{p}{n'^2\mathrm{S}^2}\sum_{0}^{\infty}[m+1]^2 q^m$$
$$+\frac{2p\theta}{n'\mathrm{S}}\left\{\sum_{\mathrm{N}-\mathrm{K}}^{2\mathrm{N}-1-\mathrm{K}}[m+1]q^m+2\sum_{2\mathrm{N}-\mathrm{K}}^{3\mathrm{N}-1-\mathrm{K}}[m+1]q^m\right.$$
$$\left.+3\sum_{3\mathrm{N}-\mathrm{K}}^{4\mathrm{N}-1-\mathrm{K}}[m+1]q^m+\ldots\right\}$$
$$+p\theta^2\left\{\sum_{\mathrm{N}-\mathrm{K}}^{2\mathrm{N}-1-\mathrm{K}}q^m+2^2\sum_{2\mathrm{N}-\mathrm{K}}^{3\mathrm{N}-1-\mathrm{K}}q^m+\ldots\right\}$$

* Notice that the simple result (7) could also be arrived at by a very rough reasoning, disregarding the haphazardness of the case, viz., as the overall time $\mathrm{T}+\theta$ divided by the number of hits $n'a\mathrm{T}$. But a rigorous treatment has seemed desirable not only because it is more convincing, but prepares also the way for the next computation which will run on similar lines.

The first term, not containing θ, has already been evaluated in connexion with (t^2). Its value is

$$\frac{1+q}{n'^2a^2}=(1+q)\tau'^2.$$

The bracketed coefficient of θ^2 can be written

$$q^{-K}[q^N+2^2q^{2N}+3^2q^{3N}+\dots]\sum_0^{N-1}q^m=\frac{(1+q^N)q^{N-K}}{p(1-q^N)^2}.$$

The bracketed coefficient of θ is

$$q^{-K}\Big[q^N\sum_{m=0}^{N-1}(m+1+N-K)q^m+2q^{2N}\sum_0^{N-1}(m+1+2N-K)q^m$$
$$+3q^{3N}\sum_0^{N-1}(m+1+3N-K)q^m+\dots\Big]$$
$$=q^{-K}\Big\{\frac{q^N}{(1-q^N)^2}\sum_0^{N-1}(m+1-K)q^m$$
$$+N(q^N+2^2q^{2N}+3^2q^{3N}+\dots)\sum_0^{N-1}q^m\Big\}$$
$$=\frac{q^{N-K}}{p(1-q^N)^2}\Big\{\frac{q-q^N}{p}+N+1-(1-q^N)K\Big\}$$
$$=\frac{q_N{}^{-K}}{p(1-q^N)^2}\Big\{\frac{1-q^N}{p}+N-(1-q^N)K\Big\}.$$

Thus,

$$(t_K'^2)=(1+q)\tau'^2+\theta^2\frac{(1+q^N)q^{N-K}}{(1-q^N)^2}$$
$$+\frac{2\theta}{n'S}\cdot\frac{q^{N-K}}{(1-q^N)^2}\Big\{\frac{1-q^N}{p}+N-(1-q^N)K\Big\}.$$

When this is summed over K, as in (8), one finds after simple reductions, rigorously,

$$(t'^2)=(1+q)\tau'^2+\frac{2\theta}{n'S}\cdot\frac{2q}{Np^2}+\theta^2\frac{q(1+q^N)}{pN(1-q^N)}.$$

Now, by (5), $pN=n'aT=T/\tau'$ and $n'S.Np^2=T/\tau'^2$. Thus, and using the approximation $q=1-\frac{a}{S}\doteq 1$,

$$(t'^2)=\tau'^2\Big\{2+4\frac{\theta}{T}+\frac{T}{\tau'}\frac{1+q^N}{1-q^N}\frac{\theta^2}{T^2}\Big\}.$$

On the other hand, by (7),

$$(t')^2 = \tau'^2 \left\{ 1 + 2\frac{\theta}{T} + \frac{\theta^2}{T^2} \right\}.$$

Hence, the square of the required standard deviation,

$$\Delta'^2 = \tau'^2 \left\{ 1 + 2\frac{\theta}{T} + \left(\frac{T}{\tau'} \cdot \frac{1+q^N}{1-q^N} - 1 \right) \frac{\theta^2}{T^2} \right\}.$$

Since a/S is a small fraction, we can write

$$q^N = \left(1 - \frac{a}{S}\right)^{\frac{S}{a} \cdot n'aT} \doteq e^{-n'aT} = e^{-\frac{T}{\tau'}}.$$

Ultimately, therefore, the standard deviation of the intervals in the intermittent exposure is given by

$$\Delta'^2 = \tau'^2 \left\{ 1 + \frac{2\theta}{T} + \frac{\theta^2}{T^2} \left(\frac{x(e^x+1)}{e^x-1} - 1 \right) \right\}, \quad . \quad (9)$$

where

$$x = \frac{T}{\tau'} = Tn'a.$$

Having thus obtained the average interval between successive hits of a grain and its standard deviation for both kinds of exposures, let us now compare the intermittent exposure specified by n', T, θ/T with a continuous exposure specified wholly by its intensity n, the wavelength of the monochromatic light being assumed to be the same in both.

In the first place, let us require that the probable or average intervals for the two exposures (t) and (t'), shall be equal. Such exposures may be called equivalent. If this requirement is satisfied and if the total (overall) duration of the two exposures is the same, a grain of any size will sustain in both the same total number of hits by light-quanta, each carrying the same amount of energy. In this and only in this sense, then, are the contemplated two exposures "equivalent." Their photographic effects, however, will, in general, be different. In fact, what is technically called intermittency effect is the difference in blackening produced by just such equivalent (iso-energetic) exposures. On the discrete light structure view this effect can only be due to the different deviations of the actual intervals from, or their distribution about,

the two (equal) average intervals. And since this distribution is most essentially characterized by the standard deviation (and only in a secondary way by the third and higher order deviations, skewness, flatness, etc.), it seems reasonable to expect that the intermittency effect will disappear or, as we will say, the two equivalent exposures will become photographically indiscernible from each other, when their standard deviations, Δ' and Δ, are also equal. The two haphazard successions of hits can then be said to coincide to the second order.

We assume, in fine, that the intermittent and the continuous exposures become indiscernible when

$$(t')=(t) \quad \text{and} \quad \Delta'=\Delta. \quad . \quad . \quad . \quad . \quad (10)$$

This assumption is less arbitrary than might appear at first sight. In fact, the first equality imposes a condition upon the intensity n' in relation to n, and the second will bind x or, ultimately, the frequency of flash, and (since θ/T must be kept entirely free) we are left without further parameters to satisfy third or higher order conditions (equality of skewness, etc.). If, therefore, the two exposures do at all become indiscernible (and experiment teaches us that they do so become, for any θ/T whatever), this ought to be the case when the, at any rate necessary, requirements (10) are satisfied.

The first of these requirements gives, by (7) and (2),

$$\tau'\left(1+\frac{\theta}{\mathrm{T}}\right)=\tau, \quad . \quad . \quad . \quad . \quad . \quad (11)$$

or

$$n' : n = 1+\frac{\theta}{\mathrm{T}}, \quad . \quad . \quad . \quad . \quad . \quad (11\,a)$$

which reads simply: average intensity of intermittent equal to intensity of continuous exposure. Such an adjustment of intensities has been applied in all our experiments.

The ratio of the standard deviations (9) and (4) now becomes, by (11),

$$\frac{\Delta'}{\Delta}=\frac{\sqrt{1+2\frac{\theta}{\mathrm{T}}+\frac{\theta^2}{\mathrm{T}^2}\psi(x)}}{1+\frac{\theta}{\mathrm{T}}}, \quad . \quad . \quad . \quad (12)$$

where $$\psi(x) = \frac{x(e^x+1)}{e^x-1} - 1. \quad . \quad . \quad . \quad . \quad . \quad (13)$$

Here $x = T/\tau' = \frac{T+\theta}{\tau}$, and since the frequency of flash is defined by $f = 1 : (T+\theta)$,

$$f = \frac{1}{x\tau} = \frac{na}{x} \quad . \quad . \quad . \quad . \quad . \quad . \quad (14)$$

The second requirement, $\frac{\Delta'}{\Delta} = 1$, leads to

$$\psi(x) + 1,$$

a transcendental equation for x. Now, the only (real) root of this equation is $x = 0$ or $f = \infty$. Thus, speaking rigorously, the intermittent exposure would never coincide with, but tends asymptotically, with increasing frequency of flash, to become indiscernible from the continuous exposure. Practically, however, the function $\psi(x)$ differs from unity very little for moderately small values of x, *i. e.*, for moderate frequencies f (with na as unit frequency). Thus, *e. g.*, $\psi(0{\cdot}10) = 1{\cdot}0011$, $\psi(0{\cdot}5) = 1{\cdot}0415$. What is ultimately relevant is not so much the value of $\psi(x)$ itself, as the closeness of the ratio Δ'/Δ, the right-hand member of (12), to unity. One can expect the two exposures to become experimentally indiscernible when, say, $\Delta'/\Delta = 1{\cdot}01$ or even $1{\cdot}05$. The corresponding value of x will be the smaller, *i. e.*, the required frequency of flash f will be the greater, the greater the ratio θ/T of the dark to the luminous intervals. Moreover, when the ratio θ/T increases indefinitely, the frequency f required for making the two exposures with any degree of accuracy indiscernible tends to a certain finite upper limit, which depends only on the accuracy claimed, *i. e.*, on the desired closeness of Δ'/Δ to unity.

A clear insight into these relations is obtained by plotting the values of Δ'/Δ against f for a few different values of the ratio (sector ratio)

$$\rho = \frac{\theta}{T},$$

in accordance with the formulæ (12) and (14), *i. e.*,

$$\frac{\Delta'}{\Delta} = \frac{\sqrt{1+2\rho+\rho^2\psi(x)}}{1+\rho}, \quad \frac{f}{na} = \frac{1}{x} \quad . \quad . \quad . \quad (12a)$$

Such curves are drawn in fig. 1 for $\rho=1$, 3, 32, and ∞ *. The equation of the last of these, the limiting curve, is simply

$$\frac{\Delta'}{\Delta}=\sqrt{\psi(x)}.$$

The ordinate in this diagram is the value of Δ'/Δ, and the abscissa, the frequency of flash f with $na=1/\tau$ as unit frequency. The curves are, of course, all asymptotic to both coordinate axes. Any straight line $\Delta'/\Delta=$const.

Fig. 1.

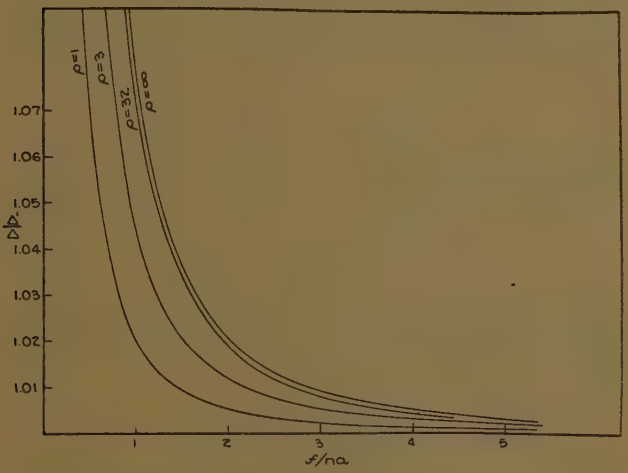

cuts these curves at frequencies f which steadily increase with increasing sector ratio ρ up to the limiting f-value for $\rho=\infty$. Thus, *e. g.*, if we take $\Delta'/\Delta-1=0{\cdot}01$, which would seem amply small enough for ensuring practical indiscernibility of the intermittent exposure from the continuous one, the corresponding frequencies of flash are :—

for	$\rho=1$	3	32	∞
	$f=1{\cdot}45$	$2{\cdot}16$	$2{\cdot}75$	$2{\cdot}907\ na$.

* The case of fractional $\rho=\theta/T$, such as 1/2 and smaller, is of slight practical interest, since the corresponding intermittency effect is difficult to observe at all.

All the curves for $\rho > 32$ being crowded into a very narrow region, barred by the $\rho = \infty$ curve, an increase of the ratio $\rho = \theta/T$ beyond 32 to any extent whatever has only a very small influence upon the flash frequency required for indiscernibility. In fact, as will be seen in the sequel, the experimental behaviour of an exposure with $\rho = 127$ could barely be distinguished from that of an equivalent exposure with $\rho = 32$ or 31. From the last set of numbers, as well as from the diagram, one sees that the frequency for $\rho = \infty$ is very nearly twice that for $\rho = 1$. This peculiarity is readily accounted for. In fact, consider any two equivalent intermittent exposures specified by different values ρ_1, ρ_2 of the ratio θ/T, and let x_1, x_2 be the corresponding x-values at which Δ'/Δ acquires for both exposures the same value. Then, by (12 *a*),

$$\frac{\psi(x_1)-1}{\psi(x_2)-1} = \left[\frac{(1+\rho_1)\rho_2}{(1+\rho_2)\rho_1}\right]^2.$$

Now, the function $\psi(x)$, as defined by (13), can be developed into the power series, convergent for all $x < 2\pi$,

$$\psi(x) = 1 + 2\left\{B_2\frac{x^2}{2!} + B_4\frac{x^4}{4!} + B_6\frac{x^6}{6!} + \cdots\right\}, \quad . \quad (15)$$

where $B_2 = 1/6$, $B_4 = -1/30$, $B_6 = 1/42$, etc., are Bernoulli's numbers. For small x, even up to 1, the x^2-term only need be retained, so that $\psi(x) - 1 = x^2/6$, and the last equation becomes, by (14),

$$\frac{f_2}{f_1} = \frac{x_1}{x_2} = \frac{(1+\rho_1)\rho_2}{(1+\rho_2)\rho_1}, \quad . \quad . \quad . \quad . \quad (16)$$

whence, *e. g.*, for $\rho_1 = 1$ and $\rho_2 = \infty$, $f_1/f_2 = 2$, as announced. Also, if both ρ_1 and ρ_2 are large numbers, $f_1 \doteq f_2$.

It is instructive to represent these relations in yet another way, namely, by drawing the curves of constant Δ'/Δ, with ρ and f as coordinates. If we put $(\Delta'/\Delta)^2 = 1 + c$, the equation of any such curve becomes

$$\psi(x) = \psi\left(\frac{na}{f}\right) = 1 + c\left(1 + \frac{1}{\rho}\right)^2, \quad . \quad . \quad (17)$$

and for small x,

$$\frac{na}{f} = \sqrt{6c}\left(1 + \frac{1}{\rho}\right). \quad . \quad . \quad . \quad . \quad . \quad (17\,a)$$

For a numerically fixed c and any ρ, $\psi(x)$ follows at once from (17), whence x and $f/na = 1/x$ are readily computed with the aid of a little table of $\psi(x)$ which need not be reproduced here. In this way a few curves were computed which are drawn in fig. 2. Each of these curves tends, asymptotically to a frequency determined by $\psi(x) = 1 + c$. A curve such as $c = 0{\cdot}02$, *i.e.*, $\Delta'/\Delta = 1{\cdot}01$, gives the frequency at which the intermittency effect can be expected to become imperceptible, for various values of the ratio $\rho = \theta/\mathrm{T}$.

The lower curves correspond to greater values of Δ'/Δ and thus to increasingly perceptible intermittency

Fig. 2.

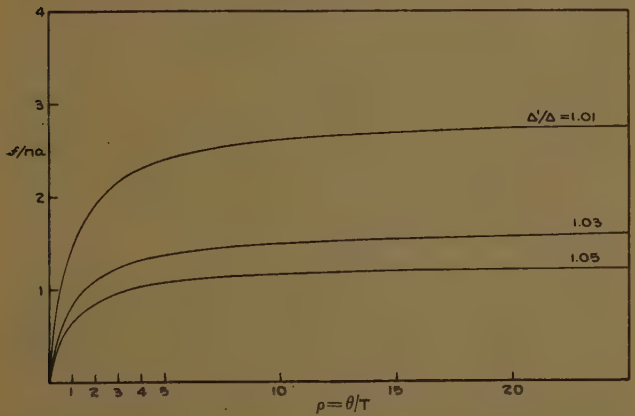

effects. The whole set of curves in fig. 2 is also interesting inasmuch as they should represent at least the general character of the (f, ρ) curves of constant intermittency effect derivable from experimental data.

To sum up. The frequency of flash, at which an intermittent exposure of sector ratio $\rho = \theta/\mathrm{T}$ becomes indiscernible from an equivalent continuous exposure, is expressed by

$$f = \frac{1}{x_0} na, \quad . \quad . \quad . \quad . \quad . \quad . \quad (14a)$$

where x_0 is the value of the pure number x which reduces $\frac{\Delta'}{\Delta} - 1$, as expressed by $(12a)$, to a small fraction. This

frequency is thus proportional to the size (a) of the grain and to the intensity (n) of the continuous, and therefore also to the average, intensity of the intermittent exposure, and depends also, through x_0, on the sector ratio ρ, increasing with ρ asymptotically to a finite limit, which is nearly twice the frequency for $\rho=1$. The curves of constant intermittency effect are expressed by (17) and should thus display, at any rate, the general character of those drawn in fig. 2.

Before closing this part of the paper a few remarks must be made about the " size " of the emulsion grains. We have, so far, considered grains of a given, fixed size (area) a, while actually every emulsion consists of grains of a more or less wide range of sizes.

Now, as to the first condition, $(t')=(t)$, it will manifestly be satisfied for grains of all sizes a, provided it is satisfied for any one size, and this is taken care of by the adjustment of intensities $\frac{n'}{n}=1+\frac{\theta}{\mathrm{T}}$. For $\frac{n'a}{na}=\frac{\tau}{\tau'}=1+\frac{\theta}{\mathrm{T}}$ is identical with $(t')=(t)$, whatever the value of a.

The case of the second condition, $\Delta'\doteq\Delta$, is different. If this is satisfied with sufficient accuracy by a flash frequency adapted to a given grain-size a_1, i. e., $f=na_1/x_1$, it will be satisfied the more closely for all smaller grains, since for these $x=na/f<x_1$, and therefore Δ'/Δ more close to unity. The grains larger than a_1, however, will call for a higher frequency. To satisfy all grains, one would have to suit f to the largest grains. But, then, these occur only sporadically and do not, therefore, contribute much to the final photographic effect. As a compromise, some size above the average can be taken, *e. g.*, the size of those grains whose relative contribution to the total area is a maximum, *i. e.*, if $\mathrm{F}(a)da$ be the fraction of all grains whose sizes are contained between a and $a+da$, that size for which $a\mathrm{F}(a)$ attains a maximum, to wit, $a=-\mathrm{F}(a)/\mathrm{F}'(a)$, which obviously lies on the descending branch of the size-frequency distribution curve and is greater than the average size. But these niceties need not be much insisted upon. It may be that not the whole but only a more or less restricted part of the area of a grain is actually sensitive to light, and this may vary from emulsion to emulsion and from grain

to grain. Under these circumstances one may as well insert for a in our formula the average grain-size, and what can then be expected is, of course, not a strict proportionality of the fusion-frequency to, but merely a qualitative increase of f with increasing average grain-size. Such a parallelism has, in fact, been observed, as will be seen in the sequel.

The increase of the fusion-frequency with light intensity should, on the other hand, be much more marked, and such, in fact, will be seen to be the case. Theoretically, a simple proportionality is claimed, but deviations from proportionality are sufficiently accounted for by the fact that the fusion-frequency can be located only within rather wide limits. It will be recalled that, rigorously, there is no such thing as a "critical" frequency (as supposed in the older investigation, *l. c.*), but an asymptotic tendency of the intermittent to the equivalent continuous exposure with indefinitely increasing flash frequency. Under these circumstances the qualitative agreement between experiment and theory as to the effects of grain-size, light intensity, and sector ratio is all that could be expected.

Experimental Part.

On the basis of the foregoing theoretical considerations, a number of predictions have been made concerning the behaviour of the intermittency effect as encountered in photographic exposure. Some of these have been confirmed by experiments already carried out on this subject, while others have been confirmed by experiments recently performed and now to be described.

The theory has shown (*cf.* formula 14 a and fig. 1) that the frequency at which an intermittent exposure should become experimentally indiscernible from a continuous one is directly proportional to the intensity of the exposing radiation and the size of the photographic emulsion grain, and should, besides, increase in a more complicated manner with the sector ratio, $\rho=\theta/\mathrm{T}$, of dark to luminous periods. The first of these provisions, relative to the increase of frequency with intensity and grain-size, *i. e.*, roughly the average grain-size, has been confirmed already through experiments carried out by one of us (J. Opt. Soc. Amer. xxiii. no. 5, p. 157, 1933).

The results from this earlier work are repeated here in Tables I. and II. The data of Table I. illustrate the manner in which the fusion-frequency varies with intensity for a fixed grain-size, while Table II. illustrates how this frequency varies with emulsions of different grain-size when the intensity remains constant. These tables

TABLE I.

Emulsion.	f (flashes/sec.).	$n.10^{-8}$.	a(obs. av. size).	$\rho=\theta/T$.	f/na.
I.	1250	870	0·7	3	2
II.	960	870	0·7	3	1·5
II.	7·5	3·4	0·7	3	2·7
III.	960	870	0·5	3	2·2
III.	5	0·85	0·5	3	10
IV.	240	870	0·1	3	2·7
IV.	15	14	0·1	3	10
				Av	4·4

TABLE II.

Emulsion.	f.	$n.10^{-8}$.	a(obs. av.).	$\rho=\theta/T$.
I.	1250	870	0·7	3
II.	960	870	0·7	3
III	960	870	0·5	3
IV.	240	870	0·1	3

show that the frequency behaves, at least qualitatively, as predicted by theory. The values of f have been inserted in column 6 of Table I., in terms of na. The average value of f is seen to be 4·4 na with a taken as average grain-size. A value of grain-size of two or three times the average would probably be more nearly the proper value to use here, in which case f would become approximately

$2na$, which is in good agreement with the value $2{\cdot}16\,na$ calculated on page 13 for the case of $\theta/T=3$, and based on the requirement of $\Delta'/\Delta=1{\cdot}01$. This result confirms that, also otherwise reasonable, requirement as to the degree of closeness of the two standard deviations to equality. It must be realized that measurements of the kind presented here are subject to a rather large experimental error and do not, therefore, afford as good a quantitative check on the theory as might be desired. Hence, only qualitative agreement between theory and observation is to be expected. To this extent the concordance of the above experimental results with the theory is thought to be fairly satisfactory.

The theoretical conclusion that the flash frequency required for making the intermittent and the continuous exposures indiscernible is also dependent on the sector ratio θ/T has been tested by special experiments designed for this purpose and described below. These experiments consisted in measurements of photographic density as a function of frequency of flash, at constant exposure (intensity $\times$ time), for several widely different values of the sector ratio θ/T.

Experimental Procedure.

The exposures in these experiments were made with monochromatic light of wave-length 4360 Å.U. The source of radiation was a mercury arc enclosed in a metal lamp house. The lamp house had a circular window 1·5 inches in diameter, directly behind which the arc was mounted. The window was covered with three pieces of ground glass which served as a diffusing medium. An adjustable brass diaphragm limiting the light beam was placed in front of the ground-glass screen, and in front of this diaphragm was placed the Corning glass filter No. 7·1 (Noviol A shade + Blue purple Ultra, 4 mm.) for isolating the 4360 Å.U. radiation. The lamp was mounted on a track 12 metres in length extending out from the sensitometer, and the intensity of light used for exposure was varied by moving the lamp along this track. The angular diameter of the source in all positions used was sufficiently small to justify the application of the inverse square law for computing relative intensities. The sensitometer used in this work was a time-scale instrument, of the step, logarithmic-sector-disk

type. Its sector had ten power-of-two steps for impressing the exposure scale upon the emulsion. In all exposures the time of rotation of the sector was so adjusted that the time of the maximum exposure step was 4096 seconds, this being a convenient setting of the instrument in the region in which it was desired to work. Immediately in front of the sensitometer sector disk was placed the sector for interrupting the exposing light beam, thus rendering the exposure intermittent. This sector was of sufficient dimensions to cover the entire aperture exposed and thus to interrupt the light beam over the complete exposure curve. The exposures were made upon a high speed panchromatic emulsion, this emulsion being chosen because of its large intermittency effect at low intensities.

Measurement of the absolute value of energy radiated per square cm. per second from the lamp was made by comparison of the density obtained in an exposure to this light source with the densities on a calibrated plate. The energy in absolute units required to produce a known density upon this calibrated plate was determined on a special monochromatic sensitometer with a thermopile incorporated for energy measurements. This thermopile was calibrated by means of a Hefner amylacetate lamp according to a method given by Coblentz *.

After selection of a sector of the desired ratio, θ/T, a series of preliminary exposures of varying intensities was made, using a high frequency of flash (over 120 per second) in order to determine the correct position of the light source, and hence the correct intensity, to produce a density of unity on the maximum exposure step †. Using the intensity thus determined, the main series of exposures was then made for frequencies of flash varying over a wide range of values. This procedure was repeated for each sector of chosen ratio θ/T. The characteristic exposure curves for a single value of the ratio θ/T were taken on a 4 by 5 inch piece of film by means of a series of dark slides having slots cut at appropriate positions. Grouping the exposures in this manner on a small area of film reduces to a minimum any errors arising from

* W. W. Coblentz, Bureau of Standards, Paper 11, 1915, p. 87.

† Experiment has shown that this frequency was well past the value at which the intermittency effect had vanished and thus past the value at which the intermittent and the continuous exposures had become indiscernible.

slight irregularities occurring in emulsion sensitivity or coating thickness. The emulsions, after exposure, were developed by the brush method in the standard Eastman developer, D-90, for a period of 4 minutes at a temperature of 68° F. The formula of this developer is as follows, the solutions A and B being used in equal proportions :—

A. Sodium bisulphite 17 g., pyro 20 g., sodium sulphite 70 g., water to make 1 litre.

B. Sodium carbonate 75 g., potassium bromide 1 g., water to make 1 litre.

Densities were read on a Martens polarization photometer type of visual densitometer. In deriving the final data, the characteristic exposure curves for any single value of the sector ratio θ/T were plotted on one graph sheet. A vertical line extended across these curves at a constant exposure value gave the densities produced by this exposure for the various frequencies of flash. The values of density as function of the frequency of flash thus obtained are represented by the curves of fig. 3. The intensity of light in all exposures of these curves was $n = 1{\cdot}3 \cdot 10^8$ quanta/cm.^{2} sec. This might be termed an average intensity value, since it was obtained by multiplying the intensity n' of the flash period T into the transmission factor of the sector, *i. e.*,

$$n = n' \frac{T}{T+\theta} = 1{\cdot}3 \cdot 10^8 \text{ quanta/cm.}^2 \text{ sec.}$$

as required by formula (11 *a*).

The curves of fig. 3 show how the density values vary with increasing frequency of flash and how they ultimately tend asymptotically to the value which would be obtained in the continuous exposure * of the same intensity, n. The main feature to be noted in these curves is the manner in which this frequency of practical fusion varies with the sector ratio θ/T. It is clear from the curves that this fusion-frequency becomes greater for the higher values of the ratio θ/T, in accordance with theory. Again, it has been shown on theoretical grounds (*cf.* fig. 2) that this frequency should approach a finite limiting value for high, indefinitely increasing values

* Vanishing of the intermittency effect was the criterion here used for " indiscernibility " of intermittent and continuous exposures.

of the ratio θ/T. This is distinctly brought out in the experimental curves by the practical equality of the values of the fusion-frequency for the two cases, $\theta/T=31$ and $\theta/T=127$.

While there is no sharp value of frequency for which the intermittency effect actually disappears, there is, for each sector ratio θ/T, a sufficiently sharply defined frequency for which the intermittency effect has decreased to any fixed *finite* value. Plots of such frequencies against the sector ratios will give curves of constant intermittency

Fig. 3.

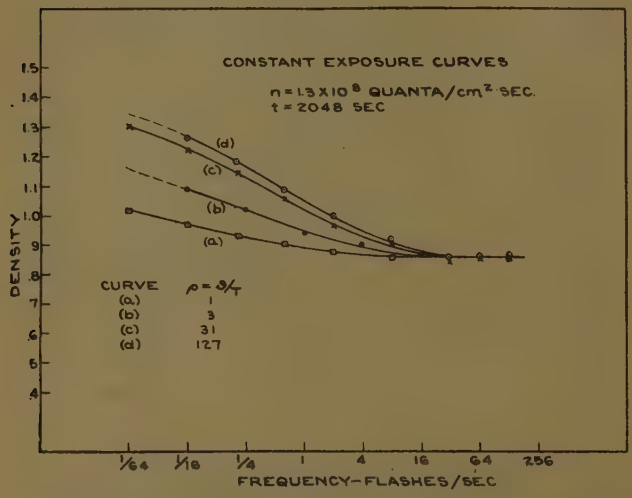

effect which should correspond to the theoretical curves of constant ratio Δ'/Δ (*cf.* fig. 2). Now, a series of such (experimental) values of frequency as a function of θ/T may be readily obtained from the curves of fig. 3 by drawing a horizontal line across these curves and reading the values of frequency f at the intersection points. Two curves obtained in this way for two values of constant intermittency effect, $\Delta D=0{\cdot}04$ and $\Delta D=0{\cdot}14$, are drawn in fig. 4. On the other hand, theoretical curves of constant proportionate difference of the standard deviations of intervals, $\frac{\Delta'-\Delta}{\Delta}$, and thus also Δ'/Δ, for several values

of Δ'/Δ, are given in fig. 2. A comparison of the experimental curves, fig. 4, of constant intermittency effect with these theoretical curves will show that they are of very much the same character, both families of curves tending asymptotically to finite limiting frequencies $f(\rho=\infty)$, whose values increase with decreasing intermittency effect ΔD and Δ'/Δ respectively, and resembling each other closely in shape.

There is thus a fair qualitative agreement between experiment and theory. This not only confirms the assumption of the discrete structure of light, which is otherwise well founded, but shows also that the grains of a photographic emulsion as targets are small enough

Fig. 4.

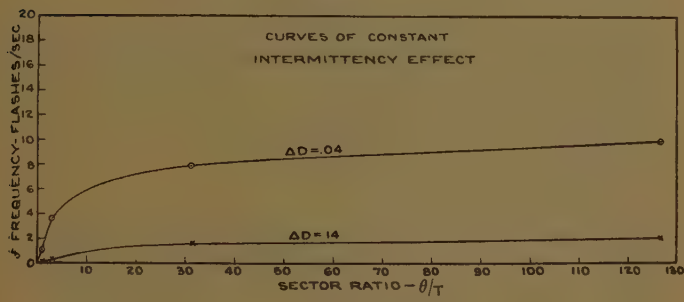

to disclose this discrete structure and the haphazard character of distribution of its elements, the light-quanta, in much the same way as microscopic particles suspended in a liquid are small enough to disclose, through their Brownian movement, the granular structure of the liquid and the chance impacts of its molecules.

In conclusion, it may be pointed out that an additional corroboration of the view here adopted is afforded by the behaviour of X-rays. The intermittency effect, more generally, any departure from Roscoe's reciprocity law, is, according to this view, most essentially conditioned by the circumstance that a silver halide grain must be hit by many quanta of visible (or near ultra-violet) light before it becomes developable. Now, in the case of X-ray exposures, it can be considered as an established fact that a hit by a *single* quantum is sufficient to make

a grain developable *. This is, no doubt, closely connected with the circumstance that an X-ray quantum, even one of the " softer " rays (as, *e. g.*, of wave-length 1·5 Å.U.) carries several thousand times as much energy as a blue light-quantum, but we need not enter into the mechanism by which such a powerful quantum (similarly as an impinging alpha-particle) makes a grain developable †. It suffices to know that it does produce this result. Now, such being the case, it is manifestly irrelevant how the hits of any given grain by X-ray quanta, following upon the first, are distributed in time. Consequently, there should be no intermittency effect, more generally, no failure of the reciprocity law, with X-rays. This negative conclusion agrees with experiment. In fact, as is generally known, no trace of an intermittency effect or of any reciprocity failure has ever been observed in X-ray exposures. The photographic effect of such an exposure (fraction of all grains present made developable) depends only on the total number of X-ray quanta thrown upon the emulsion regardless of their distribution in time.

Rochester, N.Y.
October 17, 1933.

II. *The Sound Radiation from a Condenser Discharge.* *By* Walter McFarlane, *M.A., B.Sc., Lecturer in Natural Philosophy in the University of Glasgow* ‡.

1. THE discharge of a condenser through a spark-gap is much used as a convenient source of sound in many investigations where a single sound-pulse of large pressure amplitude is desired, and particularly in the study of building acoustics, where, with such a source, the propagation of sound throughout a small model can be determined by optical means. The main objects of the present experiments were the determination of the relation between the intensity of the sound emitted and the electrical constants of the circuit employed, and a study of the propagation of the spark-pulse. It was

* *Cf.* Phil. Mag. ix. pp. 787–800 (1930).
† *Loc. cit.*
‡ Communicated by the Author.

hoped that from the latter some information might be obtained on the problem of the propagation of sound-waves of finite amplitude.

2. *Mechanism of Sound Production.*

When a condenser of capacity C is charged to a potential V and discharged through an inductance L and resistance R, the current at any instant t is given by

$$i = \frac{V}{2\pi n L} e^{-\frac{Rt}{2L}} \sin 2\pi n t,$$

where n, the frequency of oscillation, is

$$\frac{1}{2\pi}\sqrt{\frac{1}{LC} - \frac{R^2}{4L^2}}.$$

When the discharge takes place across an air-gap there is, of course, introduced the additional variable resistance offered by the gap itself. This, however, is known to be small, and does not affect appreciably the frequency and current as calculated from the above expressions. With a leyden jar connected to a spark-gap directly, or through a coil of a few turns of thick wire, the maximum of the above current is very large, and is developed in a very short interval of time ($1/4n$ sec.), and is confined to a very small volume of the air. The consequence of this sudden acquisition of a large kinetic energy by the ions and the electrons in the discharge path is the development of a high pressure and temperature.

It has been shown that the initial stage of a condenser discharge is a bright spark of small diameter in which the air only is involved [1]. This is followed by a low-potential oscillatory discharge which passes mainly through the vapour of the electrodes and takes the form of an arc, the total volume of vapour involved being much larger than in the initial spark. When a condenser discharge is photographed it consists of a bright core (the initial spark) surrounded by a less bright sheath (the arc).

The pressure variations which are propagated in the surrounding medium are exactly what would be expected from the above view of the discharge. They were first observed and photographed by M. Töpler [2], using the

Schlieren method of sound-wave photography. The author used a modification of the shadow-method developed by Dvorak [3] and Foley [4]. With a discharge of a frequency of the order of 10^5 the initial spark sends out a sharp well-defined pulse of large condensation and rarefaction, which at the commencement is cylindrical with hemispherical ends, but rapidly assumes spherical form. The subsequent oscillations of current cause fluctuations in pressure in the discharge which send out aerial waves of a frequency double that of the electrical oscillations. These waves, however, are of a much smaller pressure variation than the first pulse. This is due to the lower potential at which the current passes, with consequent diminution in energy, and to the much larger volume occupied by the discharge.

When the inductance of the spark-circuit is reduced the first pulse becomes more intense and the oscillations fainter, until the latter cannot be seen at all. This is due partly to the shortness of the wave-length and partly to the attenuation of the sound-waves, which varies as the square of the frequency. The shortest wave-length photographed in the present investigation was about $\frac{1}{2}$ mm. Neklepajev [5] made observations on the absorption of the sound oscillations produced by a condenser discharge, and he found that their intensity diminished with distance (r), according to the expression $I = I_0 e^{-\alpha r/\lambda^2}$, where $\alpha = \cdot 00073$, λ being the wave-length. Thus waves of a wave-length $\cdot 1$ mm. would have their intensity reduced to one-hundredth in a distance of 6 mm. Such waves would be emitted from a condenser discharge of frequency $1 \cdot 66 \cdot 10^6$, which is only a moderate value. It may thus be safely assumed that any pressure effect measured at a distance of several centimetres from a spark-discharge with a frequency of this order will be produced by the initial pulse only. It is of course possible that with very high frequencies the observed pulse really represents the cumulative effect of the whole discharge.

The only quantitative measurements made on the intensity of the sound radiation are those of Haschek and Mache [6]. In their experiments they enclosed the spark in a bulb and measured the steady deflexion of a column of liquid in a manometer connected to the bulb, using continuous sparking produced by a high-tension transformer. Such a method has many serious defects. The

sparking potential and mechanism of discharge when a continuous train of sparks is being produced are entirely different from those of a single discharge. In the former case the discharge passes mainly through the metallic vapour of the electrodes. Since the pressure effect due to each spark is really impulsive, the steady pressure indicated by the above arrangement is the result of the rapid succession of the discharges and the large inertia of the measuring liquid, and ought therefore to be directly proportional to the number of sparks per second if no change takes place in the nature of the discharge. The statement by the authors that the pressure tended to a limit as the number of sparks per second was increased can only indicate a change in the nature of the discharge, most probably a lowering of the sparking potential. Also no account was taken of the fact that the indicated pressure will be a cumulative effect of many reflexions inside the bulb. These defects of the method undoubtedly tend to vitiate their estimate of the pressure inside the spark, which was calculated on the assumption that the pressure indicated multiplied by the surface area of the bulb was equal to the pressure in the spark multiplied by the surface area of the spark.

3. *Method of Measurement of Impulse of Sound-Pulse.*

The impulse was measured by the deflexion of a ballistic torsion-pendulum. A thin mica vane was attached to one end of a thin aluminium wire which carried a counterpoise at its other end. This system was supported at its centre of gravity by a strip of phosphor-bronze and carried a mirror which indicated the deflexion. In order to limit the motion of the pendulum to one of rotation only, a wire, which projected downwards into a small vessel of oil, was mounted in line with the suspension. A torsion-head permitted the adjustment of the zero. The vane most frequently in use was 1 cm. square, but the sensitivity of the instrument could be varied by attaching vanes of different area.

The moment of torsion (μ) of the suspension was obtained by suspending bodies of calculable moment of inertia and measuring the period of torsional oscillations. It was found to be 0·356 dyne-cm. per radian. It is

easily shown that the impulse P, corresponding to a deflexion θ radians of the pendulum, is given by

$$P = \frac{\mu T \theta}{2\pi d} e^{\lambda/2},$$

where T is the period of oscillation of the pendulum, d is the distance between the centre of the vane and the suspension, and λ is the logarithmic decrement for free oscillations.

If it is assumed that complete absorption of the sound energy takes place at the vane, then P, as calculated above, is the measure of the impulse in the spark-pulse. On the other hand, if perfect reflexion takes place P is double the true value. The latter assumption cannot be correct, since the energy given to the pendulum would be unaccounted for. In order to compare the effect of a different absorbability a light paper cone was tried instead of a vane. The cone had an opening 1 cm. in diameter and was 4 cm. long, so that about ten reflexions would take place inside it. The value of P, as calculated by the above formula, was practically the same as with a vane for the same spark. It seems then that the assumption of complete absorption by the vane gives the best approximation. This question arises only when an absolute value of the impulse is desired. The instrument was mainly used in the following experiments for purposes of comparison, and in this case the impulse can be taken proportional to the angle of deflexion whatever the absorbability.

In the experiments the pendulum and the spark-gap were mounted in a box which was lined with cotton-wool to prevent reflexion at the walls. The torsion-head of the pendulum, a rod for controlling the distance between the gap and the vane, and the connecting wires to the spark-gap projected from the box.

The potential applied to the condenser was obtained from an induction-coil, the primary current being always adjusted to the minimum necessary to produce a discharge. Steady conditions were obtained only when the electrodes had been in use for some time, since the sparking potential for clean electrodes is a little less than when a coating of oxide is formed. Another effect which had to be obviated was the lowering of the sparking potential when sparks succeed each other rapidly. The interval

of time between observations, from two to three minutes, was sufficient to ensure that the effect of the previous discharge had disappeared.

It was found that when a high potential (a large gap) was used or when the electrodes were close to the pendulum a small electrostatic attraction between the electrodes and the vane was called into play. This of course tended to reduce the deflexion of the pendulum due to the sound-pulse. The correction to be applied was found by fitting a similar spark-gap in parallel with the other, but situated outside the box. When this was adjusted so that the discharge just passed through it in preference to the sound-gap the potential variation across the sound-gap remained practically the same as before, and the deflexion registered was that due to the electrostatic attraction only. An attempt to obviate this necessity was made by erecting between the gap and the pendulum an earthed metal screen which contained an aperture sufficiently large to allow the pulse to encounter the whole vane. Although this practically removed the electrostatic attraction errors were found to be introduced by diffraction at the aperture.

The measured deflexion corresponding to any spark showed slight variations on repetition. The value taken was usually an average of about ten trials.

The impulsive effect produced by the pulse will be $\int p\,dt$, where p is the excess of pressure in the pulse over the atmospheric pressure, and the integration is taken over the duration of the pulse. It was thought at first that the "intensity" of the pulse (the energy content) would be proportional to the square of this quantity since the intensity of continuous sound-waves is proportional to the square of the pressure amplitude. The radiation pressure of continuous waves, which is proportional to the intensity, is, however, calculated in precisely the same way as the above impulse, viz., $\int p\,dt$, and it is only the rapid succession of the waves that gives the effect of a steady pressure. An impulsive effect could no doubt be produced with ordinary sound-waves by an arrangement whereby waves could be emitted only for a brief interval of time. The effect on a vane would be an impulse proportional to the radiation pressure. It is thus evident that the impulse produced

by the sound-pulse measured here is to be regarded as a measure of its intensity, and not of the pressure amplitude.

4. *Distribution of Intensity of the Pulse.*

The source of the sound (the spark) is in the form of a line, or, at least, a cylinder of small diameter. Accordingly it is to be expected that it would exhibit directional properties, with varying intensity in a plane passing through the spark. This was indeed obvious from the appearance of the shadow of the pulse which, with a point-gap, indicated the most intense condensation in the direction of the perpendicular bisector of the spark, with a rapid diminution of intensity on each side. The pulse from a sphere-gap showed rather less variation.

In order to investigate the distribution of intensity a spark-gap was constructed which could be rotated about an axis through the centre of the gap. The electrodes were elevated above the gap supports, so that little obstruction was offered to the pulse (apart from the electrodes themselves) at small angles with the spark. By rotating the gap and keeping the pendulum fixed the impulse could be measured at any angle with the spark. The angle was reckoned from a line drawn through the spark from anode to cathode. Thus 90° corresponds to the perpendicular bisector, which was always the direction of maximum impulse (P_0). The vane used was 5×1 cm. in size, with the long side vertical, it being assumed that the impulse would be uniform in a plane perpendicular to the spark. The distance from the gap to the vane was 17 cm., so that the vane intercepted an angular width of about $3\frac{1}{2}°$.

The distribution curves obtained with electrodes 2 cm. in diameter and with steel needles are shown in fig. 1 in the form of polar diagrams ($C = \cdot 0036\,\mu F$). In both cases the curves deviate slightly from symmetry about 90°, the impulse on the side of the anode being a little greater than that at the corresponding angle on the side of the cathode. This difference is larger than the experimental error involved and appeared consistently. It is in agreement with some observations made by Hertz[7], who found that the explosive effects of a condenser discharge were more violent at the anode than at the cathode.

The striking features about the sphere-gap are the existence of very distinct minima and the fact that the

impulse rises to a maximum again at 0° and 180°, although these directions are in the optical shadow cast by the source. Even with 3 cm. spheres and a gap of 5 mm., when the optical shadow extends to 48·5°, the impulse in the directions 0° and 180° was about 70 per cent. of P_0. The minimum impulse and the angle at which it occurs depend on the diameter of the spheres. These are indicated in Table I., the minimum between 0° and 90° only being given.

Fig. 1.

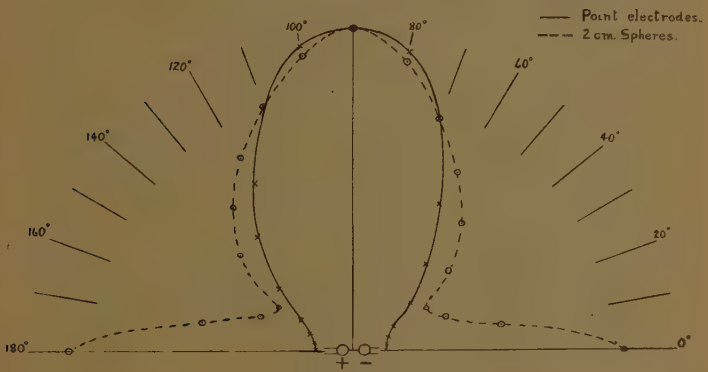

TABLE I.

Diameter of electrode (cm.).	Gap. (mm.).	Angle of min. impulse.	Min. impulse in terms of P_0.	Mean impulse in terms of P_0.
Points ..	10	0°	·11	·344
1	5	35°	·48	·446
2	5	26°	·24	·406
3	5	20°	·20	·370

Since no maximum is found at 0° with needle electrodes the cause in the case of spheres must lie in the volume or sphericity of the electrodes. Lord Rayleigh[8] dealt analytically with the influence of a rigid sphere situated close to a source of sound, and proved that the sphere does not cast a sound-shadow if its diameter is not

excessively large compared with the wave-length of the sound. Indeed, for the case where the circumference of the sphere is equal to or less than the wave-length the intensity behind the sphere exceeds that in a direction tangential to it. This analysis of course was concerned with continuous waves, but it is quite evident that similar phenomena are exhibited by a sound-pulse, although the explanation of these phenomena may be on different lines.

Experiments showed that the distribution did not depend on the length of the gap as long as this was less than half the electrode diameter. For longer gaps the minimum impulse became greater although the shape of the curve remained similar. The distribution was unaffected by variation of the intensity of the spark or the frequency of oscillation of the spark-circuit. As a result of these observations it is concluded that the only factor which determines the shape of the distribution curve for small gaps is the diameter of the electrodes.

These curves enable a determination of the mean impulse per unit area over the whole pulse to be made in terms of P_0, assuming that the distance between the source and the vane is great enough for the pulse to be considered spherical. It is easily proved that the mean impulse is given by

$$\tfrac{1}{2}\int_0^{\pi} P \sin\phi \, d\phi,$$

where P is the impulse per unit area and is a function of ϕ, the angle with the spark, as given by the distribution curve. The mean values of the impulse, as calculated from the observations for the electrodes investigated, are shown in Table I.

5. *The Variation of Intensity with Distance.*

It was found that for weak sparks—that is, using a small capacity or gap—the measured impulse varied exactly as the inverse square of the distance from the spark. In fig. 2 curve A shows the observations for a spark where $C = \cdot 00363\,\mu F$ with a gap of 4 mm. between zinc spheres 2 cm. in diameter. The impulse is expressed as a percentage of the value at a distance of 7 cm., which was the nearest convenient position to the vane which the gap

could occupy. (It was inadvisable to bring the gap closer, since the electrostatic attraction on the vane increased rapidly with diminution in distance. Errors would also be introduced by the fact that the pulse is not spherical at very small distances.) The full curve is that obtained from the inverse square law.

This experiment offers confirmatory evidence of the views expressed in § 3, viz., that the impulsive effect indicated by the pendulum is a measure of the energy in the pulse rather than the pressure amplitude. It is to be expected that the pressure amplitude would vary

Fig. 2.

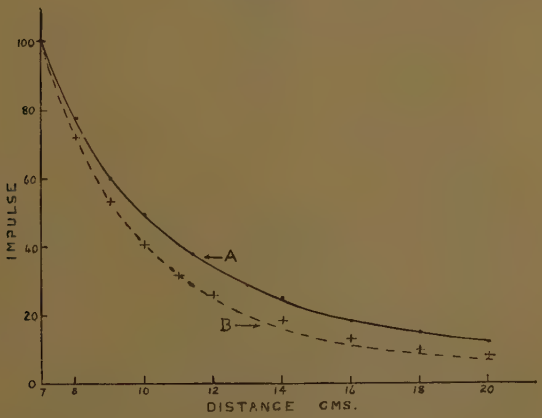

as $1/r$ rather than $1/r^2$. F. Ritter [9] found the former relation to hold approximately for the sound-pulse emitted by an explosion, and an examination of the wave-forms of spark-pulses as given by Okubo and Matuyama [10] indicate an even slower variation with distance. It might be suspected that the more rapid variation found in these experiments might be due to attenuation, but it was found that even the weakest spark which would give an appreciable deflexion gave an impulse exactly proportional to $1/r^2$.

With sparks above a certain intensity the variation of impulse at the smaller distances is more rapid than $1/r^2$. This is illustrated by the crosses in fig. 2, which show the

observations when the above gap was opened to 14 mm., thus producing a discharge of about seven times as much energy as the previous one. The dotted curve B is the curve calculated from the equation $P=Qe^{-kr}/r^2$, where Q is a constant and $k=0{\cdot}051$. It is seen that this curve, while fitting the observations closely at the smaller distances, passes below them at the larger distances. Indeed, the value of Pr^2 tends towards a definite limit as r increases, showing that ultimately the intensity of the sound-pulse will follow the inverse square law. In other words k is not constant throughout the progress of the pulse, but is a function of P, decreasing with it. The attenuation of the sound-pulse is of course due to

Fig. 3.

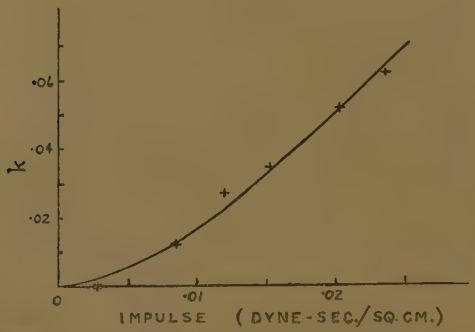

viscosity and heat-loss, and it is natural to expect the effect of these factors to vary with the intensity of the pulse. This variation of the rate of degradation of acoustical energy with sound intensity has been shown by M. D. Hart[11] to exist also with continuous waves.

The relation between P and r was obtained for various spark intensities and the value of k found which gave a curve fitting the observations between the distances 8 and 12 cm. These are shown in Table II. and are ascribed to the values of P in each case at a distance of 10 cm. P is expressed in dyne-sec per sq. cm. as calculated from the expression for P in § 3. While such a method is not exactly rigorous it provides some indication of how the absorption factor k varies with the impulse. The relation between P and k is illustrated by fig. 3.

Table II. also provides an illustration of the magnitude in absolute units of the impulsive effect of particular discharges at a distance of 10 cm. The condenser was connected directly to the gap by two copper-wire leads (26 S.W.G.), each of length 50 cm.

TABLE II.

C=·00363 μF. 2 cm. Zn electrodes.

Gap (mm.)	P (dyne-sec/sq. cm.).	*k*.
4	·0029	0
8	·0085	·012
10	·0120	·027
12	·0154	·034
14	·0205	·051
16	·0237	·062

6. *The Relation between the Intensity of the Sound-pulse and the Electrical Quantities involved in the Spark-circuit.*

The intensity was found to change with variation of the capacity, potential (or gap-length), frequency, and resistance of the spark-circuit. Difficulties were encountered in separating these variables and elucidating the effect of any one. One cannot, for example, change the capacity of the condenser without altering the frequency of the circuit, and consequently also the resistance of the wires involved. Thus, although the variation with capacity is more important from a practical point of view, it is necessary, in order to provide a logical sequence, to describe the effects of resistance and frequency first.

In these experiments the intensity measured was that on the perpendicular bisector of the spark, which in the succeeding paragraphs will be denoted simply by P, and the spark intensities were, where possible, such that the attenuation with distance was negligible. The electrodes used were zinc spheres 2 cm. in diameter.

(a) *Potential.*—The only quantity varied here was the gap-length. Care was taken not to disturb the positions

and lengths of the connecting wires, because even a small alteration of position or length was sufficient to alter the frequency of the circuit. The change of gap-length only, within the range of the experiment, did not affect the frequency. When an induction-coil is just producing a discharge across a gap the potential is directly proportional to the primary current, i_0. It was found preferable in this experiment to retain i_0 as a measure of V instead of using one of the published tables of sparking potentials, since these do not agree among themselves, and, in any case, are usually given for steady potentials.

Fig. 4.

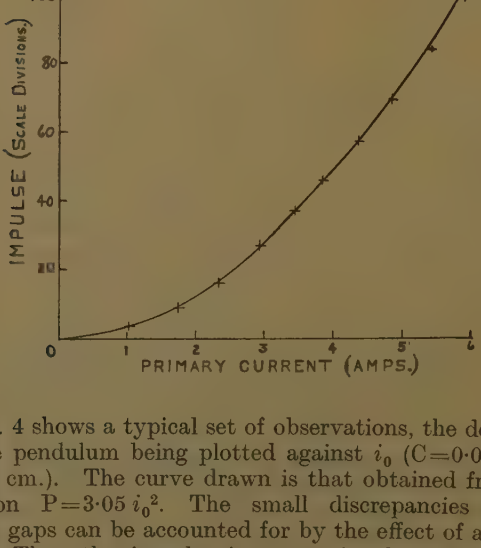

Fig. 4 shows a typical set of observations, the deflexion of the pendulum being plotted against i_0 ($C=0{\cdot}0018\,\mu F$, $r=20$ cm.). The curve drawn is that obtained from the relation $P=3{\cdot}05\,i_0^2$. The small discrepancies at the larger gaps can be accounted for by the effect of attenuation. Thus the impulse is proportional to the square of the potential to which the condenser is charged. The natural conclusion one would make from this alone is that the intensity of the spark-pulse is proportional to the energy given to the condenser ($\frac{1}{2}CV^2$), but the subsequent experiments will show that other factors are involved.

The same relation was found to hold for point-electrodes as well as spheres, but a decided difference existed between the intensity of the pulse in the two cases under the same conditions. For the same primary current, *i. e.*, the same potential, the intensity for points was found to be 1·9 times as large as that for spheres. The explanation no doubt lies in the greater volume of air involved in the spark, the gap-length for points (when fresh steel needles were used) being almost four times that for 2 cm. spheres.

When the primary current supplied to an induction-coil is gradually increased from the minimum the discharge passes from a single-spark to a multiple-spark discharge, in which the number of sparks increases with the primary current. Each separate spark, of course, sends out a separate sound-pulse. With such a discharge it was found that the average impulse per spark diminishes as the number increases. In an experiment in which the number of sparks was counted by photographing the discharge by means of a revolving mirror the results were :—

No. of sparks	1	2	3	5	7	13
Impulse (scale divisions)	20	29	42	65	82	108

It seems then that the average amount of energy in each spark diminishes as the number increases. This is probably due to the diminution in sparking potential which occurs when one spark rapidly succeeds another. Further increase in primary current causes the discharge ultimately to change its form[12]. It consists of a single spark followed by a pulsating glow or arc, and may terminate in another spark or group of sparks. The impulsive effect of the sound radiation from a discharge of this kind is small compared to that of the multiple spark. Most of the energy supplied to the discharge is consumed in the glow or arc, in which the current variation is slow.

(b) *Resistance.*—It was early realized that resistance in the spark-circuit, even when small, affected appreciably the intensity of the sound-pulse. Differences could be detected with different lengths and diameters of connecting wires from the condenser to the gap. This effect of course might be ascribed to a change of inductance as well as resistance. In order to examine the effect

of resistance alone liquid resistances were used consisting of copper plates dipping into dilute copper sulphate solution. The resistance could be varied by varying the area of contact of the metal and the solution, or by varying the concentration of the solution. Sufficient inductance was included in the circuit to ensure that the addition of the resistance did not appreciably affect the frequency. The results of one experiment are shown in fig. 5 ($C = \cdot 0087\ \mu F$, gap $= 5$ mm., $r = 13 \cdot 5$ cm.). The value of R

Fig. 5.

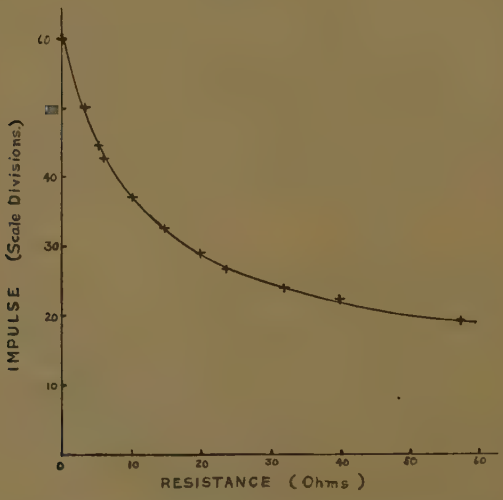

indicated is the direct current resistance added to the circuit. Even if the liquid resistance used varies in value with the frequency, it is probable that the value will be proportional to its direct current resistance, since the frequency is constant. The curve drawn is calculated from the relation $P = \beta/\sqrt{R + R_0}$, where $\beta = 150$ and $R_0 = 6 \cdot 25$ ohms. The constant R_0 may doubtless be interpreted as the resistance of the circuit apart from the resistance inserted, and will include the resistance of connecting wires and any leakage which takes place through brush discharges. It is possible that it may include even the effective resistance of the gap. Miss Brooks[13] has found that

for a spark 6 mm. long the amount of heat generated was equivalent to that which would have been produced by a wire of 2 ohms resistance. It may thus be asserted that the impulse produced by the sound-pulse is inversely proportional to the square root of the total resistance, when C, V, and n are constant.

(c) *Frequency.*—The inductance of the spark-circuit was varied by inclusion of different numbers of turns (29 cm. diameter) of copper wire (16 S.W.G.). The resistance of the

Fig. 6.

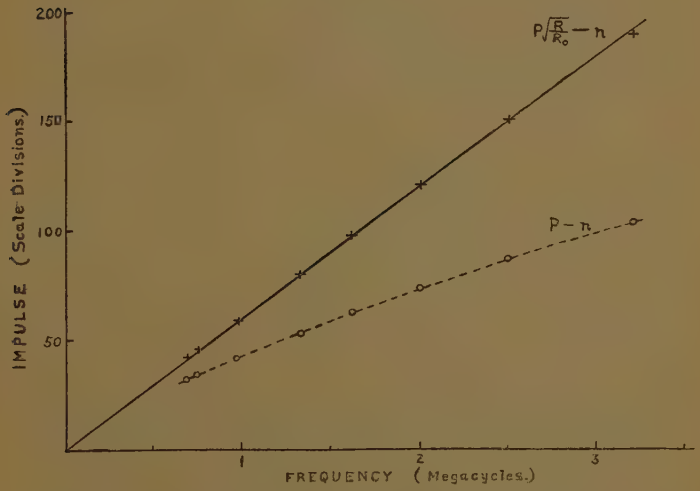

connecting wires was made great enough to render the resistance of the coil negligible. The frequency was measured by a calibrated wave-meter. It was considered preferable to measure the frequency of the circuit directly rather than attempt to measure or calculate the small inductances involved. The variation of impulse with frequency is shown in fig. 6 ($C = \cdot 00094\,\mu F$, gap = 10 mm., $r = 10$ cm.). The observations deviate slightly but consistently from a straight line, the deviations being greatest at the higher frequencies. It has been shown that even a small alteration of resistance in the circuit affects the observed impulse, so that in the present

case the change of resistance with frequency must be taken into account. The main resistance in the circuit was that of the copper connecting wires (26 S.W.G.). The values of R/R_0, where R is the resistance at frequency n and R_0 is the D.C. resistance, were calculated from the usual formula [14]. Since the impulse varies inversely as the square root of the resistance, the correction for resistance is made by multiplying P by $\sqrt{R/R_0}$. The graph of $P\sqrt{R/R_0}$ against n is shown

Fig. 7.

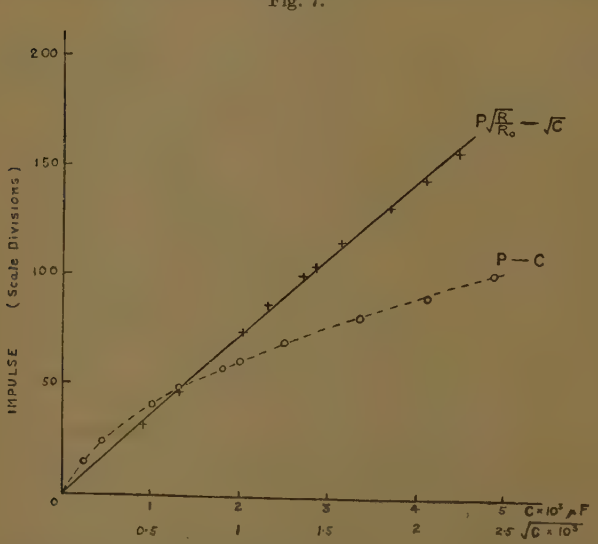

in fig. 6, the observations lying close to a straight line passing through the origin. Hence we may write $P \propto n/\sqrt{R}$. Since C has been kept constant, apart from the small self-capacity of the inductance-coil, the relation may also be stated in the form $P \propto 1/\sqrt{LR}$ when C and V are constant.

(d) *Capacity.*—The variation of the intensity of the sound-pulse when the capacity alone was varied is illustrated by fig. 7 (gap = 5 mm., $r = 13{\cdot}5$ cm.). Since it was found that the impulse is proportional to V^2, it was at first expected that it would also be proportional

to C, but the variation is more suggestive of the law $P \propto \sqrt{C}$. The reason, of course, lies in the alteration of frequency, which may be taken as $1/2\pi\sqrt{LC}$. Thus an increase in energy given to the discharge is partially counteracted by the resultant decrease in frequency. The relation $P \propto \sqrt{C}$, however, does not fit the observations perfectly, the deviations being greatest at low values of C, *i. e.*, at the higher frequencies. Applying a correction for resistance in the same manner as before, a graph of $P\sqrt{R/R_0}$ against $\sqrt{C}$ is drawn in fig. 7. The graph is approximately linear, and therefore gives the relation $P \propto \sqrt{C/R}$ when V and L are constant.

(e) *Electrode Material.*—It was found that, within the limits of experimental error, the intensity of the sound-

TABLE III.

Material.	i_0 (amp.).	Impulse (P) (scale divisions).	P/i_0^2.
Iron	5·70	59·5	1·83
Copper	5·20	51·0	1·89
Aluminium ...	5·62	58·3	1·86
Zinc	5·13	49·0	1·86

wave did not vary with the material of the electrodes. In one series of observations electrodes of diameter 1 cm. were used and the gap was adjusted in each case to 5 mm., keeping the other conditions of the spark-circuit the same. The results are given in Table III.

The probable error in adjustment of the gap was 0·05 mm., and since P is proportional to V^2 this leads to a probable error of 2 per cent. in P. Hence within the probable error P/i_0^2 is constant, and any difference which exists in the value of P for different electrodes is due to a difference in sparking potential.

This is a very different result from that given by Haschek and Mache[6], who found very different pressures generated by different materials, the value for iron being about three times that for copper. The continuous sparking method which they adopted, however, would

naturally lead to variation with material, since the sparks were really passing through the vapour of the electrodes. The sparks were produced at the rate of eighty per second.

The absence of any effect of the material when single discharges are used shows that the development of the main sound-pulse takes place before there is any appreciable evaporation of the metal—that is, is conditioned only by the initial discharge through the air.

(f).—Collecting the results of the above experiments we find that the impulse produced by the sound-pulse at a given distance is given by

$$P = AV^2\sqrt{C/LR},$$

where A is a constant for any given electrodes. The value of A varies slightly for electrodes of different diameter, and, in particular, its value for fresh needle-points is 1·9 times that for spheres 2 cm. in diameter.

The first current maximum in the discharge is, if R is small, given by $V\sqrt{C/L}$. During the development of this current the potential across the gap falls in some manner from V to a small value. If we assume that the average value of the potential during this time is proportional to V the work done in the discharge up to the first current maximum will be proportional to $V^2\sqrt{C/L}$. The impulse, which is proportional to the sound energy, varies with these quantities in the same way, and it may therefore be said that the sound energy generated is proportional to the work done in building up the current from zero to its first maximum.

The author can find no adequate explanation of the experimental relation between P and R. According to the simple theory of the circuit the first current maximum is, if R is taken into account,

$$V\sqrt{\frac{L}{C}}\left(1-\frac{CR^2}{4L}\right)^{-\frac{1}{4}}e^{-R/2L},$$

but the observations as shown in fig. 5 bear no resemblance to this relation.

It is observed that the sound energy emitted is not directly proportional to the energy supplied to the condenser. Even if it is supposed that L and R are constant, $P \propto \sqrt{C}V^2$. An interesting consequence of this relation

is that a discharge of small capacity and high potential is much more efficient as a sound producer than one of large capacity and low potential if the total energy supplied is the same.

It follows from the above that no simple numerical relation can exist between the sound energy emitted and the energy supplied to the condenser. The sound energy in any particular case, however, can be estimated from a knowledge of the impulse if we adopt a fairly reasonable analogy with continuous wave-motion. If E is the energy density of the sound-waves and F the radiation pressure then $F=\frac{1}{2}(\gamma+1)E$ (where γ is the ratio of specific heats of air), on the assumption of complete absorption. The energy in one wave-length (λ) per unit area of wave-front will be

$$E\lambda=\frac{2F\lambda}{\gamma+1}=\frac{2Fct}{\gamma+1},$$

where c is the velocity of sound and t the periodic time of vibration. But Ft may be considered as the impulse (P) produced by the impact of one wave on a vane of unit area. The total energy in a single spherical wave will thus be given by

$$\frac{2c}{\gamma+1}\int P\,dS,$$

where the integral extends over the sphere. This integral can be evaluated for the spark-pulse from the results of the distribution experiments in Table I. Selecting the observation in Table II. which is free from attenuation, we have

$C=0{\cdot}00363\,\mu F$. Gap $=4$ mm., *i. e.*, $V=14{,}700$ volts.

$r=10$ cm. $P=0{\cdot}0029$ dyne-sec/sq. cm.

Energy supplied to condenser $=\frac{1}{2}CV^2=3{\cdot}9\,.\,10^6$ ergs.

$$\text{Sound energy}=\frac{2c}{\gamma+1}\,.\,4\pi r^2\,.\,(0{\cdot}41)P=4{\cdot}1\,.\,10^4 \text{ ergs.}$$

Thus approximately 1 per cent. of the energy supplied to the condenser is dissipated in sound in this combination of C and V. The same percentage approximately would be obtained for the same C and any V, but a decrease in C would increase the percentage.

7. *The Diameter of Spark-core.*

It is natural to expect that the intensity of the sound-pulse will be related in some way to the size of the source, which obviously changes with the capacity etc. of the circuit. The sparks were photographed with a camera giving an enlarged image, using a very small aperture and a slow plate. In this way the core, which is the main source of sound, could be distinguished from the sheath, but the edges of the image, the source of light being a luminous column of gas, were not sharply defined. In addition, certain photographic difficulties, such as the effect of the time of development and the Clayden effect, had to be overcome. Thus the experimental error in estimating the diameter of the core (D) was large. The best results were obtained with point-electrodes.

Many series of photographs were taken with a view to determining the relation between D and each variable in turn, using the same circuits as in the previous experiments. The evidence, on the whole, led to the result that the cross-sectional area of the spark-core is directly proportional to the first current maximum, $V\sqrt{C/L}$. An interesting consequence of this relation is that the maximum current density in the air is constant. An average value found for this quantity was $1{\cdot}3 \cdot 10^5$ amp. per sq. cm. Prof. S. R. Milner[15] made some observations on the current density in a condenser discharge with variation of inductance only. He found that the average current density was of the order of $5 \cdot 10^4$ per sq. cm. Since it can be assumed for these experiments that V is proportional to the gap-length within the range employed, it follows that the volume of the spark-core is proportional to $V^2\sqrt{C/L}$.

The observations on the relation between D and R showed that D definitely diminished with R, but the measurements in this case were too variable to form an opinion of the exact relationship.

It is evident from the above that the intensity of the sound-pulse, at least when R is small, is directly related to the volume of air involved in the source, since both vary with the properties of the circuit in the same manner

8. The result that, with any given electrodes, the energy content of the spark (as far as the sound is concerned) is proportional to the impulse, which, in turn, is proportional

to the volume of the spark-core, leads to the conclusion that the maximum energy density in the core is the same for any spark, and hence also the pressure developed is approximately constant. In the case cited above, for which the sound energy was estimated to be $4{\cdot}1 \cdot 10^4$ ergs, the diameter of the core was found to be about 0·7 mm. If it is assumed that this energy is originally concentrated in the core, it leads to an estimate of seventeen atmospheres for the maximum pressure developed. Since this estimate is based on the assumption of complete absorption by the vane, the value is probably too large.

The influence on the intensity of the sound-pulse of change of inductance does not really lie in the resultant change of frequency, but in its influence on the amplitude of the current (and consequently on the volume of the source). This may be illustrated by considering a case in which C and L in a given current are both doubled, V and R remaining the same. No change in impulse, current, or volume would result, and yet the frequency would be halved. This indicates that the development of the pulse is not due to the rate of development of the current, or, in other words, to an expansion of the gas involved in the spark. The conditions seem rather to resemble the sound propagation produced when a region of high condensation is supposed instantaneously created and then left to itself. Such a problem, when the initial region is spherical and the condensation small, has a simple solution. If this initial condensation is s_0 throughout a sphere of radius a, a pulse is propagated which at any instant t is confined to a spherical shell of thickness $2a$, the condensation s being given by $s = s_0(r - ct)/2r$ for $r + a > ct > r - a$. s is positive in the outer half of the pulse and negative in the inner half. The wave-form of this pulse is very suggestive of the wave-form of the spark-pulse as observed by Okubo and Matuyama[10]. These writers found, however, that in the spark-pulse the pulse-length increased with distance and the positive condensation was greater than the negative. Both results are of course consequences of the very large initial condensation, and are to be expected on the theory of sound-waves of finite amplitude.

In conclusion, the writer desires to acknowledge his indebtedness to Prof. Taylor Jones for his helpful advice and criticism.

References.

(1) Beams, Phys. Rev. xxxv. p. 24 (1930).
(2) Töpler, *Ann. d. Physik*, xxvii. (1908).
(3) Dvorak, *Ann. d. Physik*, ix. p. 502 (1880).
(4) Foley, Phys. Rev. xxxv. p. 373 (1912).
(5) Neklepajev, *Ann. d. Physik*, xxxv. p. 175 (1911).
(6) Haschek and Mache, *Ann. d. Physik*, lxviii. p. 740 (1899).
(7) Hertz, Wied. *Ann.* xix. p. 78 (1883).
(8) Rayleigh, 'Theory of Sound,' vol. ii. p. 222 (1878).
(9) Ritter, *Beiträge Z. Physik d. Freien Atmosphäre*, Bd. xii. (1925).
(10) Okubo and Matuyama, Phys. Rev. xxxiv. p. 1474 (1929).
(11) Hart, Proc. Roy. Soc. cv. p. 80 (1924).
(12) McFarlane, Phil. Mag. xvi. p. 865 (1933).
(13) Brooks, Phil. Mag. vi. p. 92 (1901).
(14) Moullin, 'Radio Frequency Measurements,' p. 238.
(15) Milner, Phil. Mag. xxiv. p. 709 (1912).

III. *An Apparent Paradox in the Theory of the Heats of Dilution of completely dissociated Electrolytes.* *By* O. Gatty, *M.A., B.Sc.*†

I. *Introduction.*

In careful investigations of the properties of solutions it is necessary to distinguish between the constant volume and the constant pressure work functions which are respectively the available energy A, and the free energy F, of the system. It follows that a similar distinction ought to be applied to heats of dilution according to whether the mixing of solvent and solution be one where the initial pressures of the solvent and the solution are both equal to the final pressure, or alternatively the volume of the final solution is equal to the sum of the volumes of the two initial solutions. In practice measurements of heats of dilution refer to the former quantity, but expressions for the latter have been given by Bjerrum [1] and Gatty [2] for the case of dilute solutions of strong electrolytes. These equations are based on Debye and Hückel's [3] theory of strong electrolytes and lead to an apparent paradox, as was pointed out by Guggenheim [4]. In the range of concentrations in which the simplest Debye and Hückel theory is valid the contribution of the electrical charges on the ions to the free energy, F, of the solution is sensibly equal to their contribution to the

† Communicated by the Author.

available energy, A, of the solution. That is to say that the electrical contributions to the constant pressure and constant volume work functions are sensibly equal. Nevertheless, there is a significant difference between the electrical contributions to the heat changes on constant pressure and constant volume dilution if the equations given are correct.

At first sight the difference in both cases would be expected to be of the order of the compressional work accompanying the constant pressure dilution, and the equations therefore are suspect. In the present paper the equations are shown to be correct and the apparent paradox is elucidated. The difference in the constant pressure and constant volume work function terms tend at low concentrations to a small quantity of the second order, while the corresponding difference in the heats of dilution tends to a small quantity of the first order. The separate work function and heat of dilution terms under these conditions all tend to a small quantity of the first order. The method of analysis given below is independent of the actual value for the electrical contribution to heats of dilution, and is, in fact, applicable to the corresponding contributions of any type of field of force round solute molecules, provided only that the work necessary to build these fields of force reversibly under some specified conditions can be calculated. The actual orders of magnitude of the various small quantities do, however, depend on the particular type of force being investigated.

II. *Heat Changes and Equilibrium Conditions.*

The first law of thermodynamics may be expressed

$$d\mathrm{E}=\delta\mathrm{Q}-p d\mathrm{V}+\delta\mathrm{W}', \quad . \quad . \quad . \quad . \quad . \quad (1)$$

where $d\mathrm{E}$ is the increase in energy of any system during an infinitesimal change, $\delta\mathrm{Q}$ is the corresponding amount of heat supplied to the system, $d\mathrm{V}$ is the corresponding increase in volume of the system, p is the pressure on the system, and $\delta\mathrm{W}'$ is any work other than the compressional work, $-p d\mathrm{V}$, which is done on the system. The work necessary to introduce fresh particles into the system is to be included in $\delta\mathrm{W}'$. It may also be written

$$d\mathrm{H}=\delta\mathrm{Q}+\mathrm{V}dp+\delta\mathrm{W}', \quad . \quad . \quad . \quad . \quad . \quad (2)$$

where $\mathrm{H}=\mathrm{E}+p\mathrm{V}$.

Equations (1) and (2) become

$$dE = \delta Q_{vw'} \quad . \quad . \quad . \quad . \quad . \quad . \quad . \quad (3)$$

and

$$dH = \delta Q_{pw'}, \quad . \quad . \quad . \quad . \quad . \quad . \quad (4)$$

which show that the heat supplied to any system during any process whatsoever, whether it be thermodynamically reversible or not, is equal to the increment in internal energy of the system, provided only that the process takes place at constant volume so that no compressional work is done on the system, and provided, further, that no other work is done on the system. Similarly, for any process at constant pressure while $\delta W' = 0$ the increase in total heat content, H, is equal to the heat supplied to the system during the process. Equations (1) to (4) are independent of the second law of thermodynamics, being based only on the first law of thermodynamics, and they are therefore valid for irreversible as well as reversible processes. The second law is introduced in the form

$$\delta Q = T dS \quad . \quad . \quad . \quad . \quad . \quad . \quad . \quad (5)$$

for any reversible process, where T denotes the absolute temperature and dS an infinitesimal increase in the entropy, S, of the system. The equations for reversible changes and therefore for infinitesimal displacements at equilibrium are then given by

$$\left.\begin{aligned} dE &= T dS - p dV + \delta W', \\ dH &= T dS + V dp + \delta W', \\ dA &= -S dT - p dV + \delta W', \\ dF &= -S dT + V dp + \delta W', \end{aligned}\right\} \quad . \quad . \quad . \quad (6)$$

where

$$A \equiv E - TS \quad \text{and} \quad F \equiv E + pV - TS.$$

III. *The Contribution of the Intermolecular Field of Force to the Thermodynamic Functions of a System.*

If a thermodynamically reversible process on a sub-atomic scale is used so as to modify the field of force round the particles in a homogeneous mass the work that is involved may be set equal to $\int \delta W'$, if, apart from this process, no additional external work be done on the system apart from compressional work. Denoting $\int dG$ during such a process by ΔG, where G is any variable, and using

subscripts X and Y to show that X and Y remain constant during the process, equations (6) may be transformed into

$$\left.\begin{aligned}\Delta E_{vs}&=\Delta W'_{vs},\\ \Delta H_{ps}&=\Delta W'_{ps},\\ \Delta A_{vT}&=\Delta W'_{vT},\\ \Delta F_{pT}&=\Delta W'_{pT}.\end{aligned}\right\} \quad . \quad . \quad . \quad . \quad . \quad . \quad . \quad (7)$$

Thermodynamically reversible processes of the subatomic type indicated above have no existence in fact; but for the case of ions in solution Debye and Hückel [3] have been able to calculate the work required to discharge ions by a reversible process of this nature. They have calculated $\Delta W'$ at two concentrations, say c_1 and c_2, and given an expression for ${}^{c_1}\Delta W' - {}^{c_2}\Delta W'$ in the limit as c_2 tends to zero. Their expression is only valid in dilute solutions where ${}^{c_1}\Delta W' - {}^{c_2}\Delta W'$ becomes small, and where it also becomes independent of whether the terms refer to $\Delta W'_{pT}$ or $\Delta W'_{vT}$. In order to discuss the orders of magnitude of small quantities, expressions for $\Delta W'_{pT} - \Delta W'_{vT}$ must be obtained.

These can be derived on general thermodynamical grounds. A convention as to notation, however, is needed if $\Delta W'_{xY}$ and $\Delta W'_{xZ}$ are to be contrasted. If these two terms are to bear any relationship to one another it is essential that Δ in each case should refer to the same modification in the molecular fields of force. In addition, either the initial or the final state must be the same in both processes, and in this paper the initial states with the completed fields of force are assumed to be identical and to be at a pressure p, a temperature T, and possess volume V. From equation (6)

$$dF_{pT}=\delta W'_{pT}, \quad . \quad . \quad . \quad . \quad . \quad . \quad . \quad . \quad (8)$$

$$dA_{pT}=\delta W'_{pT}-p\,dV_{pT}, \quad . \quad . \quad . \quad . \quad (9)$$

and these can be integrated for some subatomic process giving

$$\Delta F_{pT}=\Delta A_{pT}+p\Delta V_{pT}. \quad . \quad . \quad . \quad . \quad (10)$$

Similarly, it may be shown that

$$\Delta F_{vT}=\Delta A_{vT}+V\Delta p_{vT}. \quad . \quad . \quad . \quad . \quad (11)$$

In order to relate ΔG_{pT} and ΔG_{vT}, where G is any variable, the process is supposed to be split into two stages,

the second of which is a pure compressional term in which both the pressure and volume are altered, while during the first process the reversible alteration of the molecular fields of force takes place either at constant pressure or at constant volume. In the present paper the pure compressional term is taken to refer always to the second stage in order of time, so that it operates always on the final stage and not on the initial stage.

From equations (6)

$$\Delta A_{pT} = \Delta A_{vT} - \int_{V}^{V+\Delta v_{pT}} p\, dV_T, \quad . \quad . \quad (12)$$

$$\Delta F_{pT} = \Delta F_{vT} - \int_{p}^{p+\Delta p_{vT}} V\, dp_T, \quad . \quad . \quad (13)$$

where the suffix T in the integrands denotes that the compressional process on the final solutions takes place at constant temperature. It also takes place at $dW' = 0$. From equations (7) and (10) to (13) it may be shown that

$$\Delta W'_{pT} - \Delta W'_{vT} = p\Delta V_{pT} - \int_{V}^{V+\Delta v_{pT}} p\, dV^*_T \quad . \quad (14)$$

$$= V\Delta p_{vT} - \int_{p}^{p+\Delta p_{vT}} V\, dp^*_T, \quad . \quad (15)$$

the asterisks showing that the process is performed on the modified solutions. In equations (14) and (15) the integrands vary respectively between p and $p+\Delta p_{vT}$ in the one case, and V and $V+\Delta V_{pT}$ in the other, so that both equations lead to the inequality

$$|\Delta W'_{pT} - \Delta W'_{vT}| < |\Delta p_{vT}.\Delta V_{pT}|. \quad . \quad . \quad (16)$$

If $\Delta W'_{pT}$ and $\Delta W'_{vT}$ refer to the removal respectively at constant pressure and temperature and at constant volume and temperature of some portion of the fields of force of solute molecules in a solution, they tend towards a limiting value as the dilution is increased by increasing the number of solvent particles in the system while the number of solute molecules is kept unaltered. For these conditions the inequality (16) becomes interesting. After the process $\Delta W'_{pT}$ the solution is left at a volume $V+\Delta V_{pT}$ and a pressure p; after the process $\Delta W'_{vT}$ the solution is left at a volume V and pressure $p+\Delta p_{vT}$, and in both cases the solutions are at the same temperature T.

Thus $$\Delta p_{vT} = \int_{v+\Delta v_{pT}}^{v} \left(\frac{\partial p}{\partial V}\right)_T^* dV_T^*, \quad . \quad . \quad . \quad (17)$$

where the integrand and the process of integration refer to the solution with the reduced fields of force, and this is shown by the asterisk in the equation. Denoting the compressibility of the solution with the reduced fields of force by κ^* and its volume by V^*, equation (17) becomes

$$\Delta p_{vT} = -\int_{v+\Delta v_{pT}}^{v} \frac{dV_T^*}{\kappa^* V^*}. \quad . \quad . \quad . \quad . \quad (18)$$

By increasing the solvent particles indefinitely at constant solute particles, while $\Delta W'$ refers to a process on the solute particles only, it is possible to increase V^* indefinitely. ΔV_{pT}, on the other hand, can hardly be many times greater than the total volume of the solute particles in the solution, so that ΔV_{pT} cannot increase without limit under these conditions. Like $\Delta W'_{pT}$ it tends to a limiting value at low concentrations, and from equations (6) and (7) a general thermodynamic relationship,

$$\left(\frac{\partial \Delta W'_{pT}}{\partial p}\right)_{TW'} = \Delta V_{pT}, \quad . \quad . \quad . \quad . \quad (19)$$

can be deduced. Similarly,

$$\left(\frac{\partial \Delta W'_{vT}}{\partial V}\right)_{TW'} = -\Delta p_{vT}. \quad . \quad . \quad . \quad (20)$$

Since ΔV_{pT} does not increase without limit on the addition of solvent molecules, $\frac{\Delta V_{pT}}{V^*}$ will decrease without limit under these conditions.

Thus

$$\underset{v\to\infty}{\text{Lt}} \ \Delta p_{vT} = 0. \quad . \quad . \quad . \quad . \quad . \quad (21)$$

In consequence, when V^* is big and Δp_{vT} is small and κ^* may be assumed to be constant throughout the integration,

$$\begin{aligned}\Delta p_{vT} &= -\frac{1}{\kappa^*}\int_{v+\Delta v_{pT}}^{v} d\ln V^* \\ &= +\frac{1}{\kappa^*}\ln\left(1+\frac{\Delta V_{pT}}{V^*}\right) \\ &\approx \frac{\Delta V_{pT}}{\kappa^* V^*} \quad . \quad . \quad . \quad . \quad . \quad . \quad . \quad . \quad (22)\end{aligned}$$

Thus for dilute solutions where $\Delta W'$ refers to a fixed gram molecular quantity of solute particles only, inequality (16) becomes in the limit

$$\left| \Delta\bar{\bar{W}}'_{p\mathrm{T}} - \Delta\bar{\bar{W}}'_{v\mathrm{T}} \right| < \left| \frac{(\Delta\bar{\bar{V}}_{p\mathrm{T}})^2}{\kappa V^*} \right| , \quad . \quad . \quad (23)$$

where κ is the compressibility of the pure solvent and equals κ^* for the dilute solutions considered, and the double bar indicates the work and volume changes are per mole of solute. In the limit, therefore, there is a quantity, varying directly as the concentration of the solution, which always exceeds $|\Delta\bar{\bar{W}}'_{p\mathrm{T}} - \Delta\bar{\bar{W}}'_{v\mathrm{T}}|$. In regions where the concentration is small the quantity

$$\frac{\Delta\bar{\bar{W}}'_{p\mathrm{T}} - \Delta\bar{\bar{W}}'_{v\mathrm{T}}}{\Delta\bar{W}'_{p\mathrm{T}}}$$

is also small, its ratio to the concentration tending to a definite limit as the concentration tends to zero. In cases where the concentration can be looked upon as a small quantity of the second order it is possible to write

$$\Delta\bar{W}'_{p\mathrm{T}} = \Delta\bar{\bar{W}}'_{v\mathrm{T}} = \Delta\bar{\bar{W}}'_{\mathrm{T}}. \quad . \quad . \quad . \quad . \quad (24)$$

Let ${}^{1}x_2\Delta\bar{\bar{W}}'_{\mathrm{T}}$ and ${}^{2}x_2\Delta\bar{\bar{W}}'_{\mathrm{T}}$ denote the values for $\Delta W'_{\mathrm{T}}$ when the mole fraction of the solute is ${}^{1}x_2$ and ${}^{2}x_2$ respectively, and let a quantity be defined by

$${}^{1}\Delta^{2}\Delta\bar{\bar{W}}'_{\mathrm{T}} \equiv {}^{1}x_2\Delta\bar{\bar{W}}'_{\mathrm{T}} - {}^{2}x_2\Delta\bar{\bar{W}}'_{\mathrm{T}}. \quad . \quad . \quad (25)$$

Further, for any variable L let a notation defined by the following identity hold,

$${}^{1}x\Delta\bar{\bar{L}} - {}^{2}x\Delta\bar{\bar{L}} \equiv {}^{1}\Delta^{2}\Delta\bar{\bar{L}}.$$

Then Debye and Hückel have calculated values for ${}^{1}\Delta^{2}\Delta\bar{\bar{W}}'_{\mathrm{T}}$, where the second concentration refers to the limit of zero concentrations of solute and the first term to a dilute solution, and have shown it to be proportional to the square root of the molar concentration, and therefore to $({}^{1}x_2)^{\frac{1}{2}}$.

Thus on the Debye-Hückel theory

$${}^{1}\Delta^{0}\Delta\bar{\bar{W}}'_{\mathrm{T}} \propto ({}^{1}x_2)^{\frac{1}{2}}, \quad . \quad . \quad . \quad . \quad . \quad (26)$$

while

$$|{}^{1}\Delta^{0}\Delta\bar{\bar{W}}'_{p\mathrm{T}} - {}^{1}\Delta^{0}\Delta\bar{\bar{W}}'_{v\mathrm{T}}| < |\mathrm{X}| \quad \text{where } \mathrm{X} \propto {}^{1}x_2,$$

where the affix ^{0} shows that the second solution is to be regarded as at zero concentration. Thus it may be said that

$$^1\Delta^0\Delta\bar{\bar{W}}'_{p\mathrm{T}}-{}^1\Delta^0\Delta\bar{\bar{W}}'_{\mathrm{vT}}$$

is a small quantity of the second order, while

$$^1\Delta^0\Delta\bar{\bar{W}}'_{p\mathrm{T}}$$

is a small quantity of the first order in dilute solutions for the case of solutions following the theory of Debye and Hückel. From equations (6)

$$\left.\begin{aligned} d\mathrm{H}_{p\mathrm{T}}&=\delta\mathrm{W}'_{p\mathrm{T}}+\mathrm{T}\,d\mathrm{S}_{p\mathrm{T}},\\ d\mathrm{E}_{p\mathrm{T}}&=\delta\mathrm{W}'_{p\mathrm{T}}+\mathrm{T}\,d\mathrm{S}_{p\mathrm{T}}-p\,d\mathrm{V}_{p\mathrm{T}},\\ d\mathrm{H}_{\mathrm{vT}}&=\delta\mathrm{W}'_{\mathrm{vT}}+\mathrm{T}\,d\mathrm{S}_{\mathrm{vT}}+\mathrm{V}\,dp_{\mathrm{vT}},\\ d\mathrm{E}_{\mathrm{vT}}&=\delta\mathrm{W}'_{\mathrm{vT}}+\mathrm{T}\,d\mathrm{S}_{\mathrm{vT}}, \end{aligned}\right\} \quad . \quad . \quad . \quad (27)$$

and from these, by integration,

$$\left.\begin{aligned} \Delta\mathrm{H}_{p\mathrm{T}}&=\Delta\mathrm{E}_{p\mathrm{T}}+p\Delta\mathrm{V}_{p\mathrm{T}},\\ \Delta\mathrm{H}_{\mathrm{vT}}&=\Delta\mathrm{E}_{\mathrm{vT}}+\mathrm{V}\Delta p_{\mathrm{vT}}, \end{aligned}\right\} \quad . \quad . \quad . \quad . \quad (28)$$

and

$$\Delta\mathrm{H}_{\mathrm{vT}}=\Delta\mathrm{H}_{p\mathrm{T}}+\int_{p}^{p+\Delta p_{\mathrm{vT}}}\mathrm{V}\,dp^*_{\mathrm{T}}+\int_{p}^{p+\Delta p_{\mathrm{vT}}}\mathrm{T}\,d\mathrm{S}^*_{\mathrm{T}}, \quad (29)$$

$$\Delta\mathrm{E}_{p\mathrm{T}}=\Delta\mathrm{E}_{\mathrm{vT}}-\int_{\mathrm{v}}^{\mathrm{v}+\Delta\mathrm{v}_{p\mathrm{T}}}p\,d\mathrm{V}^*_{\mathrm{T}}-\int_{\mathrm{v}}^{\mathrm{v}+\Delta\mathrm{v}_{p\mathrm{T}}}\mathrm{T}\,d\mathrm{S}^*_{\mathrm{T}}, \quad (30)$$

while

$$\Delta\mathrm{H}_{p\mathrm{T}}-\Delta\mathrm{E}_{\mathrm{vT}}=+p\Delta\mathrm{V}_{p\mathrm{T}}-\int_{\mathrm{v}}^{\mathrm{v}+\Delta\mathrm{v}_{p\mathrm{T}}}p\,d\mathrm{V}^*_{\mathrm{T}}+\int_{\mathrm{v}}^{\mathrm{v}+\Delta_{p\mathrm{T}}}\mathrm{T}\,d\mathrm{S}^*_{\mathrm{T}} \quad . \quad . \quad . \quad (31)$$

$$=\mathrm{V}\Delta p_{\mathrm{vT}}-\int_{p}^{p+\Delta p-}\mathrm{V}\,dp^*_{\mathrm{T}}-\int_{p}^{p+\Delta p_{\mathrm{vT}}}\mathrm{T}\,d\mathrm{S}^*_{\mathrm{T}}. \quad . \quad . \quad . \quad (32)$$

From equation (14), therefore,

$$\Delta\mathrm{H}_{p\mathrm{T}}-\Delta\mathrm{E}_{\mathrm{vT}}=\Delta\mathrm{W}'_{p\mathrm{T}}-\Delta\mathrm{W}'_{\mathrm{vT}}+\int_{\mathrm{v}}^{\mathrm{v}+\Delta\mathrm{v}_{p\mathrm{v}}}\mathrm{T}\,d\mathrm{S}^*_{\mathrm{T}}. \quad (33)$$

In dilute solutions if $\Delta\bar{\bar{\mathrm{G}}}$ refer to the alteration of any property by making a definite change in the fields of force of a gram molecule of solute particles, $\Delta\bar{\bar{\mathrm{G}}}$ always tends

to a definite limiting value as the dilution is increased by addition of solvent. In the limit $\Delta\bar{\bar{W}}'_{pT}-\Delta\bar{\bar{W}}'_{vT}$ has been shown to vanish by expression (23), but expression (33) shows that in general this is not the case for $\Delta H_{pT}-\Delta\bar{E}_{vT}$, which tends to a value

$$T\left(\frac{\partial s}{\partial V}\right)_T \Delta\bar{\bar{V}}_{pT}=T\left(\frac{\partial p}{\partial T}\right)_V \Delta\bar{\bar{V}}_{pT}.$$

IV. *The Process of Dilution.*

Consider two solutions, A and B, whose pressures, temperatures, volumes, internal energies, and heat contents are denoted by p_A, p_B, T_A, T_B, V_A, V_B, E_A, E_B, H_A, and H_B respectively. Let these two solutions be irreversibly mixed and allowed to come to a steady state, which is called solution C and whose properties are denoted by the usual symbols together with a suffix C.

A constant pressure dilution is defined as one in which

$$T_A=T_B=T_C \quad \text{and} \quad p_A=p_B=p_C$$

and is supposed to take place without the addition or subtraction of particles to the system. If, therefore, the solutions contain N_1—N_r—N_s gram molecules of sorts 1—r—s, the further conditions

$$N_{rA}+N_{rB}=N_{rC} \quad (r=1, 2, \ldots j \ldots s)$$

must hold for every chemical component of the system. A constant volume dilution is defined by

$$T_A=T_B=T_C, \quad p_A=p_B, \quad V_C=V_A+V_B,$$

and

$$N_{rA}+N_{rB}=N_{rC} \quad (r=1, 2, \ldots j \ldots s).$$

Equations (3) and (4) show that if ∇Q_{pT} and ∇Q_{vT} are defined as the heat absorbed on constant pressure and constant volume dilution respectively so that they are equal but of opposite sign to the heats of dilution,

$$\nabla Q_{pT}=[H_C]_{pT}-H_A-H_B, \quad . \quad . \quad . \quad (34)$$

$$\nabla Q_{vT}=[E_C]_{vT}-E_A-E_B. \quad . \quad . \quad . \quad . \quad (35)$$

In general, let ∇G_{XY} refer to a process of dilution at X and Y constant, where $X_A=X_B=X_C$ if X is any intensive property of the system that is independent of its

bulk and where $X_A+X_B=X_C$ if X is an extensive property that is directly proportional to the total quantity of the system. Furthermore, when comparing any two ∇G's let it be assumed that the two initial solutions were the same in each case. Then if G itself is an extensive property,

$$\nabla G_{XY}=[G_C]_{XY}-G_A-G_B, \quad . \quad . \quad . \quad (36)$$

where $[G_C]_{XY}$ refers to G for solution C after a process of mixing at X and Y constant.

V. *Heat and Volume Changes on Dilution of Perfect Solutions.*

The further analysis of equations (34) to (36) involves the properties of perfect solutions which in turn have to be discussed in terms of partial molal derivatives. If L denotes any property of a system and is, therefore, an extensive property of the system, it may be shown [5] that

$$L=\sum_1^s N_r\bar{L}_r, \quad . \quad . \quad . \quad . \quad . \quad . \quad (37)$$

where the system consists of N_1-N_s moles of sorts $1-r-s$ where the partial molal L or r in the system, $\bar{L}_r$, is defined by

$$\bar{L}_r\equiv\left(\frac{\partial L}{\partial N_r}\right)_{pTN_kW'}, \quad . \quad . \quad . \quad . \quad . \quad (38)$$

the suffix N_k showing that all the N's, other than N_r, are kept constant.

Equation (36) can, therefore, be transformed into

$$\nabla G_{XY}=\left[\sum_1^s N_{rC}\bar{G}_{rC}\right]_{XY}-\left[\sum_1^s N_{rA}\bar{G}_{rA}\right]$$
$$-\left[\sum_1^s N_{rB}\bar{G}_{rB}\right] \quad (r=1, 2\ldots j\ldots s). \quad (39)$$

This equation reduces to $\nabla G_{XY}=0$, provided

$$\left[\bar{G}_{rC}\right]_{XY}=\bar{G}_{rA}=\bar{G}_{rB}$$

for every component, owing to the fact that

$$N_{rC}=N_{rA}+N_{rB}$$

for each component. For perfect solutions it is easy to show that H_r, $\bar{V}_r$, and $\bar{E}_r$ are independent of the dilution provided the dilution be one at constant pressure and temperature and, therefore, that ∇H_{pT}, ∇V_{pT}, and ∇E_{pT} are all equal to zero.

Thus in ordinary solutions

$$\bar{F}_1 = F_1^0(pT) + RT \ln x_1 + RT \ln x\xi_1 \quad \underset{x_1 \to 1}{\text{Lt}}\ \xi_1 = 1, \qquad (40)$$

$$\bar{F}_r = \bar{F}_r^0(pt) + RT \ln x_r + RT \ln \xi_r \quad \underset{xr \to 0}{\text{Lt}}\ \xi_r = 1 \quad (r = 2, 3, \ldots j \ldots s),$$

where component 1 is the solvent, $\bar{F}_j$ denotes the partial molal free energy of j in the system, x_j denotes the mole fraction of it in the system, and ξ_j is an activity coefficient which is made to satisfy the given conditions by assigning a suitable value to the arbitrary constant $\bar{F}_j^0(pT)$ which for a given solvent is a function only of the temperature and the pressure. For these solutions it may be shown [6] that

$$\bar{H}_1^{x_1=1} - \bar{H}_1^{x_1} = RT^2 \left(\frac{\partial \ln \xi_1}{\partial T} \right)_{pN}, \qquad (41)$$

$$\bar{H}_r^{x_r=0} - \bar{H}_r^{x_r} = RT\xi \left(\frac{\partial \ln \xi_r}{\partial T} \right)_{pN} \quad (r = 2, 3 \ldots j \ldots s), \qquad (41)$$

$$\bar{V}_1^{x} - \bar{V}_1^{x_1=1} = RT \left(\frac{\partial \ln \xi}{\partial p} \right)_{TN}, \qquad (43)$$

$$\bar{V}_r^{x_r} - \bar{V}_r^{x_r=0} = RT \left(\frac{\partial \ln \xi_r}{\partial p} \right)_{TN} \quad (r = 2, 3 \ldots j \ldots s). \qquad (44)$$

For a perfect solution, ξ_1 and all the ξ_r are by definition equal to unity, so that their logarithms vanish and all the terms on the left of equations (41) to (44) become zero at all concentrations which proves the proposition. Having chosen standard states in this way, the solution need only be a dilute one, in which it tends to perfection on account of its dilution, and the results $\nabla H_{pT} = 0$ and $\nabla V_{pT} = 0$ will still hold in the dilute region. The result $\nabla E_{pT} = 0$ follows at once since $H = E + pV$, and therefore $\bar{H} = \bar{E} + p\bar{V}$. If $\bar{H}$ and $\bar{V}$ are independent of the concentration and p is made so by diluting at constant pressure,

then $\overline{E}$ must also be independent of the dilution. Another way of looking at the process of dilution of perfect solutions is that $\nabla V_{pT}=0$, and therefore equals ∇V_{vT}. In consequence $\nabla p_{vT}=0$ and ∇G_{pT} and ∇G_{vT} refer to the same process.

VI. *The Effects of Intermolecular Fields of Force on Heats of Dilution.*

For imperfect solutions the heat of dilution at constant pressure may be calculated from equations (39) to (44), but it can also be calculated from the following process:—

(*a*) Reduce the fields of force on the solute molecules in solution A at molar fraction ${}^1x_r$, until they form a perfect solution. This process is to take place at constant pressure and temperature. The work required for this process is ${}^1x_r \Delta W_{pT}$ and the change in heat content is ${}^1x_r \Delta H_{pT}$.

(*b*) To the perfect solution so formed add the requisite amount of solvent at pressure p and temperature T, and perform a constant pressure dilution to molar fraction of solute ${}^2x_r$. A constant pressure dilution of a perfect solution is one in which $\nabla H_{pT}=0$.

(*c*) Restore reversibly the solute fields of force at constant pressure and temperature. At this stage the heat change is ${}^2x_r \Delta H_{pT}$.

The result of processes (*a*), (*b*), and (*c*) is at constant pressure dilution of the solution, and the total heat change is given by

$$\nabla Q_{pT}=\nabla H_{pT}={}^1x \Delta H_{pT}-{}^2x \Delta H_{pT}={}^1\Delta^2 \Delta H_{pT}. \quad (45)$$

In the case of heats of constant volume dilution, the calculation must be performed indirectly because the solutions, after the requisite portion of the fields of force round the solute molecules has been removed, will no longer be at the same pressure in the case of the removal of fields of force at two different dilutions, and neither will they be at the same pressure as the solvent, which must be at the initial pressure of the stronger solution.

∇Q_{vT} equals ∇E_{vT}, and this must be calculated by first calculating ∇E_{pT}, which is the change in E of the system on a constant *pressure* dilution. And then finding the change in E that accompanies the subsequent compressional process to restore the condition of constant

volume. Considering a cycle similar to that used for deducing equation (45), it is evident that

$$\nabla E_{pT} = {}^1\Delta\,{}^2\Delta E_{pT} \quad . \quad . \quad . \quad . \quad . \quad (46)$$

and

$$\nabla V_{pT} = {}^1\Delta\,{}^2\Delta V_{pT}; \quad . \quad . \quad . \quad . \quad (47)$$

furthermore,

$$\nabla E_{vT} = \nabla E_{pT} + \int_{v_A + v_B}^{v_A + v_B + \nabla v_{pT}} \left(\frac{\partial E}{\partial \bar{V}}\right)_T^{**} dV_T^{**}, \quad (48)$$

where the double asterisk shows that the integral represents a process performed on the solution C after dilution and with the molecules possessing their normal fields of force. But

$$\left(\frac{\partial E}{\partial V}\right)_T = -p - T\left(\frac{\partial p}{\partial \bar{V}}\right)_T \left(\frac{\partial V}{\partial T}\right)_p, \quad . \quad . \quad . \quad (49)$$

so that

$$\nabla E_{vT} = \nabla E_{pT} + \int_{v_A + v_B}^{v_A + v_B + \nabla v_{pT}} \left[p + T\left(\frac{\partial p}{\partial T}\right)_T \left(\frac{\partial V}{\partial \bar{T}}\right)_p\right]^{**} dV_T^{**}. \quad . \quad . \quad . \quad (50)$$

From equations (28), (45), (46), and (50),

$$\nabla E_{vT} = \nabla H_{pT} - p\nabla V_{pT} + \left[\int p\, dV_T^{**} + \int T\left(\frac{\partial p}{\partial V}\right)_T \left(\frac{\partial V}{\partial T}\right)_p dV_T^{**}\right]_{T_A + v_B}^{v_A + v_B + \nabla v_{pT}}. \quad . \quad . \quad . \quad (51)$$

In dilute solutions the integrands may be assumed to approximate to constancy throughout the integration process, so equation (51) reduces to

$$\nabla E_{vT} = \nabla H_{pT} + T\left(\frac{\partial p}{\partial \bar{V}}\right)_T \left(\frac{\partial V}{\partial \bar{T}}\right)_p \nabla V_{pT}. \quad . \quad (52)$$

From equations (52), (47), and (19), it follows that

$$\nabla E_{vT} = \nabla H_{pT} + T\left(\frac{\partial\, {}^1\Delta\,{}^2\Delta W'_{pT}}{\partial V}\right)_T \left(\frac{\partial V}{\partial \bar{T}}\right)_p \quad . \quad (53)$$

for dilute solutions. For these solutions if

$$\frac{{}^1\Delta\,{}^2\Delta \bar{\bar{W}}'_{pT}}{T}$$

be denoted by Z,

$$\nabla\bar{\bar{H}}_{pT} = -T^2\left(\frac{\partial Z}{\partial T}\right)_p, \quad . \quad . \quad . \quad . \quad (54)$$

since

$$\left(\frac{\partial F/T}{\partial T}\right)_p = -\frac{H}{T^2},$$

as may be shown from equations (6) ; while

$${}^1\Delta^2\Delta W'_{pT} = {}^1\Delta^2\Delta F_{pT} \quad \text{and} \quad {}^1\Delta^2\Delta H_{pT} = \nabla H_{pT}$$

from equation (45).

Thus

$$\begin{aligned}\nabla\bar{\bar{E}}_{vT} &= -T^2\left(\frac{\partial Z}{\partial T}\right)_p + T^2\left(\frac{\partial Z}{\partial V}\right)_T\left(\frac{\partial V}{\partial T}\right)_p \\ &= -T^2\left[\left(\frac{\partial Z}{\partial T}\right)_p - \left(\frac{\partial Z}{\partial V}\right)_T\left(\frac{\partial V}{\partial T}\right)_p\right] \\ &= -T^2\left(\frac{\partial Z}{\partial T}\right)_v. \quad . \quad . \quad . \quad . \quad . \quad . \quad . \quad . \quad (55)\end{aligned}$$

Equation (55) is the equation that was employed by Gatty [2] in order to get the expression (vii. *a*) in his paper, and is seen to be justified. In dilute solutions, therefore,

$$\begin{aligned}\nabla\bar{\bar{E}}_{vT} - \nabla\bar{\bar{H}}_{pT} &= T^2\left(\frac{\partial Z}{\partial V}\right)_T\left(\frac{\partial V}{\partial T}\right)_p \quad . \quad . \quad (56) \\ &= -T^2\left(\frac{\partial Z}{\partial p}\right)_T\left(\frac{\partial p}{\partial T}\right)_v.\end{aligned}$$

From the definitions for the ${}^1\Delta^0\Delta$G's and expression (23), the term

$$[{}^1\Delta^0\Delta\bar{\bar{W}}'_{pT} - {}^1\Delta^0\Delta\bar{\bar{W}}'_{vT}]$$

is always less than a quantity that varies directly as the first power of the concentration and further, if Z′ denote

$$\frac{{}^1\Delta^2\Delta\bar{\bar{W}}'_{vT}}{T},$$

it is evident from equations (6) and (7) that

$${}^1\Delta^2\Delta E_{vT} = -T^2\left(\frac{\partial Z'}{\partial T}\right)_v. \quad . \quad . \quad . \quad (57)$$

Thus for dilute solutions where $Z-Z'$ is a second order small quantity (that is to say, varies as the concentration)

$$[\nabla\bar{\bar{E}}_{vT}-{}^1\Delta^0\Delta\bar{\bar{E}}_{vT}]$$

is a small quantity of the second or some higher order from equations (55) and (57).

Debye and Hückel calculated ${}^1\Delta^0\Delta W'_{eT}$ for the reversible isothermal work for simultaneously charging the ions of a solution at the mole fractions of solute ${}^1x_2$ and zero. They give

$$\left.\begin{aligned} {}^1x_2\Delta W'_{eT} &= \sum_1^s \int_0^{{}^1} \frac{N_r z_r \epsilon^2}{a_r D} \cdot \lambda d\lambda + \sum_1^s \int_0^{{}^1} \frac{N_r z_r \epsilon^2}{D} \cdot \kappa \cdot \lambda^2 d\lambda \\ \text{and} \\ {}^0\Delta W'_{eT} &= \sum_1^s \int_0^{{}^1} \frac{N_r z_r \epsilon^2}{a_r D} \cdot \lambda d\lambda, \end{aligned}\right\} \quad (58)$$

where the solution contains $N_l \ldots N_r \ldots N_s$ moles of sorts $1 \ldots r \ldots s$ (and N_0 of solvent), carrying charges $z_1\epsilon \ldots z_r\epsilon \ldots z_s\epsilon$, where $-\epsilon$ denotes the charge on a negative electron. The calculation for ${}^0\Delta W'_{eT}$ is not supposed to be free from error, but the errors are assumed to cancel out by subtraction when an expression for ${}^1\Delta^0\Delta W'_{eT}$ is calculated The radius of the ionic atmosphere is given by $1/\kappa$, where

$$\kappa^2 = \frac{4\pi\epsilon^2}{RT} \frac{\Sigma N_r z_r{}^2}{DV},$$

where V denotes the volume of the solution, and D the dielectric constant of the pure solvent under the given conditions of temperature and pressure. This method of integration corresponds, in theory, to building up the charges on the ions by a method such that at any instant T the charge on all the ions of a given species is a fraction λ of its final value. Debye and Hückel then integrate these expressions at constant D, a_r, and V. For ${}^0\Delta W'_{eT}$ this procedure is justifiable, but at the finite concentration ${}^1x_2$ this is not possible. Thus ${}^1x_2\Delta W_{eT}$ is neither strictly a ${}^1x_2\Delta W'_{vT}$ nor a ${}^1x_2\Delta W'_{pT}$ term. If it is decided to integrate at constant volume and temperature both integrals in the expression for ${}^1x_2\Delta W'_{eT}$ will be affected by the small pressure change and its corresponding effect upon the dielectric constant D, which is

here assumed to be independent of the concentration of the electrolyte. If the integration is at p and T, constant D and the a_r will presumably vary still to a lesser extent, but κ will also alter its value, because κ varies as the reciprocal of the square root of the volume. For either process of integration fractional changes in D, κ, and possibly also the a_r are proportional to the first power of the concentration, so that ${}^{1}x_2\Delta W'_{eT}$, which tends to a limiting value ${}^{0}\Delta W'_{eT}$, will differ from ${}^{1}x_2\Delta W'_{pT}$ and ${}^{1}x_2\Delta W'_{vT}$, which both tend to the same value ${}^{0}\Delta W'_{eT}$ at low concentrations, by a quantity that varies as the concentration and which is therefore said to be small to the second order.

Debye and Hückel give

$$ {}^{1}\Delta^{0}\Delta W'_{eT} = \frac{\Sigma N_r z_r^2 \epsilon^2}{3D} \cdot \kappa, $$

where κ varies as the square root of the concentration. Therefore, denoting

$$ \frac{{}^{1}\Delta^{0}\Delta\overline{\overline{W}}'_{pT}}{T}, \quad \frac{{}^{1}\Delta^{0}\Delta\overline{\overline{W}}'_{vT}}{T}, \quad \text{and} \quad \frac{{}^{1}\Delta^{0}\Delta\overline{\overline{W}}'_{eT}}{T}, $$

respectively by Z, Z′, Z_e, the results of this paper as applied to dilute solutions of electrolytes, following Debye and Hückel's simple theory, may be summarized as follows :—

(1) Z—Z′ is a small quantity of the second order from expression (23) and the definition of the $\Delta\Delta$ symbols.

(2) Z and Z′ both differ from Z_e by a small quantity of the second order.

(3) Z_e is a small quantity of the first order.

(4) $$ T\left(\frac{\partial Z}{\partial p}\right)_T = {}^{1}\Delta^{0}\Delta\overline{\overline{V}}_{pT} = {}^{1}\nabla^{0}\overline{\overline{V}}_{pT}. $$

(5) $T\left(\frac{\partial(Z_e-Z)}{\partial p}\right)_T$ must be small to the second or a higher order, since Z_e—Z is small to the second order.

(6) $T\left(\frac{\partial Z_e}{\partial p}\right)_T$ is small to the first order. Therefore, ${}^{1}\nabla\,{}^{0}V_{pT}$ is small to the first order.

(7) $-T\left(\frac{\partial Z'}{\partial V}\right)_T = +{}^1\Delta^0\Delta p_{VT} = +{}^1\nabla^0 p_{VT}$, and this has been shown to be a small quantity of the second order by equation (22).

(8) $-T^2\left(\frac{\partial Z}{\partial T}\right)_p = {}^1\Delta^0\Delta\bar{\bar{H}}_{pT} = {}^1\nabla^0\bar{\bar{H}}_{pT}$, and is a small quantity of the first order since $-T^2\left(\frac{\partial Z_e}{\partial T}\right)_p$ is of the first order and differs from it by a term that is of the second order or is smaller still.

(9) $-T^2\left(\frac{\partial Z}{\partial T}\right)_v = {}^1\nabla^0\bar{\bar{E}}_{VT}$;

$-T^2\left(\frac{\partial Z_e}{\partial T}\right)_v$ is of the first order;

$-T^2\left(\frac{\partial Z'}{\partial T}\right)_v = {}^1\Delta^0\Delta\bar{\bar{E}}_{VT}$.

(10) Therefore ${}^1\nabla^0\bar{\bar{E}}_{VT} - {}^1\Delta^0\Delta\bar{\bar{E}}_{VT}$ is small to the second or some higher order.

(11) $\nabla\bar{\bar{H}}_{pT} - \nabla\bar{\bar{E}}_{VT} = T^2\left(\frac{\partial Z}{\partial p}\right)_T\left(\frac{\partial p}{\partial T}\right)_v$, and this by (4), (5), and (6) may be shown to be a small quantity of the first order.

Throughout this paper terms which vary directly as the concentration have been considered to vanish at low concentrations by comparison with the terms that vary as the square root of the concentration. The actual dilutions at which this procedure becomes justifiable depend on the numerical coefficients of the terms. The Debye and Hückel values of these coefficients have already been examined in a former paper [2], which showed that volume terms were not negligible. For heat changes an inspection of the Debye formulæ shows at once that the terms that are independent of the concentration are the same as those for the corresponding work terms except for a factor of the order of unity. Thus the procedure of neglecting terms that vary as the concentration by comparison with terms that vary as the square root of the concentration is justified.

Summary.

An apparent paradox in the theory of heats of dilution of electrolytes that obey the Debye-Hückel formulæ is investigated. A number of terms become small in dilute solutions in proportion to the square root of the concentration and others become small in proportion to the concentration The various heat and volume changes on dilution and on discharging the ions are classified according to which of the above classes contains them. The methods here developed are applicable to the general problem of molecular interaction and not merely to the fields of force round electrically-charged ions.

References.

(1) Bjerrum, *Zeit. f. Phys. Chem.* cix. p. 145 (1926).
(2) Gatty, Phil. Mag. (7) xi. p. 1082 (1931).
(3) Debye and Hückel, *Phys. Zeit.* xxiv. p. 185 (1923).
(4) Guggenheim, private communication.
(5) Lewis and Randell, 'Thermodynamics' (McGraw Hill).
(6) Macfarlane and Gatty, Phil. Mag. (7), xiii. p. 283 (1932).

Rothamsted Experimental Station.

IV. *The Surface Resistivity of Adsorbed Moisture Films on Glazed Porcelain.* *By* F. W. Johnson, *B.Sc.**

Introduction.

UNDER normal atmospheric conditions most solid insulating surfaces have the property of retaining an invisible yet electrically conducting film of moisture, the nature of which depends on the material of the surface. This film is stable under normal conditions, and, therefore, is in equilibrium with the water-vapour molecules present in the surrounding air, although there must be constantly a transference of moisture from the surface film to the air by evaporation, that is balanced by an equal number of molecules returning to the surface by condensation or deposition. The mass of the film is, therefore, a function of the humidity. In all electrical measurements, especially when high-tension voltages are used, these films are of great importance, and, where a high order of accuracy is required, insulating materials must be used on which

* Communicated by Prof. W. M. Thornton, O.B.E., D.Sc.

such films do not form. This is particularly the case in the measurements of volume resistivity of insulating materials, the capacity of condensers, voltage by flash-over between spheres, and in methods where the charging of a condenser is used to measure either current or voltage.

The value of the resistivity of the film on any surface is dependent on the humidity, the type of surface, and upon the state of the surface. The influence of the film can only be reduced by having the surface as clean as possible, a maximum length of leakage path, and the atmosphere in which measurements are taken as dry as possible, although the application of certain paints and varnishes to the surface greatly increases the resistivity of the leakage path. In high-tension apparatus the presence of this conducting surface on the insulators, as well as producing a leakage current and a loss of power, alters the distribution of stress across the apparatus and tends to give lower break-down or flash-over voltage values.

The most comprehensive study of leakage films on insulating surfaces was made by Curtis *, who examined a large number of substances. He concluded that, in general, the mass of the film on the surface is insufficient to produce the conductivity obtained as a pure film, but that the film was, rather, composed of a solution of the insulator surface in the film. Traces of foreign matter on the surface also dissolve partially in the surface solution, thus producing a further lowering of the resistivity. The first attempt to deduce laws of formation of these films with respect to the humidity was made by Smail, Brooksbank, and Thornton †, who studied the effect of surface temperature, dew-point and air-pressure upon the surface films on glass. They found that the relation between the surface resistivity per square centimetre of the film and the humidity could be expressed as

$$\rho_s = \rho_{s(\alpha)} \epsilon^{k(1-p_a/p_s)^2},$$

where $\rho_{s(\alpha)}$ is the surface resistivity immediately before the dew-point is reached, p_a the actual vapour-pressure to produce the required humidity, and p_s that required to give the saturation value of the air at the same temperature. They also found that at all humidities there is a

* 'Bulletin of the Bureau of Standards,' 1915.
† J. I. E. E. lxix. (1931).

very sharply defined critical pressure above which the resistivity falls as the pressure rises, and below which both fall together. The change of resistivity with respect to the surface temperature at one humidity was found to be exponential in form. Near the dew-point the film became unstable, and very marked and definite changes occurred. From the exponential character of the laws of formation and change the authors concluded that the film was wholly or partially of an adsorbed nature.

The above researches were confined to low-tension direct current, and no attempt was made to measure the change in resistivity produced by contamination of the surface or by the influence of the applied voltage. The laws of formation of adsorbed moisture films on solids have never been derived or measured except by these electrical methods. Since high-tension alternating fields are usual in practice, the work was continued, essentially by the same method, but with the apparatus reconstructed, using high-tension alternating current with a glazed porcelain specimen. The changes of resistivity with respect to the time of application of the voltage and the humidity were studied, and gave rise to exponential functions similar to those previously derived. The nature of the laws of formation and change of the film under these conditions indicates that it is very complex and probably of two parts, one adsorbed and the other a surface solution. This is in agreement with the conclusions of previous workers. The nature of the adsorbed film depends upon the nature of the insulator surface, while the surface solution depends upon the materials of the surface soluble in the film, and is a saturated solution. It must be so, since the mass of the soluble matter is greatly in excess of the solvent. The experimental work is always lengthy when dealing with films of this nature owing to the length of time taken for the solution state to be established, and often a period of over a week must be allowed in order that the film may reach its equilibrium state. The account given is only a brief survey of the results obtained on one porcelain specimen.

Experimental Results on Glazed Porcelain.

The investigation was carried out on alternating current, using a constant applied potential of 3000 volts,

obtained from a transformer connected to an 80 cycle supply, so that there was little, if any, electrolytic action. The electrodes, of fine tinned-copper wire, were placed on a tubular specimen of glazed porcelain, which was very carefully cleaned. The capacity of the specimen was made as low as possible by placing an earthed sheath inside the tube, a device which also served to reduce to a minimum the error due to the volume resistivity. The measurements were made by an electrometer connected in series with the specimen on the earthed side. The electrical arrangement is shown in fig. 1.

Fig. 1.

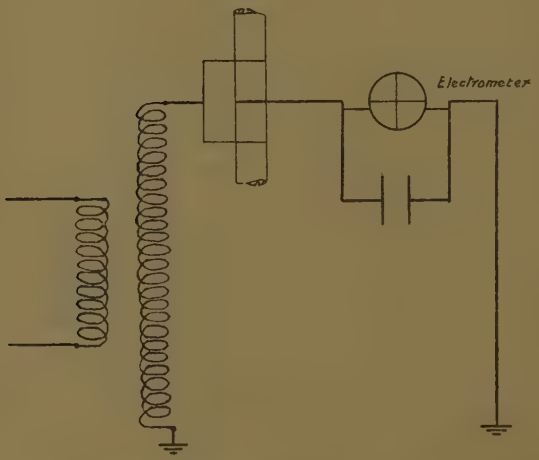

By this arrangement the change of resistivity of the surface film could be readily observed over a period of time varying between one and two hours ; the formation of corona on the electrodes was shown by the rapid deflexion of the electrometer. The method was found to have a limit when the resistivity of the surface reached a value of 10^{11} ohms per centimetre square of surface, due to the fact that the capacity of the specimen could not be reduced below 1 micro-micro-farad. The results were, therefore, confined to humidities between 100 per cent. and 65 per cent. Six surface conditions of the one insulator were examined ; these different surface conditions

were not intentional, but were obtained when attempting to clean the surface after each set of results had been obtained. It is impossible to reproduce exactly the same surface conditions, for when great cleanliness is attempted small impurities have a marked effect on the surface resistivity of glazed porcelain. In one case the surface condition was changed by coating the surface with a solution of sodium sulphate (4 grams in 100 c.c. of distilled water) and allowed to dry.

The humidities were obtained by the sulphuric acid solutions method given by Griffiths *, and a period of

Fig. 2.

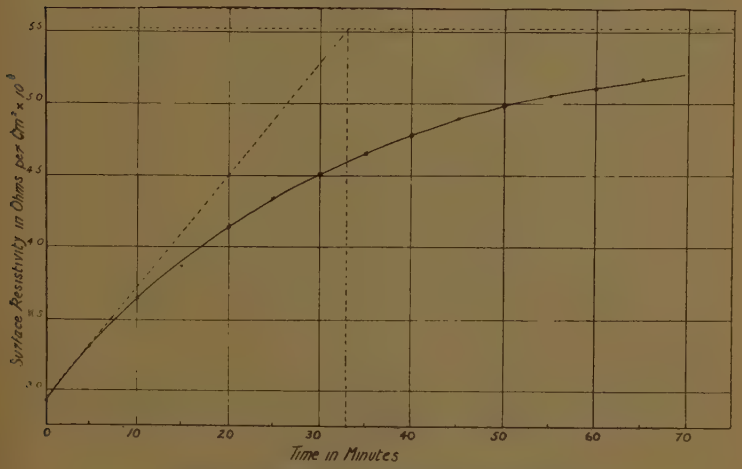

Surface condition (2). Humidity 100 per cent.
Observed change of resistivity with respect to the time of application of the voltage. The initial resistivity is below the critical value. Equation to curve of change (1.2).

several days was allowed to elapse before any readings were taken.

The change of resistivity was observed with the applied voltage constant in all cases for the six different surface conditions. Typical curves connecting the change of resistivity with the time of application of the constant applied voltage are shown in figs. 2 and 3 for two humidities.

* N.P.L. Researches, v. p. 19 (1926).

These curves reveal a new condition of film formation and change. The equations relating the change of resistivity to the time of application of the voltage for any humidity are found to be of the form

$$r = r_0 + (r_\infty - r_0)(1 - \epsilon^{-At}), \quad . \quad . \quad . \quad . \quad (1.2)$$

where r_0 is the resistivity at zero time, that is, before the voltage is applied, and r_∞ is the resistivity finally reached, provided that r_0 was below a certain fixed value. If r_0 was above this value, the change was according to

$$r = r_0 - (r_0 - r_\infty)(1 - \epsilon^{-At}). \quad . \quad . \quad . \quad . \quad (2.2)$$

Fig. 3.

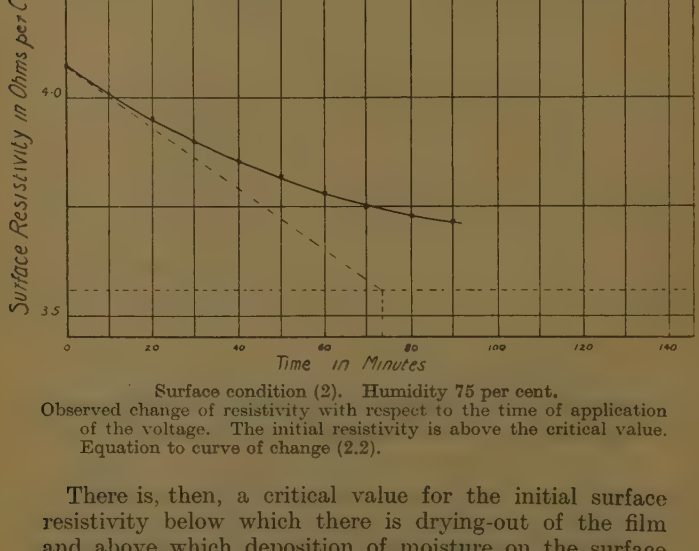

Surface condition (2). Humidity 75 per cent.
Observed change of resistivity with respect to the time of application of the voltage. The initial resistivity is above the critical value. Equation to curve of change (2.2).

There is, then, a critical value for the initial surface resistivity below which there is drying-out of the film and above which deposition of moisture on the surface occurs when a voltage is applied. The effect of contamination of the surface is only to move the critical value to a higher or lower humidity without affecting its actual value.

The indices, A, of these expressions for the change of resistivity are found to be proportional only to the

humidity, and independent of the surface condition. Fig. 4 shows how A varies with the humidity.

The equations relating A to the humidity were found from the curve to be

$$A = A_{100}\epsilon^{-k_4(1-h)}, \quad . \quad . \quad . \quad . \quad . \quad (3.2)$$

where A_{100} is the value of A at 100 per cent. humidity, viz., 0·0303 at 3000 volts (r.m.s.).

Fig. 4.

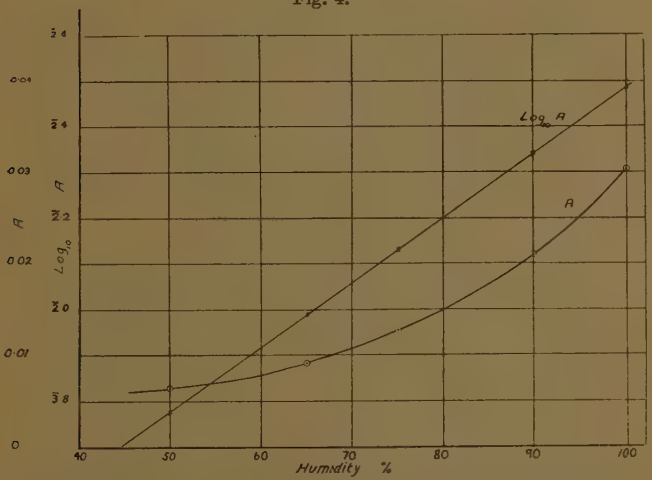

Observed values of the rate of deposition factor A for various humidities when the applied voltage is 3000 volts (r.m.s.).

TABLE I.

Humidity, per cent.	A.	Log_{10} A.
100.....	1/33	$\bar{2}\cdot4814$
90.....	1/45·5	$\bar{2}\cdot3429$
75.....	1/73·5	$\bar{2}\cdot1342$
65.....	1/101	$\bar{2}\cdot9957$
50.....	1/163·5	$\bar{3}\cdot7889$

The values of the initial and final resistivities r_0 and r_∞ respectively, obtained for the six surfaces, are shown in figs. 5*a* and 5*b*. The curves of $\log_{10} r_0$ and $\log_{10} r_\infty$ cross for

Fig. 5*a*.

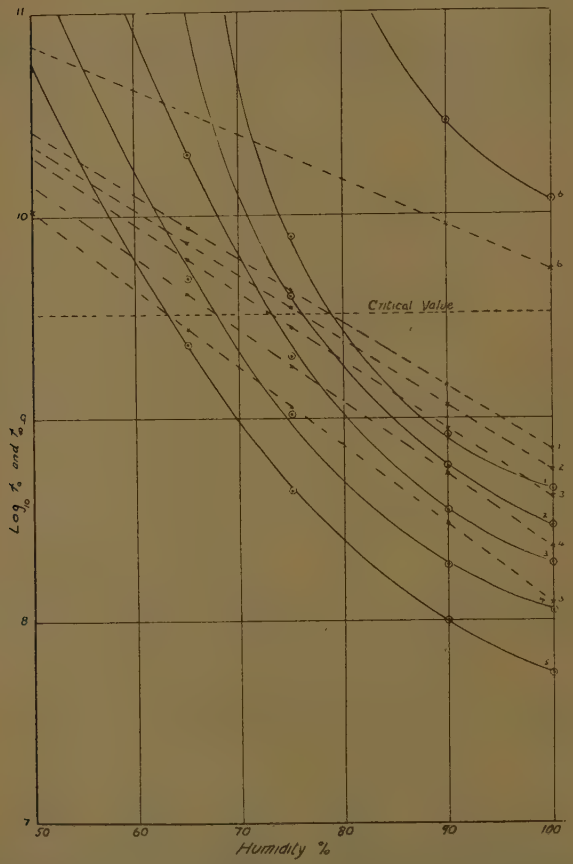

Observed curves of the logarithms (to the base 10) of the initial and final resistivities, r_0 and r_∞, to a base of humidity. The numerals 1, 2, 3, etc., indicate the different surface conditions. Initial resistivity shown —⊙——⊙—. Final resistivity shown – – × – – – × – –.

each surface condition at the same value of the resistivity, indicating that there is a critical value for the given

specimen at $3{\cdot}25 \times 10^9$ ohms per cm.^{2} It is interesting to note that under all conditions of the surface the value of r_∞ at zero humidity is the same, viz., $9{\cdot}55 \times 10^{11}$

Fig. 5 *b*.

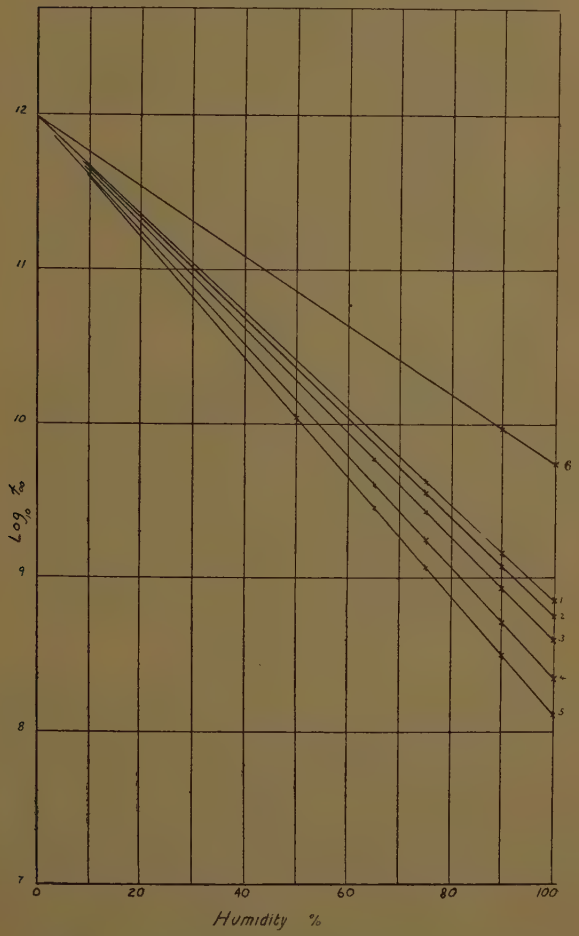

Values of the logarithms (to the base 10) of the final resistivities to a base of humidity.

ohms per cm.^{2} It can be inferred from this that the final resistivity is unaffected by the presence of foreign matter at zero humidity.

TABLE II.

Equations to the Initial Resistivity with respect to the Humidity.

$$\left.\begin{array}{lll}
(1)\ r_0 = 3{\cdot}07\ \epsilon^{[3{\cdot}232(1-h)+0{\cdot}2776\epsilon^{8{\cdot}68(1-h)}]} \times 10^8 & \text{ohms per cm.}^2 & \\
(2)\ r_0 = 2{\cdot}134\epsilon^{[3{\cdot}773(1-h)+0{\cdot}2158\epsilon^{8{\cdot}465(1-h)}]} \times 10^8 & ,, & ,, \\
(3)\ r_0 = 1{\cdot}337\epsilon^{[4{\cdot}173(1-h)+0{\cdot}198\epsilon^{8{\cdot}25(1-h)}]} \times 10^8 & ,, & ,, \\
(4)\ r_0 = 0{\cdot}820\epsilon^{[4{\cdot}723(1-h)+0{\cdot}1759\epsilon^{8{\cdot}0(1-h)}]} \times 10^8 & ,, & ,, \\
(5)\ r_0 = 0{\cdot}403\epsilon^{[5{\cdot}975(1-h)+0{\cdot}1443\epsilon^{7{\cdot}65(1-h)}]} \times 10^8 & ,, & ,,
\end{array}\right\} \quad . \quad . \quad . \quad (4.2)$$

TABLE III.

Equations to the Final Resistivity with respect to the Humidity.

$$\left.\begin{array}{lll}
(1)\ r_\infty = 7{\cdot}08\epsilon^{7{\cdot}206(1-h)} \times 10^8 & \text{ohms per cm.}^2 & \\
(2)\ r_\infty = 5{\cdot}52\epsilon^{7{\cdot}456(1-h)} \times 10^8 & ,, & ,, \\
(3)\ r_\infty = 4{\cdot}02\epsilon^{7{\cdot}769(1-h)} \times 10^8 & ,, & ,, \\
(4)\ r_\infty = 2{\cdot}22\epsilon^{8{\cdot}366(1-h)} \times 10^8 & ,, & ,, \\
(5)\ r_\infty = 1{\cdot}22\epsilon^{8{\cdot}966(1-h)} \times 10^8 & ,, & ,, \\
(6)\ r_\infty = 5{\cdot}40\epsilon^{5{\cdot}174(1-h)} \times 10^9 & ,, & ,,
\end{array}\right\} \quad . \quad (5.2)$$

The Change of Resistivity under the Influence of Voltage.

Under the initial conditions, before the application of the constant voltage, the leakage film is in equilibrium with the mass of the moisture present in the surrounding air. When the voltage is applied to the film, a current passes, heating it and causing evaporation, in proportion to the amount of energy dissipated. This evaporation disturbs the equilibrium state previously attained, and there is also an attraction due to the presence of the electrostatic field between the moisture present on the surface and the molecules of water vapour in the surrounding air. The theory of this is as follows.

Consider one square centimetre of the surface situated so that the current-flow across it is uniform between any two opposite sides. Let the total mass of the moisture on this unit-surface area be m, the resistance of the film between the two given sides be r, the density per cm.^{3} be σ, the resistivity per cm.^{3} be ρ, the thickness of the film be s, and the potential applied between the two sides be e.

The resistance r of the film, is given in terms of the mass m present on the surface by

$$r=\rho.\frac{l}{a}=\rho\frac{1}{s}=\rho\frac{1}{\overline{V}}=\rho\sigma\frac{1}{m}, \quad . \quad . \quad . \quad (1.3)$$

and since the area of the film considered is one square centimetre, r is the resistivity per cm.^{2} of the film, and is called the " surface resistivity."

The energy dissipated in the film is $\frac{e^2}{r}$ and the rate of evaporation will be $K\frac{e^2}{r}$ per unit mass of moisture on the surface. The factor K is dependent on the state of the film and upon the vapour-pressure of the surrounding air, that is, upon the humidity. If the state of the surface remains constant, the factor K is dependent only upon the humidity. At the maximum humidity, when the fractional humidity as represented by h equals unity, the rate of evaporation factor is a minimum equal to some value K_{100}. If the humidity is changed from its maximum value to some other value h, the change in K produced with respect to the humidity is

$$\frac{dK}{dh}=K_{100}(1-h)k_1,$$

where, when $h=1$, $K=K_{100}$, and there is 100 per cent. humidity.

The solution of this equation is

$$K=K_{100}\epsilon^{k_1(1-h)}. \quad . \quad . \quad . \quad . \quad . \quad (2.3)$$

The rate of deposition of moisture per unit mass of moisture on the surface will be proportional to the humidity, and for any given humidity will be constant for one particular potential applied to the film, since the quantity of water-vapour molecules available for deposition is proportional only to the humidity. The state of the

surface or the mass of the film can have no effect on the rate of deposition per unit mass of the film, since it only serves to hold the attracting charge. The deposition will occur, therefore, at a constant rate A per unit mass of moisture on the surface for a given value of the humidity and applied potential. If at the initial point the humidity is at saturation value, that is, $h=1$, A is a maximum, and may be represented by A_{100}. If the change of humidity is considered as being from this point to a fractional value h, the rate of change of A with respect to the humidity will be

$$\frac{dA}{dh} = -A_{100}(1-h)k_2,$$

where, when $h=1$, $A=A_{100}$, and there is 100 per cent. humidity.

The solution is

$$A=A_{100}\epsilon^{-k_2(1-h)}. \quad . \quad . \quad . \quad : \quad . \quad . \quad (3.3)$$

This is in agreement with the equation (3.2) derived from the experimental results.

If the film can be considered as being of two parts, one adsorbed and the other a surface solution of the insulator surface, evaporation must take place initially from the surface solution. This evaporation will disturb the equilibrium state existing between the adsorbed film and the surface solution, and transference of moisture occurs between the two portions of the film in order to maintain the equilibrium state. If the change takes place slowly, the surface solution remains saturated and the relative proportions of the two parts of the film remain constant, that is, the film will not change in type. The conductivity, the density, and the rate of evaporation factor K are constant.

For any given surface condition, under the influence of the constant applied potential, the factors K and A are constant, and the rate of change of the mass m of the film on the unit area with the time of application of the constant applied potential is given by

$$\frac{dm}{dt} = -K\frac{e^2}{r}.m+Am, \quad . \quad . \quad . \quad . \quad (4.3)$$

where ρ, σ, K, A are constant throughout the change; but $r=\rho\sigma.\frac{1}{m}$ by equation (1.3) above, so

$$-\frac{\sigma\rho}{r^2}\cdot\frac{dr}{dt}=\frac{dm}{dt},$$

$$-\frac{\sigma\rho}{r^2}\cdot\frac{dr}{dt}=-\mathrm{K}\frac{e^2}{r}\cdot\frac{\sigma\rho}{r}+\mathrm{A}\frac{\sigma\rho}{r},$$

$$\frac{dr}{dt}=\mathrm{K}e^2-\mathrm{A}r,$$

$$r\epsilon^{\mathrm{A}t}=\mathrm{K}e^2\cdot\frac{1}{\mathrm{A}}\epsilon^{\mathrm{A}t}+\mathrm{C},$$

$$r=\frac{\mathrm{K}e^2}{\mathrm{A}}+\mathrm{C}\epsilon^{-\mathrm{A}t}.$$

If at $t=\infty$, $r=r_\infty$, the final value of the resistivity, then

$$r_\infty=\frac{\mathrm{K}e^2}{\mathrm{A}}, \quad . \quad . \quad . \quad . \quad . \quad . \quad . \quad (5.3)$$

and at $t=0$, $r=r_0$, the initial value of the resistivity before the voltage is applied,

$$r_0=r_\infty+\mathrm{C};$$

therefore

$$r=r_\infty+(r_0-r_\infty)\epsilon^{-\mathrm{A}t},$$

or

$$r=r_0+(r_\infty-r_0)(1-\epsilon^{-\mathrm{A}t}), \quad . \quad . \quad . \quad (6.3)$$

which is in agreement with the equation (1.2) above.

There are three possible cases that may arise :

(*a*) $r_0<r_\infty$, then $\frac{dm}{dt}<0$, since $\mathrm{K}\frac{e^2}{r_0}>\mathrm{A}$.

The rate of evaporation is then greater than the rate of deposition, and drying-out of the surface must occur. The change is then according to

$$r=r_0+(r_\infty-r_0)(1-\epsilon^{-\mathrm{A}t}).$$

(*b*) $r_0=r_\infty$, then $\frac{dm}{dt}=0$, since $\mathrm{K}\frac{e^2}{r_0}=\mathrm{K}\frac{e^2}{r_\infty}=\mathrm{A}$.

There is no change of resistivity, and this is the critical value.

(*c*) $r_0>r_\infty$, then $\frac{dm}{dt}>0$, since $\mathrm{K}\frac{e^2}{r_0}<\mathrm{A}$.

The rate of evaporation is then less than the rate of deposition, and deposition of moisture on the surface occurs and the change in resistivity is according to

$$r = r_0 - (r_0 - r_\infty)(1 - \epsilon^{-At}).$$

The final value of the resistivity r_∞ is attained when a new equilibrium state between the surface film and the surounding air has been reached. Let the state be considered for the saturation value of the humidity, that is, 100 per cent. humidity, then by equation (5.3)

$$r_{\infty_{100}} = \frac{K_{100}}{A_{100}} . e^2 . \quad . \quad . \quad . \quad . \quad . \quad (7.3)$$

If the humidity of the air is changed to a value h, while the film is still under the influence of the constant applied potential when equilibrium is attained, the rate of deposition factor A will have become, by equation (3.3),

$$A_h = A_{100} \epsilon^{-k_2(1-h)},$$

and the rate of evaporation factor K will have become, by equation (2.3),

$$K_h = K_{100} \epsilon^{k_1(1-h)},$$

and the final resistivity will have changed from $r_{\infty_{100}}$ to r_{∞_h}, where again

$$r_{\infty_h} = \frac{K_h}{A_h} . e^2, \quad . \quad . \quad . \quad . \quad (8.3)$$

and, by comparing the equations (7.3) and (8.3),

$$r_{\infty_{100}} = \frac{K_{100}}{A_{100}} . e^2,$$

$$r_{\infty_h} = \frac{K_{100} \epsilon^{k_1(1-h)}}{A_{100} \epsilon^{-k_2(1-h)}} . e^2;$$

therefore

$$r_{\infty_h} = r_{\infty_{100}} \epsilon^{(k_1+k_2)(1-h)}. \quad . \quad . \quad (9.3)$$

The final resistivity is, therefore, an exponential function of the humidity, of the form

$$r_\infty = r_{\infty_{100}} \epsilon^{k_3(1-h)}, \quad . \quad . \quad . \quad . \quad . \quad (10.3)$$

where

$$k_3 = k_1 + k_2. \quad . \quad . \quad . \quad . \quad . \quad . \quad (11.3)$$

The equations relating the initial resistivity to the humidity cannot be so derived, and are of a more complex form. The most suitable form found from the experimental results is

$$r_0 = r'_{0_{100}} \epsilon^{\left[k_4(1-h)+Ce^{k_5(1-h)}\right]},$$

where the point $r'_{0_{100}}$ is not the actual value found at 100 per cent. humidity, as indicated in fig. 5, but may be explained from the work of Smail, Brooksbank, and

Fig. 6.

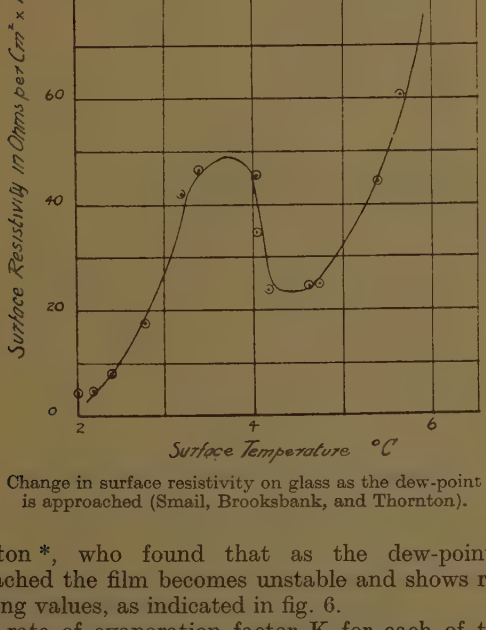

Change in surface resistivity on glass as the dew-point is approached (Smail, Brooksbank, and Thornton).

Thornton *, who found that as the dew-point was approached the film becomes unstable and shows rapidly changing values, as indicated in fig. 6.

The rate of evaporation factor K for each of the six surface conditions may be calculated from the equation (5.3),

$$K\frac{e^2}{r_{\equiv}} = A,$$

* *Loc. cit.*

from the experimental results obtained. The values of $\log_{10} K$ so obtained are shown in fig. 7.

Also from the experimental results Table IV. shows the agreement obtained between the indices of the equations

Fig. 7.

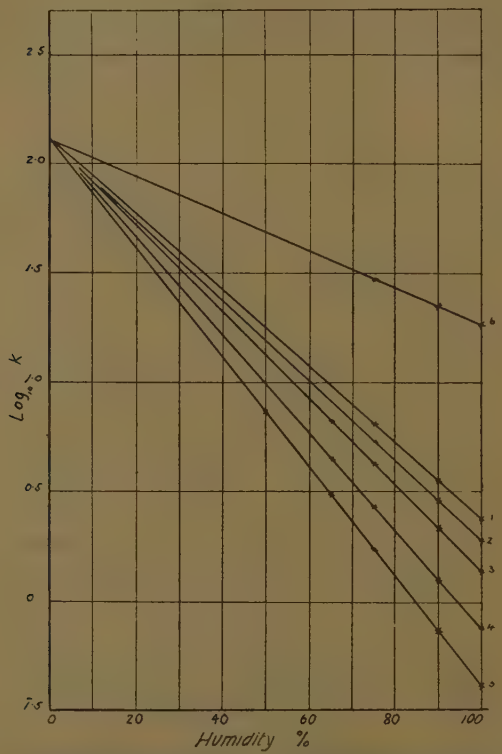

Calculated values of the rate of evaporation factor K for the six surface conditions.

of K, A, and r_∞, with respect to the humidity, as expressed by the equation (11.3).

Surface condition 6 was obtained by using the solution of sodium sulphate.

The good agreement between the figures in the last two columns shows that the exponential forms of the

observed curves of drying and deposition can be regarded as a close approximation to the change of state of moisture films on insulating surfaces.

TABLE IV.

Surface condition.	k_1. Index of K.	k_2. Index of A.	k_1+k_2.	k_3. Index of r_∞.
1	4·017	3·189	7·206	7·206
2	4·257	3·189	7·446	7·456
3	4·582	3·189	7·771	7·769
4	5·169	3·189	8·358	8·366
5	5·776	3·189	8·965	8·966
6	1·963	3·189	5·152	5·174

Conclusion.

From the experimental results there is every indication that the leakage film, if continuous, has two components, one adsorbed and the other a surface solution. Changes in the surface conductivity due to the deposition of foreign matter on to the surface, such as dust, are due to the change in state of the surface solution which is always saturated. The solution must be saturated and the relative proportions of the adsorbed film and the surface solution components must be constant for one humidity in order that the exponential character of the laws of formation and change under the influence of either surface temperature or applied potential is possible. Under these circumstances it follows that a substance that is almost insoluble in the film will have a higher surface resistivity than one that is soluble. Waxy or bituminous substances in which little or no adsorption can take place, and whose surfaces are insoluble in the film, have high surface resistivities, for a continuous film cannot form. In all this work surface tension plays no part. The adsorbed film under the influence of voltage is unstable except after an indefinitely long period, and this, coupled with the fact that the value of the resistivity of the film is so variable, depending on a large number of factors, makes the problem of the complete elimination of the

effects of leakage on any insulating surface a matter of great difficulty. The only practical solution appears to be in the discovery of some paint or varnish with exceptional properties of resisting the formation of these films on its surface. Even in this case, since part of the film is adsorbed and difficult to remove, the surface to be treated with the paint or varnish must be previously dried by heating, or *in vacuo*, as thoroughly as possible.

The research was carried out in the ElectricalEngineering Laboratory at Armstrong College, Newcastle-on-Tyne, and the author wishes to thank Professor Thornton for his constant advice and interest.

V. *Energy, Temperature, and Atomic Weight: A Rapid Interconversion Scale.* By C. H. Douglas Clark, *M.Sc., A.R.C.S., D.I.C., Assistant Lecturer in Chemistry in the University of Leeds* *.

1. *Introduction.*

THE appropriate interrelation of energetic magnitudes is often a matter of considerable importance in modern research. In order to facilitate the necessary interconversions, the author, in an earlier communication [1], has provided the requisite factors for a considerable variety of magnitudes, using the best accredited values of the physical constants concerned (electronic charge, Planck's constant, velocity of light, etc.) at present available. It has occurred to him that it might prove of additional advantage to prepare suitable scales, whereby interconversions might be made with considerable accuracy and at the same time more rapidly than by the intermediate employment of factors. A measure of precedence may, in fact, be claimed for this procedure. Mecke [2] has independently pointed out that a scale of this type has been found very convenient in the rapid determination of spectroscopic energy equivalence in connexion with photochemical reactions. The present author was thereby encouraged to continue with the task he had independently commenced, and it is hoped that the resulting scale, here

* Communicated by Prof. R. Whiddington, D.Sc., F.R.S.

presented, will be found of value in practice in different kinds of research. The interconversion factors will doubtless continue to be used in cases where further accuracy is required.

In a preliminary paper, the author [3] has devised a scale showing the relation between various energetic and related magnitudes over 90 octaves of the electromagnetic wave-band, from the region of very long waves to that of cosmic rays at the other extreme. Interconversions may be made over this range by means of the scale with an accuracy of about 3 per cent. It appears desirable to present another scale for general use, with certain additions detailed in the following paragraph. Moreover, it is found that the accuracy of reading can be materially extended by this means. The present scale applies also to the wave-band, for use as required.

It appears that the results presented earlier (*loc. cit.* [1]) can be made more useful by the introduction of further magnitudes directly or indirectly related to those in which energy may be expressed. It seems desirable to achieve this by (1) consideration of the gas constant, which has energy dimensions; (2) introduction of the conception of temperature corresponding to energy of maximum density; and (3) inclusion of atomic masses on the O=16 scale, with the requisite factors in each of the three cases. Each of these further additions appears to be important in some way or other in connexion with matters which are occupying the attention of investigators at the present time.

2. *The Gas Constant.*

Consideration of the relation between energy and temperature involves knowledge of the gas constant R occurring in the relation $PV=nRT$, where n is the number of (gram-) molecules of gas present in volume V at pressure P and absolute temperature T. Depending on the ways in which P and V are expressed, R (which has energy dimensions) assumes different numerical values. Let **R** represent the value of R in ergs*, **H** in calories, **G** in gram-centimetres, and **L** in litre-atmospheres, per degree of temperature, per gram-molecule of gas,

* Denoted by K in the earlier paper [1].

respectively. Further, let k be the value in ergs per degree per individual molecule (Boltzmann's constant). The relations between these magnitudes are then as follows :—

$$\mathrm{R} = \frac{\mathrm{H}}{10^3 k} = \mathrm{N}\mathrm{k} = g\mathrm{G} = 10^3 dg\mathrm{P}\mathrm{L} \quad . \quad . \quad . \quad (1)$$

where k, N, d, g, and P are constants defined in Table III.

TABLE I.

Interconversion Factors for the Gas Constant and related Magnitudes.

H **CALORIES** per degree per gr.-mol.	$\mathrm{H} = 10^3 k\mathrm{N}\mathrm{k}$ $16{\cdot}1612 + \log \mathrm{k}$ $1{\cdot}449 \times 10^{16}\mathrm{k}$	$\mathrm{H} = 10^3 kg\mathrm{G}$ $\bar{5}{\cdot}3702 + \log \mathrm{G}$ $2{\cdot}345 \times 10^{-5}\mathrm{G}$	$\mathrm{H} = 10^6 \mathrm{P}dgk\mathrm{L}$ $1{\cdot}3843 + \log \mathrm{L}$ $24{\cdot}23\mathrm{L}$
$\mathrm{k} = \frac{1}{10^3 k\mathrm{N}}\mathrm{H}$ $\bar{17}{\cdot}8388 + \log \mathrm{H}$ $6{\cdot}900 \times 10^{-1}\mathrm{H}$	**k** **ERGS** per degree per mol.	$\mathrm{k} = \frac{g}{\mathrm{N}}\mathrm{G}$ $\bar{21}{\cdot}2090 + \log \mathrm{G}$ $1{\cdot}618 \times 10^{-21}\mathrm{G}$	$\mathrm{k} = \frac{10^3 \mathrm{P}dgk}{\mathrm{N}}\mathrm{L}$ $\bar{15}{\cdot}2231 + \log \mathrm{L}$ $1{\cdot}672 \times 10^{-15}\mathrm{L}$
$\mathrm{G} = \frac{1}{10^3 kg}\mathrm{H}$ $4{\cdot}6298 + \log \mathrm{H}$ $4{\cdot}264 \times 10^{4}\mathrm{H}$	$\mathrm{G} = \frac{\mathrm{N}}{g}\mathrm{k}$ $20{\cdot}7910 + \log \mathrm{k}$ $6{\cdot}180 \times 10^{20}\mathrm{k}$	**G** **GRAM-CENTIMETRES** per degree per gr.-mol.	$\mathrm{G} = 10^3 \mathrm{P}d\mathrm{L}$ $6{\cdot}0142 + \log \mathrm{L}$ $1{\cdot}033 \times 10^{6}\mathrm{L}$
$\mathrm{L} = \frac{1}{10^6 \mathrm{P}dgk}\mathrm{H}$ $\bar{2}{\cdot}6157 + \log \mathrm{H}$ $4{\cdot}128 \times 10^{-17}\mathrm{H}$	$\mathrm{L} = \frac{\mathrm{N}}{10^3 \mathrm{P}dg}\mathrm{k}$ $14{\cdot}7769 + \log \mathrm{k}$ $5{\cdot}982 \times 10^{14}\mathrm{k}$	$\mathrm{L} = \frac{1}{10^3 \mathrm{P}d}\mathrm{G}$ $\bar{7}{\cdot}9859 + \log \mathrm{G}$ $9{\cdot}679 \times 10^{-7}\mathrm{G}$	**L** **LITRE-ATMOSPHERES** per degree per gr.-mol.

Table I. is constructed on the same lines as the interconversion table of the earlier paper to show the relationships existing between **H**, **k**, **G**, and **L**. The relation between ergs and calories, previously given, is not included.

In calculating the value of the gas constant, the starting-point is the figure due to Birge [4] $\mathrm{R} = 8{\cdot}3136 \times 10^7$ ergs, or 8·3136 joules per degree per gram-molecule. Using the conversion factor from ergs to calories, $\mathrm{H} = (8{\cdot}314 \times 10^7) \times (2{\cdot}390 \times 10^{-8}) = 1{\cdot}987$ calories per degree per gram-molecule. Further, by the conversion factors of Table I., $\mathrm{G} = 1{\cdot}897 \times (4{\cdot}264 \times 10^4) = 8\,473 \times 10^4$ gram-centimetres, and $\mathrm{L} = 1{\cdot}987 \times (4{\cdot}128 \times 10^{-2}) = 8{\cdot}202 \times 10^{-2}$ litre-atmospheres, per degree per gram-molecule respectively. The value of

the Boltzmann constant then becomes $\mathbf{k}=1{\cdot}987\times(6{\cdot}900\times10^{-17})=1{\cdot}371\times10^{-16}$, which agrees with Birge's estimate $\mathbf{k}=1{\cdot}3709\times10^{-16}$ erg per degree per molecule. A self-consistent set of numbers is thus obtained. Table I. may evidently be used quite generally for gas energy values in the stated units, and need not apply only to the gas constant. The value of **H** may be used as a link with the earlier table.

A further check on the above set of values is provided by evaluating the gram-molecular volume of a gas at N.T.P. This is **L** multiplied by the absolute temperature corresponding to 0° C., or 273·18° K., or $0{\cdot}08202\times273{\cdot}2=22{\cdot}41$ litres. Birge gives 22·414 litres. Agreement is thus obtained within the limits of accuracy used, that attainable by the use of four-figure logarithms.

3. *Energy and Temperature.*

In the theory of temperature radiation, if λ is the wave-length (in Å.U.) of radiant energy of maximum density in a closed space at **T**° K., then (see section 4 of [1]) :—

$$\lambda\mathbf{T}=2{\cdot}884\times10^{7} \quad . \quad . \quad . \quad . \quad . \quad . \quad (2)$$

Further, if **E** is the value of the maximum energy in ergs available at **T**° K.,

$$\mathbf{E}=\frac{\alpha}{\mathbf{N}}\mathbf{RT}=\alpha\mathbf{kT}=a\mathbf{T} \quad . \quad . \quad . \quad . \quad . \quad (3)$$

where α is the solution of the equation $\alpha=5(1-e^{-\alpha})$, whereby $\alpha=4{\cdot}9651$ (accidentally given as 4·9561 in the earlier paper). Inserting the value of the Boltzmann constant **k** obtained in the foregoing section, it follows that the constant a connecting **E** and **T** is given by $a=\alpha\mathbf{k}=4{\cdot}965\times(1{\cdot}371\times10^{-16})=6{\cdot}807\times10^{-16}$ erg per degree per molecule, whilst $\lambda\mathbf{T}$ is given by $10^{8}hc/a$.

When the relation between energy of maximum density and corresponding temperature is included in the other expressions for **E**, as in the equations (4), it becomes possible to construct a table connecting **T** with other energetic magnitudes. This is carried through in Table II. (A). For meaning of symbols, see Tables III. and IV.

The $h\nu$'s here considered correspond to the largest energy quanta available at temperature **T**° K. Conversely, the temperatures are the lowest for which quanta of frequency ν can be produced by heat effects alone.

Table II.

Interconversion Factors between energetic and related Magnitudes and (A) Temperature, (B) Atomic Weight.

A		B	
TEMPERATURE **T** **°K**	$\mathbf{T=(c^2/aN)A}$ $12{\cdot}3379+\log \mathbf{A}$ $2{\cdot}177\times10^{12}\mathbf{A}$	**ATOMIC WEIGHT** **A** **O=16**	$\mathbf{A=(aN/c^2)T}$ $\bar{1}3{\cdot}6621+\log \mathbf{T}$ $4{\cdot}593\times10^{-13}\mathbf{T}$
$\mathbf{J=(a/10^7)T}$ $\bar{2}3{\cdot}8330+\log \mathbf{T}$ $6{\cdot}807\times10^{-23}\mathbf{T}$	$\mathbf{T=(10^7/a)J}$ $22{\cdot}1670+\log \mathbf{J}$ $1{\cdot}469\times10^{22}\mathbf{J}$	$\mathbf{J=(c^2/10^7N)A}$ $\bar{1}0{\cdot}1710+\log \mathbf{A}$ $1{\cdot}483\times10^{-10}\mathbf{A}$	$\mathbf{A=(10^7N/c^2)J}$ $9{\cdot}8290+\log \mathbf{J}$ $6{\cdot}745\times10^{9}\mathbf{J}$
$\mathbf{V=(ac/10^8e)T}$ $\bar{4}{\cdot}6313+\log \mathbf{T}$ $4{\cdot}278\times10^{-4}\mathbf{T}$	$\mathbf{T=(10^8e/ac)V}$ $3{\cdot}3687+\log \mathbf{V}$ $2{\cdot}337\times10^{3}\mathbf{V}$	$\mathbf{V=(c^3/10^8eN)A}$ $8{\cdot}9694+\log \mathbf{A}$ $9{\cdot}320\times10^{8}\mathbf{A}$	$\mathbf{A=(10^8eN/c^3)V}$ $\bar{9}{\cdot}0306+\log \mathbf{V}$ $1{\cdot}073\times10^{-9}\mathbf{V}$
$\mathbf{v=\sqrt{2a/m}T^{\frac{1}{2}}}$ $6{\cdot}0890+\frac{1}{2}\log \mathbf{T}$ $1{\cdot}228\times10^{6}\mathbf{T}^{\frac{1}{2}}$	$\mathbf{T=(m/2a)v^2}$ $\bar{1}3{\cdot}8219+2\log \mathbf{v}$ $6{\cdot}637\times10^{-13}\mathbf{v^2}$	$\mathbf{v=c\sqrt{2/m\bar{N}}A^{\frac{1}{2}}}$ $12{\cdot}2581+\frac{1}{2}\log \mathbf{A}$ $1{\cdot}811\times10^{12}\mathbf{A}^{\frac{1}{2}}$	$\mathbf{A=(mN/2c^2)v^2}$ $\bar{2}5{\cdot}4839+2\log \mathbf{v}$ $3{\cdot}047\times10^{-25}\mathbf{v^2}$
$\mathbf{E=aT}$ $\bar{1}6{\cdot}8330+\log \mathbf{T}$ $6{\cdot}807\times10^{-16}\mathbf{T}$	$\mathbf{T=(1/a)E}$ $15{\cdot}1670+\log \mathbf{E}$ $1{\cdot}469\times10^{15}\mathbf{E}$	$\mathbf{E=(c^2/N)A}$ $\bar{3}{\cdot}1710+\log \mathbf{A}$ $1{\cdot}483\times10^{-3}\mathbf{A}$	$\mathbf{A=(N/c^2)E}$ $2{\cdot}8290+\log \mathbf{E}$ $6{\cdot}745\times10^{2}\mathbf{E}$
$\mathbf{H=10^3akT}$ $\bar{2}3{\cdot}2114+\log \mathbf{T}$ $1{\cdot}627\times10^{-23}\mathbf{T}$	$\mathbf{T=(1/10^3ak)H}$ $22{\cdot}7886+\log \mathbf{H}$ $6{\cdot}147\times10^{22}\mathbf{H}$	$\mathbf{H=(10^3c^2k/N)A}$ $\bar{1}1{\cdot}5493+\log \mathbf{A}$ $3{\cdot}542\times10^{-11}\mathbf{A}$	$\mathbf{A=(N/10^3c^2k)H}$ $10{\cdot}4507+\log \mathbf{H}$ $2{\cdot}823\times10^{10}\mathbf{H}$
$\mathbf{U=akNT}$ $\bar{3}{\cdot}9941+\log \mathbf{T}$ $9{\cdot}866\times10^{-3}\mathbf{T}$	$\mathbf{T=(1/akN)U}$ $2{\cdot}0059+\log \mathbf{U}$ $1{\cdot}014\times10^{2}\mathbf{U}$	$\mathbf{U=c^2kA}$ $10{\cdot}3321+\log \mathbf{A}$ $2{\cdot}148\times10^{10}\mathbf{A}$	$\mathbf{A=(1/c^2k)U}$ $\bar{1}1{\cdot}6679+\log \mathbf{U}$ $4{\cdot}655\times10^{-11}\mathbf{U}$
$\mathbf{\nu=(a/h)T}$ $11{\cdot}0169+\log \mathbf{T}$ $1{\cdot}039\times10^{11}\mathbf{T}$	$\mathbf{T=(h/a)\nu}$ $\bar{1}2{\cdot}9831+\log \nu$ $9{\cdot}618\times10^{-12}\nu$	$\mathbf{\nu=(c^2/Nh)A}$ $23{\cdot}3549+\log \mathbf{A}$ $2{\cdot}264\times10^{23}\mathbf{A}$	$\mathbf{A=(Nh/c^2)\nu}$ $\bar{2}4{\cdot}6451+\log \nu$ $4{\cdot}417\times10^{-24}\nu$
$\mathbf{w=(a/ch)T}$ $0{\cdot}5401+\log \mathbf{T}$ $3{\cdot}468\mathbf{T}$	$\mathbf{T=(ch/a)w}$ $\bar{1}{\cdot}4599+\log \mathbf{w}$ $0{\cdot}2884\mathbf{w}$	$\mathbf{w=(c/Nh)A}$ $12{\cdot}8780+\log \mathbf{A}$ $7{\cdot}551\times10^{12}\mathbf{A}$	$\mathbf{A=(c/hN)w}$ $\bar{1}3{\cdot}1220+\log \mathbf{w}$ $1{\cdot}324\times10^{-13}\mathbf{w}$
$\mathbf{\lambda=(10^8ch/a)T^{-1}}$ $7{\cdot}4599-\log \mathbf{T}$ $2{\cdot}884\times10^{7}\mathbf{T^{-1}}$	$\mathbf{T=(10^8ch/a)\lambda^{-1}}$ $7{\cdot}4599-\log \lambda$ $2{\cdot}884\times10^{7}\lambda^{-1}$	$\mathbf{\lambda=(10^8h\bar{N}/c)A^{-1}}$ $\bar{5}{\cdot}1220-\log \mathbf{A}$ $1{\cdot}324\times10^{-5}\mathbf{A^{-1}}$	$\mathbf{A=(10^8h\bar{N}/c)\lambda^{-1}}$ $\bar{5}{\cdot}1220-\log \lambda$ $1{\cdot}324\times10^{-5}\lambda^{-1}$
$\mathbf{M=(a/c^2)T}$ $\bar{3}7{\cdot}8793+\log \mathbf{T}$ $7{\cdot}574\times10^{-37}\mathbf{T}$	$\mathbf{T=(c^2/a)M}$ $36{\cdot}1207+\log \mathbf{M}$ $1{\cdot}320\times10^{36}\mathbf{M}$	$\mathbf{M=(1/N)A}$ $\bar{2}4{\cdot}2172+\log \mathbf{A}$ $1{\cdot}649\times10^{-24}\mathbf{A}$	$\mathbf{A=N.M}$ $23{\cdot}7828+\log \mathbf{M}$ $6{\cdot}064\times10^{23}\mathbf{M}$

It is easily possible to verify, for instance, that: (1) very long waves correspond to temperatures very near the absolute zero; (2) 300° K. comes in the infra-red region; (3) visible light is emitted between about 4000° and 8000°; (4) ultra-violet light, X-rays and γ-rays, the last named involving nuclear disturbance, between 10^4 and 10^9 degrees; (5) cosmic rays, which can apparently explode nuclei, at about 10^{10} degrees; and (6) the temperature necessary for the synthesis of a hydrogen atom from a proton and electron pair is about $2{\cdot}2\times10^{12}$ degrees. See [3], [5].

4. *Energy and Atomic Weight.*

In the table given in the earlier paper [1] the masses considered were **M** on the gram scale; actually, in most modern work, for instance in that on mass spectra, the unit chosen is that of the chemist, equal to one-sixteenth of the weight of an oxygen atom. The atomic weight is represented by **A**, where $\mathbf{A}=\mathrm{N}\mathbf{M}$, since it is to this scale that the Avogadro Number N refers. Conversions between energy values (generally expressed in electron-volts) and weights on the O=16 scale are frequently made in practice, and it is therefore deemed advisable to include masses expressed in this way in the general interconversion scheme. The absolute mass of 1 unit on the O=16 scale is the reciprocal of the Avogadro Number, or $1{\cdot}649\times10^{-24}$ gram. The absolute mass of a hydrogen atom will be this multiplied by 1·008, or $1{\cdot}662\times10^{-24}$ gram. Using the conversion factors between masses and electron-volts, it is found that one unit on the atomic weight scale is equal to $(1{\cdot}649\times10^{-24})\times(5{\cdot}652\times10^{32})=9{\cdot}320\times10^{8}$ electron-volts, and that 10^6 electron-volts correspond to $1{\cdot}073\times10^{-3}$ units of mass. The complete table for interconversion between atomic weights and energetic and related magnitudes previously taken into account is included in Table II. (B).

Two examples of the applicability of the atomic weight conversion factors may be given. First, the "loss of mass" occurring on assembling complex nuclei from their constituent protons and electrons has been associated, on relativistic grounds, with an evolution of energy. It may be calculated that the loss in the case of the oxygen nucleus is 0·1238 unit of atomic weight [3]. This corresponds, using the appropriate conversion factor given

above, to $1{\cdot}154\times10^8$ electron-volts, a very large figure, but quite consistent with the remarkable stability of the oxygen nucleus, and the observed impossibility of breaking it up by bombardment with α-particles. Secondly, reference to the experiment of Cockcroft and Walton[6] may be made, in which a lithium nucleus (presumably Li (7)) is caused to break up into two α-particles by bombardment with high-speed protons. The reaction and masses involved are :—

$$\begin{array}{cccc} \mathrm{Li}\ (7)+\mathrm{H}\ (1) & = & 2\mathrm{He}\ (4)+17{\cdot}2\times10^6 & \text{electron-volts} \\ 7{\cdot}0104 & & 1{\cdot}0072 \quad 8{\cdot}0022. & \end{array}$$

The loss of mass is therefore $7{\cdot}0104+1{\cdot}0072-8{\cdot}0022=0{\cdot}0154$ unit, which corresponds to $14{\cdot}3\times10^6$ electron-volts. The difference between the observed and calculated evolution of energy may possibly be associated with the uncertainty in knowledge of the exact mass of the Li (7) isotope. The conversion factor is $9{\cdot}320\times10^8$ in each of the above two examples.

5. *The Interconversion Scale.*

The various energetic and related magnitudes of which account is here taken are shown on the left-hand side of the interconversion scale (Table IV.). The relations between them may be expressed as follows :—

$$\mathbf{E}=c^2\mathbf{M}=\frac{c^2}{\mathbf{N}}\mathbf{A}=\frac{10^8e}{c}\mathbf{V}=\frac{m}{2}\mathbf{v}^2=10^7\mathbf{J}=\mathbf{Nk}=g\mathbf{G}=10^3dg\mathbf{PL}$$

$$=\frac{1}{10^3k}\mathbf{H}=\frac{1}{k\mathbf{N}}\mathbf{U}=h\nu=ch\mathbf{w}=10^8ch\frac{1}{\lambda}=a\mathbf{T}. \quad . \quad . \quad . \quad (4)$$

Evidently interconversions may be made between any pair of the fifteen chosen magnitudes, though the experimental significance of all of these possibilities has not yet been realized. The values of the constants occurring in equations (4) are shown in Table III. Some of the assigned values are those adopted in the earlier paper [1] after some critical discussion. They still appear to be the best available, within the desired accuracy limits.

Table IV. is constructed so that corresponding values of the various constants may be found directly, by placing one edge of a (preferably transparent) set-square on either of the reference lines placed at the top and foot of the scale. The order of symbols is that considered most likely to be

convenient, so that scales which may be more frequently used in conjunction are placed as close as possible together. The accuracy of reading is about that of an ordinary slide rule, in the neighbourhood of $\pm 0{\cdot}5$ per cent., whilst that using interconversion factors is about $\pm 0{\cdot}1$ per cent.

In using the scale, the number to be converted must first be expressed with *one digit only before the decimal place*, using the appropriate power of 10: thus, 156×10^5 would be written $1{\cdot}56 \times 10^7$, $9{\cdot}75$ as $9{\cdot}75 \times 10^0$, and $0{\cdot}000563$ as $5{\cdot}63 \times 10^{-4}$. The converted number will then be expressed in the same way. Powers of 10 (7, 0, and -4 in the above instances) of a number to be converted to another scale are shown as functions of a quantity x over ranges denoted by the dotted lines running over the scales. It is not generally necessary to evaluate x, and greater speed can generally be attained without doing so. As an example, supposing it is desired to convert $\mathbf{A} = 0{\cdot}1238$ to the **V** scale, the number is first written $1{\cdot}238 \times 10^{-1}$, which comes in the range denoted by $x+27$, whilst the value of **V**, read from the scale as about $1{\cdot}155$, is in a range marked $x+36$. Evidently an increase in the power of 10 from 27 to 36, that is 9 units, must be allowed for, giving the new power as $-1+9=8$, so the value $\mathbf{V} = 1{\cdot}155 \times 10^8$ electron-volts is reached (value by calculation: $1{\cdot}154 \times 10^8$, as in the first example in section 4). This method is of general applicability in making conversions between any pair of magnitudes.

TABLE III.

Values of the Physical Constants used in calculating Interconversion Factors.

Symbol.	Significance.	Value.	Units.
e	Electronic charge	$4{\cdot}770 \times 10^{-10}$	Electrostatic.
c	Veclocity of light	$2{\cdot}998 \times 10^{10}$	Cm. per second.
m	Electronic rest mass ...	$9{\cdot}035 \times 10^{-28}$	Gram.
k	Heat equivalent of work	$2{\cdot}390 \times 10^{-11}$	Kil.-cals. per erg.
N.....	Avogadro Number	$6{\cdot}064 \times 10^{23}$	Per gram-mol.
h	Planck's Constant	$6{\cdot}547 \times 10^{-27}$	Erg second.
a	Energy - Temperature constant	$6{\cdot}807 \times 10^{-16}$	Erg per degree.
g	Acceleration due to gravity (Greenwich) .	$9{\cdot}812 \times 10^2$	Cm. per sec^2.
P	Normal atmospheric pressure	$7{\cdot}600 \times 10$	Cm. Hg.
d	Density of Hg	$1{\cdot}3595 \times 10$	Grams per cm^3.

in section 4). This method is of general applicability in making conversions between any pair of magnitudes.

Table IV.—An Interconversion Scale.

It may be noted that on account of the appearance of the square of electron velocity in the energy equations (4), it becomes necessary to use two lines of scale, the upper line corresponding to *odd* values of x, and the lower line to *even* or *zero* values of x. This should be observed in choosing the right velocity scale when making conversions from other scales into the **v** scale. The x functions here take the form $\frac{1}{2}(x+n)$, so it may be more convenient to note the actual values of x in these cases.

Further, the λ scale of wave-length represents an inverse function of energy, so that the scale runs in the direction opposite to that of the other scales, and the functions of x are of the form $-(x+n)$. In making conversions involving this scale, therefore, the principle explained above may be used, without necessarily considering the actual value of x, but remembering that in making the change and after the change is made, a reversal of sign must be observed, as in the following example. Suppose it is desired to find the temperature **T** corresponding to energy of maximum density of wave-length $\lambda=3{,}750=3{\cdot}75\times10^3$ Å.U., in the region marked $-(x+33)$. The temperature scale reading is about 7·70, and this is in the range $x+39$; hence there is a *negative increase* from 33 to 39, which amounts to a *decrease* of 6 units, yielding the new exponent of 10 as $3-6=-3$, whence, reversing the sign, the value is $+3$, giving $\mathbf{T}=7{\cdot}70\times10^3$ (compare $7{\cdot}690\times10^3$ degrees absolute, obtained by calculation from equation (2)). This slightly complicating factor may therefore be allowed for without serious difficulty.

6. *Conclusion.*

In conclusion, the presentation of so many scales, involving apparently diverse magnitudes, in close interrelation may possess some attributes of special interest, apart from the question of their direct and immediate usefulness. Before the advent of the quantum theory, it might have seemed futile to connect together spectroscopic numbers with energetic magnitudes ; still more perhaps, before the general theory of relativity, might the interconversion of mass and energy have seemed without significance. Actually, the equations $\mathbf{E}=h\nu$ and $\mathbf{E}=c^2\mathbf{M}$ are now found of vital importance in general physical and astrophysical work. Further, by a combina-

tion of both theories, masses and spectroscopic numbers may sometimes be usefully brought into relation. It therefore seems pertinent to enquire whether other magnitudes, such as gas energies and spectroscopic numbers, here assembled together, perhaps for the first time, may not be found capable of being related by experiment. At least, there seems to exist no limitation upon the arithmetical relation of any pair of quantities given in the set of equations (4), in so far as these relations are applicable. The scale presented may therefore perhaps prove itself useful, not only in present researches, but also in types of experiment as yet unrealized.

References.

(1) C. H. Douglas Clark, Phil. Mag. (7) xiv. p. 291 (1932).
(2) R. Mecke, Trans. Faraday Society, xxvii. p. 514 (1931).
(3) C. H. Douglas Clark, Proc. Leeds Phil. Soc. ii. p. 513 (1934).
(4) R. T. Birge, Phys. Rev., Supplement, i. p. 1 (1929).
(5) F. G. Donnan, 'Nature,' cxxviii. p. 290 (1931).
(6) J. D. Cockcroft and E. T. S. Walton, Proc. Roy. Soc. A, cxxxvii. p. 229 (1932).

Corrigenda.

In the paper of reference (1) above,

Page 296, line 28, *for* $\alpha=4{\cdot}9561$ *read* $\alpha=4{\cdot}9651$.
Table III., compartment (16), middle line, *for* 4·0914 *put* $\bar{4}{\cdot}0914$.
Table III., compartment (27), bottom line, *for* **M** *put* $\mathbf{M}^{\frac{1}{3}}$.
Table III., compartment (35), middle line, *for* 8·2930 *put* $\bar{8}{\cdot}2930$.
Table III., compartment (43), middle line, *for* 24·6713 *put* $\overline{24}{\cdot}6713$.
Table III., compartment (81), middle line, *for* $+\log \mathbf{M}$ *put* $-\log \mathbf{M}$.
Table III., compartment (86), middle line, *for* 14·6679 *put* $\overline{14}{\cdot}6679$.

Department of Inorganic Chemistry,
The University of Leeds.
January 20th, 1934.

VI. *X-ray Diffraction in Liquid Mixtures.*—Part I.

By S. Parthasarathy *.

[Plates I.–III.]

1. Introduction.

A LARGE mass of data has accumulated on the diffraction of X-rays in liquids since the discovery of the effect in 1916 by Debye and Scherrer †. Various

* Communicated by the Author.
† *Nach. Gott.* xvi. p. 16 (1916).

theories have been put forward in the meantime to explain adequately the diffraction maxima observed with liquids. Notably we may mention those of Ehrenfest, Brillouin *, and of Raman and Ramanathan †, but the theory of Raman and Ramanathan is essentially based on the fact that the liquid state approaches a crystal nearer in the arrangement of molecules following some regularity, and that they are not wholly oriented at random. The treatment is an extension of that of Einstein and Smoluchowski for scattering in the visible region, to the region of X-rays, and arrives at a formula for the intensity and spacing agreeing well with experimental facts. More recently Stewart ‡ has advanced the view of the cybotactic state of liquid, which assumes that in a liquid there are always groups of molecules existing, other than associated molecules, if any, which give rise to diffraction patterns.

If groups of molecules exist, then in a mixture of two liquids there ought to be a single diffraction pattern instead of one for each liquid separately, as the probability of two kinds of molecules conspiring to form a single group is as much as for molecules of the same kind. A good number of mixtures of organic liquids have been studied by various authors §, but differences still exist. We may mention notably Meyer, who observes, in the case of the mixtures studied, a single major peak shifting with concentration. Raman and Ramanathan's theory demands a superposition of the two maxima due to each liquid, while Stewart's view requires a single peak, as obtained by Meyer, due to conglomeration of the two groups of molecules. Other particulars regarding the intensity of general scattering at small angles and the behaviour of possible inner rings in the case of associated or polar liquids are lacking, and the work is undertaken to examine more closely the results of X-ray diffraction in binary liquid mixtures, in view of similar work on scattering of light by the author ||.

* *Annales de Physique*, 1922, p. 88.

† Proc. Ind. Ass. Cult. Sci. viii. p. 127 (1923).

‡ Phys. Rev. xxxii. p. 558 (1928); also Ind. Journ. Phys. vii. p. 603 (1933).

§ Wyckoff, Am. J. Sc. v. p. 455 (1923). Krishnamurti, Ind. Journ. Phys. ii. p. 501 (1928); iii. pp. 209, 307, 331, & 507 (1928–29); v. p. 489 (1930). Meyer, Phys. Rev. xxxviii. p. 1083 (1931).

|| In the course of publication in the Indian Journal of Physics, viii. p. 275 (1933–34).

2. Apparatus and Technique.

In order that the diffraction ring may be as sharp as can be consistent with the nature of the liquid, the slit of the camera was made very narrow in a cylindrical block of lead. The camera was covered all over with thick lead sheet. The incident beam was the copper K_α radiation.

A small cell about 1 mm. in thickness, with mica windows, placed behind the slit served as container for the liquid mixture. Since mica gives rise to only Laue spots, the rings given were those by mixtures only, and not at all interfered with in any way. The mica windows were firmly fixed to the sides of cell by either gum or rubber solution or sodium silicate, depending on the nature of the liquid under investigation.

Ilford Iso-Zenith plates were used in these investigations.

3. Liquids chosen.

The liquids selected for investigation have been studied by various authors, and in this laboratory by Sogani and Krishnamurti. The idea borne in mind in the selection was the great difference in the diameter of the rings for the two liquids, such that, a mixture of the two, if giving only a superposition of the ring patterns, would give distinctly separated peaks. Such pairs of mixtures were :

i. Benzene and ethyl phthalate.
ii. Ethyl phthalate and pyridine.
iii. Ethyl phthalate and *m*-xylene.
iv. Pyridine and ethyl benzene.
v. Acetic acid and *m*-xylene.
vi. Acetic acid and ethyl benzene.

If the mixtures give only a single major peak without their respective patterns, then a distinct change in position of the single peak could be easily noted.

The diameter of the ring was measured and the spacing calculated, using Bragg's formula

$$d = \frac{\lambda}{2 \sin \frac{\theta}{2}},$$

where the letters have the usual significance.

4. Results.

i. *Benzene and Ethyl Phthalate.*

Benzene gives a halo with a spacing of 4·82 Å.U., while ethyl phthalate gives two of 4·05 Å.U. and 7·20 Å.U., both of them equally intense and much sharper than the one given by benzene. For the ratio 1 : 2 for benzene and phthalate the ring has shifted in position, while general scattering inside the ring has increased. The inner ring of ethyl phthalate is greatly weakened. For 1 : 1 ratio the spacing as measured is 4·47 Å.U., while the inner ring of the phthalate has completely disappeared. The progressive shifts in position of the inner ring could be followed very easily for the concentrations studied. The table below gives the results *. (Figs. 1–5, Pl. I.)

Liquid.	Inner ring.		Outer ring.	
	θ.	λ in Å.U.	θ.	λ in Å.U.
Benzene	—	—	18·5	4·82
Solution 2 : 1	—	—	19·3	4·60
„ 1 : 1	—	—	19·7	4·47
„ 1 : 2	12·2	7·20	20·8	4·27
Ethyl phthalate.....	12·2	7·20	22·0	4·05

ii. *Pyridine and Ethyl Phthalate.*

The diffraction ring for pure pyridine is much sharper than the one for benzene, and the spacing is 4·60 Å.U.

Liquid.	Inner ring.		Outer ring.	
	θ.	λ in Å.U.	θ.	λ in Å.U.
Pyridine	—	—	19·3	4·60
Solution 2 : 1	—	—	19·6	4·50
„ 1 : 1	—	—	20·5	4·33
„ 1 : 2	12·2	7·20	21·8	4·08
Ethyl phthalate.....	12·2	7·20	22·0	4·05

The mixture in 1 : 1 ratio gives the greatest small angle scattering, while for the other two mixtures it is much less. For 67 per cent. of pyridine in the mixture the

* Krishnamurti has also studied this solution.

spacing is 4·45 Å.U., while for the same percentage of the phthalate in the mixture, the pattern remains almost unchanged. The results are set forth in the preceding table. (Figs. 6–10, Pl. II.)

iii. *Ethyl Phthalate and* m-*xylene.*

Pure *m*-xylene gives a ring, slightly diffuse outwards, with a spacing of 5·54 Å.U. This diffuseness persists even in mixtures up to 1 : 1, while the shifting of the maximum is clearly visible. The diffraction pattern gets wider, instead of the two rings being superposed. For more of ethyl phthalate (2 : 1) the spacing is practically the same as the one for pure liquid. The following table gives the results :—

Liquid.	Inner ring.		Outer ring.	
	θ.	λ in Å.U.	θ.	λ in Å.U.
m-xylene	—	—	16·0	5·54
Solution 2 : 1	—	—	18·2	4·87
„ 1 : 1	—	—	19·8	4·47
„ 1 : 2	12·2	7·20	22·0	4·05
Ethyl phthalate.....	12·2	7·20	22·0	4·05

iv. *Pyridine and Ethyl Benzene.*

Each liquid gives only one diffraction ring. Ethyl benzene gives slightly wider ring, but a small one at that, giving a spacing of 5·30 Å.U. only. While the maxima can be followed easily in the photograms, the pattern for more of ethyl benzene is characterized by slightly greater width.

Liquid.	Diffraction ring.	
	θ.	λ in Å.U.
Pyridine	19·3	4·60
Solution 2 : 1	18·8	4·71
„ 1 : 1	18·0	4·92
„ 1 : 2	17·2	5·15
Ethyl benzene	16·8	5·30

v. *Acetic Acid and* m-*xylene.*

Pure acetic acid gives two rings with spacings of 4·10 Å.U. and 7·20 Å.U. The latter one is usually ascribed to molecular association, and it is naturally less intense than the outer one. For the ratio 2 : 1 of acetic acid to *m*-xylene the inner ring is greatly weakened, while the position of the outer one is not much altered. The mixture of the acid and *m*-xylene in the ratio 1 : 2 shows diffuseness with a distinct maximum. The shifts in position of the maxima are as below. (Figs. 11–15, Pl. III.)

Liquid.	Inner ring.		Outer ring.	
	θ.	λ in Å.U.	θ.	λ in Å.U.
Acetic acid	12·2	7·20	21·8	4·10
Solution 2 : 1	12·2	7·20 (weak)	21·6	4·11
„ 1 : 1	—	—	20·1	4·42
„ 1 : 2	—	—	18·2	4·87
m-xylene	—	—	16·0	5·54

vi. *Acetic Acid and Ethyl Benzene.*

The difference in the maxima for the two principal rings of these liquids is 1·20 Å.U., and the shift is distinct and marked. General internal scattering at small angles is marked of the mixture with more of ethyl benzene.

Liquid.	Inner ring.		Outer ring.	
	θ.	λ in Å.U.	θ.	λ in Å.U.
Acetic acid	12·2	7·20	21·8	4·10
Solution 2 : 1	12·2	7·20 (very weak)	21·1	4·19
„ 1 : 1	—	—	18·8	4·71
„ 1 : 2	—	—	17·5	5·06
Ethyl benzene	—	—	16·8	5·30

5. Discussion.

The above results favour the view that in a mixture it is the combined group of the two kinds of molecules

which scatter the X-rays, giving rise to diffraction patterns with a single maximum. Otherwise, the mixture pattern ought to be a superposition of those of the individual patterns, which is not found to be the case. A general treatment has been given for liquids by Dr. K. Banerjee *.

In a liquid the crystalline structure of orderly arrangement is preserved to a certain degree, and Stewart's idea for the origin of these rings is that they are caused by such groups, or the cybotactic state of the molecule. The fact that even in a mixture instead of separate maxima we get only a combined major peak, has been advanced by Stewart as a strong case for this state of the molecule.

In all the liquid mixtures studied above there has been obtained in each case only one maximum, as against Wyckoff. In general, the shift of the maximum does not seem to be proportional to concentration. In some cases, as with polar, the differences are marked in the increased general scattering and in the shift of the peak of maximum intensity.

In the selection of the mixtures some have been chosen for being polar, as, for example, pyridine and acetic acid. Their general behaviour seems to be a little different from that of others. When only about 33 per cent. of the second component is present the shift for any of the two mentioned above is not appreciable, while for the next 50 : 50 ratio the maximum moves much forward. This is so only with polar compounds. This is easily explained on the view that the groups are present to a greater strength in these liquids, and that only the larger groupings or the associated molecules are disrupted by the addition of the other compound to about 33 per cent. without definite groups being formed. The groups of the first component are still present, and the presence of the second one merely decreases the number of the associated molecules, at the same time increasing the groups of the first kind, while perhaps there are not many free molecules of the first kind to form a common group with those of the second. The results with mixtures of acetic acid with ethyl benzene and *m*-xylene, and of pyridine with ethyl phthalate and ethyl benzene, clearly support this view.

The increased general scattering at small angles observed in some of the foregoing cases indicates a greater random-

* Ind. Journ. Phys. iv. p. 541 (1930).

ness of orientation of the molecules and less number of molecular groups.

The inner rings being destroyed in acetic acid and greatly weakened for 33 per cent. of the second component also indicates that the molecular association is destroyed, though not completely. Such a view is supported by Krishnamurti's observation on acetic acid and water mixture, and also by the effect of heat on the acid.

The giving of such single major peak in a mixture of liquids indicates that a solution has been formed, a solution wherein the two components enter into the formation of a single type or group of molecules. In a case where this is not possible we expect to get the superposition alone of the two individual spacings, which has not been observed in any of the cases studied in this paper by the author.

The foregoing experimental work was carried out at the Laboratory of the Indian Association for the Cultivation of Science, Calcutta, and the author takes this opportunity of thanking Sir C. V. Raman, F.R.S., N.L., for facilities afforded for this work.

"Dvaraka,"
Mylapore, Madras.

VII. *On the Theory of the Combination Coefficients for large Ions and for uncharged Particles at any Pressure.* *By* W. R Harper, *Ph.D., Research Associate, Wills Physical Laboratory, University of Bristol* *.

Abstract.

By extending a previous theory of the author, a formula is derived for the frequency of approach to within a distance σ of particles suffering random Brownian displacements, the formula being valid for all values of σ/λ where λ is the mean free path. A further extension generalizes the effect of mutual electrostatic attraction on this frequency to nearly all values of σ/λ. This enables the recombination coefficients for large ions to be calculated, different formulæ being obtained for different

* Communicated by Prof. A. M. Tyndall, D.Sc., F.R.S.

values of the radius of the ion and different pressures. The recombination of multiply charged large ions is shown to be peculiar. The combination coefficients for small ions with uncharged nuclei are calculated, and the relation between them and the recombination coefficients shown to be different from that announced recently by Whipple. The results for atmospheric pressure are exhibited graphically and compared with the available experimental data. Finally, it is shown how, from observations on large ions, the mass of a clustered small ion could be found without making any assumptions about the size or structure of the cluster.

---

1. *Introduction.*

IN a recent paper to the Physical Society * Whipple derived certain theoretical relations between the coefficients of recombination and formation of large atmospheric ions. The derivation was similar to that originally given by Langevin † in his treatment of the recombination coefficient for small ions. I have, however, shown ‡ that the original treatment of Langevin must lead to incorrect results, even at high pressures, because it fails to make due allowance for the Brownian movement of the ions. This is also true of the modification—or extension—proposed by Whipple. In my previous paper (*loc. cit.*), I re-developed the theory of the recombination of small ions at high pressures, obtaining a formula quite different from any previously given, but agreeing with experiment. The difficulties encountered in attempting to extend the theory to lower pressures—including atmospheric—are absent when the ions are large, and this extension will be made in the present paper.

It should again be emphasized that whereas the theory pays due attention to all the physical phenomena involved, the mathematical methods used are approximate, and do not, therefore, lead to formulæ which are *numerically* exact. The notation will correspond with that of my

* Proc. Phys. Soc. xlv. p. 367 (1933).
† *Ann. de Phys.* xxviii. p. 433 (1903).
‡ Proc. Camb. Phil. Soc. xxviii. p. 219 (1932).

previous paper *, and therefore differ slightly from that used by Whipple †.

2. *The General Collision Frequency in the Absence of Mutual Attraction.*

We shall consider a gas in which there is a random distribution per c.c. of n_1 small positive ions, n_2 small negative ions, N_1 large positive ions, N_2 large negative ions, and N_0 uncharged nuclei; it being assumed that these quantities are of the usual order of magnitude. It then follows from Paper I., Section 2, that encounters between ions (or uncharged particles) are due primarily to thermal agitation, and that the effect of mutual electrostatic attraction may be calculated as a correction. The collision frequency in the absence of mutual attraction will therefore first be calculated. Calling approach to within a distance σ (between centres) a σ collision, the frequency of σ collisions for $\sigma << \lambda$ where λ is the mean free path is well known to be $\pi n' n'' \sigma^2 U$, where U is the mean relative gas kinetic velocity of any two kinds of ions (or uncharged particles) whose numbers per c.c. are n' and n''. It was shown in Paper I., Section 4, that this formula breaks down if σ is comparable with, or greater than, λ. For σ considerably greater than λ it was shown to become $\pi n' n'' \sigma (D' + D'')$ where D' and D'' are the diffusion coefficients of the two ions (or uncharged particles) concerned.

A calculation of the precise form of the intermediate formula for σ comparable with λ would be almost impossible, since none of the approximations which make the calculations for the extreme cases feasible are then permissible. The procedure will therefore be adopted of choosing the simplest interpolation formula which tends asymptotically to the two required forms for $\sigma >> \lambda$ and $\sigma << \lambda$, and passes smoothly from the one to the other in the proper region, namely at $\sigma \approx \lambda$. A knowledge of the relation between the diffusion coefficient and the mean velocity of agitation is required before the choice can be made. Meyer's ‡ relation is $D' + D'' = \frac{2}{3}\lambda U$ if we do not differentiate between the mean free paths of the two

* Hereinafter referred to as Paper I.

† σ and N are used in different senses by him, and he uses w for the mobility whereas k is used in the present paper.

‡ Jeans, 'Dynamical Theory of Gases,' 4th ed. p. 310.

ions concerned, as is permissible in an approximate theory when considering a pair of small or a pair of large ions.

Using this relation the required formula for the collision frequency is

$$\nu'(\sigma)=\pi n' n''\sigma(D'+D'')[1-\exp\{-U\sigma/(D'+D'')\}]. \quad (2.1)$$

The dotted curves in fig. 1 show the two forms to which it must tend for large and small values of σ/λ, the full line being equation (2.1). The change from one form to the

Fig. 1.

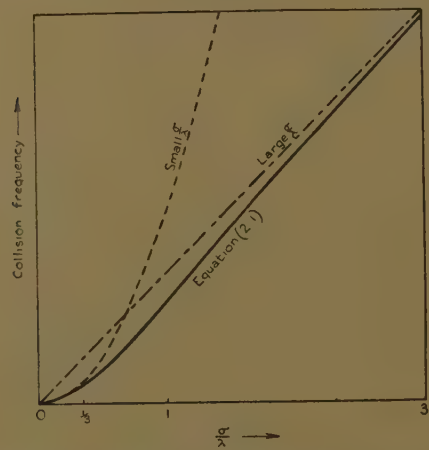

other takes place almost completely in the range of σ a few times greater than λ to a few times smaller than λ. This leads one to expect that the theory developed in Paper I. from the formula for the upper range will apply quite well some way into the intermediate range, where the approximations used are ceasing to be justifiable, that is for rather too low pressures *. This was found to be the case, but it should perhaps be regarded as a confirmation of the interpolation rather than a prediction of the theory.

For a small and a large ion only the D for the small ion need be retained, so that $D''=0$ and $D'=\frac{1}{3}\lambda U$ where λ

* See the first footnote on p. 228 of Paper I.

here refers to the small ion. Replacing $\frac{2}{3}\lambda U$ by $\frac{1}{3}\lambda U$ in (2.1) alters, however, the value of σ/λ at which the change over from one form to the other occurs, and this is inconsistent with the consideration on p. 223 of Paper I. The contradiction arises from attempting to work more accurately than is justified by the approximations. The matter being therefore arbitrary, it seems best to retain the $\frac{2}{3}$ throughout, which is equivalent to replacing $D'+D''$ by $2D'$ when D'' is dropped. So far we have been discussing the exponential term in the collision frequency. That the same replacement must be made in the other term follows from p. 225 of Paper I. Intermediate ions and electrons do not fall within the scope of the theory.

3. *The General Attraction Factor.*

The collision frequency just calculated will be increased from ν' to ν_c' as a result of mutual electrostatic attraction. The attraction factor $f(\sigma)$ is defined by the equation $\nu_c'(\sigma)=f(\sigma)\nu'(\sigma)$. In Paper I. it was calculated for σ considerably greater than λ, and shown to be

$$1+\frac{\sigma_0}{\sigma}\log\frac{N^{-\frac{1}{3}}}{2(\sigma+\sigma_0)},$$

provided that $\sigma\geq\sigma_0$, where $N=n_1+n_2+N_1+N_2$. σ_0 is the separation at which the drift together due to electrostatic attraction just balances (on the average) the drift apart due to Brownian movement, and is equal to $6{\cdot}1\,.\,10^{-6}\times 273/\theta$ cm. for singly charged ions, θ being the absolute temperature. If the ions have b' and b'' elementary charges respectively, then σ_0 is increased by the factor $b'\,b''$, but the value of $f(\sigma)$ in terms of the new σ_0 is unaltered.

For smaller σ the attraction factor cannot be calculated on the assumption that the motion of the ions is fundamentally a Brownian movement. The circumstances are then more like those for ions colliding with each other, but not with the gas molecules, when the value of $f(\sigma)$ is *

$$1+\frac{2(m'+m'')b'b''e^2}{m'm''U^2\sigma}.$$

where m' and m'' are the masses of the two ions, and e the electronic charge.

* Thomson, 'Conduction of Electricity through Gases,' i. p. 43 (1928).

We must now consider the case of $\sigma \geq \sigma_0$, but with no restriction on λ, neither formula being then applicable. In approaching the sphere σ surrounding the one ion, the other ion will, in general, during its journey from a large distance, pass successively through a region in which its motion is fundamentally a Brownian movement, through an intermediate region, and through a region where it is unlikely to collide with a gas molecule. These regions are bounded by concentric spheres. The first region extends from a large distance down to a radius several times greater than λ, the second extends from this radius down to a radius several times less than λ, and the third is the region inside this last sphere. The attraction factor is now the product of three parts :—

(a) The attraction factor for the sphere of diameter several times λ as given by the formula of Paper I. ; times

(b) the attraction factor for the sphere of diameter several times smaller than λ for ions starting at the first sphere ; times

(c) the Thomson attraction factor for ions starting at the inner sphere. The Thomson factor can at once be generalized for ions not starting at infinity by referring the electrostatic potential to the starting-point instead of to infinity. If first we omit (b), assuming that (a) is applicable down to $\sigma = \lambda$, and that thereafter (c) is applicable, we have for $\sigma > \lambda > \sigma_0$

$$1 + \frac{\sigma_0}{\sigma} \log \frac{N^{-\frac{1}{3}}}{2(\sigma + \sigma_0)},$$

and for $\lambda > \sigma > \sigma_0$

$$\left\{1 + \frac{\sigma_0}{\lambda} \log \frac{N^{-\frac{1}{3}}}{2(\lambda + \sigma_0)}\right\} \left\{1 + \frac{2(m' + m'')b'b''e^2}{m'm''U^2}\left(\frac{1}{\sigma} - \frac{1}{\lambda}\right)\right\}.$$

Except when σ is considerably greater than λ, the contribution of the Brownian movement term in these formulæ will be too large, because in the range (b) conditions are giving way to ones more like those obtaining in the range (c), and for a given $\sigma > \sigma_0$ the Brownian movement factor is greater than the Thomson factor. The Thomson factor will, however, be but little affected by collisions inside the λ sphere, since from the nature of its derivation a considerable number of collisions are required for it

to be much altered. To correct the formulæ it is therefore only necessary to modify the Brownian movement term so that when σ is less than several times λ it tends asymptotically to the constant value required in the second formula. This constant value is the Brownian movement factor for a $\xi\lambda$ sphere instead of the factor for a λ sphere where $\xi>1$. The modification may be carried out most simply by substituting $\sigma/\{1-\exp(-\sigma/\xi\lambda)\}$ for σ. This has only a small effect for σ greater than several times $\xi\lambda$, but makes the factor tend asymptotically to that for a $\xi\lambda$ sphere for decreasing σ. The σ in the log term has so little effect on the magnitude of the factor that it is superfluous to alter it in an approximate theory. The same Brownian movement factor may now be used throughout the whole range of λ, so that if the Thomson factor is dropped for $\sigma>\lambda$ we may write for $\sigma\geq\sigma_0$ and all λ

$$f(\sigma)=\left[1+\frac{\sigma_0}{\sigma}\{1-\exp(-\sigma/\xi\lambda)\}\log\frac{N^{-\frac{1}{3}}}{2(\sigma+\sigma_0)}\right]$$
$$\times\left[1+\left\{\frac{2(m'+m'')b'b''e^2}{m'm''\mathrm{U}^2}\left(\frac{1}{\sigma}-\frac{1}{\lambda}\right)\text{ or }0\right\}\right]. \quad (3.1)$$

This formula will clearly also hold for all σ if $\lambda>\sigma_0$, but not if $\lambda<\sigma_0$ since then the Brownian movement factor is incorrect. If, however, λ is a few times less than σ_0 it was shown in Paper I. that a σ_0 collision leads to recombination.

4. *The Combination Coefficients involving Ions.*

The general combination equations for time t are

$$\frac{dn_1}{dt}=-\alpha n_1n_2-\eta_{12}n_1\mathrm{N}_2-\eta_{10}n_1\mathrm{N}_0,$$

$$\frac{dn_2}{dt}=-\alpha n_1n_2-\eta_{21}n_2\mathrm{N}_1-\eta_{20}n_2\mathrm{N}_0,$$

$$\frac{d\mathrm{N}_1}{dt}=-\eta_{21}n_2\mathrm{N}_1-\alpha'\mathrm{N}_1\mathrm{N}_2+\eta_{10}n_1\mathrm{N}_0,$$

$$\frac{d\mathrm{N}_2}{dt}=-\eta_{12}n_1\mathrm{N}_2-\alpha'\mathrm{N}_1\mathrm{N}_2+\eta_{20}n_2\mathrm{N}_0,$$

$$\frac{d\mathrm{N}_0}{dt}=-\eta_{10}n_1\mathrm{N}_0-\eta_{20}n_2\mathrm{N}_0,$$

defining the recombination coefficients α, α', η_{12}, η_{21}; and the coefficients η_{10} and η_{20}, which determine the formation of large ions from small ions and uncharged nuclei. α' is in general negligible, since the diffusion coefficient of a large ion is extremely small compared with that of a small ion. If, however, the large ions are multiply charged, α' is not necessarily negligible. J. J. Nolan and O'Keeffe * have reported large ions with as many as several thousand elementary charges. For such ions σ_0 may amount to nearly a metre. Paper I., Section 6, then implies that if two such ions approach to within this distance in an otherwise unionized gas of large extent, they will continue to approach each other until eventually they recombine. In the absence of an external field they would in effect be already recombined. A quite small applied field could, however, suffice to prevent recombination, since it would only have to overcome their mutual attraction, which is very small at this distance. The recombination coefficient for such ions will, therefore, depend very markedly on the applied field. Moreover, it is not possible to define a unique radius for capture when this is comparable with the average distance between the ions, and the speed of recombination will depend very much on the precise initial distribution of the ions. The recombination process is, therefore, not amenable to mathematical treatment, so it will be assumed in what follows that b' and b'' are not greater than a few units.

The frequency of encounters between small ions and uncharged nuclei will be given by (2.1), since the effect of mutual attraction may be neglected. In the formula we must put $\sigma=a_0$ the radius of the nucleus and $D'+D''=2D_2$, or $2D_2$ where D_1 and D_2 are the diffusion coefficients for the small ions †. We may assume that every collision leads to combination, so that

$$\eta_{10}n_1N_0=2\pi n_1N_0a_0D_1\{1-\exp(-Ua_0/D_1)\}$$

holds for the formation of positive large ions, with a similar equation for the negative ions. Using Meyer's relation the equation may be written

$$\eta_{10}=2\pi a_0D_1\{1-\exp(-3a_0/2\lambda_1)\},$$

* Proc. Roy. Irish Acad. xli. p. 26 (1933).

† See p. 101.

where λ_1 refers to the positive small ion. Now if k_1 is the mobility of the small positive ion in e.s.u., we have $D_1/k_1=P/eN(\theta)$, where P is the standard atmosphere in dynes cm.$^{-2}$, and $N(\theta)$ is the number of molecules per c.c. of a perfect gas at this pressure and at a temperature of $\theta°$ abs. This gives

$$\eta_{10}=\frac{2\pi P a_0 k_1}{eN(\theta)}\{1-\exp(-3a_0/2\lambda_1)\} \quad . \quad . \quad (4.1)$$

and

$$\eta_{20}=\frac{2\pi P a_0 k_2}{eN(\theta)}\{1-\exp(-3a_0/2\lambda_2)\}, \quad . \quad (4.2)$$

where k_2 and λ_2 refer to the small negative ion. These equations will hold for dust particles as well as for nuclei. For dust particles the exponential term may be neglected, when the formulæ reduce to

$$\eta_{10}=4{\cdot}9\times10^{-4}a_0k_1\theta/273$$

and

$$\eta_{20}=4{\cdot}9\times10^{-4}a_0k_2\theta/273,$$

after making the necessary numerical substitution. The rate of combination of small ions and dust particles therefore depends only on the radius of the particle, on the mobility of the small ion, and on the temperature. Moreover, $\eta_{10}/\eta_{20}=k_1/k_2$, a relation which should be much more accurate than the absolute values of either η_{10} or η_{20}, since the least reliable result of the theory is the numerical constant which has cancelled in the ratio. It might be expected on general grounds that this relation would hold for nuclei also, but (4.1) and (4.2) show that this is *not* the case.

The recombination coefficients η_{12} and η_{21} have now to be calculated. Let a_1 and a_2 be the radii of the positive and negative large ions respectively.

Suppose first that σ_0 is greater than these radii, and also at least several times greater than the mean free path of the small ion. Then, as in Paper I., σ_0 collisions will ultimately lead to recombination, and we have

$$\eta_{12}n_1N_2=\nu'(\sigma_0)f(\sigma_0),$$

where $\nu'(\sigma_0)$ is given by (2.1) and $f(\sigma_0)$ by (3.1). Therefore, if the positive and negative large ions have b_1 and b_2 elementary charges respectively,

$$\eta_{12}=2\pi\sigma_0D_1\left\{1+\log\frac{N^{-\frac{1}{3}}}{4\sigma_0}\right\},$$

in which $\sigma_0=b_2e^2N(\theta)/P$. Moreover, from Paper I. Section 2, $D_1=ek_1b_2/\sigma_0$, whence

$$\eta_{12}=2\pi ek_1b_2\left\{1+\log\frac{N^{-\frac{1}{3}}P}{4b_2e^2N(\theta)}\right\}, \quad . \quad . \quad (4.3)$$

and similarly,

$$\eta_{21}=2\pi ek_2b_1\left\{1+\log\frac{N^{-\frac{1}{3}}P}{4b_1e^2N(\theta)}\right\}. \quad . \quad . \quad (4.4)$$

If $b_1=b_2$ these equations give $\eta_{12}/\eta_{21}=k_1/k_2$ ($=\eta_{10}/\eta_{20}$ for dust particles).

If now σ_0 is less than the mean free path, then the criterion for recombination is collision with the large ion, whatever the relative values of σ_0 and the radius of the ion, as is also the case for the radius of the ion greater than σ_0 and any value of the mean free path. We then have

$$\eta_{12}n_1N_2=\nu'(a_2)f(a_2)$$

where $\nu'(a_2)$ is given by (2.1) and $f(a_2)$ by (3.1). This gives

$$\eta_{12}=\eta_{10}(a_2)f(a_2)$$

where $\eta_{10}(a_2)$ is η_{10} for an uncharged nucleus of radius a_2. If m_1 and m_2 are the masses of the positive and negative small ions respectively, we therefore have

$$\eta_{12}=\eta_{10}(a_2)\left[1+\frac{\sigma_0}{a_2}\{1-\exp(-a_2/\xi\lambda_1)\}\log\frac{N^{-\frac{1}{3}}}{2(a_2+\sigma_0)}\right]$$
$$\times\left[1+\left\{\frac{2b_2e^2}{m_1U^2}\left(\frac{1}{a_2}-\frac{1}{\lambda_1}\right)\text{ or }0\right\}\right].$$

Now, since the velocity of agitation of the large ion is small compared with that of the small, $\frac{1}{2}m_1U^2=\frac{3}{2}B\theta$, where B is Boltzmann's constant. σ_0 is here $b_2e^2N(\theta)/P$, giving

$$\eta_{12}=\eta_{10}(a_2)\left[1+\frac{b_2e^2N(\theta)}{a_2P}\{1-\exp(-a_2/\xi\lambda_1)\}\right.$$
$$\left.\times\log\frac{N^{-\frac{1}{3}}}{2\{a_2+b_2e^2N(\theta)/P\}}\right]$$
$$\times\left[1+\left\{\frac{2b_2e^2}{3B\theta}\left(\frac{1}{a_2}-\frac{1}{\lambda_1}\right)\text{ or }0\right\}\right], \quad (4.5)$$

the alternative " or 0 " to be taken when $a_2>\lambda_1$. $\eta_{10}(a_2)$ is given by (4.1) on replacing a_0 by a_2, and, of course, η_{21}

is obtainable from (4.5) by interchanging the subscripts 1 and 2. Note that $\eta_{12}/\eta_{21} \neq k_1/k_2$.

5. *Application to Atmospheric Large Ions.*

The relation derived by Whipple (*loc. cit.*), is in the notation of this paper (and for $b_2=1$)

$$\eta_{12}=\eta_{10}(a_2)+4\pi e k_1,$$

and is incompatible with the relations here derived.

In applying the new theoretical results to large atmospheric ions the difficulty at once arises that we do not know the magnitude of the mean free path of the small ions. We do know, however, that it is comparable with both σ_0 and the radius of the large ion, so that its magnitude is important, and, furthermore, we are unfortunately interested in the range where the theory is at the same time most complicated and least reliable. We shall, therefore, postpone choosing a value for the mean free path and investigate how the various coefficients depend on the radius for different values of the mean free path between 10^{-5} and 10^{-6} cm.

In fig. 2 η_{10} and η_{20}, as given by (4.1) and (4.2) for atmospheric ions at 760 mm. pressure and 15° C., are plotted as functions of a_0 for different assumed values of λ_1 and λ_2 respectively. The numbers on the curves are the values of the mean free path in 10^{-6} cm. k_1 is taken as 357 and k_2 as 414 e.s.u.

η_{12} and η_{21} are functions of the ionic concentration N, whereas, of course, η_{10} and η_{20} are not *. The dependence is, however, slight, and quite insufficient to account for the variation with ionic concentration found by P. J. Nolan†, which was therefore probably due to a progressive change in the magnitude of the radius of the large ions. In the ensuing calculation N will be taken as 10^4 per c.c.

The theory of the recombination of small ions at high pressures developed in Paper I., in which the criterion for recombination was σ_0 collision, was found to be inapplicable to pressures less than about five atmospheres, whence it follows that σ_0 collision does not imply recombination at atmospheric pressure. This will be true whether, as in Paper I., the σ_0 sphere is occupied by a small

* α also is a function of N.

† Proc. Roy. Irish Acad. xxxviii. p. 49 (1929).

ion or whether, as here, it is occupied by a large ion. (4.3) and (4.4) are therefore only applicable to pressures greater than five atmospheres (and for $a_0 < \sigma_0$). As is to be expected from Paper I., they then give $\eta_{12}+\eta_{21}=2\alpha$.

Turning to (4.5) we find that it is applicable at atmospheric pressure for all values of $a_2 > \sigma_0$, but that it only holds for $a_2 < \sigma_0$ if $\sigma_0 < \lambda_1$, which, unfortunately, is probably not the case. Let us, however, investigate the possibilities of extrapolation. J. J. Nolan, Boylan, and

Fig. 2.

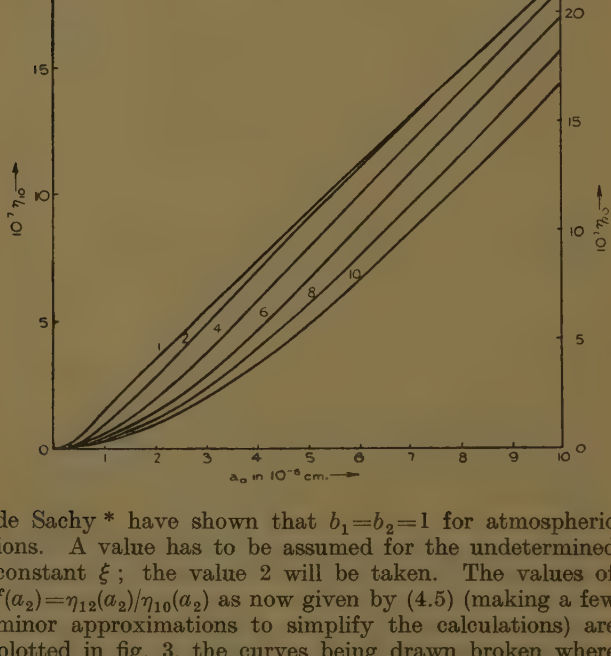

de Sachy * have shown that $b_1=b_2=1$ for atmospheric ions. A value has to be assumed for the undetermined constant ξ; the value 2 will be taken. The values of $f(a_2)=\eta_{12}(a_2)/\eta_{10}(a_2)$ as now given by (4.5) (making a few minor approximations to simplify the calculations) are plotted in fig. 3, the curves being drawn broken where the theory is inapplicable. $f(a_1)$ has the same value in terms of a_1 and λ_2 as $f(a_2)$ in terms of a_2 and λ_1. The numbers on the curves again refer to the mean free path

* Proc. Roy. Irish Acad. xxxvii. p. 1 (1925).

in 10^{-6} cm. For $a_2 > \lambda_1$ $f(a_2)$ for a value of ξ other than 2 is given by the curve for a mean free path $\frac{1}{2}\xi\lambda_1$.

$\eta_{12}(a_2) = f(a_2)\eta_{10}(a_2)$ and $\eta_{21}(a_1)$ are plotted in fig. 4. The inapplicability of the theory where the curves are shown broken is at once apparent for curves 1 and 2, since the

Fig. 3.

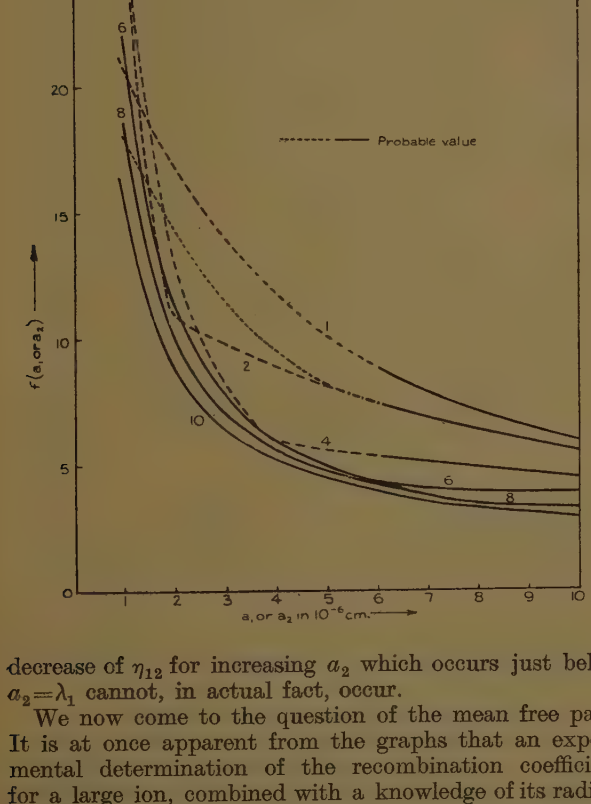

decrease of η_{12} for increasing a_2 which occurs just below $a_2 = \lambda_1$ cannot, in actual fact, occur.

We now come to the question of the mean free path. It is at once apparent from the graphs that an experimental determination of the recombination coefficient for a large ion, combined with a knowledge of its radius, enables the value of the mean free path of the small ion to be read off from fig. 4 by finding what value of the mean free path gives a curve through the point determined

by the recombination coefficient and the radius. This value of the mean free path is the proper one to substitute in the equation relating the mean free path and the mean velocity of agitation to the diffusion coefficient, whence the mean velocity of agitation may be found since the diffusion coefficient is known from the mobility. The law of equipartition of energy then gives the mass of the ion

Fig. 4.

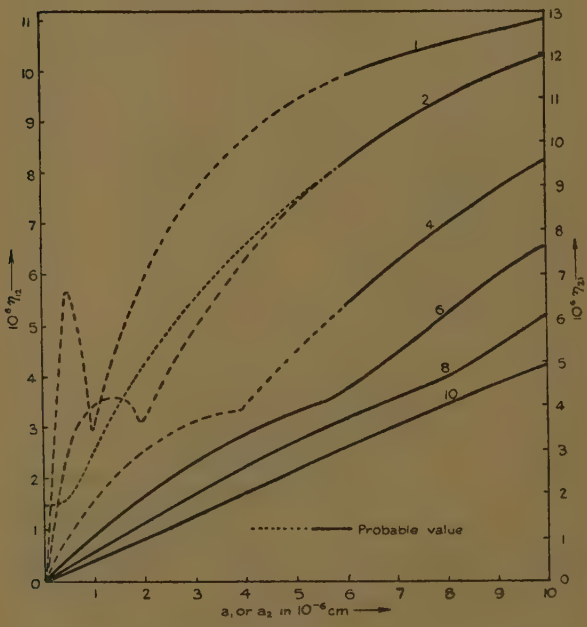

from its mean velocity of agitation. The mass of the small ion is easily seen to be

$$m_1 = \frac{\lambda_1^2 e^2 B\theta N^2(\theta)}{3P^2 k_1^2}.$$

An independent value for m_1 can be obtained if λ_1 is determined experimentally from η_{10} and a_0 using fig. 2. In this way it is theoretically possible to find the mass of a clustered ion *without requiring a knowledge of its size.*

So far as the author is aware, no other method has been proposed which dissociates the effect of mass from the effect of size, and which, therefore, does not pre-suppose a knowledge of the structure of the cluster in obtaining its mass. Unfortunately, the accuracy of the experimental results does not at present justify an investigation of the mass of clusters from the formation and recombination coefficients for large ions, quite apart from the insufficient numerical accuracy of the theory.

We must therefore take a plausible value for the mean free path in order to calculate the coefficients. The self diffusion coefficient of air is about six times the diffusion coefficient of small atmospheric ions in air, the difference being due to the combined effect of a change in the mean velocity of agitation due to clustering and a change in the mean free path due both to clustering and to the effect of charge. If there were no clustering the mean free path for air would be six times that for the ion. If there were no effect of charge then the ratio would be 3·3 if we assume that the cluster increases the collision area in the same proportion as the mass, as would be the case for a loose cluster. For a closely packed cluster for which the mass is proportional to the $\frac{3}{2}$ power of the collision area the ratio is 2·8. The mean free path in air being 9.10^{-6} cm. we ought, therefore, to be safe in assuming the mean free path for the ion to be between 1·5 and 3.10^{-6} cm. In default of further information the mean value $2{\cdot}25.10^{-6}$ cm. will be chosen, and this will be rounded off to 2.10^{-6} cm. The corresponding curves for the recombination coefficients and attraction factor are only applicable down to $a_0=6.10^{-6}$ cm. The recombination coefficient for a large ion and a small ion cannot, however, be less than the recombination coefficient for a pair of small ions, one of which is held fixed. From Paper I. this gives $\eta_{12}+\eta_{21}>2\alpha$, and α is $1{\cdot}6.10^{-6}$. Below $a_0=6.10^{-6}$ cm. therefore curve 2 in fig. 4 should decrease steadily to a lower limit of $\eta_{12}=1{\cdot}5.10^{-6}$ at $a_0=0$ instead of passing through a maximum and then falling off to zero. This enables the curve to be extrapolated with considerable certainty through the region where the theory is inapplicable. The extrapolated curve is shown dotted. Similar extrapolations for alternative assumed values of the mean free path could easily be carried out if desired. It is to be noted, however, that

at the most this would only alter the recombination coefficient by about 50 per cent., if the extremes calculated above for the mean free path are admitted. The extrapolated curve implies a different value of the attraction factor which is plotted in fig.3. Its shape (shown dotted) is more reasonable than the original shape, the sharp bend having now been eliminated. It would seem therefore that the final curves of figs. 3 and 4 cannot be greatly in error. Let us now compare their predictions with experiment.

6. *Comparison with Experiment.*

Considerable uncertainty attaches to the available experimental data, as is clear from a general survey by Israel *, who shows that the value obtained for the attraction factor depends to a large extent on the conditions prevailing at the time and place of measurement. That the experimental values depend also to a large extent on the interpretation of the measurements is illustrated by the fact that P. J. Nolan †, in re-interpreting some of his earlier work with O'Brolchain, reduced the value of η_{12} from $5{\cdot}7.10^{-6}$ to $1{\cdot}9.10^{-6}$. J. J. Nolan, Boylan, and de Sachy ‡, on the other hand, find $\eta_{12}=8{\cdot}7.10^{-6}$. It is probable that the ions on which the experiments were carried out were the Langevin ions, for which the radius may be deduced from the mobility with comparative certainty, using Stokes's law as modified by Cunningham, the radius being § $4{\cdot}5.10^{-6}$ cm. The theoretical value of η_{12} is therefore $7{\cdot}2.10^{-6}$. This agrees very well with the value of J. J. Nolan, Boylan, and de Sachy, and with the earlier value of P. J. Nolan, but not with his revised value. The revised value would, however, imply an improbably small radius for the large ion, so, on the whole, it would seem that the Langevin value of the radius is confirmed. Assuming the nuclei to have had the same radius as the large ions the attraction factor should therefore be 8·7. J. J. Nolan, Boylan, and de Sachy find 1·3 and P. J. Nolan 2·1, values which would

* Gerland's Beiträge, xl. p. 29 (1933).

† Proc. Roy. Irish Acad. xli. p. 61 (1933).

‡ Proc. Roy. Irish Acad. xxxvii. p. 1 (1925); and J. J. Nolan and de Sachy, Proc. Roy. Irish Acad. xxxvii. p. 71 (1927).

§ Thomson, 'Conduction of Electricity through Gases,' i. p. 189 (1928).

imply a very much larger and improbable value for the radius, and which cannot be reconciled with their values of η_{12} by assuming a different value for the mean free path. The value 4·8 found by Wait and Torreson * is in better agreement, but still differs from the theoretical one by nearly a factor of 2. Moreover, Israel (*loc. cit.*) finds that a value about 4 is very frequent. An attraction factor as high as 8·7 finds no support from experiment. Here therefore is a discrepancy which, unless it shows the theory to be numerically in error to an extent which seems improbable to the author, demands a new interpretation of the observations.

7. *The Combination Coefficient for uncharged Particles.*

Equation (2.1) may be used as a basis for calculating the combination coefficient for uncharged particles. If the particles are homogeneous and spherical and combine whenever they come into contact, we have, in fact, for a coagulation coefficient χ defined by the equation

$$\frac{dN_0}{dt} = -\chi N_0^2,$$

$$\chi N_0^2 = \pi N_0^2 (2a_0)(2D_0)[1-\exp\{-Ua_0/D_0\}],$$

where D_0 is the diffusion coefficient of the uncharged particle and is given by the well-known theory of Stokes as modified by Cunningham. Using Meyer's relation we have

$$\chi = 4\pi a_0 D_0[1-\exp\{-3a_0/\lambda_0\}], \quad . \quad . \quad (7.1)$$

where λ_0 is the mean free path of the particle. If λ_0 is considerably less than a_0 the equation reduces to $\chi = 4\pi a_0 D_0$. It must be generalised to allow for inhomogeneity of the particles, the possibility of their not being spherical, and for other factors before being compared with experiment. This is being discussed in detail elsewhere † with reference to a comparison of (7.1) with the similar formula of Smoluchowski which has hitherto been applied to the coagulation of uncharged smoke and colloid particles. It must not be overlooked that the effect of heterogeneity and other factors may also be of importance in the application of the other equations of this paper.

* 'Congrès Internationale D'Electricité,' Paris, 1932.

† In a paper submitted to the 'Transactions of the Faraday Society.'

VIII. *An X-ray Investigation of the Arsenic-Tin System of Alloys.* *By* W. H. Willott, *B.Sc. and Prof.* E. J. Evans, *D.Sc., Physics Department, University College, Swansea* *.

VARIOUS compounds of arsenic and tin have been reported from time to time. The first systematic work was carried out by Stead[1], who described the preparation and isolation of crystals of Sn_3As_2. Jolibois and Dupruis[2] examined the system thermally, from pure tin to an alloy containing 50 per cent. by weight of arsenic, and obtained the compounds Sn_4As_3 and SnAs. Parravano and de Cesaris [3], by studying the arrests in the cooling curves of the alloys, obtained three phases extending over the following ranges of composition, pure tin to 30 per cent. of arsenic, 30 per cent. of arsenic to 40 per cent. of arsenic, and 40 per cent. of arsenic to 50 per cent. of arsenic respectively, and concluded from their results that the compounds Sn_3As_2 and SnAs existed.

Mansuri [4], by means of a thermal and micrographic analysis, obtained the equilibrium diagram illustrated in fig. 1. The phase from 0 to 29·6 per cent. of arsenic consists of a mixture of pure tin and the compound α which is Sn_3As_2. The $\alpha+E$ phase is a mixture of the compound α and the phase E which corresponds to 34·5 per cent. of arsenic. This is followed by a phase, which is a mixture of E and the compound β, which is SnAs and corresponds to a composition of 38·7 per cent. of arsenic. The homogeneous γ phase is a solid solution of arsenic in the compound SnAs and has a range extending from 38·7 to 46·0 per cent. of arsenic. This is followed by two mixture phases, the first consisting of the γ and E′ phases, and the other, a mixture of the E′ with the δ phase, which is a solid solution of tin in arsenic ranging from 68·0 per cent. of arsenic to the end of the series.

This diagram is similar to that obtained by Guertler [5] for the antimony-tin system of alloys, except that in the latter case there is a solid solution of antimony in tin. Bowen and Morris Jones [6] examined the antimony-tin system and found no crystal evidence of the compound

* Communicated by Prof. E. J. Evans.

Sn_3Sb_2, but obtained solid solutions on both sides of the compound SnSb having ranges extending from 40 to 50 per cent. of antimony, and from 50 to 54 per cent. of antimony. The alloy containing 50 per cent. of antimony corresponds to the compound SnSb.

The present investigation was undertaken to examine fully the crystal structure at room-temperature of the arsenic-tin system of alloys by means of X-rays. The experimental results will be discussed in relation to the equilibrium diagram.

Fig. 1.

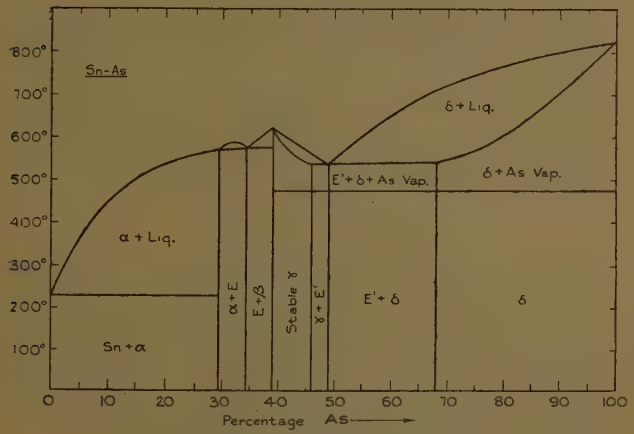

Mansuri's equilibrium diagram.

Preparation of the Alloys.

The alloys of low arsenic content were prepared in evacuated pyrex tubes, hermetically sealed. The tube, containing sufficient metal to yield an ingot of about 10 grams in weight, was placed vertically in a small crucible and transferred to a gas-fired muffle furnace. Great difficulty was experienced in preparing alloys containing more than 60 per cent. of arsenic by weight, as the vapour pressure of the arsenic was sufficient to expand and burst the tube. An attempt was made to overcome this difficulty by placing the tube in an iron bomb, tightly packed with sand, but without success

The difficulty was eventually overcome by the use of quartz tubes of the same volume as the pyrex tubes, and by the employment of much smaller quantities of arsenic and tin in the preparation of the alloys.

Owing to the tendency of arsenic to sublime and condense on the sides of the tube, an additional 10 per cent. of arsenic was added when preparing alloys of a desired composition. The resulting alloys were carefully examined for homogeneity, and if unsatisfactory were discarded.

Annealing.

The alloys were placed in pyrex tubes which were evacuated and sealed. The tubes were then placed in an electric furnace and the temperature measured by a calibrated copper-constantan thermo-couple. The three alloys of lowest arsenic content were annealed for three weeks at 200° C., and the remainder at 400° C. for the same period. All the alloys were finally annealed down to room-temperature.

Analysis of the Alloys.

The analysis of the alloys presented difficulties. Mansuri's method, which relies on dissolving the alloys in nitric acid, collecting the precipitated metastannic acid, thoroughly washing, and weighing the tin as oxide, was not wholly satisfactory. The alloys of high arsenic content took days to dissolve in the hot acid, and as it was difficult to determine when solution was complete the tin oxide almost invariably contained arsenic.

The following method was finally adopted, as it was found that on analysing known mixtures of pure tin and arsenic the method gave results which were accurate to within 0·2 per cent.

About half a gram of roughly powdered alloy was carefully weighed, and was then dissolved in the least quantity of nitric acid to which a drop or two of hydrochloric acid was added. The alloy, even if it contained a high percentage of arsenic, dissolved fairly rapidly, and when the action was complete the whole of the solution was evaporated to dryness. About 30 c.c. of concentrated nitric acid were then added, and the solution was again evaporated to dryness. This process of adding nitric acid and evaporating was further repeated to ensure

the complete removal of hydrochloric acid. When the bulk of liquid had reached 10 c.c. the final evaporation was arrested, and the liquid was diluted to 250 c.c. by the addition of water.

After almost neutralising with ammonia, the slightly acid solution was allowed to stand overnight, when the tin was precipitated as metastannic acid. The solution was filtered and the precipitate washed free from acid.

The precipitate, after being transferred together with the filter paper to a flask, was dissolved in concentrated hydrochloric acid, a small piece of pure iron added, and the solution was kept just on the boil for half an hour. The nascent hydrogen evolved partially reduced the stannic chloride, whilst the iron threw any trace of arsenic out of solution.

The paper pulp and precipitated arsenic were filtered off and the solution made up to exactly 100 c.c. The tin was then reduced to the stannous state by means of pure nickel, and the solution was titrated against standard iodine solution in the usual manner.

The Experimental Method.

The well-known powder method, depending on the use of the Debye-Scherrer camera, was employed in the investigation of the crystal structure of the alloys.

A demountable Coolidge tube, fitted with a copper target, produced the X-ray beam, which was deprived of the K_β radiation by passing the beam through a thin nickel foil. The tube was run at 23 milliamperes and 45,000 volts, and was kept exhausted by means of a mercury vapour pump backed by a rotary oil pump.

The camera was a 9 cm. brass cylinder, fitted with a lead slit 1 mm. in diameter. The film was wrapped round the outside and firmly held in position by a wide rubber band.

Most of the alloys were brittle and were ground to a fine powder in an agate mortar, but a few of high tin content had to be rubbed down on fine emery paper. The fine powder was painted on a thin copper wire to a thickness of $0{\cdot}75 \pm 0{\cdot}05$ mm., cellulose acetate being used as the adhesive.

Kodak duplitized X-ray films were used in taking the photographs. The distance between the lines on these

films was measured on a Bellingham Stanley's low power travelling microscope.

The openings running round the camera terminated in knife edges on opposite sides of the slit, and these edges gave two fiducial marks on the films. These marks were used to correct the film for shrinkage.

TABLE I.

Alloy.	Percentage by wt. of arsenic.	Crystal structure.	Dimensions of unit cell in A.U.
Tin	0	Simple tetragonal.	a_0 5·81$_7$ c_0 0·546
A	12·4	Simple tetragonal.	a_0 5·83$_3$ c_0 0·546
B	24·0	Simple tetragonal.	a_0 5·84$_2$ c_0 0·546
C	28·8	Simple tetragonal.	a_0 5·85$_4$ c_0 0·546
D	32·6	Simple tetragonal and Sodium chloride.	a_0 5·85$_5$ c_0 0·546 a_0 5·71$_3$
E	33·6	Simple tetragonal and Sodium chloride.	a_0 5·85$_3$ c_0 0·546 a_0 5·71$_4$
F	38·0	Sodium chloride.	a_0 5·68$_8$
G	40·8	Sodium chloride.	a_0 5·68$_6$
H.....	43·0	Sodium chloride.	a_0 5·69$_6$
I	47·4	Sodium chloride.	a_0 5·71$_3$
J	52·8	Sodium chloride and Face-centred rhombohedral.	a_0 5·71$_3$ a_0 5·59$_0$ α85° 0′
K.....	55·3	Sodium chloride and Face-centred rhombohedral.	a_0 5·71$_4$ a_0 5·59$_4$ α 85° 0′
L	62·6	Sodium chloride and Face-centred rhombohedral.	a_0 5·71$_3$ a_0 5·59$_3$ α 85° 0′
M.....	65·4	Sodium chloride and Face-centred rhombohedral.	a_0 5·71$_7$ a_0 5·59$_1$ α 85° 0′
N	76·8	Face-centred rhombohedral.	a_0 5·59$_1$ α 84° 50′
O	87·0	Face-centred rhombohedral.	a_0 5·59$_0$ α 84° 40′
Arsenic ..	100·0	Face-centred rhombohedral.	a_0 5·59$_0$ α 84° 36′

The calibration of the camera was carried out by taking films of sodium chloride, and from its known plane spacings obtaining a correction curve. This correction curve was employed in the calculation of the lattice constants of pure tin, and the results obtained were in good agreement with those determined by Bowen and Morris Jones [6] and Westgren and Phragmén [7].

Bradley and Jay's [8] method of computing crystal parameters was tried, but the quality of the films in the region of large angles of diffraction did not permit its use, as the intensity of the general scattering in this region was comparable with that of the diffraction lines.

The results are estimated to be correct to within 1 in 1000.

The Experimental Results.

A summary of the results is shown in Table I., which gives the composition, crystal structure, and lattice

Fig. 2.

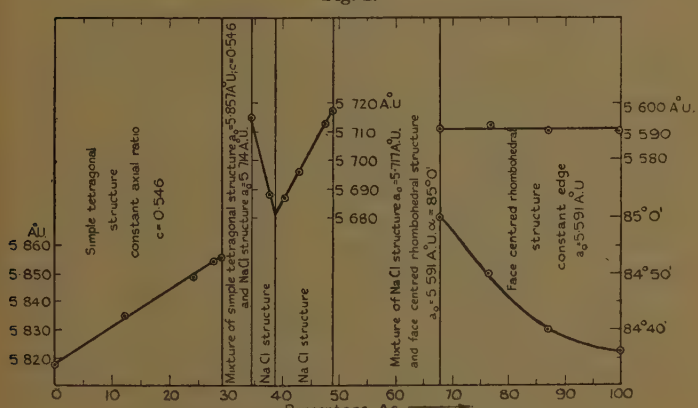

The crystal structure of the arsenic-tin alloys.

dimensions of each alloy. The variations of the crystal lattices are also shown in fig. 2.

The results indicate that the phase from 0 to 29·5 per cent. of arsenic is a solid solution and not a mixture of tin and Sn_3As_2. There is no evidence of the compound Sn_3As_2. The compound SnAs has a sodium chloride structure, which persists as a homogeneous phase over the range extending from 34·5 to 49·0 per cent. of arsenic, and is accompanied by changes of lattice constant, showing that the compound SnAs dissolves both tin and arsenic. The sodium chloride structure has a range extending from 29·5 to 68·0 per cent. of arsenic, indicating the presence of two mixture phases, one extending from

29·5 to 34·5 per cent. of arsenic and the other from 49·0 to 68·0 per cent. of arsenic respectively. The existence of a solid solution of tin in arsenic is confirmed.

The full X-ray data obtained from the films are given in Tables II. to VI. Column 1 gives the Miller indices of the plane spacings, while the relative intensities of the lines on the films are denoted by St. (strong), M. (medium), W. (weak), and V.W. (very weak) in column II. The other columns give the plane spacings and lattice constants, as deduced from measurement of the films.

The Homogeneous Phase from 0 *to* 29·5 *per cent. of Arsenic.*

The equilibrium diagram (fig. 1) shows this phase to be a mixture of pure tin and the compound Sn_3As_2. Its crystal structure was investigated by means of pure tin and alloys A, B, and C containing 12·4, 24·0, and 28·8 per cent. of arsenic respectively.

The data obtained from the films are given in Table II. All the lines belong to a simple tetragonal structure, and there is no evidence of a structure corresponding to Sn_3As_2.

The plane spacings of pure tin correspond to a simple tetragonal lattice of axial ratio 0·546 and a lattice constant (a_0) $5{\cdot}81_7$ Å.U., which are in good agreement with the results of Bowen and Morris Jones [6], and also with the results of Westgren and Phragmén [7].

Alloys A, B, and C, which are also tetragonal, have the same axial ratio 0·546 and lattice constants (a_0) $5{\cdot}83_5$, $5{\cdot}84_9$, and $5{\cdot}85_4$ Å.U. respectively.

These alloys must therefore lie inside the limits of a homogeneous phase, as no evidence of the α component is obtained. Alloys D and E show that the limit of expansion of the above lattice is $5{\cdot}85_7$ Å.U., which fixes the end of the solid solution at 29·5 per cent. of arsenic. The phase extending from 0 to 29·5 per cent. of arsenic is therefore a solid solution, which causes the lattice to expand from $5{\cdot}81_7$ Å.U. to $5{\cdot}85_6$ Å.U. at 29·5 per cent. of arsenic, the limit of the solid solution (see fig. 2).

The Mixture Phase between 29·5 *and* 34·5 *per cent. of Arsenic.*

Alloys D and E, which contain 32·6 and 33·6 per cent. of arsenic respectively, were examined in this phase. Their X-ray data are shown in Table III.

TABLE II.

The Homogeneous Phase between 0 and 29·5 per cent. of Arsenic.

Plane.	Relative intensity.	Pure tin.		Alloy A.		Alloy B.		Alloy C.	
		0% As.	100% Sn.	12·4% As.	87·6% Sn.	24·0% As.	76·0% Sn.	28·8% As.	71·2% Sn.
		d/n.	a_0 in A.U.	d/n.	a_0 in A.U.	d/n.	a_0 in A.U.	d/n.	a_0 in A.U.
100 (2)...	St.	2·908	5·816	2·921	5·842	2·926	5·852	2·924	5·848
101 (2)...	St.	2·786	5·818	2·794	5·840	2·805	5·854	2·805	5·854
110 (2)...	W.	2·058	5·820	2·066	5·843	—	—	2·074	5·865
211.....	St.	2·011	5·816	2·024	5·852	2·024	5·852	2·022	5·848
301.....	M.	1·656	5·821	1·661	5·838	1·661	5·838	1·665	5·859
112.....	M.	1·480	5·814	1·487	5·844	1·495	5·858	—	—
100 (4)...	W.	1·454	5·816	1·460	5·840	1·459	5·838	—	—
231.....	M.	1·439	5·821	1·443	5·836	1·445	5·843	1·446	5·849
120 (2)...	W.	1·301	5·818	1·304	5·827	1·311	5·860	1·312	5·865
411.....	W.	1·289	5·817	1·292	5·830	1·295	5·842	1·296	5·847
312.....	M.	1·203	5·820	1·206	5·833	1·209	5·849	1·210	5·852
431.....	W.	1·094	5·817	1·095	5·826	1·097	5·844	1·100	5·862
103.....	W.	1·039	5·803	1·044	5·833	1·047	5·853	1·048	5·857
113.....	W.	1·025	5·818	1·026	5·824	1·030	5·850	1·031	5·855
123.....	W.	0·980	5·818	0·982	5·827	0·985	5·849	—	—
101 (3) ..	M.	0·928	5·807	0·933	5·837	0·938	5·860	0·935	5·847
233.....	W.	0·885	5·818	0·887	5·831	0·889	5·842	—	—
541.....	W.	0·873	5·824	—	—	0·875	5·843	0·875	5·843
413.....	W.	0·846	5·818	0·849	5·838	—	—	—	—
631.....	W.	0·837	5·826	0·837	5·826	—	—	—	—
		Mean .. 5·817		Mean .. 5·835		Mean .. 5·849		Mean .. 5·854	

Structure.—Simple tetragonal. Constant axial ratio c_0=0·546.

Both alloys show the presence of a simple tetragonal lattice, together with a sodium chloride type lattice. The dimensions of the tetragonal lattice are practically constant, the axial ratio being 0·546 in each case, and the edge of the lattice $5{\cdot}85_5$ and $5{\cdot}85_8$ Å.U. respectively, while the dimensions of the cubic lattice, which are also constant within experimental error, are $5{\cdot}71_3$ and $5{\cdot}71_4$ Å.U.

TABLE III.

The Mixture Phase between 29·5 and 34·5 per cent. of Arsenic.

Plane.	Relative intensity.	Alloy D.		Alloy E.	
		32·6% As.	67·4% Sn.	33·6% As.	66·4% Sn.
		d/n.	a_0. in Å.U.	d/n.	a_0 in Å.U.
100 (2) ...	**M.**	**2·930**	**5·860**	**2·932**	**5·864**
100 (2) ...	St.	2·854	5·708	2·853	5·706
101 (2) ...	**M.**	**2·807**	**5·857**	**2·810**	**5·865**
211	**M.**	**2·023**	**5·848**	**2·026**	**5·854**
101 (2) ...	St.	2·018	5·706	2·019	5·709
310	**W.**	**1·664**	**5·857**	**1·664**	**5·857**
111 (2) ...	M.	1·650	5·713	1·650	5·714
112	**W.**	**1·493**	**5·852**	**1·494**	**5·855**
231	**W.**	**1·447**	**5·857**	**1·448**	**5·860**
210	W.	1·278	5·718	1·277	5·713
312	**W.**	**1·208**	**5·852**	**1·208**	**5·852**
110 (4) ...	V.W.	0·952	5·714	0·954	5·720
101 (3) ...	**V.W.**	**0·934**	**5·862**	**0·933**	**5·859**
310 (2) ...	W.	0·905	5·719	0·904	5·717
311 (2) ...	W.	0·861	5·714	0·862	5·718
		Means..	5·713 **5·855**	Means..	5·714 **5·858**

Structure.—Mixture of simple tetragonal $a_0=5{\cdot}856$ Å.U. $c_0=0{\cdot}546$ and sodium chloride type $a_0=5{\cdot}71_4$ Å.U.
Lines of tetragonal in heavy type.

The Homogeneous Phase from 34·5 to 49·0 *per cent. of Arsenic including the Compound SnAs.*

The structure of these phases was investigated by means of the alloys F, G, H, and I, whose X-ray data are shown in Table IV.

These results show that all alloys in this region have a cubic structure of the sodium chloride type.

TABLE IV.

The Homogeneous Phase between 34·5 and 49·0 per cent. of Arsenic.

Plane	Relative intensity.	Alloy F.		Alloy G.		Alloy H.		Alloy I.	
		38% As.	62% Sn.	40·8% As.	59·2% Sn.	43% As.	57% Sn.	47·4% As.	52·6% Sn.
		d/*n*.	a_0 in Å.U.	*d*/*n*.	a_0 in Å.U.	*d*/*n*.	a_0 in Å.U.	*d*/*n*.	a_0 in Å.U.
111	V.W.	3·279	5·679	—	—	3·276	5·675*	—	—
100 (2)...	St.	2·842	5·684	2·840	5·680	2·847	5·694	2·850	5·700
110 (2)...	St.	2·009	5·682	2·010	5·684	2·015	5·700	2·022	5·720
310.....	V.W.	1·793	5·670*	—	—	—	—	—	—
311.....	V.W.	1·717	5·694*	—	—	—	—	—	—
111 (2)...	M.	1·641	5·684	1·639	5·679	1·645	5·700	1·649	5·711
100 (4)...	W.	1·420	5·684	1·419	5·679	1·422	5·688	1·429	5·714
210 (2)...	M.	1·272	5·690	1·269	5·678	1·273	5·693	1·278	5·716
211 (2)...	M.	1·161	5·690	1·160	5·686	1·162	5·698	1·166	5·718
110 (4)...	V.W.	1·005	5·690	1·006	5·691	1·007	5·700	1·010	5·714
100 (6)...	M.	0·950	5·699	0·949	5·696	0·949	5·696	0·952	5·715
310 (2)...	M.	0·899	5·691	0·900	5·695	0·900	5·695	0·903	5·713
311 (2)...	M.	0·858	5·696	0·859	5·699	0·859	5·699	0·861	5·714
		Mean .. 5·688		Mean .. 5·686		Mean .. 5·696		Mean .. 5·713	

Structure.—Sodium chloride.

* Lines very faint; too weak to measure accurately. Have not been used in determining the mean.

The lattice dimension of alloy F, containing 38·0 per cent. of arsenic, is $5{\cdot}68_8$ Å.U., while alloys G, H, and I, which contain a greater percentage of arsenic than the compound SnAs and have compositions corresponding to 40·8, 43·0, and 47·4 per cent. of arsenic, give lattice dimensions of $5{\cdot}68_6$, $5{\cdot}69_5$, and $5{\cdot}71_3$ Å.U. respectively.

From these values and those of the cubic lattices in the adjacent mixture phases, it is found that the limit of the solid solution of arsenic in the compound is situated at 49·0 per cent. of arsenic, while the limit of the solubility of tin in the compound is at 34·5 per cent. of arsenic (see fig. 2). The compound SnAs has a lattice dimension of $5{\cdot}68_1$ Å.U.

Reference to Mansuri's equilibrium diagram (fig.1) shows the existence of these phase boundaries. The phase ranging from 34·5 per cent. of arsenic to the compound SnAs is recorded as a mixture of E and SnAs; but the present investigation indicates that tin dissolves in SnAs, forming a solid solution, which increases the lattice from $5{\cdot}68_1$ Å.U. to $5{\cdot}71_4$ Å.U. at the limit of the solution. The existence of the solid solution of arsenic in the compound SnAs is confirmed, but it extends over a longer range (from 38·7 to 49·0 per cent. of arsenic) than given in Mansuri's equilibrium diagram. This solution of arsenic causes an expansion of the lattice from $5{\cdot}68_1$ to $5{\cdot}71_7$ Å.U.

Goldschmidt [9], who has made a special study of the relationship of crystal structure to chemical constitution, determined the lattice constant of the compound SnAs and obtained the value $5{\cdot}70_8$ Å U, which is higher than that obtained in the present work

The atomic radii of Sn^{+3} and As^{-3}, as determined by Pauling [10], are 0·75 and 2·22 Å U. respectively, and these results applied to SnAs give a lattice constant of 5·94 Å.U., which is decidedly larger than the experimental value. According to Goldschmidt [9] the coordination number of the sodium chloride structure is 6, and the atomic radii of tin and arsenic, having a coordination number 8, are 1·53 and 1·36 Å.U. respectively. These values of the radii reduced to a coordination number 6 become 1·484 and 1·319 Å.U., and give a sodium chloride type SnAs lattice of constant $5{\cdot}60_6$ Å.U. This lattice constant is in closer agreement with the experimental value $5{\cdot}68_1$ Å.U. than that deduced from Pauling's data.

The density of the compound SnAs, calculated on the assumption of 4 atoms per unit cell of sodium chloride type, is 6·90, which is in reasonably good agreement with the experimental value 6·85. This value was determined by the specific gravity bottle, using a small specimen of the alloy.

The Mixture Phase between 49·0 *and* 68·0 *per cent. of Arsenic.*

The alloys J, K, L, and M were examined in this phase. The films, from which the data given in Table V. were deduced, show the presence of lines corresponding to the cubic structure of the preceding phase, together with a face-centred rhombohedral lattice. The cubic lattices of the above alloys had practically constant dimensions $5{\cdot}71_8$, $5{\cdot}71_4$, $5{\cdot}71_8$, and $5{\cdot}71_7$ Å.U., while the rhombohedral lattices had an angle of 85° 0′ and an edge of practically constant dimensions $5{\cdot}59_0$, $5{\cdot}59_4$, $5{\cdot}59_2$, and $5{\cdot}59_1$ Å.U. respectively.

The Homogeneous Phase between 68·0 *and* 100·0 *per cent. of Arsenic.*

The data obtained from the films of the alloys N and O and from pure arsenic, which were examined in this phase, are shown in Table VI.

This table shows that for the alloy N, containing 76·8 per cent. of arsenic, the dimensions of the rhombohedral lattice are (a_0) $5{\cdot}59_1$ Å.U. and α 84° 50′, while for alloy O, containing 87·0 per cent. of arsenic, the angle decreases to 84° 40′, but the edge of the rhomb remains constant at $5{\cdot}59_0$ Å.U.

Pure annealed arsenic gave a face-centred rhombic lattice of dimensions (a_0) $5{\cdot}59_0$ Å.U. and α 84° 36′, agreeing to within 1 to 500 with the previously determined values, viz. :—

Bradley [11]	(a_0) $5{\cdot}60_0$ Å.U.	α 84° 36′
Jung [12]	(a_0) $5{\cdot}59_9$ Å.U.	α 84° 15′
Olhausen [13]	(a_0) $5{\cdot}59_4$ Å.U.	α 84° 12′

It is difficult to fix the limit of the solid solution of tin in arsenic with accuracy, as the change of the angle of the rhomb is so small. It is seen from an examination

Table V.

The Mixture Phase between 49·0 and 68·0 per cent. of Arsenic.

Plane.	Relative intensity.	Alloy J.		Alloy K.		Alloy L.		Alloy M.	
		52·8% As.	47·2% Sn.	55·4% As.	44·6% Sn.	62·6% As.	37·4% Sn.	65·4% As.	34·6% Sn.
		d/n.	a_0 in Å.U.	d/n.	a_0 in Å.U.	d/n.	a_0 in Å.U.	d/n.	a_0 in Å.U.
111.....	V.W.	**3·301**	**5·717**	—	—	**3·306**	**5·726***	—	—
100 (2)...	M.	2·862	5·724	2·857	5·714	2·859	5·718	2·859	5·718
100 (2)...	**M.**	**2·795**	**5·590**	**2·799**	**5·598**	**2·803**	**5·607**	**2·799**	**5·598**
110 (2)...	**M.**	**2·048**	**5·592**	**2·050**	**5·596**	**2·047**	**5·589**	**2·050**	**5·596**
110 (2)...	M.	2·022	5·720	2·019	5·710	2·022	5·720	2·022	5·720
110 (2)...	**M.**	**1·889**	**5·589**	**1·892**	**5·597**	**1·889**	**5·589**	**1·889**	**5·589**
111 (2)...	W.	1·651	5·717	—	—	—	—	1·651	5·717
111 (2)...	**M.**	—	—	—	—	**1·574**	**5·588**	**1·572**	**5·580**
100 (4)...	**W.**	**1·396**	**5·586**	**1·397**	**5·588**	1·398	**5·591**	**1·397**	**5·588**
210 (2)...	M.	1·278	5·716	1·277	5·712	1·279	5·720	1·277	5·712
210 (2)...	**W.**	**1·278**	**5·586**	**1·277**	**5·585**	**1·279**	**5·586**	**1·277**	**5·585**
211 (2)...	W.	1·166	5·718	1·165	5·716	1·165	5·716	1·166	5·718
431.....	**W.**	**1·163**	**5·595**	**1·165**	**5·602**	**1·165**	**5·602**	**1·166**	**5·602**
110 (4)...	V.W.	1·011	5·720	1·011	5·720	1·011	5·720	1·012	5·724
100 (6)...	W.	0·952	5·714	0·953	5·719	0·953	5·719	0·952	5·714
310 (2)...	W.	0·903	5·713	0·903	5·713	0·903	5·713	0·904	5·717
311 (2)...	W.	0·861	5·714	0·861	5·714	0·861	5·714	0·861	5·714
		Means	5·718 **5·590**	Means	5·714 **5·594**	Means	5·718 **5·592**	Means	5·717 **5·591**

Structure.—Mixture of sodium chloride. $a_0 = 5{\cdot}71_7$ Å.U. and face-centred rhombic; $a_0 = 5{\cdot}59_2$ Å.U.; $\alpha = 85°\ 0'$.
Lines of rhombohedral lattice in heavy type.
* Line very weak; too faint to measure accurately. **Has not been used in determining the mean.**

TABLE VI.

The Homogeneous Phase between 68·0 and 100 per cent. of Arsenic.

Plane.	Relative intensity.	Alloy N. 76·8% As. 23·2% Sn.		Alloy O. 87·0% As. 13·0% Sn.		Pure Arsenic. 100% As. 0·0% Sn.	
		d/n.	a_0 in Å.U.	d/n.	a_0 in Å.U.	d/n.	a_0 in Å.U.
100 (2)	St.	2·776	5·592	2·770	5·585	2·776	5·598
110 (2)	St.	2·047	5·586	2·063	5·603	2·049	5·587
$1\bar{1}0$ (2)	St.	1·885	5·592	1·886	5·601	1·880	5·587
320 & 321	V.W.	—	—	—	—	1·599	5·595
$1\bar{1}1$ (2)	St.	1·557	5·586	1·557	5·597	1·556	5·587
100 (4)	M.	1·389	5·596	1·388	5·593	1·385	5·584
331	W.	—	—	—	—	1·368	5·589
210 (2)	M.	1·286	5·603	1·283	5·588	1·286	5·590
111 (3)	W.	—	—	—	—	1·172	5·589
430	M.	1·164	5·605	1·163	5·591	1·161	5·588
211 (2)	M.	1·115	5·583	1·114	5·584	1·114	5·592
$\bar{2}11$ (2)	W.	—	—	—	—	1·085	5·589
$5\bar{1}0$	M.	1·070	5·590	1·081	5·586	1·070	5·589
520	M.	1·064	5·593	1·065	5·596	1·062	5·592
532 & 411	W.	—	—	1·032	—	1·032	5·592
221 (2)	W.	—	—	—	—	0·995	5·589
531	W.	—	—	—	—	0·970	5·599
$1\bar{1}0$ (4)	M.	0·942	5·599	0·941	5·589	0·942	5·598
100 (6)	W.	0·930	5·596	—	—	0·923	5·584
530	V.W.	—	—	—	—	0·918	5·598
$6\bar{1}1$	V.W.	—	—	—	—	0·897	5·590
311 (2)	W.	0·888	5·598	0·889	5·603	0·888	5·602
443	W.	—	—	—	—	0·864	5·596
$3\bar{1}0$ (2)	W.	0·855	5·594	0·854	5·588	0·854	5·585
$62\bar{1}$	V.W.	—	—	—	—	—	5·602
		Mean .. 5·591 $\alpha = 84° 50'$		Mean .. 5·590 $\alpha = 84° 40'$		Mean .. 5·590 $\alpha = 84° 36'$	

Structure.—Face-centred rhombohedral. Constant edge $5·59_0$ Å.U.

of Table VI. that, as the percentage of tin increases from 0 to 32·0 per cent., the angle changes by 24′. The experimental results indicate, however, that the end of the solid solution is in the neighbourhood of 68·0 per cent. of arsenic, as determined by Mansuri.

When investigating the antimony-tin system Bowen and Morris Jones [6] observed that the angle of the rhombohedral lattice of antimony varied from 87° 24′ for pure antimony to 86° 30′ for an alloy containing 10 per cent. of tin, which is the limit of the solid solution, while the edge of the rhomb remained constant at $6{\cdot}22_0$ Å.U. A like change, but less in extent, is noted when tin dissolves in arsenic. In this case the angle only varies from 84° 36′ to 85° 0′ over a 32·0 per cent. solid solution, the edge of the rhomb remaining constant at $5{\cdot}59_1$ Å.U.

This work shows the close resemblance of the arsenic-tin to the antimony-tin system. In both cases there exist solid solutions in tin, but the solubility of arsenic is 29·5 per cent. as compared with 9·0 per cent. for antimony. Both systems also give compounds of the form AB, bounded by solid solutions. In addition, whilst tin dissolves in both antimony and arsenic, the solubility of tin in antimony is only 10·0 per cent. as compared with its 32·0 per cent. solubility in arsenic.

References.

(1) Stead, J. Soc. Chem. Ind. xvi. p. 200 (1897).
(2) Jolibois and Dupruis, *Compt. Rend.* clii. p. 1312 (1911).
(3) Parravano and de Cesaris, *Rend. R. Accad. Lincie*, v. (20), p. 593 (1911); *Gazzetta*, xlii. p. 274 (1912).
(4) Mansuri, J. Soc. Chem. cexli. p. 123 (1923).
(5) Guertler, 'Metallographie,' i. p. 803; 'International Critical Tables,' ii. p. 417.
(6) Bowen and Morris Jones, Phil. Mag. xii. p. 441 (1931).
(7) Phragmén and Westgren, *Zeits. Anorg. Chem.* clxxv. p. 80 (1928).
(8) Bradley and Jay, Proc. Phys. Soc. pt. 6, xliv. p. 563 (1933).
(9) Goldschmidt, Trans. Faraday Soc. xxv. p. 253 (1929).
(10) Pauling, J. Amer. Chem. Soc. xliv. p. 765 (1927).
(11) Bradley, Phil. Mag. xlvii. p. 657 (1924).
(12) Jung, *Centralblat für Mineralogie, Geologie und Palaontologie*, xiv. p. 107 (1926) A.
(13) Olhausen, *Zeit. Krist.* viii. p. 250 (1925).

February 1934.

IX. *The Structure of Atomic Nuclei.*

By HAROLD J. WALKE, *B.Sc., Mardon Research Scholar, Department of Physics, Washington Singer Laboratories, University College, Exeter* *.

1. *General Introduction.*

AS a result of the classical experiments of Rutherford and Chadwick on the disintegration of the nuclei of light elements by α-particles, it has previously been supposed that the proton, which was obtained as a disintegration particle, existed within these nuclei as a free or loosely bound component. It has, indeed, been suggested that the proton existed within nuclei as a satellite in rotation about a central tightly bound core. In considering the neutron emission of the light elements and their disintegration under proton and diplon bombardment, it was found † that there was definite evidence to show that the proton was not loosely bound in these nuclei, but that it formed a stable sub-unit, the diplon, by union with a neutron. It was shown that the neutron emission could be best explained if a neutron, and not the proton, was considered as loosely bound, and though certain difficulties were apparent, it seemed from the evidence that the nuclei of the light elements consisted of a central core of the maximum number of α-particles surrounded by a looser system consisting of a diplon and zero or one neutron.

In a more recent paper ‡ it was shown, further, that it was not necessary to consider that all emitted particles existed within nuclei in the free state before emission, as it was found easier to understand the β-ray disintegrations and the very short transformation periods of AcC′, ThC′, and RaC′ if it was assumed that some of the disintegration particles were formed within the nucleus immediately before ejection.

It is the purpose of the present paper to extend both these ideas, and to show that within nuclei there exist no free protons, but that they are bound either as α-particles or as diplons. On this view the neutrons are less firmly bound, and form a shell system in the heavier elements

* Communicated by Prof. F. H. Newman, D.Sc.

† Walke, Phil. Mag. xvii. p. 793 (1934).

‡ Walke, Phil. Mag. xvii. p. 1176 (1934).

surrounding the nuclear core. Proton emission is considered to be due to the formation of these particles within the nucleus as a result of interaction between the bombarding α-particle and the nucleus.

2. *The Proton and Neutron.*

The presence of electrons in the nucleus has always led to insuperable difficulties in proposed nuclear structure. At the time when the electron was regarded as a simple spherical electric charge of definite size, it was shown experimentally that the dimensions of the nuclei of the heavy atoms were altogether too small to accommodate the numerous electrons they were supposed to contain. Later, when the wave-mechanics were applied, other difficulties arose, and it was recently concluded by Bohr * that the theoretical treatment of electrons, as such, in nuclei must be abandoned. The view now in favour is that the electrons within nuclei must be combined in the form of stable nuclear sub-units. Until quite recently it was supposed that negative electrons exist within nuclei, being combined in the form of neutrons or α-particles.

It was first assumed by Chadwick † that the neutron consisted of a proton and an electron in close combination, the proton regarded as the fundamental unit of nuclear structure, being a simple particle. The experiments of Lewis, Livingston, and Lawrence ‡, and Kurie §, and the theoretical arguments from quantum mechanics and the spins of the light nuclei brought forward by Chadwick in the Bakerian Lecture for 1933, however, indicate that the neutron is a simple neutral particle, being the fundamental unit of mass. The proton is accordingly complex, and consists of a combination of a neutron and a positive electron. In this paper it is assumed that the proton is thus constituted, and further, it will be assumed that by interaction with a negative electron a neutron will be produced together with a quantum of radiation resulting from the disappearance of the two electrons. The positive charge on the nucleus is thus looked upon as due to positive electrons equal in

* Bohr, Volta Congress, Rome (1932).
† Chadwick, Proc. Roy. Soc. A, cxxxvi. p. 692 (1933).
‡ Lewis, Livingston, and Lawrence, Phys. Rev. xliv. p. 56 (1933).
§ Kurie, Phys. Rev. xliv. p. 463 (1933).

number to the extranuclear electrons. These positive electrons are, however, considered as combined with neutrons to form nuclear α-particles and protons.

3. *The Diplon as a Nuclear Component.*

In a previous paper * it has been shown that the disintegration of the light elements by high speed protons and diplons could be explained by assuming that within the nuclei of certain of these elements a proton and neutron exist as a diplon, forming a stable nuclear sub-unit. In addition, postulating that the diplon and neutron surrounded a tightly bound core of α-particles, it was further found possible to explain the neutron emission of these elements under α-particle bombardment. However, it was difficult to explain the proton emission of these elements, though this form of disintegration was explicable by assuming that the diplon was broken up by the impact, the neutron remaining in the resultant nucleus as forming the more stable configuration. In addition, the positron emission of aluminium † could be explained on this hypothesis, and it was predicted that positrons would be obtained by the α-particle disintegration of fluorine. It was further pointed out that diplogen H_1^2 should be disintegrable by high energy α-particles emitting protons and neutrons It is significant, that although Rutherford and Kempton‡ were unable to detect with certainty the presence of disintegration neutrons when they bombarded heavy water with the α-particles of polonium, Lewis, Livingston, and Lawrence §, using protons accelerated by their ingenious apparatus to 3×10^6 e.v., have shown that heavy water disintegrates under bombardment by these particles into protons and neutrons, indicating that the diplon has the constitution they originally assumed for it. In the following section it is shown that by making the same assumptions as in the previous paper ‖, namely, that one proton and one neutron in certain of the light nuclei are united to form a diplon, the other neutron being regarded as loosely bound, an explanation of all the disintegrations by

* Walke, Phil. Mag. xvii. p. 793 (1934).
† Curie and Joliot, *Comptes Rendus*, cxcvi. p. 1885 (1933).
‡ Rutherford and Kempton, Proc. Roy. Soc. A, cxliii. p. 724 (1934).
§ Lewis, Livingston and Lawrence, Phys. Rev. xlv. (1934).
‖ Walke, Phil. Mag. xvii. p. 793 (1934).

α-particle bombardment can be given, in addition to the disintegrations by proton and diplon bombardment already dealt with *. According to this hypothesis, one neutron and not the proton, as it was formerly supposed, is assumed to be loosely bound to the nuclear core.

4. *The Stability of α-particles within Nuclei.*

The α-particle is a particularly stable entity, and such particles are constituents of all nuclei, exceedingly stable nuclei being composed solely of α-particles. Until Rutherford and Chadwick † published their results on artificial disintegration, all elements of mass $4n$ were recorded to have withstood bombardment by swift α-particles without detachment of a proton, but the results of these experimenters place neon, magnesium, silicon, sulphur, and argon on the list of disruptable nuclei. However, these elements contain isotopes of atomic mass other than $4n$, to which the protons might be attributed. It is significant that the proton emission of these elements is very weak in intensity, and the protons ejected are of relatively short range compared with the proton emission of the other elements. Recent work by F. Perrin ‡ confirms the view that the nuclei of atomic mass $4n$ are stable structures.

Perrin has shown that pairs of electrons can be produced by the impact of a moving particle with another particle at rest. He shows that in general the minimum kinetic energy required by a particle of mass M_1 to produce a pair of electrons on impact with a particle at rest of mass M_2 is given by the formula

$$\text{kinetic energy of } M_1 = 2mc^2\left(\frac{m+M_1+M_2}{M_2}\right),$$

where m is the rest mass of an electron and c the velocity of light. Since $2mc^2 = 1{\cdot}01 \times 10^6$ e.v. approximately, the minimum kinetic energy necessary for M_1 to produce a pair of electrons in such a collision is approximately

$$\left(\frac{M_1+M_2}{M_2}\right) \times 10^6 \text{ e.v.},$$

if the masses M_1 and M_2 are large compared with that of an electron. Thus an α-particle of mass 4 will produce a

* Walke, *loc. cit.*
† Rutherford and Chadwick, 'Nature,' cxiii. p. 457 (1924).
‡ F. Perrin, *Comptes Rendus*, cxcvii. p. 1302 (1934).

pair of electrons on impact with a boron nucleus of mass 10 if its kinetic energy is greater than

$$\left(\frac{10+4}{10}\right)\times 10^6 \text{ e.v.} = 1{\cdot}5\times 10^6 \text{ e.v. approximately.}$$

In general, as the mass of the nucleus increases, the kinetic energy of the α-particle necessary for the production of pairs of electrons in nuclear collisions decreases. For the light elements, however, it can be assumed that pairs of electrons will be formed if the kinetic energy of the α-particles is greater than about $1{\cdot}5\times 10^6$ e.v.

We may thus explain the emission of protons by neon, magnesium, silicon, sulphur, and argon as due to the formation of pairs of electrons when α-particles bombard the nuclei of these elements. In this way we can retain the hypothesis of the stability under α-particle bombardment of nuclei which are regarded as composed of α-particles, since the action can be assumed to occur with other isotopes. It is significant that

$$Ne_{10}^{21},\ Ne_{10}^{22};\ Mg_{12}^{25},\ Mg_{12}^{26};\ Si_{14}^{29},\ Si_{14}^{30};\ S_{16}^{33},\ S_{16}^{34};\text{ and } Ar_{18}^{40}$$

exist, as well as the more abundant isotopes

$$Ne_{10}^{20},\ Mg_{12}^{24},\ Si_{14}^{28},\text{ and } S_{16}^{32},$$

which are assumed to consist entirely of α-particles, the nuclei of these isotopes being of the form

$$Ne_{10}^{20}(5\alpha);\ Mg_{12}^{24}(6\alpha);\ Si_{14}^{28}(7\alpha);\text{ and } S_{16}^{32}(8\alpha),$$

adopting the notation used in the previous paper*.

The reaction may occur as follows:—

$$Ne_{10}^{21}\quad\{[5\alpha]+(n)\}+\alpha\rightarrow\{[6\alpha]+(n)+\overset{-}{e}+\overset{+}{e}\},$$

$\overset{-}{e}+\overset{+}{e}$ representing the formation of a pair of electrons within the nucleus, the positive electron uniting with the neutron to produce a proton which is then emitted with the mass defect energy of the action, viz.,

$$\{[6\alpha]+(n)+\overset{-}{e}+\overset{+}{e}\}\rightarrow[6\alpha]+\overset{\nearrow}{p}+\overset{-}{e}\quad Mg_{12}^{24}.$$

The proton may thus be accompanied by an electron. Such electrons, if of low energy, would not be easily detected, and would certainly not be detected in any scintillation experiments. In this connexion it is significant

* Walke, Phil. Mag. xvii. p. 793 (1934).

that Rutherford *, considering certain disintegrations photographed by Blackett, mentions the possibility of electron emission which might not have been detected in such experiments.

A similar action is applicable to the other neon isotope Ne^{22}_{10}, so that the proton emission could result from the disintegration of both isotopes. For the other elements we have the following nuclear reactions :—

$$Mg^{25}_{12} \quad \{[6\alpha]+(n)\}+\alpha \rightarrow \{[7\alpha]+(n)+\overset{-}{e}+\overset{+}{e}\}$$
$$\rightarrow [7\alpha]+\overset{\nearrow}{p}+\overset{-}{e} \quad Si^{25}_{14},$$

$$Si^{29}_{14} \quad \{[7\alpha]+(n)\}+\alpha \rightarrow \{[8\alpha]+(n)+\overset{-}{e}+\overset{+}{e}\}$$
$$\rightarrow [8\alpha]+\overset{\nearrow}{p}+\overset{-}{e} \quad S^{32}_{16},$$

$$S^{33}_{16} \quad \{[8\alpha]+(n)\}+\alpha \rightarrow \{[9\alpha]+(n)+\overset{-}{e}+\overset{+}{e}\}$$
$$\rightarrow [9\alpha]+\overset{\nearrow}{p}+\overset{-}{e} \quad Ar^{36}_{18},$$

$$Ar^{40}_{18} \quad \{[9\alpha]+(n+n+n+n)\}+\alpha$$
$$\rightarrow \{[10\alpha]+(n+n+n+n)+\overset{-}{e}+\overset{+}{e}\}$$
$$\rightarrow \{[10\alpha]+(n+n+n)\}+\overset{\nearrow}{p}+\overset{-}{e} \quad Ca^{43}_{20}.$$

On these assumptions, therefore, the α-particle interacts directly with the core of the nucleus, pairs of electrons being produced by the impact, and the loosely bound neutron is ejected in the form of a proton. These reactions will be considered again in Section 7. It is to be noted that by similar actions protons may be ejected from the other isotopes of magnesium, silicon, and sulphur.

5. *The Disintegration of other Light Nuclei by α-particles.*

From the other light elements protons are emitted under α-particle bombardment by boron, nitrogen, fluorine, sodium, aluminium, and phosphorus in relatively large numbers, and by chlorine and potassium in relatively small numbers. Of these elements the most abundant isotopes of fluorine, sodium, aluminium, phosphorus, chlorine, and potassium have similar nuclear structures, whereas

* Rutherford, Chadwick, and Ellis, 'Radiations from Radioactive Substances.'

nitrogen and if we accept the suggestion previously made regarding the origin of the protons of boron in B_5^{10}, are different. Also neutrons have been obtained by bombarding fluorine, sodium, aluminium, and boron with high energy α-particles, and further positrons have been found to accompany the neutron emission of aluminium, fluorine, and boron. It will be shown in this section that all these reactions are explicable if we assume the stability of the diplon in these nuclear disintegrations and adopt the mechanism of pair formation used to explain the proton of the elements considered in section 4.

On this view, in nuclei containing a proton and neutrons, one neutron and the proton form a diplon which is stable under the impact of the α-particle with the core, the other neutron, which is regarded as less tightly bound, being emitted in the form of a disintegration proton. The proton emission may therefore be shown by the following reactions

$$F_9^{19} \quad \{[4\alpha]+(\overbrace{p+n}+n)\}+\alpha \rightarrow \{[5\alpha]+(\overbrace{p+n}+n+\overset{-}{e}+\overset{+}{e})\}$$
$$\rightarrow \{[5\alpha]+(\overbrace{p+n})+\overset{-}{e}\}+\overset{\nearrow}{p} \rightarrow \{[5\alpha]+(n+n)\}+\overset{\nearrow}{p}+\gamma \quad Ne_{10}^{22},$$

the assumption being made that in this nucleus the electron produced unites with the positron of the proton in the diplon to produce γ-radiation.

Similarly we have

$$Na_{11}^{23} \quad \{[5\alpha]+(\overbrace{p+n}+n)\}+\alpha \rightarrow \{[6\alpha]+(\overbrace{p+n}+n)+\overset{-}{e}+\overset{+}{e}\}$$
$$\rightarrow \{[6\alpha]+(\overbrace{p+n})+\overset{-}{e}\}+\overset{\nearrow}{p} \rightarrow \{[6\alpha]+(n+n)\}+\overset{\nearrow}{p}+\gamma \quad Mg_{12}^{26},$$

$$Al_{13}^{27} \quad \{[6\alpha]+(\overbrace{p+n}+n)\}+\alpha \rightarrow \{[7\alpha]+(\overbrace{p+n}+n)+\overset{-}{e}+\overset{+}{e}\}$$
$$\rightarrow \{[7\alpha]+(\overbrace{p+n})+\overset{-}{e}\}+\overset{\nearrow}{p} \rightarrow \{[7\alpha]+(n+n)\}+\overset{\nearrow}{p}+\gamma \quad Si_{14}^{30},$$

$$P_{15}^{31} \quad \{[7\alpha]+(\overbrace{p+n}+n)\}+\alpha \rightarrow \{[8\alpha]+(\overbrace{p+n}+n)+\overset{-}{e}+\overset{+}{e}\}$$
$$\rightarrow \{[8\alpha]+(\overbrace{p+n})+\overset{-}{e}\}+\overset{\nearrow}{p} \rightarrow \{[8\alpha]+(n+n)\}+\overset{\nearrow}{p}+\gamma \quad S_{16}^{34},$$

$$Cl_{17}^{35} \quad \{[8\alpha]+(\overbrace{p+n}+n)\}+\alpha \rightarrow \{[9\alpha]+(\overbrace{p+n}+n)+\overset{-}{e}+\overset{+}{e}\}$$
$$\rightarrow \{[9\alpha]+(\overbrace{p+n})+\overset{-}{e}\}+\overset{\nearrow}{p} \rightarrow \{[9\alpha]+(n+n)\}+\overset{\nearrow}{p}+\gamma \quad Ar_{18}^{38},$$

$$K_{19}^{39} \quad \{[9\alpha]+(\overbrace{p+n}+n)\}+\alpha \rightarrow \{[10\alpha]+(\overbrace{p+n}+n)+\overset{-}{e}+\overset{+}{e}\}$$
$$\rightarrow \{[10\alpha]+(\overbrace{p+n})+\overset{-}{e}\}+\overset{\nearrow}{p} \rightarrow \{[10\alpha]+(n+n)\}+\overset{\nearrow}{p}+\gamma \quad Ca_{20}^{42}.$$

These same reactions allow for the neutron and positron emission from the nuclei concerned. We must suppose that when the α-particle energy is sufficiently high, the kinetic energy of the positive electron is increased to such an extent that it can leave the nucleus without uniting with the neutron, the two being expelled as if the proton had been resolved into its components. We can thus explain the emission of neutrons and positrons by fluorine and aluminium under bombardment with high energy α-particles, the actions being otherwise the same as above, viz. :—

$$\mathrm{F}_{9}^{19} \quad \{[4\alpha]+(\overline{p+n}+n)\}+\alpha \rightarrow \{[5\alpha]+(\overline{p+n}+n)+\bar{e}+\overset{+}{e}\}$$
$$\rightarrow \{[5\alpha]+(\overline{p+n})+\bar{e}\}+\overset{\nearrow}{n}+\overset{+\nearrow}{e}$$
$$\rightarrow \{[5\alpha]+(n+n)\}+\overset{\nearrow}{n}+\overset{+\nearrow}{e}+\gamma \quad \mathrm{Ne}_{10}^{22},$$

$$\mathrm{Al}_{13}^{27} \quad \{[6\alpha]+(\overline{p+n}+n)\}+\alpha \rightarrow \{[7\alpha]+(\overline{p+n})+\bar{e}+\overset{+}{e}\}$$
$$\rightarrow \{[7\alpha]+(\overline{p+n})+\bar{e}\}+\overset{\nearrow}{n}+\overset{+\nearrow}{e}$$
$$\rightarrow \{[7\alpha]+(n+n)\}+\overset{\nearrow}{n}+\overset{+\nearrow}{e}+\gamma \quad \mathrm{Si}_{14}^{30}.$$

By a similar reaction we should expect positive electrons to accompany the neutron emission of sodium. Similarly phosphorus, chlorine, and potassium would emit neutrons and positrons if the energy of the bombarding α-particles was sufficiently great. As, however, the proton emission of chlorine and potassium is weak (probably on account of their high atomic numbers), it is doubtful whether α-particle sources of sufficient energy exist to produce the neutrons and positrons expected from these elements. But we might reasonably look for neutrons and positrons from phosphorus when disintegrated by high energy α-particles.

In considering these actions and the ideas formulated, it is interesting to note that neutrons have been obtained from neon and magnesium *, and, further, that positive electrons have been found accompanying the neutrons of magnesium †. The actions already given to explain the proton emission of these elements show that these

* Chadwick, Bakerian Lecture (1933).
† Curie and Joliot, *Comptes Rendus*, cxcviii. p. 254 (1934).

actions occur as a result of the increased energy of the positive electron, thus :—

$$Mg_{12}^{25} \quad \{[6\alpha]+(n)\}+\alpha \rightarrow \{[7\alpha]+(n)+\overset{-}{e}+\overset{+}{e}\}$$
$$\rightarrow [7\alpha]+\overset{\nearrow}{n}+\overset{+\nearrow}{e}+\overset{-}{e} \quad Si_{14}^{28}$$

and similarly,

$$Ne_{10}^{21} \quad \{[5\alpha]+(n)\}+\alpha \rightarrow \{[6\alpha]+(n)+\overset{-}{e}+\overset{+}{e}\}$$
$$\rightarrow [6\alpha]+\overset{\nearrow}{n}+\overset{+\nearrow}{e}+e \quad Mg_{12}^{24}.$$

Thus positive electrons may accompany the neutrons of neon. In addition, considering the actions required to explain the proton emission of silicon, sulphur, and argon, with α-particles of sufficient energy these elements may disintegrate by emitting neutrons and positive electrons.

Formerly it has been assumed in considering the disintegration of boron by α-particles that the least abundant isotope B_5^{10} gives rise to the proton emission, whereas B_5^{11} ejects the neutron according to the reactions :—

$$B_5^{10} \quad \{[2\alpha]+(\overline{p+n})\}+\alpha \quad \rightarrow \{[3\alpha]+(n)\}+\overset{\nearrow}{p} \quad C_6^{13},$$

$$B_5^{11} \quad \{[2\alpha]+(p+\overline{n+n})\}+\alpha \rightarrow \{[3\alpha]+(p+\overline{n})\}+\overset{\nearrow}{n} \quad N_7^{14}.$$

But it has been found by Curie and Joliot * that the neutron emission of boron is accompanied by positive electrons. It seems likely, therefore, that both proton and neutron emissions result from the disintegration of the heavy isotope by reactions of the same form as those suggested for aluminium, viz. :—

$$B_5^{11} \quad \{[2\alpha]+(\overline{p+n}+n)\}+\alpha \rightarrow \{[3\alpha]+(\overline{p+n}+n)+\overset{-}{e}+\overset{+}{e}\}$$
$$\rightarrow \{[3\alpha]+(\overline{p+n})+\overset{-}{e}\}+\overset{\nearrow}{p} \rightarrow \{[3\alpha]+(n+n)\}+\overset{\nearrow}{p}+\gamma \quad C_6^{14},$$

$$B_5^{11} \quad \{[2\alpha]+(\overline{p+n}+n)\}+\alpha \rightarrow \{[3\alpha]+(\overline{p+n}+n)+\overset{-}{e}+\overset{+}{e}\}$$
$$\rightarrow \{[3\alpha]+(p+\overline{n})+\overset{-}{e}\}+\overset{\nearrow}{n}+\overset{+\nearrow}{e}$$
$$\rightarrow \{[3\alpha]+(n+n)\}+\overset{\nearrow}{n}+\overset{+\nearrow}{e}+\gamma \quad C_6^{14}.$$

* Curie and Joliot, *loc. cit.*

It is interesting, too, to note that Curie and Joliot (*loc. cit.*) have also observed positive electrons accompanying the neutron emission of beryllium. The reaction is probably similar to those considered for magnesium and neon

$$\mathrm{Be}_4^9 \quad \{[2\alpha]+(n)\}+\alpha \rightarrow \{[3\alpha]+(n)+\overset{-}{e}+\overset{+}{e}\}$$
$$\rightarrow [3\alpha]+\overset{\nearrow}{n}+\overset{+\nearrow}{e}+\overset{-}{e} \quad \mathrm{C}_6^{12}.$$

There is the probability, therefore, that protons might be emitted by beryllium according to the action

$$\mathrm{Be}_4^9 \quad \{[2\alpha]+(n)\}+\alpha \rightarrow \{[3\alpha]+(n)+\overset{-}{e}+\overset{+}{e}\}$$
$$\rightarrow [3\alpha]+\overset{\nearrow}{p}+\overset{-}{e} \quad \mathrm{C}_6^{12}.$$

Some evidence * of proton emission from this element has been obtained. By a similar action we should expect positive electrons to accompany the neutron emission of lithium. These have not been detected, however.

The proton emission of nitrogen seems to form an exception to the examples considered, as it would appear that the isotope $\mathrm{N}_7^{14}\{[3\alpha]+(\overbrace{p+n}^{})\}$ is disintegrated under the α-particle bombardment. It is possible that in this nucleus the diplon is disintegrated by the impact, leading to the proton emission. On account of the great stability of O_8^{16} it would be expected, however, that both neutron and proton would be emitted, whereas the expansion chamber photographs show that only a disintegration proton is observed, and that no other particle of comparable mass is emitted. However, Chadwick has stated in the Bakerian Lecture for 1933, that all the light elements up to aluminium except hydrogen, helium, oxygen, and carbon emit neutrons under α-particle bombardment, so that we must conclude that nitrogen also emits neutrons. As Blackett's photographs give no evidence of neutrons accompanying the protons, we must conclude that the neutron and proton emission occur separately.

In this connexion it is of interest to consider the rarer isotope of nitrogen N_7^{15}. This isotope, which is only present in the proportion 1 to 350 of the main isotope, could give rise to both protons and neutrons as in the

* Kirsch and Petterson, Phil. Mag. xlvii. p. 500 (1924).

other examples already considered, the resultant nucleus being the stabler of the two heavy oxygen isotope O_8^{18}.

The action could be considered as follows :—

$$N_7^{15} \quad \{[3\alpha]+(\overline{p+n}+n)\}+\alpha \rightarrow \{[4\alpha]+(\overline{p+n}+n)+\bar{e}+\overset{+}{e}\}$$
$$\rightarrow \{4\alpha]+(\overline{p+n})+\bar{e}\}+\overset{\nearrow}{p} \rightarrow \{[4\alpha]+(n+n)\}+\overset{\nearrow}{p}+\gamma \quad O_8^{18},$$

resulting in the proton emission, and

$$N_7^{15} \quad \{[3\alpha]+(\overline{p+n}+n)\}+\alpha \rightarrow \{[4\alpha]+(\overline{p+n}+n)+\bar{c}+\overset{+}{e}\}$$
$$\rightarrow \{[4\alpha]+(\overline{p+n})+\bar{e}\}+\overset{\nearrow}{n}+\overset{+\nearrow}{e}$$
$$\rightarrow \{[4\alpha]+(n+n)\}+\overset{\nearrow}{n}+\overset{+\nearrow}{e}+\gamma \quad O_8^{18},$$

resulting in the neutron emission.

While these actions probably take place, it appears that N_7^{15} is not sufficiently abundant to account for the whole of the proton emission of nitrogen, and it would seem that in N_7^{14} the diplon itself is disintegrated. In view, however, of the comparative instability of O_8^{17} (as shown by its small abundance), it is difficult to understand why the neutron and proton are not simultaneously emitted.

According to the hypothesis of pair formation adopted in this paper it would appear that positrons should accompany most neutron emissions. However, since the neutron emission is weak in many cases, the number of positive electrons would be small, and in consequence of their easy conversion into γ-radiation by interaction with negative electrons, they would not easily be detected.

It appears, however, that there is other evidence to indicate pair formation by interaction between α-particles and the nucleus, as Slater * has found that when heavy atoms, such as gold, are bombarded by α-particles, a small amount of γ-radiation is emitted which, from its penetrating power, he judged to have its origin in the nucleus. This radiation might, however, easily arise as a result of the disappearance of the positive electrons of electron pairs produced by the interaction of α-particles and the nucleus.

In addition, Chadwick, Blackett, and Occhialini † have reported that positrons are emitted by lead irradiated by

* Slater, Phil. Mag. xlii. p. 904 (1921).

† Chadwick, Blackett and Occhialini, Proc. Roy. Soc. A, cxliv. p. 235 (1934).

the radiations of boron and fluorine bombarded by polonium α-particles. These they attribute to a secondary effect of internal conversion of γ-rays emitted by the excitation or disintegration of lead nuclei in neutron collisions. It seems possible, however, that these positrons arise directly as a result of the interaction of the neutron and the nucleus in a similar manner to the α-particle actions considered above. It appears, therefore, that the interaction between an α-particle and nucleus must be of the nature discussed. These reactions, therefore, confirm definitely the fundamental rôle played by the α-particle and the diplon in nuclear structure. It appears that a "free" proton has no existence in any nuclei, and that the diplon is an essential component of all nuclei of odd atomic number.

These disintegrations can be compared with an induced form of radioactivity. In the normal radioactive substances α-particles leave the nucleus, and the conversion of their energy in the form of pairs of electrons in the negative potential field of the nucleus results in the expulsion of β-particles and the formation of more complex nuclei *. In normal radioactivity, too, α-particle disintegration results in a lowering of atomic number and a less complex nucleus, whereas β-ray changes raise the atomic number and as shown produce a more complex nucleus. In the actions considered so far, the reverse processes occur, α-particles enter the nucleus, and often positive electrons are emitted. In these disintegrations the entry of the α-particle produces a more complex nucleus, whereas the departure of the positive electron results in a simpler nucleus. The disintegration processes are, therefore, complementary to the radioactivity of the heavy atoms and α-particles, pairs of electrons, and neutrons in both forms of activity, play a fundamental part in all nuclei. In addition, the importance of high frequency γ-radiation in all these actions and the obvious relation that exists between electrons, α-particles, and γ-radiation show that high-frequency quanta may play a fundamental part in nuclear structure.

In this connexion Compton †, to explain his results on the variation of cosmic radiation with geomagnetic latitude, requires an electron component in the primary

* Walke, Phil. Mag. xvii. p. 793 (1934).
† Compton, Phys. Rev. xliii. p. 835 (1933).

cosmic radiation, and, further, Alvarez and Compton * and Johnson † have shown by the azimuthal asymmetry of the rays at Mexico City that this charged component must be mainly positive. They conclude that the beam consists mainly of positive electrons, such as were discovered by Anderson ‡ in the cosmic ray showers observed in expansion chambers. In addition, Millikan and Regener's depth-ionization curves seem only explicable on a quantum beam hypothesis, and, further, the Hoffmann-stösse or ionization bursts due to nuclear disintegrations by cosmic radiation appear to require a neutron component. If we assume that the primary beam entering the earth's atmosphere contains all these components, then cosmic radiation is produced by the formation of more complex nuclei analogous to the disintegrations we have considered. Probably, therefore, cosmic rays arise as a result of the formation of the more complex elements in the depths of space, and not from the break up of heavy elements into their components. This point will receive further consideration in Section 8.

6. *The Stability and Abundance of Atoms.*

There is no known method of testing the stability of the lighter atoms, but apparently the more stable atoms should be more abundantly formed, and to a certain extent this is undoubtedly true. It is certain that there is a direct relation between the abundance of the elements and nuclear structure, and that there is no very marked relation to the periodic system of Mendelejeff. Sufficiently good data might therefore be obtained from the earth's crust, and while this is to a great extent true, there are factors which cause our knowledge of the quantitative composition of such to be of less value in this respect. For example, the common idea that sodium is a very abundant element undoubtedly has its origin in the fact that the solubility of its salts has caused their very considerable concentration in the oceans. Again, the salts of sodium are more fusible than similar ones of the alkaline earths and most other metals in the rocks, and this fact may have caused it to be segregated by magmatic solution and redisposition. Thus, while in the average

* Alvarez and Compton, Phys. Rev. xliii. p. 835 (1933).
† Johnson, *ibid.* xliii. p. 834 (1933).
‡ Anderson, *ibid.* xli. p. 405 (1932).

igneous rock found on the surface of the earth there is about 2·23 per cent. of sodium, it is not improbable that this is a larger percentage than would be found in the earth as a whole.

In spite of such difficulties, however, the relative abundance of the different atomic species in known materials gives an index which indicates the most important stability relations of the different types of nuclei.

There is, in addition to the lithosphere of the earth, meteorite material available. The general relations between the abundance of the elements found in meteorites and the earth's crust are similar, and while it is difficult to be certain that the various analyses of the relative abundance of the elements in meteorites and the lithosphere represent the average composition of matter, certain general conclusions can safely be drawn. In both sources it is found that the helium system elements are most abundant. Also the light elements up to atomic number 28 are much more abundant than the heavier elements; in fact, the number of atoms per light element is 5000 times as large as the number per heavy element, and since there are many more isotopes of the heavy elements than of the light ones, the number of atomic species is extremely small above $Z=28$.

The two even numbered elements oxygen and silicon together are responsible for 75 per cent. of the material of the earth, while less than 0·2 per cent. is contributed by elements of higher atomic numbers 28 to 92. Thus if we suppose that the elements are built up of neutrons and positrons or of simple combinations of these units, it is to be anticipated that the lighter stable nuclei would be formed in much greater quantity than the heavier and more complex nuclei. The comparative rarity of the elements of atomic number greater than thirty is thus an indication that the nuclei arise from the synthesis of simple units into more complex structures rather than from the disintegration of some heavy element or elements.

7. *α-particle Groups in Atomic Nuclei.*

The general evidence of nuclei from mass spectroscopy strongly supports the view that the α-particle is of primary importance as a unit of the structure of nuclei in general, and particularly of the heavy elements. This is supported by radioactive evidence, for the stability of the α-particle

is shown by the fact that it is not disintegrated when emitted from radioactive nuclei with speeds of $2{\cdot}0 \times 10^9$ cm. sec.

In addition, Rutherford *, from a study of the artificial disintegrations of the elements, states that carbon and oxygen represent very stable structures composed of helium nuclei. It is possible, he suggests, that oxygen nuclei may be the structural basis of some of the elements following oxygen. It is now shown that oxygen, and more especially carbon nuclei, form the basis of nuclear structure. According to the view put forward, the α-particle is the primary nuclear component (consisting of two neutrons and two protons), though groups of α-particles are formed in the more stable nuclei. In considering relative nuclear stability as shown by abundance, hydrogen, helium, and carbon are not considered, as their lack of abundance is merely evidence in favour of the tendency of these units to form more complex nuclei.

Consider the four most abundant even numbered elements (omitting aluminium, which will be considered later). In order of abundance they are :—

Element.	Atomic number.	Atomic weight.	Number of α-particles.	
Oxygen	8	16	[4α]	1α+3α
Silicon	14	28	[7α]	1α+2.3α
Iron	26	52	[13α]	1α+4.3α
Calcium.....	20	40	[10α]	1α+3.3α

Since the atomic number of iron 26 is near the end of the light element group of atomic numbers from 1–28, for these elements the 3α-particle group is a definite nuclear component. It will be shown that by assuming the greater stability of the 3α-group in nuclei, the radioactivity of potassium and rubidium by β-ray emission is accounted for, and, further, the comparative rarity of the inert gases is explicable.

8. *The Radioactivity of Potassium and Rubidium.*

Potassium and rubidium both show a weak β-ray activity, which is specific to these elements. Tests for

* Rutherford, Journ. of Franklin Inst. cxcviii. p. 725 (1924).

the presence of an emanation in the substances by Campbell and Wood * gave negative results, and they concluded that the observed emission of β-rays was a property of potassium and rubidium atoms. Subsequent investigations have confirmed the conclusion that the β-radiations are not due to radioactive impurities, but to the elements themselves. In both cases only β-rays are emitted, no α-rays having been observed, and no transformation products of either potassium or rubidium have so far been detected. Biltz and Ziegert † have shown that the isotope of mass 41 is mainly, if not wholly, responsible for the β-radiation of potassium.

All these facts are explicable on the assumption that the 3α-particle group is a very stable nuclear unit, and, further, the β-radiation must arise from the isotope of mass 41. In a previous paper ‡ it was shown that in some cases β-ray disintegration involves the formation of α-particles in the nuclei of disintegrating atoms, which are in some cases bound into a vacant place, and so complete a shell of α-particles. Applying these ideas, which resulted from the assumption that the emission of a β-particle resulted in the formation of a positron in the nucleus, the β-ray disintegration of potassium occurs as follows :—

$$K_{19}^{41} \quad \{[9\alpha]+(\overline{p+n}+n+n+n)+\overset{+}{e}\}+\overset{-}{e}\nearrow$$

$$\rightarrow\{[9\alpha]+(\overline{p}+n+\overline{p+n}+n)\}\rightarrow\{[10\alpha]+(n)\} \quad Ca_{20}^{41}.$$

On this view an α-particle is formed as a result of the production of a proton by the union of the positive electron and one neutron. The diplon, proton, and one neutron then unite to form an α-particle, which completes the stable core $1\alpha+3.3\alpha$ of the calcium isotope. Thus only a single β-ray change could occur, and no α-particles would be emitted. Moreover, the β-ray disintegration of K_{19}^{39} would not be possible, as the nucleus

$$K_{19}^{39} \quad \{[9\alpha]+(\overline{p+n}+n)\}$$

would not produce the new α-particle by so changing. However, the β-ray disintegration of an isotope of mass 40

* Campbell and Wood, Proc. Camb. Phil. Soc. xiv. p. 15 (1906).
† Biltz and Ziegert, *Phys. Zeit.* xxix. p. 197 (1928).
‡ Walke, Phil. Mag. xvii. p. 793 (1934).

would produce the more stable calcium isotope of mass 40, so that possibly the radioactivity of potassium is due to a rare isotope of mass 40.

Further, no emanation could be produced, and no series of disintegrations would occur. In addition, though one might expect sodium to be similarly radioactive because of its similarity in chemical properties to potassium, the above reasoning shows that this would be impossible. In fact, of the known isotopes of mass less than 42, only two, viz., K_{19}^{41} and Cl_{17}^{37}, could be radioactive by β-ray disintegration on the above hypothesis, since in no other nuclei is there a sufficient number of neutrons to produce an α-particle which would complete the stable core. In this connexion the possible β-ray disintegration of Cl_{17}^{37} is doubtful, as the production of an α-particle would not complete the stable 3α grouping. In this connexion we should not expect aluminium to be radioactive (for it might be imagined, on account of the variety of its disintegration products under α-particle bombardment, that it was unstable), though on this hypothesis its easy disintegration is due to the great tendency to form the stable core

$$[6\alpha]+\alpha\rightarrow[7\alpha]=1\alpha+2.3\alpha.$$

We should, therefore, not expect an aluminium isotope of mass 28, nor a nitrogen isotope of mass 16, as both would probably be radioactive by β-ray emission, and produce silicon and oxygen thus :—

$$Al_{13}^{28}\quad \{[6\alpha]+(\overline{p+n}+n+n)+\overset{+}{e}\}+\overset{-}{e}$$

$$\rightarrow\{[6\alpha]+(\overline{p+n}+\overline{p+n})\}\rightarrow[7\alpha]\quad Si_{14}^{28},$$

$$N_{7}^{16}\quad \{[3\alpha]+(\overline{p+n}+n+n)+\overset{+}{e}\}+\overset{-}{e}$$

$$\rightarrow\{[3\alpha]+(\overline{p+n}+\overline{p+n})\}\rightarrow[4\alpha]\quad O_{8}^{16}.$$

As rubidium is radioactive and emits β-rays, results similar to those with potassium would be expected, the resulting nucleus containing $1\alpha+N.3\alpha$.

The reaction is as follows :—

$$Rb_{37}^{87}\quad \{[18\alpha]+(\overline{p+n}+13n)+\overset{+}{e}\}+\overset{-}{e}$$

$$\rightarrow\{[18\alpha]+(\overline{p+n}+\overline{p}+\overline{n}+11n)\}\rightarrow\{[19\alpha]+(11n)\}\quad Sr_{38}^{87}.$$

It is significant that $19\alpha = [1\alpha + 6.3\alpha]$, so that the stability of the 3α-particle group in nuclear structure seems existent up to atomic number 38.

By a similar action β-ray radioactivity of manganese resulting in the production of iron is feasible, *i. e.*,

$$Mn_{25}^{55} \quad \{[12\alpha]+(\overline{p+n}+5n)+\overset{+}{e}\}+\overset{-}{e}\nearrow$$

$$\rightarrow \{[12\alpha]+(\overline{p+n}+\overline{p+n}+3n)\} \rightarrow \{[13\alpha]+(3n)\} \quad Fe_{26}^{55}.$$

Such an isotope of iron has, however, not been detected. In this, and other possible radioactive disintegrations which will be considered, it must be remembered that the neutron configuration plays a definite part in nuclear stability, so that while these actions are theoretically possible, the disintegrations may not occur if the resulting neutron stability is too low (see Landé *).

For example, we might expect the gallium isotope of mass 71 to become a germanium isotope of the same mass—

$$Ga_{31}^{71} \quad \{[15\alpha]+(\overline{p+n}+9n)+\overset{+}{e}\}+\overset{-}{e}\nearrow$$

$$\rightarrow \{[15\alpha]+(\overline{p+n}+\overline{p+n}+7n)\} \rightarrow \{[16\alpha]+(7n)\} \quad Ge_{32}^{71},$$

$$16\alpha = 1\alpha + 5.3\alpha,$$

and, similarly, if the 3α-particle grouping continues, the element of atomic number 43 might be radioactive. It is significant in this connexion that the element has not been detected; non occurrence may be evidence of instability. It is to be noted that on these views that strontium of atomic number 38 and ruthenium 44 should be more abundant than neighbouring elements. Russell's diagram † of the abundance of the elements in the sun's atmosphere shows, in addition to the maxima at oxygen, calcium, and iron, smaller maxima at atomic numbers 38 and 44.

Quite apart from these speculations, the two known radioactive substances potassium and rubidium, together with the easy disintegration of aluminium, support the idea that the 3α-particle grouping is an important nuclear component.

* Landé, Phys. Rev. xliii. p. 620 (1933).

† R. d'E. Atkinson, Astrophys. Journ. lxxiii. p. 275 (1931).

9. *The Inert Gases.*

The chemical properties by which the elements are divided into groups depend entirely on the outermost shells of electrons. The absence of chemical properties of the inert gases is thus attributed to the fact that the electronic configurations of these elements represent closed or completed shells. The inertness of these elements is therefore not directly dependent on their nuclear structure, and although their nuclei may be considered to consist mainly of α-particles, their comparative rarity forces us to the conclusion that in the nuclei of these gases the α-particle configurations are comparatively unstable.

If we consider the group neon, argon, krypton, and xenon (we omit helium because, as already stated, it is considered as a fundamental nuclear unit) it will be seen, that except for neon, all have α-particle nuclear configurations which are less by one than the arrangements $1\alpha+\mathrm{N}$. 3α which have been shown to be very stable thus:—

Element.	Atomic number.	α-particles.	Stable group.
Argon	18	9α	$10\alpha=1\alpha+3.3\alpha$
Krypton	36	18α	$19\alpha=1\alpha+6.3\alpha$
Xenon	54	27α	$28\alpha=1\alpha+9.3\alpha$

On account of this relation the rarity of these gases is to be attributed to the stability of the 3α grouping, for the addition of a single α-particle would produce these stable units. The 3α-groups form some kind of shell system, so that the rare gases have nuclei in which there exists one vacancy as it were. In consequence the absorption of α-particles in their nuclei would be easy, and we can imagine that if in the process of forming elements these gases ever existed in large quantities, they would absorb α-particles very rapidly, and would change into the stabler groupings. We should, therefore, expect α-particles to be absorbed by the nuclei of these atoms without disintegration. This idea might be tested with argon for the absorption of an α-particle with the formation of the stable Ca_{20}^{40} or Ca_{20}^{44} would produce a recoil nucleus which might be registered photographically by means of a

Wilson expansion chamber. We can compare the rare gases and their neighbours with radium and radon. Radon with one α-particle less than radium is much less stable, as shown by the half transformation periods 1600 years and 3·825 days.

It is interesting to note that on this hypothesis neon differs from the other inert gases as far as nuclear structure is concerned, for the neon nucleus has two α-particles less than the next stable 3α-group. This shows quite definitely that the inertness of these gases is determined, not directly by their nuclear structure, but by their extranuclear electron groups. It is difficult to understand what distinction the difference in nuclear structure will make between neon and the other rare gases, but it may be of significance that the protons emitted by neon bombarded with α-particles have a shorter range than those from argon. The stability of the 3α-group would cause a greater release of energy when the shell is completed as with the absorption of an α-particle in argon, than with neon in the nucleus of which absorption of an α-particle would still leave the group incomplete. The difference in energy of the protons emitted may be due to this difference in structure.

Thus, considering the most stable elements, the radioactivity of potassium and rubidium, and the small abundance of the inert gases, it is suggested that a stable group or shell of 3α-particles is a definite nuclear component, and we may therefore suppose that the more stable elements above atomic number 8 may be formed primarily of oxygen and carbon nuclei, though they themselves are formed of helium, oxygen further being formed from helium and carbon [1α+3α]. Helium itself is thus the basis of nuclear structure, and since it is formed of neutrons and protons only neutrons and positrons are required for nuclear structures. The last section shows how the elements may be formed from these units.

10. *α-particle Shells in the Nucleus.*

Rutherford * has suggested that if the helium nucleus is taken as a combining unit, we should ultimately expect many of the neutrons in heavy nuclei to form α-particles.

* Rutherford, *loc. cit.*

These helium nuclei would tend to collect together and form definite systems, and it seems not unlikely that they will group themselves in orderly structures analogous to the regular arrangement of atoms to form crystals. These ideas expressed by Rutherford are in agreement with the views already expressed in this paper. In addition, Aston * has suggested that in the lighter elements the nucleus is composed of a combination of α-particles, protons, and neutrons. At first a concentrated and firmly bound nucleus is formed, and for an atom of about atomic weight 120 a minimum mass is reached representing the closest binding of the constituent particles. With successive additions of mass the α-particle becomes less and less tightly bound, until the heaviest element is reached. There is always a probability that the inner highly condensed nucleus may form a compact and definitely orientated structure surrounded by a number of α-particles as satellites.

Rutherford †, in his satellite theory of the radioactive bodies, also suggested that at first sight it is natural to suppose, since the end product of the radioactive series is in an isotope of lead, that one of these isotopes forms a central core. It may, however, well be that the radioactive processes cease when there is still a number of satellites remaining. If this is so the core may be of smaller charge and mass than lead. Rutherford suggested that this core may correspond to an element near platinum of mass 192. Previously a theory of the radioactive transformations ‡ was developed by extending Landé's § ideas, and evidence was brought forward to show that the 41α-particle configuration of lead indicated a closed shell system.

In connexion with this shell theory, the remarks of Aston already quoted are significant, and it is probable that the nucleus of mass 120, *i. e.*, an isotope of tin, represents the completed nuclear α-particle core, and that above this α-particles are bound in shells outside the core. The atomic number of tin, 50, corresponds to an α-particle configuration $25\alpha = 1\alpha + 8.3\alpha$, and we may therefore suppose that 3α is a fundamental unit in the building

* Aston, 'Mass Spectra and Isotopes.'
† Rutherford, *loc. cit.*
‡ Walke, *loc. cit.*
§ Landé, *loc. cit.*

of the core. In addition, if we combine Rutherford's suggestion and that already mentioned, then 41α represents the complete stable shell system, and a nucleus of mass 192 represents a configuration with one complete shell less than this. Osmium of atomic number 76 has an isotope of mass 192, and its α-particle configuration 38α indicates that above osmium a closed shell of 3α-particles is formed to give the last stable nucleus. Above lead it has already been suggested that a group of four, or perhaps five, α-particles form another shell.

Between atomic numbers 50 and 76, that is from 25α to 38α, there is little evidence to indicate how the α-particles are distributed, but the proved radioactivity of samarium by α-particle emission may be of value in indicating a possible shell formation. It has been shown that the least stable α-particle group (as shown by the shortest half transformation period) was formed when the nucleus contained one α-particle above the completed shell. If, therefore, we assume that the presence of an α-ray radioactive substance in a group of non-radioactive elements indicates that this nucleus is the least stable of the group, then by analogy we are led to conclude that samarium contains in its nucleus one α-particle more than the first complete α-particle shell surrounding the core of 25α-particles.

As samarium (atomic number 62) contains 31α-particles, it is feasible to assume that 30α represents a first closed shell of 5α-particles. Thus above the stable core of maximum closeness of packing we assume three α-particle shells containing 5α, 8α, and 3α-particles respectively. Thus, as far as α-particles are concerned, nuclei are built up with a core by successive groups of 3α-particles until the core is complete at [1α+8.3α], when three shells of less tightly bound particles are added outside the core, to form the remaining stable nuclei, the last of which consists of

$$([1\alpha+8.3\alpha)+5\alpha+8\alpha+3\alpha)-\text{lead}.$$

In considering these α-particle shells and the core the neutron configurations have been omitted, as they have been very adequately discussed by Landé *.

In considering these stable nuclear groupings, the relative abundance of the elements is of significance.

* Landé, *loc. cit.*

R. d'E. Atkinson * (following Russell), has shown the relative abundance of elements in the sun by means of a smooth curve. If, however, instead of drawing such a curve representing the general abundance of elements, the points are joined by means of a curve which will indicate the detailed abundance relations, it is found that there is definite evidence of maxima at atomic numbers 8, 14, 20, 26, 38, 44, and 50, though the latter is not so definite as the others. These maxima correspond to the stable 3α-groups $[1\alpha+3\alpha]$, $[1\alpha+2.3\alpha]$, $[1\alpha+3.3\alpha]$, $[1\alpha+4.3\alpha]$, $[1\alpha+6.3\alpha]$, $[1\alpha+7.3\alpha]$, and $[1\alpha+8.3\alpha]$. If is to be noted, however, that there does not appear to be any evidence of a maximum of abundance at $z=32$ $[1\alpha+5.3\alpha]$. As we have assumed that these particular α-particle configurations would be more stable than intermediate arrangements, we should expect these nuclei to be correspondingly more abundant. It would appear, therefore, that the results quoted above are confirmatory evidence in favour of the stable 3α nuclear core unit.

In addition, d'E. Atkinson states that from $Z=55$ upwards we should expect to find a maximum of abundance at first, and possibly a second maximum in the lead region. As we should expect closed shells to be stable configurations, we should expect on the hypothesis suggested, maxima of abundance at $Z=60$ and $Z=82$, with, however, a further maximum at $Z=76$. The curve already mentioned shows some evidence of a slight increase of abundance at $Z=74$ with definite maxima at $Z=82$ and approximately $Z=60$. It appears, therefore, that there is some astrophysical evidence in favour of the shell systems suggested.

11. *The Origin of the Elements and Cosmic Radiation.*

According to the assumptions already made, the nuclei of all the elements can be formed from combinations of neutrons and positrons. One can visualize the formation of all the elements from neutrons only, and simply as a result of gravitational attraction.

Jeans has shown that if all the matter of the universe were evenly scattered throughout space so as to form "the primæval chaos from which most scientific theories

* d'E. Atkinson, *loc. cit.*

of cosmogony have started," then, as a result of the gravitational attractions of the component particles one to another and by the process of "gravitational instability," the material would condense into a very large number of gigantic condensation, which he considers are the extra galactic nebulæ. By similar considerations he is able to indicate how stars, planets, and their satellites are formed, and concludes that it is fair to say that gravitational instability appears to be the agency primarily responsible for the main architecture of the universe. It is probable that this agency is also responsible for the evolution of the main material components.

The general theoretical considerations of gravitational instability can be applied to any mass of gas. Consider that all matter has been resolved into its components. On the view adopted in this paper, the result would be a primæval distribution throughout space of neutrons, for the positive and negative electrons equal in number would be annihilated in the form of γ-radiation. Thus the origin of matter can be pictured as a "cosmic neutron cloud" such as suggested by Elsassar and Guggenheimer *. This distribution of neutrons would be like a gas of atomic number zero incapable of emitting light. Such a gas which has been called "neuton" by Harkins † would only differ from other gases in being incapable of becoming luminous. Though neutral, the neutrons would attract each other by gravitation, and in consequence of "gravitational instability" giant condensations would occur which would increase in size and density to form the extragalactic nebulæ. In consequence of the increased density and rise in temperature caused by the shrinkage of the condensation, the mean free paths of the neutrons would decrease, and their kinetic energy would increase so that collisions would become more frequent. When the kinetic energy of the particles was as high as $2{\cdot}00 \times 10^6$ e.v., pairs of electrons would be formed in collisions according to Perrin's theory and hydrogen would be produced, the proton resulting from the union of one of the neutrons and the positive electron. As the condensation continues to contract collisions will be more

* Elsaser and Guggenheimer, *Comptes Rendus*, cxcvii. p. 1629 (1933).
† Harkins, 'Nature,' p. 23, Jan. 7th (1933).
‡ Perrin, *loc. cit.*

frequent, and the next units to appear would be diplons, formed either by the combination of a proton and neutron or resulting directly from the interaction of two neutrons. As a result a quantum of γ-radiation is produced which is probably fairly "soft." It is significant that Millikan has shown that the major part of the ionization of the atmosphere is due to a soft cosmic ray band, which is of such low frequency that it is practically inappreciable at sea-level. It seems probable that this soft band represents the formation of hydrogen in the way suggested. Since in addition the hydrogen nucleus is simpler than any other, the early state of this nebula and any stars formed in it by further gravitational instability is one of remarkable simplicity, consisting of neutrons, protons, and diplons.

In the development of any theory of the complexity of stars and of the chemical elements there is one obvious difficulty that has been pointed out by d'E. Atkinson*. On the view that the proton is the unit of nuclear structure and that nuclei are built up of protons and negative electrons, the simplest direct synthesis from hydrogen to any other element is the formation of helium according to the reaction

$$4H^+ + 2\bar{e} \rightarrow He^{++} + h\nu.$$

This, as he states, requires a six body collision, and is so improbable a process that he disregards it as playing any important part in supplying stellar energy at all. However, as he points out, granted the helium, then it is not difficult to suppose that many or all other known elements might be formed by cumulative synthesis.

According to the view expressed, however, the difficulty of helium synthesis from hydrogen is removed, for we can imagine that α-particles will be produced by the collision of two diplons. Thus diplogen will be rare as a hydrogen isotope, though formed at an early stage on account of its conversion into helium. The formation of helium will give rise to a quantum of high frequency γ-radiation which will thus be a fundamental cosmic ray quantum. When helium is formed cumulative synthesis probably occurs in the manner suggested by d'E. Atkinson. He supposes that protons can penetrate light nuclei and

* d'E. Atkinson, *loc. cit.*

remain inside, and that approximately every other time this happens the nucleus becomes able to take up, and sooner or later does take up, a free electron as well. It seems more likely in view of the fact that all stable nuclei of odd atomic number contain a diplon that the synthesis occurs by the interaction of nuclei and diplons and neutrons. When such synthesis does occur, however, it is certain that some α-particles must be produced by diplon and nuclear actions, and that in this way, as he suggests, helium is also formed. For example, while we can visualize the formation of Li_3^6 by the union of an α-particle and a diplon, we would expect the addition of another diplon to produce two α-particles by the action

$$Li_3^6 \quad \{[\alpha]+(\overline{p+n})\}+p+n \rightarrow \overset{\nearrow}{\alpha}+\overset{\nearrow}{\alpha}.$$

Thus, there is probably disintegration as well as synthesis with the production of α-particles from diplons.

However, when α-particles are formed it is probable that oxygen, silicon, iron, and calcium soon appear, as the result of the aggregation of the α-particles, to form the stable groups considered. Carbon and oxygen are probably the first elements to appear, the interaction of the 3α-groups with simpler nuclei producing those elements mentioned. We should thus expect Be_4^8 to be a rare isotope, as this nucleus would be transformed into 3α by impact with an α-particle. We can thus visualize the formation of the more stable elements by two body collisions. In all these actions, and in the nuclear collisions occurring, pairs of electrons are produced, some of which are probably emitted forming the high energy electron component of cosmic radiation. We should expect, further, that cosmic radiation would be emitted in the form of high frequency quanta corresponding to the formation of oxygen from helium and carbon, and to the formation of silicon, iron, and calcium from oxygen and carbon. In addition, the presence of uncombined neutrons, protons, diplons, and α-particles would lead gradually to the formation of the more complex nuclei by processes similar to the disintegrations we have considered in section 5. We should, therefore, expect positive electrons to predominate in the primary cosmic ray beam. Further, neutrons would be emitted in many of these processes,

so that cosmic radiation would consist of high-frequency quanta, positive and negative electrons moving with high speeds and neutrons. A primary cosmic ray beam consisting of these three components is sufficient to explain all the observed phenomena. The high-frequency quanta account for Millikan and Cameron's ionization-depth curves, and probably the showers. The electron beam, in which positrons predominate, explains the variation of cosmic ray intensity with geomagnetic latitude and the azimuthal variation noted by Alvarez and Compton.

The pairs and showers would be formed by either the electron component or the high-frequency quanta. Thus if a photon or electron produces a single pair of electrons, on interaction with the potential field near a nucleus, of very high energies then at the moment of formation, both these electrons may have sufficient energies to produce pairs of electrons. If, again, these pairs produce pairs, we may account for the showers, since it has been shown by Oppenheimer and Plesset that electrons of high energy will produce pairs to practically the same extent as high-frequency γ-radiation. The electrons and photons give rise to the observed residual ionization in electroscopes by ionizing secondaries, since the primary rays themselves are almost certainly non-ionizing, as Swann has shown that very high energy electrons would not be able to ionize gases through which they pass.

The neutrons in the primary cosmic ray beam would be capable of nuclear disintegrations, and may give rise to the bursts of ionization known as Hoffmannstösse. Such a neutron beam may play an important part in the disintegration and formation of elements, so that cosmic radiation, while probably arising as a result of the formation of elements, may itself be an important factor in further synthesis in other parts of the univeres.

This work was carried out under the direction of Prof. F. H. Newman, D.Sc., to whom my best thanks are due for valuable criticism and help in preparing this paper.

X. *The Radioactivity of Light Elements.* *By* HAROLD J. WALKE, *B.Sc., Mardon Research Scholar, Department of Physics, Washington Singer Laboratories, University College, Exeter* †.

IN a previous paper ‡ it has been shown that we can understand the emission of protons by nuclei which do not contain a free proton as part of their structure when bombarded by α-particles, if it is assumed that pairs of electrons are formed as a result of the collision between the bombarding particle and the nucleus. In addition, it was shown that the neutron-positron emission of these nuclei could be explained by the same action. It has been proved, however, by Curie and Joliot § and Ellis and Henderson ‖ that the positron emission of aluminium, magnesium, and boron does not cease when the α-particle bombardment is stopped, and this effect has been supposed to be due to the radioactivity of the unstable nuclei resulting from the neutron emission. Further, Danysz and Zwÿ ¶ have observed similar radioactivity by positron emission when nitrogen was bombarded by high-energy α-particles. It will be shown in this paper that this induced radioactivity is explicable on the hypothesis previously suggested.

In this connexion the experiments of Oliphant, Harteck, and Rutherford ** are significant. These investigators used diplons to bombard compounds like ammonium chloride and ammonium sulphate in which ordinary hydrogen was in part replaced by diplogen. Enormous numbers of fast protons were found to be emitted, the main group having a range of 14 cm. in air and of energy 3×10^6 e.v. In addition to this group, another strong group of singly charged particles was observed of range in air of only 1·6 cm. as well as large numbers of neutrons.

In order to account for these observations it was suggested that, as a result of a collision between two

† Communicated by Prof. F. H. Newman, D.Sc.
‡ Walke, Phil. Mag. xviii. p. 129 (1934).
§ Curie and Joliot, *Comptes Rendus*, cxcviii. p. 254 (1934).
‖ Ellis and Henderson, ' Nature,' cxxxiii. p. 531 (1934).
¶ Wertenstein, *ibid.* cxxxiii. p. 564 (1934).
** Oliphant, Harteck, and Rutherford, *ibid.* cxxxiii. p. 481 (1934).

diplons, a helium nucleus of mass 4 and charge 2 was formed which differed from the normal α-particle in having a large excess energy. The new nucleus is in consequence unstable, and breaks up into two parts in two different ways, thus :

$$D_1^2+D_1^2 \rightarrow He_2^4 \rightarrow He_1^3+p,$$
$$D_1^2+D_1^2 \rightarrow He_2^4 \rightarrow He_2^3+n_0^1,$$

and it was suggested as very probable that He_2^3 would emit a positron being transformed to H_1^3. In considering the other radioactive actions this is significant.

The cause of the two disintegrations considered is the formation of an α-particle with excess energy. It is suggested that in a similar manner the radioactivity of the light elements by positron emission is due to the formation within the nuclei concerned of a proton with excess energy. The actions are assumed the same as was considered in the previous paper, but it is further supposed that, when the energy of the α-particle increases beyond a critical value, the loosely bound neutron is emitted before uniting with the high-energy positron produced, which remains within the nucleus and unites with another neutron which is produced when the negative electron of the pair unites with the positron of the diplon to give rise to a quantum of γ-radiation. This proton, on account of the high energy of the positron, differs from the normal proton in having a large excess energy. In consequence this particle is explosive, and disintegrates comparatively rapidly by emitting a high-speed positron. According to this view, therefore, the similar radioactivity produced by bombarding aluminium, magnesium, boron, and nitrogen with high-speed α-particles is due to the presence within the new nuclei produced of this "radioproton." The varying periods of decay of this induced radioactivity is explicable on account of the differences between the various nuclear potential fields concerned. Further, on this assumption we should expect the positrons to be emitted from the nuclei with definite energies, the induced radioactivity thereby differing from the β-ray disintegrations of the normal radioactive atoms in which the disintegration electrons have a continuous range of energies.

The reactions may accordingly be presented by equations of the type

$$\mathrm{Al}^{27}_{13}\quad \{[6\alpha]+(\overline{p+n}+n)\}+\alpha \rightarrow \{[7\alpha]+(\overline{p+n}+n)+\overset{-}{e}+\overset{+}{e}\}$$
$$\rightarrow \{[7\alpha]+(n+n)+\overset{+}{e}\}+\overset{\nearrow}{n}+\gamma \rightarrow \{[7\alpha]+(n)+\overset{*}{p}\}$$
Radiophosphorus I.
$$\rightarrow \{[7\alpha]+(n+n)\}+\overset{+\nearrow}{e}\quad \mathrm{Si}^{30}_{14},$$

$\overset{*}{p}$ representing the the "radioproton."

On this view, though we should expect positive electrons to be observed accompanying the neutron emission of beryllium, we should not expect any radioactive effect, as, according to the structure of Be^{9}_{4} assumed, no radioproton could be formed after the departure of the disintegration neutron, as follows :

$$\mathrm{Be}^{9}_{4}\quad \{[2\alpha]+(n)\}+\alpha \rightarrow \{[3\alpha]+(n)+\overset{-}{e}+\overset{+}{e}\}$$
$$\rightarrow [3\alpha]+\overset{\nearrow}{n}+\overset{+\nearrow}{e}+\overset{-}{e}\quad \mathrm{C}^{12}_{6}.$$

It is significant that Curie and Joliot observed positrons when beryllium was bombarded with α-particles, but they detected no induced radioactivity.

In contrast magnesium Mg^{26}_{12} is on this view radioactive, as a radioproton is formed when the α-particle is captured and the neutron is emitted, as shown by the following reaction :—

$$\mathrm{Mg}^{26}_{12}\quad \{[6\alpha]+(n+n)\}+\alpha \rightarrow \{[7\alpha]+(n+n)+\overset{-}{e}+\overset{+}{e}\}$$
$$\rightarrow \{[7\alpha]+\overset{*}{p}\}+\overset{\nearrow}{n}+\overset{-}{e} \rightarrow \{[7\alpha]+n\}+\overset{+\nearrow}{e}\quad \mathrm{Si}^{29}_{14}$$
Radiophosphorus II.

In view of the fact that on the nuclear scheme adopted there are no stable nuclei in which a proton is not accompanied by a neutron, it seems probable that any nucleus in which a "free proton" occurs will be radioactive, and will emit a positron. We should therefore expect nuclei of the type $4n$, *i. e.*, helium, carbon, and oxygen, to emit positive electrons when bombarded by protons if the bombardment resulted in the capture of a proton. It is significant that Henderson, Livingston, and Lawrence † have observed induced radioactivity when they bombarded carbon with protons.

† Henderson, Livingston, and Lawrence, Phys. Rev. xlv. p. 429 (1934).

In considering these results and the emission of protons and neutrons discussed previously †, it might be imagined that the various disintegrations observed are due to the break-up within the nucleus of the bombarding α-particle. It will be shown there is considerable evidence to prove that this is unlikely. In the first place α-particles are emitted from radioactive nuclei with energies varying from 4 to 8×10^6 e.v., and it has never been shown that these particles are in any way unstable. Moreover, as it has been shown that the long-range α-particles are associated with γ-radiation, it is certain that the α-particles can remain within nuclei in energy states which are considerably higher than the value given above. Since the emitted α-particles resemble in every way the helium ions produced in discharge-tubes, even though they have passed through the intense nuclear fields of the radioactive atoms, it is highly improbable that they will disintegrate in passing through the much less intense potential fields of the bombarded nuclei. The disintegrations observed are due to bombardment by normal α-particles ; the disintegrations observed by Oliphant, Harteck, and Rutherford were due to helium nuclei with a large excess energy.

Further, if the emission of protons and neutrons was a phenomenon due to the disintegration of the α-particles on colliding with nuclei, we should expect disintegration particles to be observed by bombarding any of the light elements of atomic number less than 20 (the potential barriers of heavier nuclei are so high that capture of an α-particle is a rare phenomenon). On the hypothesis postulated in the preceding paper, however, no disintegration particles would be observed from helium, carbon, and oxygen under α-particle bombardment. It is significant that neither proton nor neutron emission has been detected when these elements have been bombarded by α-particles. In addition, if the protons and neutrons observed came from disintegrating α-particles there should be evidence of the recoiling H_1^3 or He_2^3 nucleus. No expansion photographs of α-particle collisions have shown any particles emitted other than the expelled proton and the recoil nucleus. Finally, it would be difficult to explain why the proton and neutron emission

† Walke, *loc. cit.*

varies so considerably from element to element if in each case disintegration of the α-particle occurred. The variation is rather to be attributed to differences of nuclear constitution. On the view expressed, the number of particles observed depends on the number of nuclei present in which one or more loosely bound neutrons exist, and except for the heavier elements chlorine, argon, and potassium (for which elements the small yield of protons is due to the increased height of the potential barrier), the small number of protons observed is due to the relatively small abundance of such isotopes.

It is to be noticed that, according to the above hypothesis, neutron emission with induced radioactivity of the resulting nucleus should be observed from all elements which give rise to protons when bombarded by α-particles.

Moreover, as radioactivity by diplon and proton bombardment has lately been observed, it is certain that the effects discussed are not due to disintegration of the bombarding α-particle ; the radioactivity of magnesium and carbon seem only explicable by means of a "radio-proton."

Lawrence and Livingston† have observed neutron radiation by bombarding many elements with diplons accelerated by a potential of three million volts. From the same targets they have observed the emission of protons in large numbers, the proton yields being found to be roughly proportional to the neutron yields, suggesting that the neutrons and protons were involved in the same nuclear reaction. This process seemed to be due to the disintegration of the diplon itself, the observed ranges agreeing well with the hypothesis if the mass of the neutron is about unity. However, in a later communication‡ induced radioactivity has been observed with many elements bombarded by diplons, and, in addition, many of these have already been observed to emit α-particles. It is probable that more than one type of reaction occurs. For example, if the diplon disintegrates into protons and neutrons of high energy (as these experimenters suggest), either of these particles may cause other nuclear disintegrations. Moreover, if the diplons are captured by nuclei, stable or unstable α-particles

† Lawrence and Livingston, *ibid.* xlv. p. 220 (1934).
‡ Henderson, Livingston and Lawrence, *ibid.* xlv. p. 429 (1934).

may be formed which appear either as normal α-particles, as, for example, with nitrogen †,

$$N_7^{14} \quad \{[3\alpha]+(\overline{p+n})\}+\overline{p+n} \rightarrow \{[3\alpha]+(\overline{p+n}+\overline{p+n})\} \rightarrow [3\alpha]+\overset{\nearrow}{\alpha} \quad C_6^{12},$$

or as H_1^3 and a proton, as has been observed by the disintegration of lithium and diplogen when an unstable α-particle is formed. And, moreover, with high-energy diplons electron pairs may also be produced.

We should thus explain the positron radioactivity of carbon bombardment by diplons as due to the capture of a proton if the diplon disintegrates before entering the nucleus, or, if it is captured by the nucleus, as due to its disintegrating on impact with the nuclear core and emitting the neutron. On either view of the action "radionitrogen" is produced, the radioactivity being due to the disintegration of the free or radioproton.

With nuclei of the type

$$\{[N\alpha]+(\overline{p+n+n})\} \quad \text{and} \quad \{[N\alpha]+(\overline{p+n})\}$$

radioactivity is probably due to capture of the diplon with the production of α-particles. If, for example, the diplon is captured by a lithium nucleus it has been shown that H_1^3 is emitted, and from considering the results of Oliphant, Harteck, and Rutherford (*loc. cit.*) it seems certain that the reaction is as follows :—

$$Li_3^6 \quad \{[\alpha]+(p+\overline{n})\}+\overline{p+n} \rightarrow \{[\alpha]+(\overline{p+n}+\overline{p+n})\} \rightarrow \overset{\nearrow}{\alpha}+\overset{*\nearrow}{\alpha}$$
$$\overset{*}{\alpha} \rightarrow H_1^3+\overset{\nearrow}{p},$$

where $\overset{*}{\alpha}$ represents the excess-energy α-particle.

However, we can envisage the disintegration of $\overset{*}{\alpha}$ by the emission of a neutron leaving He_2^3, this nucleus being radioactive by positron emission, as it may be considered to consist of a diplon and a proton. As no stable nuclei are known in which each proton is not accompanied by a neutron, the radioactivity of He_2^3 can similarly be attributed to a "radioproton." It is probable, therefore, that substances with nuclei of the form $\{[N\alpha]+(\overline{p+n})\}$ when bombarded with diplons may give rise to radioactive helium nuclei He_2^3, so that the

† Lewis, Livingston, and Lawrence, *ibid.* xliv. p. 55 (1933).

half-period of such substances may be very similar. Some such effect may be the cause of similar periods of several substances, as has been observed by Henderson, Livingston, and Lawrence. In addition with nuclei of the type $\{[N\alpha]+(\overline{p+n}+n)\}$ we may have disintegration with the emission of both α-particles and neutrons. For instance, Oliphant, Kinsey, and Rutherford † observed neutrons and α-particles from Li_3^7 according to the reaction

$$Li_3^7 \quad \{[\alpha]+(\overline{p+n}+n)\}+\overline{p+n}\rightarrow\{[\alpha]+(\overline{p+n}+\overline{p+n})\}+\overset{\nearrow}{n}$$
$$\rightarrow \overset{\nearrow}{\alpha}+\overset{\nearrow}{\alpha}+\overset{\nearrow}{n}.$$

It is possible with such a reaction that an explosive α-particle may be formed giving rise to He_2^3, as already explained. The fact that boric oxide, sodium phosphate, lithium carbonate, and ammonium nitrate have the same half-period may be due to the production of He_2^3, though it may, however, be due to a common impurity.

Finally, we have the possibility of pair formation with diplons of energy greater than about $1{\cdot}5\times10^6$ e.v. Thus the radioactivity of a nucleus of the form $\{[N\alpha]+(\overline{p+n}+n)\}$, as, for example, aluminium, may result from emission of an α-particle, as follows :—

$$Al_{13}^{27} \quad \{[6\alpha]+(\overline{p+n}+n)\}+\overline{p+n}$$
$$\rightarrow\{[6\alpha]+(\overline{p+n}+\overline{p+n})+n+\overset{-}{e}+\overset{+}{e}\}$$
$$\rightarrow\{[6\alpha]+\overset{*}{p}\}+\overset{\nearrow}{\alpha}+\overset{-}{e}\rightarrow\{[6\alpha]+n\}+\overset{+\nearrow}{e} \quad Mg_{12}^{25},$$

and by a similar reaction the radioactivity of beryllium may be considered, as follows :—

$$Be_4^9 \quad \{[2\alpha]+n+\overline{p+n}\rightarrow\{[2\alpha]+(\overline{p+n})+n+\overset{-}{e}+\overset{+}{e}\}$$
$$\rightarrow\{[2\alpha]+(n)+\overset{*}{p}\}+\overset{\nearrow}{n}+\gamma\rightarrow\{(2\alpha]+(n+n)\}+\overset{+\nearrow}{e} \quad Be_4^{10}.$$

It is possible, however, that the diplon disintegrates before entering the beryllium nucleus and that the neutron is emitted by it. In all cases, however, it is probable that the new radioactivity is due to a free proton within the nucleus, and it seems certain that the " radioproton "

† Oliphant, Kinsey, and Rutherford, Proc. Roy. Soc. A, cxli. p. 722 (1933).

and the formation of electron pairs in nuclear reactions play important parts in the synthesis of elements.

In addition, if, as suggested, the formation of pairs of electrons is a general phenomenon attending the collision of high-energy particles and nuclei, we should expect to observe positrons and γ-radiation resulting from their annihilation when α-particles interact with nuclei, even though disintegration does not take place. In this connexion the results of Slater † are significant. Slater bombarded various elements with fast α-rays and showed that a hard γ-radiation was emitted which differed but little in quality when the radiator was changed from one of high atomic number, such as lead or gold, to one of medium atomic number, such as tin. The intensity obtained was small, and only a small fraction of the impinging α-particles could have been effective. For the same absorption conditions the intensity was about 50 per cent. greater for the lead radiator than the tin. These results are what would be expected if the radiation was emitted during the close collision of an α-particle with a nucleus of one of the atoms of the radiator.

These results, namely, the observation of γ-radiation which differed little in hardness whether from an element of high or medium atomic number, are similar to those obtained by Gray and Tarrant ‡ when investigating the anomalous scattering of hard γ-radiation. It has been shown that these results are mainly due to the annihilation of positrons formed by the interaction of the high-frequency quanta and the atomic nucleus. It would, therefore, appear probable that Slater observed the γ-radiation arising as a result of annihilation of the positrons formed by the interaction of α-particles and nuclei. Moreover, as Skobeltzyn and Stepanowa § have shown that high-energy β-rays from a radioactive substance produce electron pairs by interaction with the atoms of the materials surrounding the source, it would appear that the formation of positive and negative electrons is a general phenomenon when kinetic-energy changes of the order of millions of electron-volts occur.

It was also suggested || that the α-particle configurations

† Slater, Phil. Mag. xlii. p. 904 (1921).
‡ Gray and Tarrant, Proc. Roy. Soc. A, cxxxvi. p. 662 (1933).
§ Skobeltzyn and Stepanowa, ' Nature,' cxxxiii. p. 565 (1934).
|| Walke, *loc. cit.*

of the nuclei of the elements of atomic number 60 and 76 corresponded to closed-shell systems. The atomic number 76 was assumed following a suggestion by Rutherford. By analogy with the radioactive series it was assumed that the disintegration of samarium by α-particle emission indicated that this element contained in its nucleus one α-particle more than a completed shell. It was thus deduced that the α-particles in the nucleus of atomic number 60 consisted of a closed shell of five α-particles surrounding the core, which was assumed to become complete at atomic number 50. In consequence we should similarly expect that the nucleus containing one more α-particle than the completed shells at atomic number 76 would be radioactive and emit α-particles. This nucleus of atomic number 78 is platinum, which element we should accordingly expect to emit α-particles.

In this connexion some experiments of Hoffmann † are significant. This investigator tested several non-radioactive elements for evidence of spontaneous disintegration, by means of a very sensitive electroscope. By careful attention to detail he was able to detect the ionization due to single α-particles and to separate the effects of these rays from those due to β- and γ-rays. From a statistical examination of the results he obtained he concluded that platinum and brass gave a weak α-ray activity which was specific to those substances, and which could not be attributed to the presence of known radio-elements. These results confirm the presence of a closed shell of α-particles in the osmium nucleus, above which is added a further shell of three α-particles to complete the α-particle configuration of the heaviest stable nuclei.

This work was carried out under the direction of Prof. F. H. Newman, D.Sc.

Note added in proof.—It is significant that Curie and Joliot ‡ have observed negative electrons accompanying the positrons from magnesium and beryllium. The reactions discussed in this paper predict such a result.

† Hoffmann, *Ann. d. Phys.* lxii. p. 738 (1920).
‡ Curie and Joliot, *Jour. d. Phys.* v. p. 153 (1934).

XI. *On the Solution of a Problem in Heat-conduction from a Spherical Source by the Method of Wave-trains. By* JAMES ROBERTSON, *M.A., B.Sc., Lecturer in Mathematics at Jordanhill Training College, Glasgow* *.

IN the previous papers of this series † the general method of solving problems in heat-conduction by means of wave-trains has been explained. All the ordinary problems can be solved by an investigation of the temperature wave-trains set up from suitably placed periodic heat or temperature sources of appropriate strength. The effect at any point in the medium is regarded as the resultant of the effects due to the trains so set up, and the effects due to all the other trains set up by the reflexions and transmissions of the original ones at the boundaries. The analytical expressions for all these trains are readily written down. Each such expression is a solution of the fundamental equation of heat-conduction; likewise the infinite series of them corresponding to the infinite number of reflexions, transmissions, etc., that take place is a solution. Moreover, the terms of this series naturally arrange themselves in pairs, one member of each pair representing a train incident on a boundary, the other representing the corresponding reflected train, the coefficient in any one pair of trains being so chosen that the boundary condition prevailing is satisfied. In the particular problems solved in these papers the choice of these coefficients has been a perfectly straightforward matter. We are thus enabled to obtain an expression for the temperature at any point of the medium due to the postulated periodic sources, at once adjusted to satisfy the differential equation of heat-conduction and the boundary conditions. From this result we can proceed, by what we may now regard as a known process ‡, to the case where each periodic source is replaced by the corresponding instantaneous one. It might reasonably be claimed for the wave-train method thus summarized that it throws more light on the physical processes

* Communicated by George Green, D.Sc., Applied Physics Department, The University of Glasgow.

† G. Green, Phil. Mag. iii. Suppl. (April 1927), I.; v. (April 1928), II.; ix. (Feb. 1930), III.; xii. Suppl. (Aug. 1931), IV.; J. Robertson, xv. (May 1933).

‡ *e. g.*, Green, I. pp. 787, 797.

involved than other more purely mathematical methods. Analogies from hydrodynamics, optics, and other branches of physics at once suggest themselves. Temperature wave-trains satisfy boundary conditions as to phase, intensity, etc., exactly as do the wave-trains by which any other physical state is propagated. The following-up of each train from its inception, in its successive incidences, reflexions, and transmissions, enables us to analyse more clearly the varying physical condition from point to point in the medium.

The method is specially successful in cases where flow of heat takes place across a surface of separation of two media of different conductivities. In his third paper Dr. Green has shown in full the solution of the problem of heat-flow in a finite sphere surrounded by a finite concentric sheath of different material. He has also indicated the lines of the solution for the case where the surrounding sheath is of infinite extent. While it is theoretically possible to deduce the solution of the latter problem from the former, it is more instructive to attempt it from first principles by an application of the wave-train method. The project just stated may be regarded as the objective of the present investigation.

The problem is represented, in the usual notation, by means of the following equations :—

$$0<r<a, \quad \frac{\partial v_1}{\partial t}=\kappa_1\nabla^2 v_1; \quad r>a, \quad \frac{\partial v_2}{\partial t}=\kappa_2\nabla^2 v_2. \qquad (1)$$

$$r=a, \quad v_1=v_2, \quad \text{and} \quad \mathrm{K}_1\frac{\partial v_1}{\partial r}=\mathrm{K}_2\frac{\partial v_2}{\partial r}. \qquad (2)$$

We begin by supposing that at the surface $r=r_1$ within the inner medium we have a periodic heat-source of strength qe^{ikt} per unit area. This source may be regarded as setting up a converging temperature wave-train denoted by

$$r<r_1, \quad -\frac{qr_1}{2\mathrm{K}_1 r\sqrt{\frac{ik}{\kappa_1}}}e^{ikt-(r_1-r)\sqrt{\frac{ik}{\kappa_1}}},$$

and a diverging train

$$r>r_1, \quad \frac{qr_1}{2\mathrm{K}_1 r\sqrt{\frac{ik}{\kappa_1}}}e^{ikt-(r-r_1)\sqrt{\frac{ik}{\kappa_1}}}, \qquad (3)$$

By combining with these trains all the others set up by reflexions at the surface $r=a$ and at the centre of the sphere we obtain expressions for the temperature at any point in the inner medium. Thus we follow up the original converging train and write down the contributions made by it and its various continuations to v_i and v_0, the temperatures in the two parts ($r<r_1$ and $r>r_1$) of the inner medium. We next repeat the process, beginning with the original diverging train, and then obtain total effects by addition. The details of the process have been given previously *, and need not be repeated.

Denoting $\sqrt{\frac{ik}{\kappa_1}}$ by $i\lambda$, we find that the complete expressions for v_i and v_0 are given by

$$\left.\begin{aligned} r<r_1, \qquad v_i &= \frac{qr_1e^{ikt}}{2K_1ri\lambda}\,2i\sin\lambda r\,\frac{e^{-i\lambda r_1}+Ae^{-(2a-r_1)i\lambda}}{1+Ae^{-2ai\lambda}}, \\ r>r_1, \qquad v_0 &= \frac{qr_1e^{ikt}}{2K_1ri\lambda}\,2i\sin\lambda r_1\,\frac{e^{-i\lambda r}+Ae^{-(2a-r)i\lambda}}{1+Ae^{-2ai\lambda}}, \end{aligned}\right\} \qquad (4)$$

where A is the coefficient for reflexion at the surface $r=a$. It is important to notice that v_i is finite at $r=0$; also that $v_i=v_0$ at $r=r_1$, and again that

$$-K_1\left(\frac{\partial v_0}{\partial r}-\frac{\partial v_i}{\partial r}\right)_{r=r_1}=qe^{ikt}$$

as required. It is instructive also to notice the form taken by v_0 when r_1 tends to zero. If we suppose that this limit is reached in such a way that $4\pi r_1^2q$ tends to a definite limit q_0, say, we find that the above expression for v_0 reduces exactly to the form required for the case of a point source of strength q_0e^{ikt} situated at the centre of the sphere of radius a.

We obtain the result corresponding to (4) for the outer medium by supposing that each positively travelling constituent of v_0 as indicated in (4) on arrival at the surface $r=a$ is partly reflected and partly transmitted to the outer medium. The temperature in this medium will be obtained by writing down the resultant of all the trains so transmitted. As the outer medium is of infinite extent, each transmitted train proceeds without

* Green, III. p. 246.

interruption to infinity, so that there are no reflexion effects in this medium, and consequently no further retransmission effects inwards across the surface $r=a$. To this extent the problem is simpler than when the outer medium has an outer boundary at a finite distance. Thus, taking A′ as the coefficient for transmission across the surface $r=a$ in the positive direction, we find that the temperature v_2 in the outer medium is given by

$$v_2=\frac{\mathrm{A}'qr_1e^{ikt}}{2\mathrm{K}_2r\mu i\lambda}2i\sin\lambda r_1\frac{e^{-ai\lambda-(r-a)\mu i\lambda}}{1+\mathrm{A}e^{-2ai\lambda}}, \quad . \quad . \quad (5)$$

where $$\mu=\sqrt{\frac{\kappa_1}{\kappa_2}}.$$

The results (4) and (5) apply when the periodic source is located within the inner medium. It is of equal importance to obtain the corresponding results when this source is in the outer medium. In this case the effect in the inner medium is produced by the transmission inwards across the surface $r=a$ of the primary converging train emanating from the surface $r=r_1(r_1>a)$, and by the successive reflexions of this transmitted train at $r=0$ and at $r=a$. The effect in the outer medium is compounded of (i.) that due to the original trains emanating from the surface $r=r_1$, (ii.) that due to the reflexion at $r=a$ of the original converging train, and (iii.) that due to the partial retransmission outwards across the surface $r=a$ of positively travelling trains in the inner medium. Taking C as coefficient for transmission inwards across the surface $r=a$, and C′ as coefficient for reflexion at this surface in the outer medium, A′ having its former meaning, we find that v_1, v_2, the total effects in the inner and outer media respectively, take forms indicated by

$$v_1=\frac{\mathrm{C}qr_1}{2\mathrm{K}_1ri\lambda}e^{ikt-(r_1-a)\mu i\lambda-ai\lambda}\frac{2i\sin r\lambda}{1+\mathrm{A}e^{-2ai\lambda}}, \quad . \quad . \quad (6)$$

$$a<r<r_1, \quad v_2=\frac{qr_1e^{ikt}}{2\mathrm{K}_2r\mu i\lambda}\left\{e^{-(r_1-r)\mu i\lambda}+\mathrm{C}'e^{-(r_1+r-2a)\mu i\lambda}-\frac{\mathrm{A}'\mathrm{C}e^{-2ai\lambda-(r+r_1-2a)\mu i\lambda}}{1+\mathrm{A}e^{-2ai\lambda}}\right\}, \quad . \quad (7)$$

the corresponding form for v_2 in the region $r>r_1$ being obtained from (7) by interchanging r and r_1 in the bracketed expression.

The results (4), (5) and (6), (7) give the temperature at any point in either medium due to the prescribed periodic heat sources. To obtain from them results corresponding to instantaneous initial sources we have to perform the process indicated by $\frac{1}{2\pi}\int_{-\infty}^{\infty} v\,dk$. If we use the transformation $\sqrt{\frac{ik}{\kappa_1}}=i\lambda$, we find that this process is equivalent to $\frac{i\kappa_1}{\pi}\int_C v\lambda\,d\lambda$, where the contour of integration C consists of the line $\theta=-3\pi/4$ from infinity to the origin, followed by the line $\theta=-\pi/4$ from the origin to infinity. When we apply this process to the second form of (4) we obtain, for an instantaneous source situated at $r=r_1$ within the inner medium,

$$r>r_1,\quad v_1=\frac{iq\kappa_1 r_1}{\pi \mathrm{K}_1 r}\int_C e^{-\kappa_1\lambda^2 t}\sin\lambda r_1\,\frac{e^{-i\lambda r}+\mathrm{A}e^{-(2a-r)i\lambda}}{1+\mathrm{A}e^{-2ai\lambda}}\,d\lambda, \quad (8)$$

the corresponding result in the region $r<r_1$ being obtained from this by interchanging r and r_1 in the integrand. Similarly, when the process is applied to (5), (6), and (7) we obtain, in order,

$$v_2=\frac{iq\kappa_1 r_1}{\pi \mathrm{K}_2\mu r}\int_C e^{-\kappa_1\lambda^2 t}\sin\lambda r_1\,\frac{\mathrm{A}'e^{-ai\lambda-(r-a)\mu i\lambda}}{1+\mathrm{A}e^{-2ai\lambda}}\,d\lambda, \quad . \quad . \quad . \quad (9)$$

$$v_1=\frac{iq\kappa_1 r_1}{\pi \mathrm{K}_1 r}\int_C e^{-\kappa_1\lambda^2 t}\sin\lambda r\,\frac{\mathrm{C}e^{-ai\lambda-(r_1-a)\mu i\lambda}}{1+\mathrm{A}e^{-2ai\lambda}}\,d\lambda, \quad . \quad . \quad (10)$$

$$v_2=\frac{iq\kappa_1 r_1}{2\pi \mathrm{K}_2\mu r}\int_C e^{-\kappa_1\lambda^2 t}\left\{e^{-(r_1-r)\mu i\lambda}+\mathrm{C}'e^{-(r_1+r-2a)\mu i\lambda}-\frac{\mathrm{A}'\mathrm{C}e^{-2ai\lambda-(r+r_1-2a)\mu i\lambda}}{1+\mathrm{A}e^{-2ai\lambda}}\right\}d\lambda, \quad (11)$$

$a<r<r_1$, with a corresponding form in the case of (11) for the region $r>r_1$.

The results (8) and (9) apply when the instantaneous source is within the inner medium, (10) and (11) when it is in the outer medium. For the evaluation of these integrals we require to know the forms of the various coefficients A, A′, C, C′. These have already been obtained*. Thus, with

$$d=\mathrm{K}_1+\mathrm{K}_2\mu-\frac{1}{ai\lambda}(\mathrm{K}_1-\mathrm{K}_2)$$

* Green, III. p. 255.

we have

$$\left.\begin{aligned} A&=\frac{K_1-K_2\mu+\frac{1}{ai\lambda}(K_1-K_2)}{d}; \quad A'=\frac{2K_2\mu}{d},\\ C'&=\frac{-K_1+K_2\mu+\frac{1}{ai\lambda}(K_1-K_3)}{d}; \quad C=\frac{2K_1}{d}, \end{aligned}\right\} \quad (12)$$

with the relations

$$A=C-1; \qquad A'=C'+1;$$

$$AC'-A'C=-\frac{K_1+K_2\mu+\frac{1}{ai\lambda}(K_1-K_2)}{K_1+K_2\mu-\frac{1}{ai\lambda}(K_1-K_2)}.$$

Utilising these results, we find that (8) to (11) become, after reduction,

$$v_1=\frac{iq\kappa_1 r_1}{\pi K_1 r_*}\int_C e^{-\kappa_1\lambda^2 t}\sin\lambda r_1 \times \frac{K_1\cos(a-r)\lambda-(K_1-K_2)\dfrac{\sin(a-r)\lambda}{a\lambda}+iK_2\mu\sin(a-r)\lambda}{d'}\,d\lambda,$$

. . . (13)

$$v_2=\frac{iq\kappa_1 r_1}{\pi r}\int_C e^{-\kappa_1\lambda^2 t}\sin\lambda r_1\frac{e^{-(r-a)\mu i\lambda}}{d'}d\lambda, \quad . . . . . (14)$$

$$v_1=\frac{iq\kappa_1 r_1}{\pi r}\int_C e^{-\kappa_1\lambda^2 t}\sin\lambda r\frac{e^{-(r_1-a)\mu i\lambda}}{d'}d\lambda, \quad . . . . . (15)$$

$$v_2=\frac{q\kappa_1 r_1}{2\pi K_2\mu r_*}\int_C e^{-\kappa_1\lambda^2 t}\left\{e^{-(r_1-r)\mu i\lambda}-e^{-(r_1+r-2a)\mu i\lambda}\times\frac{K_1\cos a\lambda-(K_1-K_2)\dfrac{\sin a\lambda}{a\lambda}-iK_2\mu\sin a\lambda}{d'}\right\}d\lambda, \quad (16)$$

where

$$d'=K_1\cos a\lambda-(K_1-K_2)\frac{\sin a\lambda}{a\lambda}+iK_2\mu\sin a\lambda. \quad (17)$$

Discussion of the Roots of the Equation $d'=0$.

The evaluation of the integrals appearing in the results (13) to (16) would enable us to obtain at once the solutions corresponding to the initial surface sources postulated,

and clearly from these we could obtain by volume integrations the solutions corresponding to any initial heat distribution of symmetrical type. For such evaluation we require to know the nature of the roots of the equation $d'=0$. If we rewrite this equation in the form

$$\cot a\lambda = \frac{K_1-K_2}{K_1}\frac{1}{a\lambda} - i\frac{K_2\mu}{K_1}, \quad . \quad . \quad . \quad (18)$$

and put $a\lambda=x+iy$, where x and y are real, we find, on equating real and imaginary parts,

$$\left.\begin{aligned} \frac{\sin 2x}{\cosh 2y-\cos 2x} &= \frac{K_1-K_2}{K_1}\frac{x}{x^2+y^2}, \\ \frac{\sinh 2y}{\cosh 2y-\cos 2x} &= \frac{K_1-K_2}{K_1}\frac{y}{x^2+y^2}+\frac{K_2\mu}{K_1}, \end{aligned}\right\} \quad . \quad (19)$$

and, by combining these,

$$\frac{y\sin 2x - x\sinh 2y}{\cosh 2y-\cos 2x} = -\frac{K_2\mu}{K_1}x.$$

We observe from the second of these that $y=0$ is inadmissible, so that the equation (18) has no real roots. If x is positive, the third of (19) indicates that the expression

$$xy\left(\frac{\sin 2x}{x}-\frac{\sinh 2y}{y}\right)$$

is negative, so that

$$y \text{ and } 2\left(\frac{\sin 2x}{2x}-\frac{\sinh 2y}{2y}\right)$$

are of opposite sign. Clearly the expression in the bracket is negative for all values of x and y. Thus y is positive. Similarly, if x were negative, we could again show that y is positive. It is thus shown that all the roots of the equation $d'=0$ are complex, and that they all lie in the upper half of the λ plane. Actually it will be noticed that the equation under discussion is the limiting form of Green's equation $f_1(\lambda)=0$*, encountered in the discussion of the case of the sphere surrounded by the finite sheath, when the thickness of the sheath becomes infinitely great, in which case the restriction as to real roots is abandoned.

Reverting to the results (13) to (16), since all the singularities of the integrands lie in the upper half of the complex plane, we may replace the integrals along the standard

* *Ibid.* p. 256.

contour by integrals along the real axis. Thus, after some reduction, we find in place of (13) and (14)

$$v_1 = -\frac{2q\kappa_1 K_2 \mu r_1}{\pi r}\int_0^\infty e^{-\kappa_1\lambda^2 t} \frac{\sin\lambda r_1 \sin\lambda r\, d\lambda}{\left\{K_1\cos a\lambda - (K_1-K_2)\dfrac{\sin a\lambda}{a\lambda}\right\}^2 + K_2{}^2\mu^2\sin^2 a\lambda}, \quad (20)$$

$$v_2 = \frac{2q\kappa_1 r_1}{\pi r}\int_0^\infty e^{-\kappa_1\lambda^2 t}\sin\lambda r_1 \times \frac{\left\{K_1\cos a\lambda - (K_1-K_2)\dfrac{\sin a\lambda}{a\lambda}\right\}\sin\mu(r-a)\lambda + K_2\mu\sin a\lambda\cos\mu(r-a)\lambda}{\left\{K_1\cos a\lambda - (K_1-K_2)\dfrac{\sin a\lambda}{a\lambda}\right\}^2 + K_2{}^2\mu^2\sin^2 a\lambda} d\lambda. \quad (21)$$

The result v_1 by which (15) is replaced is found to be the same as (21) when r and r_1 are interchanged under the integral sign. The form of v_2 corresponding to (16) is shown below.

These results are shown with greater compactness if we write

$$R\cos\phi = K_1\cos a\lambda - (K_1-K_2)\frac{\sin a\lambda}{a\lambda};$$

$$R\sin\phi = K_2\mu\sin a\lambda,$$

in virtue of which (20) and (21) become

$$v_1 = -\frac{2q\kappa_1 K_2\mu r_1}{\pi r}\int_0^\infty e^{-\kappa_1\lambda^2 t}\frac{\sin\lambda r_1\sin\lambda r\, d\lambda}{R^2}, \quad . \quad . \quad (20')$$

$$v_2 = \frac{2q\kappa_1 r_1}{\pi r}\int_0^\infty e^{-\kappa_1\lambda^2 t}\frac{\sin\lambda r_1\sin\{\mu(r-a)\lambda+\phi\}}{R}d\lambda, \quad (21')$$

these being the fundamental results when the instantaneous source is in the inner medium. Similarly, when the source is in the outer medium, we have

$$v_1 = \frac{2q\kappa_1 r_1}{\pi r}\int_0^\infty e^{-\kappa_1\lambda^2 t}\frac{\sin\lambda r\sin\{\mu(r_1-a)\lambda+\phi\}d\lambda}{R}, \quad . \quad . \quad (22)$$

$$v_2 = \frac{2q\kappa_1 r_1}{\pi K_2\mu r}\int_0^\infty e^{-\kappa_1\lambda^2 t}\sin\{(r_1-a)\mu\lambda+\phi\}\sin\{(r-a)\mu\lambda+\phi\}\, d\lambda. \quad . \quad . \quad . \quad (23)$$

The full investigation of the integrals in (20) to (23) is not in the meantime attempted. Some useful idea of the kind of results to be expected, however, is obtained if we consider their approximate evaluation. Of various possible approaches we take that suggested by the special case $K_1-K_2=0$, $\mu=1$. It is readily verified that in this case all four results reduce to the form

$$v=\frac{2q\kappa_1 r_1}{\pi K_1 r}\int_0^\infty e^{-\kappa\lambda^2 t}\sin\lambda r_1 \sin\lambda r\, d\lambda, \quad . \quad . \quad (24)$$

which is the well-known form of solution for the case of the source at the surface $r=r_1$ in the infinite medium. If, *e. g.*, there is an initial heat distribution between the surfaces $r_1=a$ and $r_1=b$ given by $q=1/r_1$, the temperature at any subsequent time is given by

$$v=\frac{2\kappa_1}{\pi K_1 r}\int_a^b dr_1\int_0^\infty e^{-\kappa\lambda^2 t}\sin\lambda r_1 \sin\lambda r\, d\lambda. \quad . \quad (25$$

It seems natural to take next the case where there is a small difference between the conductivities of the two media. If, accordingly, we write

$$\sigma=\frac{K_1}{K_2\mu}; \quad \sigma'=\frac{K_1-K_2}{K_2\mu}; \quad \sigma=1+\epsilon,$$

where σ'/σ and ϵ are small quantities, we find, *e. g.*, that (20) becomes

$$v_1=\frac{2q\kappa_1 r_1}{\pi K_1 r}\int_0^\infty e^{-\kappa_1\lambda^2 t}\sin\lambda r_1 \sin\lambda r \times\left(1-\epsilon\cos 2a\lambda+\sigma'\frac{\sin 2a\lambda}{a\lambda}\right)d\lambda, \quad (26)$$

to the first order of small quantities. To interpret the various parts of this result we rewrite the second term as

$$-\frac{\epsilon q\kappa_1 r_1}{\pi K_1 r}\int_0^\infty e^{-\kappa_1\lambda^2 t}\sin\lambda r\{\sin(2a+r_1)\lambda-\sin(2a-r_1)\lambda\}d\lambda$$

and the third term as

$$\frac{\sigma' q\kappa_1 r_1}{\pi K_1 r}\int_0^\infty e^{-\kappa_1\lambda^2 t}\sin\lambda r\left\{\frac{\cos(2a-r_1)\lambda-\cos(2a+r_1)\lambda}{a\lambda}\right\}d\lambda$$

$$=\frac{\sigma' q\kappa_1 r_1}{\pi K_1 r a}\int_0^\infty e^{-\kappa_1\lambda^2 t}\sin\lambda r\int_{2a-r_1}^{2a+r_1}\sin\lambda\xi\, d\xi\, .\, d\lambda$$

$$=\frac{\sigma' q\kappa_1 r_1}{\pi K_1 r a}\int_{2a-r_1}^{2a+r_1} d\xi\int_0^\infty e^{-\kappa_1\lambda^2 t}\sin\lambda\xi\sin\lambda r\, d\lambda.$$

Thus, to the order of small quantities adopted, the effect at any point in the inner medium, on the understanding that there is now no discontinuity of medium at $r=a$, is the same as that due to the following system of spherical sources in infinite continuous media :—

(i.) The original surface source of strength q in the infinite medium of conductivity K_1 ;

(ii.) a surface sink of strength $\frac{1}{2}\epsilon q r_1/(2a+r_1)$ at the surface $r=2a+r_1$, together with a surface source of strength $\frac{1}{2}\epsilon q r_1/(2a-r_1)$ at the surface $r=2a-r_1$, both in the infinite medium of conductivity K_1 ;

(iii.) a continuous distribution of surface sources between the surfaces $2a-r_1$ and $2a+r_1$ of strength varying inversely as the distance from the centre. (See result (25) above.)

In the same way we could treat the results (21) to (23) with a view to finding the various solutions in terms of elementary sources. As we are only concerned with the general character of the solutions at present, the details for the other cases need not be reproduced.

With a view to obtaining partial verification of the general results (13) to (16) or (20) to (23), obtained as the solution of our problem, the forms taken by these results for such cases as (*a*) $K_2=0$, $r_1<a$, (*b*) $K_1=0$, $r_1>a$ should be considered, and the results compared with those obtained by the direct application of first principles. It will be found that the results deduced from the general ones here obtained reduce to correct form in every case.

The same Problem treated in Terms of Bessel Functions.

Reverting again to the results (20) to (23), and having regard to certain analogies existing between the solutions of spherical problems and the corresponding cylindrical ones, pointed out by Green in his fourth paper *, it might be useful to show that the results we have obtained here are confirmed when we adopt the special method and notation of that paper. The notation referred to is that of Bessel's functions of half-odd-integral order. It is found that when the fundamental spherical wave-trains are expressed in terms of these functions the summation processes required when we use circular functions are no longer necessary.

* p. 241.

When there is symmetry about a point, the only functions required are those of the $K_{\frac{1}{2}}$ and $I_{\frac{1}{2}}$ type and their derivatives. Thus

$$K_{\frac{1}{2}}(z)=\frac{\pi}{\sqrt{2\pi z}}e^{-z}; \quad I_{\frac{1}{2}}(z)=\frac{1}{\sqrt{2\pi z}}(e^{z}-e^{-z}). \quad . \quad (27)$$

With this notation we find that the two fundamental wave-trains emanating from the periodic source qe^{ikt} at the surface $r=r_1$ in the inner medium are given by *

$$\left.\begin{aligned} v_0&=\frac{qr_1}{K_1}\left(\frac{r_1}{r}\right)^{\frac{1}{2}}e^{ikt}I_{\frac{1}{2}}\left(\sqrt{\frac{ik}{\kappa_1}}r_1\right)K_{\frac{1}{2}}\left(\sqrt{\frac{ik}{\kappa_1}}r\right), \quad r>r_1,\\ v_i&=\frac{qr_1}{K_1}\left(\frac{r_1}{r}\right)^{\frac{1}{2}}e^{ikt}K_{\frac{1}{2}}\left(\sqrt{\frac{ik}{\kappa_1}}r_1\right)I_{\frac{1}{2}}\left(\sqrt{\frac{ik}{\kappa_1}}r\right), \quad r<r_1. \end{aligned}\right\} \quad . \quad (28)$$

Taking the first of these as $\rho r^{-\frac{1}{2}}K_{\frac{1}{2}}(i\lambda r)$, the meaning of ρ being apparent, and representing the continuations by reflexion and transmission respectively by

$$A\rho r^{-\frac{1}{2}}I_{\frac{1}{2}}(i\lambda r); \quad A'\rho r^{-\frac{1}{2}}K_{\frac{1}{2}}(\mu i\lambda r), \quad . \quad . \quad (29)$$

$$\mu=\sqrt{\frac{\kappa_1}{\kappa_2}},$$

we remark that the first of these, travelling towards the centre of the sphere, is reflected there, setting up the corresponding reflected train of the $K_{\frac{1}{2}}$ type. As has already been pointed out †, however, the converging train of the $I_{\frac{1}{2}}$ type includes as part of itself a train of the $K_{\frac{1}{2}}$ type of just the amount required to satisfy the condition at $r=0$. We can, therefore, represent the temperature in the inner medium completely by

$$r>r_1, \qquad v_1=\rho r^{-\frac{1}{2}}K_{\frac{1}{2}}(i\lambda r)+A\rho r^{-\frac{1}{2}}I_{\frac{1}{2}}(i\lambda r),$$

and that in the outer medium by

$$v_2=A'\rho r^{-\frac{1}{2}}K_{\frac{1}{2}}(\mu i\lambda r).$$

We have now to find A and A′ by taking into account the conditions obtaining at the surface $r=a$, stated in (2) above.

Noting that

$$\frac{d}{dr}\{r^{-\frac{1}{2}}K_{\frac{1}{2}}(i\lambda r)\}=-i\lambda r^{-\frac{1}{2}}K_{\frac{3}{2}}(i\lambda r),$$

$$\frac{d}{dr}\{r^{-\frac{1}{2}}I_{\frac{1}{2}}(i\lambda r)\}=i\lambda r^{-\frac{1}{2}}I_{\frac{3}{2}}(i\lambda r),$$

* *Ibid.* p. 236.
† *Ibid.*

we find that A and A′ are given by

$$\left.\begin{aligned} A&=\frac{K_1.K_{\frac{3}{2}}(i\lambda a)K_{\frac{1}{2}}(\mu i\lambda a)-K_2\mu.K_{\frac{1}{2}}(i\lambda a)K_{\frac{3}{2}}(\mu i\lambda a)}{d'}=\frac{\alpha}{d'}, \text{ say,}\\ A'&=\frac{K_1\{K_{\frac{1}{2}}(i\lambda a)I_{\frac{3}{2}}(i\lambda a)+K_{\frac{3}{2}}(i\lambda a)I_{\frac{1}{2}}(i\lambda a)\}}{d'}=\frac{K_1}{i\lambda a d'},\end{aligned}\right\} \quad . \quad . \quad . \quad (30)$$

where

$$d'=K_1I_{\frac{3}{2}}(i\lambda a)K_{\frac{1}{2}}(\mu i\lambda a)+K_2\mu I_{\frac{1}{2}}(i\lambda a)K_{\frac{3}{2}}(\mu i\lambda a).$$

From these we have, *e. g.*,

$$v_1=\frac{qr_1}{K_1}\left(\frac{r_1}{r}\right)^{\frac{1}{2}}e^{ik_1t}I_{\frac{1}{2}}(i\lambda r_1)\{K_{\frac{1}{2}}(i\lambda r)+\frac{\alpha}{d'}I_{\frac{1}{2}}(i\lambda r)\}. \quad . \quad (31)$$

If now we use the forms

$$I_{\frac{3}{2}}(z)=\sqrt{\frac{2}{\pi z}}\left(\cosh z-\frac{\sinh z}{z}\right);\ K_{\frac{3}{2}}(z)=\sqrt{\frac{2}{\pi z}}e^{-z}\left(1+\frac{1}{z}\right),$$

we find that, after reduction,

$$d'=\frac{e^{-\mu i\lambda a}}{i\lambda a\sqrt{\mu}}\left\{K_1\cos a\lambda-(K_1-K_2)\frac{\sin\lambda a}{\lambda a}+iK_2\mu\sin\lambda a\right\},$$

$$d'K_{\frac{1}{2}}(i\lambda r)+\alpha I_{\frac{1}{2}}(i\lambda r)=\sqrt{\frac{\pi}{2}}\frac{e^{-\mu i\lambda a}}{i\lambda a\sqrt{\mu i\lambda r}}\left\{K_1\cos\lambda(a-r)\right.$$
$$\left.-(K_1-K_2)\frac{\sin\lambda(a-r)}{\lambda a}+iK_2\mu\sin\lambda(a-r)\right\}.$$

When these results are used in (31), and when the usual contour integration with respect to λ is performed, we are at once led to the result (13) above. In the same way we could verify the remaining results (14) to (16).

This analysis, together with the results of Dr. Green's investigations of the analogies already referred to, suggests that ultimately evaluation of the integrals in (20) to (23) may be effected by working out in full the corresponding cylindrical problem and then replacing the Bessel functions of integral order that appear in the solution by those of the half-odd-integral order as required in the spherical case. Clearly the cylindrical problems are of much greater practical importance. These are at present being investigated.

The writer wishes to acknowledge again his indebtedness to Dr. Green for valuable advice given during the preparation of this paper.

XII. *Characteristic Numbers, Functions, and Orthogonal Properties of Difference Equations.* *By* H. Levy, *D.Sc.*, *and* E. A. Baggott, *M.Sc.**

THE properties of difference equations detailed in the present paper are analogous to those of differential equations. They are stated for difference equations of the second order, but are capable of easy and direct generalization, both for higher orders and for more general forms of the second order equation

1. In $$\Delta^2 U_x+\lambda f_{x+1} U_{x+1}=0, \quad . \quad . \quad . \quad . \quad (1)$$

if f_{x+1} is a given function of x finite in the range $0<\alpha<1<x<N+\alpha$, where N is a positive integer ≥ 2, then there exists in general $N-1$ values of λ for which the difference equation possesses a solution U_x that vanishes only at $x=\alpha$ and at $x=N+\alpha$ and nowhere else within the range at corresponding points.

Such numbers λ we call characteristic numbers and such solutions U_x, characteristic solutions

Let $U_x=\varpi_1 u_x+\varpi_2 v_x$ be a general solution of the above equation, *i. e.*, u_x and v_x form a fundamental system of solutions of the difference equation. ϖ_1 and ϖ_2 are arbitrary periodic functions of period unity.

If $U_\alpha=0$ then from the difference equation

$$U_{2+\alpha}=(2-\lambda f_{1+\alpha})(\varpi_1 u_{1+\alpha}+\varpi_2 v_{1+\alpha})$$
$$U_{3+\alpha}=\{(2-\lambda f_{2+\alpha})(2-\lambda f_{1+\alpha})-1\}\{\varpi_1 u_{1+\alpha}+\varpi_2 v_{1+\alpha}\}$$
$$. \quad . \quad . \quad . \quad . \quad . \quad . \quad . \quad . \quad . \quad . \quad . \quad .$$
$$U_{n+\alpha}=F(\lambda, \alpha)(\varpi_1 u_{1+\alpha}+\varpi_2 v_{1+\alpha}),$$

in which $F(\lambda, \alpha)$ is a polynomial in λ of degree $(n-1)$.

For $U_{n+\alpha}$ to be zero,

either $$F(\lambda, \alpha)=0 \quad . \quad . \quad . \quad . \quad . \quad . \quad (2)$$

or $$\varpi_1 u_{1+\alpha}+\varpi_2 v_{1+\alpha}=0 \quad . \quad . \quad . \quad . \quad . \quad (3)$$

The latter equation may be satisfied in two ways. Thus if ϖ_1 and ϖ_2 have a common zero at $x=\alpha$, then it follows that the solution U_x has a zero at all points $U_{s+\alpha}$, where s is any integer positive or negative. Such a

* Communicated by the Authors.

solution is therefore rejected for the purposes of the present investigation.

Again, equation (3) may be satisfied by virtue of λ being a root of this equation in λ.

Now $$\Delta(u_x v_{1+x} - v_x u_{1+x}) = 0,$$

since u_x and v_x separately satisfy the difference equation.

Hence $$u_x v_{1+\alpha} - v_x u_{1+x} = \text{constant}.$$

If $\varpi_1 = -v_\alpha$ and $\varpi_2 = u_\alpha$ in the range $0 < \alpha < 1$ the equation $\varpi_1 u_\alpha + \varpi_2 v_\alpha = 0$ is satisfied, and $U_{1+\alpha} = \varpi_1 u_{1+\alpha} + \varpi_2 v_{1+\alpha}$ is a function of λ only. Hence if $U_{1+\alpha}$ is zero by virtue of λ being a root of $U_{1+\alpha} = 0$, then U_x is identically zero everywhere.

Thus the only way in which $U_{n+\alpha}$ may be zero and U_x not have corresponding zeros at $x = s + \alpha$, or become identically zero, is for the equation

$$F(\lambda, \alpha) = 0$$

to be satisfied.

This is the characteristic equation and is of degree $(N-1)$ in λ. Corresponding to each characteristic value of λ found from this equation there is a difference equation similar to (1) with a characteristic solution, zero at $x = \alpha$ and at $x = N + \alpha$ but not at corresponding intermediate points $x = s + \alpha$, $s = 1, 2 \ldots\ldots (N-1)$. There is a different characteristic equation corresponding to each value of α. Those characteristic solutions belonging to a particular characteristic equation will be said to belong to one set.

2. If ${}_rU_x$ and ${}_sU_x$ be any two characteristic functions corresponding to the two distinct characteristic numbers λ_r and λ_s, then ${}_rU_x$ and ${}_sU_x$ satisfy the orthogonal conditions

$$\sum_{x=\alpha}^{x=\alpha+n-2} f_{n+1} \cdot {}_rU_{x+1} \cdot {}_sU_{x+1} = 0 \quad r \neq s.$$

Let ${}_rU_\alpha$ and ${}_sU_\alpha$ be two characteristic solutions of the $(n-1)$ solutions which vanish at $x = \alpha$ and $x = n + \alpha$ corresponding to the characteristic numbers λ_r and λ_s.

Then

$$\Delta^2 {}_rU_x + \lambda_r \cdot f_{x+1} \, {}_rU_{x+1} = 0$$

and

$$\Delta^2 {}_sU_x + \lambda_s \cdot f_{x+1} \, {}_sU_{x+1} = 0.$$

Hence multiplying the first equation by ${}_sU_{x-1}$ and the second by ${}_rU_{x+1}$ and subtracting

$$({}_sU_{x+1}\cdot{}_rU_{x+2}-{}_rU_{x+1}\cdot{}_sU_{x+2})-({}_sU_x\cdot{}_rU_{x+1}-{}_rU_x\,{}_sU_{x+1})$$
$$+(\lambda_r-\lambda_s)f_{x+1}\cdot{}_rU_{x+1}\cdot{}_sU_{x+1}=0.$$

Writing this equation for all integral values of n between $x=\alpha$ and $x=n+\alpha-2$ and adding, it follows, by virtue of the fact that

$${}_rU_\alpha={}_sU_\alpha={}_rU_{\alpha+n}={}_sU_{\alpha+n}=0,$$

that the bracketed terms either subtract out or vanish and hence

$$\sum_{x=\alpha}^{x=\alpha+n-2}(\lambda_r-\lambda_s)\,f_{x+1}\cdot{}_rU_{x+1}\cdot{}_sU_{x+1}=0,$$

and since $\lambda_r-\lambda_s\neq0$, it follows that any pair of characteristic solutions of a set satisfy the orthogonal stated above.

The above propositions hold equally for the more general difference equation

$$\Delta^2u_x+(g_{x+1}+\lambda f_{x+1})u_{x+1}=0.$$

3. A linear function of characteristic solutions of difference equations of the form

$$\Delta^2u_x+(g_{x+1}+\lambda f_{x+1})u_{x+1}=0,$$

can be found which is zero at $x=\alpha$ and $x=n+\alpha$ and which assumes $(n-1)$ arbitrary values V_1, $V_2\ldots V_{n-1}$, corresponding to $x=1+\alpha$, $2+\alpha,\ldots(n-1)+\alpha$. If this linear function is written

$$\sum_{r=1}^{r=n-1}a_r\cdot U_x(\lambda_r),$$

then the coefficients are given by the equations

$$a_r=\sum_{x=1+\alpha}^{x=n-1+\alpha}f_x\cdot V_xU_x(\lambda_r)\Big/\sum_{x=1+\alpha}^{x=n-1+\alpha}f_x[U_x(\lambda_r)]^2. \quad . \quad (4)$$

Let U_x be a general solution of the difference equation (1), in the form

$$U_x=\varpi_1u_x+\varpi_2v_x,$$

where u_x and v_x form a fundamental system of solutions of the difference equation. The periodic functions ϖ_1 and ϖ_2 for present purposes are taken as constants and have the values $-v_{\alpha_1}$ and u_{α_1}, so that for the particular value $x=\alpha_1$, $U_{\alpha_1}=0$.

Hence

$$U_x = -v_{\alpha_1} u_x + u_{\alpha_1} v_x.$$

In order that $U_{n+\alpha_1}$ shall be zero, the equation

$$F_{n-1}(\lambda_1, \alpha_1) = 0$$

must be satisfied, and this equation yields $(n-1)$ characteristic values each of which gives a characteristic solution zero at $x=\alpha_1$ and at $x=n+\alpha_1$. Suppose that a function which is zero at $x=\alpha_1$ and at $x=n+\alpha_1$ is known to have the values $V_{1+\alpha_1}, \ldots V_{n-1+\alpha_1}$ at $x=(1+\alpha_1) \ldots, (n-1+\alpha_1)$, then since there are $(n-1)$ characteristic solutions available such a function may be expressed as a linear function of these $(n-1)$ characteristic solutions and the $(n-1)$ constants in the linear function may be determined uniquely, since $(n-1)$ linear equations suffice to determine the $(n-1)$ constants.

If $U_x(\lambda_r)$ denote the characteristic solution corresponding to λ_r, then let

$$\sum_{r=1}^{r=n-1} a_r U_x(\lambda_r) \quad . \quad . \quad . \quad . \quad . \quad . \quad (5)$$

be the linear function of the characteristic solutions which is to assume the values $V_{1+\alpha_1} \ldots V_{n-1+\alpha_1}$ at

$$x = 1+\alpha_1, \ldots n-1+\alpha_1.$$

Let

$$V_x = a_1 U_x(\lambda_1) + a_2 U_x(\lambda_2) + \ldots + a_{n-1} U_x(\lambda_{n-1}),$$

then

$$\sum_{x=1+\alpha_1}^{x=n-1+\alpha_1} f_x V_x U_x(\lambda_r) = \sum_{x=1+\alpha_1}^{x=n-1+\alpha_1} [\{a_1 U_x(\lambda_1) + \ldots + a_{n-1} U_x(\lambda_{n-1})\} U_x(\lambda_r) . f_x]_s.$$

and since

$$\sum_{x=1+\alpha_1}^{x=n-1+\alpha_1} f_x a_s U_x(\lambda_s) . U_x(\lambda_r) = 0, \quad \lambda_r \neq \lambda_s.$$

by the condition of orthogonality it follows that

$$\sum_{x=1+\alpha_1}^{x=n-1+\alpha_1} f_x V_x U_x(\lambda_r) = \sum_{x=1+\alpha_1}^{x=n-1+\alpha_1} a_r [U_x(\lambda_r)]^2 . f_x.$$

Hence

$$a_r = \sum_{x=1+\alpha_1}^{x=n-1+\alpha_1} f_x V_x U_x(\lambda_r) = \sum_{x=1+\alpha_1}^{x=n-1+\alpha_1} f_x [U_x(\lambda_r)]^2.$$

This equation determines the coefficients of the orthogonal functions and the required linear function for V_x is (5) above.

This function assumes the $(n-1)$ arbitrary values at $x=1+\alpha_1, \ldots n-1+\alpha_1$, and is zero at $x=\alpha_1$ and at $x=n+\alpha_1$.

4. If $$\Delta^2 u_x + f_{x+}u_{x+1} = 0$$

and $$\Delta^2 v_x + g_{x+1}v_{x+1} = 0$$

are two difference equations in which

$$g_{x+1} - f_{x+1} > 0,$$

and if (i.) $$u_\alpha = v_\alpha = 0 \quad 0 \leq \alpha < 1$$

and (ii.) $$u_{1+\alpha} = v_{1+\alpha} > 0,$$

then $u_x > v_x$ up to the next zero of v_x or until it becomes negative.

Now $$u_{x+2} - 2u_{x+1} + u_x = -f_{x+1} \cdot u_{x+1},$$

$$v_{x+2} - 2v_{x+1} + v_x = -g_{x+1} \cdot v_{x+1}.$$

Multiply the first equation by v_{x+1} and the second by u_{x+1} and subtract, then

$$\Delta(u_{x+1}v_x - u_x v_{x+1}) = (g_{x+1} - f_{x+1})u_{x+1} \cdot v_{x+1}.$$

Since the right-hand side is positive until u_x or v_x becomes negative,

$$\frac{u_{x+2}}{u_{x+1}} > \frac{v_{x+2}}{v_{x+1}} + \left(\frac{v_x}{v_{x+1}} - \frac{u_x}{u_{x+1}}\right).$$

Now $$u_\alpha = v_\alpha = 0,$$

and $$u_{1+\alpha} = v_{1+\alpha},$$

therefore $$u_{\alpha+2} > v_{\alpha+2}.$$

Again $$\frac{u_{\alpha+3}}{u_{\alpha+2}} > \frac{v_{\alpha+3}}{v_{\alpha+3}} + \left(\frac{v_{\alpha+1}}{v_{\alpha+2}} - \frac{u_{\alpha+1}}{u_{\alpha+2}}\right)$$

and $$\frac{u_{\alpha+2}}{u_{\alpha+1}} > \frac{v_{\alpha+2}}{v_{\alpha+1}},$$

therefore $$\frac{u_{\alpha+3}}{u_{\alpha+2}} > \frac{v_{\alpha+3}}{v_{\alpha+2}},$$

i. e. $$u_{\alpha+3} > v_{\alpha+3} \quad \text{since} \quad u_{\alpha+2} > v_{\alpha+2}.$$

Hence, proceeding in the above manner, it follows that $u_x > v_x$ up to the second zero of v_x or until v_x becomes negative.

5. If the solutions of the equations

$$\Delta^2 u_x + f_{x+1} u_{x+1} = 0,$$

$$\Delta^2 v_x + \mathrm{M}_{x+1} v_{x+1} = 0,$$

$$\Delta^2 w_x + m_{x+1} . w_{x+1} = 0,$$

have a common zero at

$$x = \alpha, \quad 0 \leq \alpha < 1,$$

and if

$$u_{1+\alpha} = v_{1+\alpha} = w_{1+\alpha},$$

then, provided that

$$\mathrm{M}_{x+1} - f_{x+1} > 0,$$

$$f_{x+1} - m_{x+1} > 0,$$

the solution for u_x lies between those for v_x and w_x up to the first zero of v_x or where it becomes negative. The position at which u_x becomes zero or negative lies between the corresponding positions for v_x and w_x.

Since

$$\mathrm{M}_{x+1} - f_{x+1} > 0,$$

therefore $u_x > v_x$ up to the second zero of v_x or until v_x becomes negative.

Again,

$$f_{x+1} - m_{x+1} > 0,$$

therefore, $w_x > u_x$ up to the second zero of u_x or until u_x becomes negative. Hence the proposition is established.

6. In the difference equation

$$\Delta^2 u_x + (g_{x+1} + \lambda f_{x+1}) u_{x+1} = 0$$

if

$$\mathrm{M}_{x+1} - f_{x+1} > 0$$

and

$$f_{x+1} - m_{x+1} > 0,$$

then the first characteristic value λ for which

$$u_\alpha = 0 = u_{n+\alpha}, \quad \text{viz.,} \quad \lambda_\alpha$$

lies between the first characteristic values of λ for the difference equations

$$\Delta^2 v_x+(g_{x+1}+\lambda \mathrm{M}_{x+1})v_{x+}=0$$

and

$$\Delta^2 w_x+(g_{x+1}+\lambda m_{x+1})w_{x+1}=0,$$

for which

$$v_a=0=v_{n+a}$$

and

$$w_a=0=w_{n+a}.$$

Let λ_u, λ_v, λ_w be the characteristic values for the three equations.

Suppose λ_u is positive, then

$$\lambda_u(\mathrm{M}_{x+1}-f_{x+1})>0,$$

therefore $u_x>v_x$ up to the next zero of v_x, or where v_x becomes negative. For v_x to have the same second zero as u_x, then $\lambda_v-\lambda_u<0$.

Again,

$$\lambda_u(f_{x+1}-m_{x+1})>0,$$

therefore $w_x>u_x$ up to the next zero of u_x, or where u_x becomes negative. For w_x to have the same second zero as u_x,

$$\lambda_w-\lambda_u>0.$$

Thus λ_u lies between the values of λ_v and λ_w. Similar reasoning applies if λ is negative.

7. In the difference equation

$$\Delta^2 u_x+(g_{x+1}+\lambda f_{x+1})u_{x+1}=0,$$

if

$$\mathrm{M}_{x+1}-g_{x+1}>0$$

and

$$g_{x+1}-m_{x+1}>0,$$

then the first characteristic value of λ for which

$$u_a=0=u_{n+a}$$

lies between the first characteristic values of λ for the difference equations

$$\Delta^2 v_x+(\mathrm{M}_{x+1}+\lambda f_{x+1})v_{x+1}=0$$

and

$$\Delta^2 w_x+(m_{x+1}+\lambda f_{x+1})w_{x+1}=0,$$

for which

$$v_a=0=v_{n+a}$$

and

$$w_a=0=w_{n+a}.$$

Clearly these propositions admit of being combined when both g_{x+1} and f_{x+1} are replaced by M_{x+1}, N_{x+1}, such that

$$M_{x+1}-g_{x+1}>0,$$
$$N_{x+1}-f_{x+1}>0,$$

and by m_{x+1}, n_{x+1}, such that

$$g_{x+1}-m_{x+1}>0,$$
$$f_{x+1}-n_{x+1}>0$$

in the new difference equations.

8. Again, if v_x and w_x are two independent continuous solutions of the equation

$$\Delta^2 U_x+\rho(x).U_{x+1}=0,$$

then between two zeros of v_x there must be at least one zero of w_x.

For $$\Delta^2 v_x+\rho(x).v_{x+1}. \quad . \quad . \quad . \quad . \quad . \quad . \quad \text{(i.)}$$
$$\Delta^2 w_x+\rho(x).w_{x+1}. \quad . \quad . \quad . \quad . \quad . \quad . \quad \text{(ii.)}$$

Let $x=\xi$ and $x=\eta$ be two zeros of v_x.

From (i.) and (ii.)

$$w_x.\Delta^2 v_x-v_x.\Delta^2 u_x=0,$$

hence $$v_x.\Delta w_x-w_x.\Delta v_x=\text{constant}.$$

Therefore

$$[v_\eta.\Delta w_\eta-w_\eta\Delta v_\eta]-[v_\xi\Delta w_\xi-w_\xi\Delta v_\xi]=0.$$

Since $$v_\xi=v_\eta=0,$$

it follows that $$w_\xi\Delta v_\xi-w_\eta\Delta v_\eta=0.$$

Suppose that v_η is positive between $x=\xi$ and $x=\eta$, then $\Delta v_\xi>0$ and $\Delta v_\eta<0$.

Hence $$w_\eta=\frac{w_\xi\Delta v_\xi}{\Delta v_\eta}<0 \text{ if } w_\xi \text{ is positive,}$$

and $$>0 \text{ if } w_\xi \text{ is negative.}$$

Thus w_η is negative if w_ξ is positive,

and w_η is positive if w_ξ is negative,

and therefore w_x changes sign between two zeros $x=\xi$, $x=\eta$ of v_x. Hence there are 1, 3, 5, ... zeros of w_x between two consecutive zeros of v_x.

9. If p_x is a function of x zero at $x=\alpha$ and at $x=n+\alpha$, which may be taken as a first approximation to the solution of the difference equation

$$\Delta^2 u_x+\lambda f_{x+1}u_{x+1}=0,$$

then for a solution of this equation which is zero at $x=\alpha$ and at $x=n+\alpha$, and is not zero at corresponding intermediate points, the first characteristic value satisfies the inequality

$$\lambda<\sum_{x=\alpha}^{x=n+\alpha-1}(\Delta p_x)^2\Big/\sum_{x=\alpha}^{x=n+\alpha-1}f_{x+1}.p_{x+1}^2.$$

Consider the difference equation (1) in the form

$$u_{x+2}-2u_{x+1}+u_x=-\lambda.f_x.u_{x+1}.$$

Multiplying by u_{x+1} this may be written

$$u_{x+1}.\Delta u_{x+1}-u_x\Delta u_x=-\lambda.f_x.u_{x+1}^2+(\Delta u_x)^2.$$

Hence writing this equation for values of u_x ranging between u_α and $u_{n+\alpha}$, and making $u_\alpha=u_{n+\alpha}=0$.

$$u_{\alpha+1}.\Delta u_{\alpha+1}-u_\alpha.\Delta u_\alpha=-\lambda f_\alpha.u_{\alpha+1}^2+(\Delta u_\alpha)^2$$

$$u_{\alpha+2}.\Delta u_{\alpha+2}-u_{\alpha+1}.\Delta u_{\alpha+1}=-\lambda f_{1+\alpha}.u_{\alpha+2}^2+(\Delta u_{\alpha+1})^2$$

. . . . . .

$$u_{\alpha+n}.\Delta u_{\alpha+n}-u_{\alpha+n-1}.\Delta u_{\alpha+n-1}=-\lambda f_{\alpha+n-1}.u_{\alpha+n}^2+(\Delta u_{\alpha+n-1}).$$

Hence upon adding these equations

$$\sum_{x=\alpha}^{x=\alpha+n-1}(\Delta u_x)^2-\lambda\sum_{x=\alpha}^{x=\alpha+n-1}f_x.u_{x+1}^2=0,$$

and therefore,

$$\lambda=\sum_{x=\alpha}^{x=\alpha+n-1}(\Delta u_x)^2\Big/\sum_{x=\alpha}^{x=\alpha+n-1}f_x.u_{x+1}^2.$$

Hence if a solution of the difference equation is known which vanishes at $x=\alpha$ and at $x=n+\alpha$ the above expression gives the corresponding characteristic value of the constant λ.

Extension of Rayleigh's Principle.

Since if f_x is essentially positive the right-hand side of the above expression is also positive, λ is necessarily positive. Suppose that an approximate solution of the difference equation only is available In this case we

proceed as follows :—Let p_x be a function of x zero at $x=\alpha$ and at $x=n+\alpha$, and finite in the range, and suppose y_x is a solution of the equation

$$\Delta^2 y_x+\lambda f_x . y_{x+1}=0,$$

such that

$$y_\alpha=y_{n+\alpha}=0,$$

and has *not* corresponding zeros in the intermediate intervals at $x=s+\alpha$, $s=1$ to $n-1$.

Consider $\Delta\left(\dfrac{p_x^2\Delta y_x}{y_x}\right)$

$$=\frac{1}{y_x y_{x+1}}\{y_x p_{x+1}^2\Delta y_{x+1}-p_x^2\Delta y_x . y_{x+1}\}$$

$$=\frac{1}{y_x y_{x+1}}\{p_{x+1}^2 y_x\Delta y_{x+1}-(p_{x+1}-\Delta p_x)^2(y_{x+1}-y_x)(y_x+\Delta y_x)\}$$

$$=\frac{p_{x+1}^2 y_x\Delta^2 y_x}{y_x y_{x+1}}+\frac{\Delta p_x^2 y_{x+1} . y_x}{y_x y_{x+1}}$$

$$-\frac{1}{y_x y_{x+1}}\{p_{x+1}^2\Delta y_x^2-\Delta p_x^2 . y_{x+1}^2+2p_{x+1} . \Delta p_x\Delta y_x . y_{x+1}\}$$

$$=-\lambda f_x p_{x+1}^2+\Delta p_x^2-\frac{(p_x\Delta y_x-y_x\Delta p_x)^2}{y_x y_{x+1}}$$

$$=-\lambda f_x p_{x+1}^2+\Delta p_x^2-y\, y_{x+1}\left(\frac{p_{x+1}}{y_{x+1}}-\frac{p_x}{y_x}\right)^2.$$

Hence

$$\Delta\frac{p_x^2\Delta y_x}{y_x}=-\lambda f_x p_{x+1}^2+\Delta p_x^2-y_x y_{x+1}\left(\Delta\frac{p_x}{y_x}\right)^2.$$

Summing both sides of this equation from $x=\alpha$ to $x=n+\alpha-1$, we have for the first characteristic number λ

$$\lambda<\sum_{x=\alpha}^{x=n+\alpha-1}(\Delta p_x)^2\Big/\sum_{x=\alpha}^{x=n+\alpha-1} f_x . p_{x+1}^2,$$

since

$$\sum_{x=\alpha}^{x=n+\alpha-1} y_x y_{x+1}\left(\Delta\frac{p_x}{y_x}\right)^2$$

is a positive quantity and

$$\frac{p_\alpha^2\Delta y_\alpha}{y_\alpha}=0=\frac{p_{n+\alpha}^2\Delta y_{n+\alpha}}{y_{n+\alpha}}.$$

From this analysis it follows that if a finite function p_x

be taken to satisfy the boundary conditions $p_\alpha=0$ and $p_{n+\alpha}=0$, then the expression

$$\lambda \leq \sum_{x=\alpha}^{x=n+\alpha-1} (\Delta p_x)^2 \Big/ \sum_{\iota=\alpha}^{x=n+\alpha-1} f_x . p_{x+1}^2$$

provides an upper bound to the first characteristic value of λ of the difference equation—

$$\Delta^2 y_x + \lambda f_x . y_{x+1} = 0,$$

subject to $$y_\alpha = y_{n+\alpha} = 0.$$

XIII. *Generalization of Lorentz Transformation.* *By* F. Tavani *.

§ 1.

In Lorentz's transformation it is assumed that the origin of the moving frame moves with a uniform and rectilinear motion. Let us see what becomes of the transformation when the origin describes with a given law a curvilinear path, such as that described by a point taken on the earth or any other planet.

We shall consider first the case of the motion in a space of two dimensions, then of three.

Let $$P=O+I_1x_1+I_2x_2 \quad . \quad . \quad . \quad . \quad . \quad (1)$$

be the expression of a point referred to a frame OI_1I_2, and let us suppose that the moving origin O′, starting from its initial position O, describes a curve with a given law.

Let T and N be unit vectors taken respectively along the tangent and the normal to the curve. We shall have

$$T=\alpha_1I_1+\alpha_2I_2 \quad \text{and} \quad N=\beta_1I_1+\beta_2I_2\,;$$

therefore

$$I_1=\eta_1T+\eta_2N \quad \text{and} \quad I_2=\theta_1T+\theta_2N\,; \quad . \quad . \quad (2)$$

therefore, from (2) and (1),

$$P=O+(x_1\eta_1+x_2\theta_1)T+(x_1\eta_2+x_2\theta_2)N. \quad . \quad . \quad (3)$$

We shall assume, for simplicity, I_1 and I_2 to coincide with the initial positions of T and N.

* Communicated by the Author.

Since T and N represent the tangent and the normal to any point of the curve described by O′, so the equation (3) is the expression of P, referred to a frame of origin O and axes moving perpendicularly to one another while turning round O in the direction of the successive tangents and normals respectively. Comparing the transformation represented by (3) with Lorentz's transformation, we can say that, while the latter supposes the direction of the axes unchangeable with the motion of the origin, along a straight line, in (3) we have the direction of the axes moving, and the origin unchangeable. In the same way as a series of problems arise from Lorentz's transformation, considered in the theory of relativity, so there is a parallel series of similar problems derived from the equation (3) which must be considered.

§ 2.

At the time $t=0$ let the moving origin O′ coincide with O, and after an interval of time t let O′ occupy the position shown in the diagram.

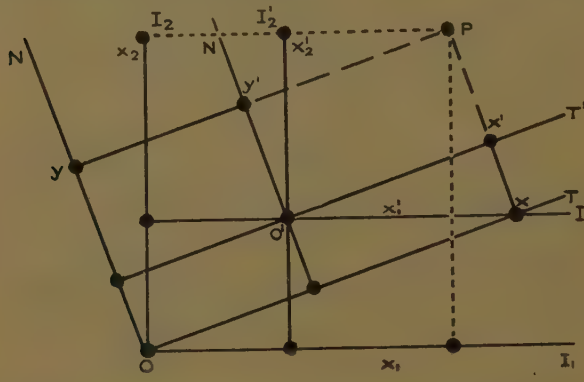

We want to determine the position of the moving axes and the coordinates of P referred to them at the time t. Let the curve described by the origin O′ be

$$O' = O_0 + \phi_1(t)I_1 + \phi_2(t)I_2.$$

By applying the transformation (3) this equation becomes

$$O' = O + (\phi_1(t)\eta_1 + \phi_2(t)\theta_1)T + ((\phi_1(t)\eta_2 + \phi_2(t)\theta_2)N, \quad (4)$$

which determines the position of O′ relatively to the frame OTN. Having thus obtained the position of O′, let us reproduce the positions of the axes as in O by drawing first $I_1'I_2'$ through O′, and then turn them in the direction of T and N.

By a process similar to that followed for passing from (1) to (3) we pass from the initial expression of P relative to the frame $O'I_1'I_2'$, viz.,

$$P=O'+x_1'I_1'+x_2'I_2'$$

to

$$P=O'+(x_1'\eta_1+x_2'\theta_1)T+(x_1'\eta_2+x_2'\theta_2)N.$$

So the quantities x and x' of Lorentz's transformation, where the rotation is zero, become in the more general transformation respectively $(x_1\eta_1+x_2\theta_1)$ and $(x_1'\eta_1+x_2'\theta_1)$.

Let us now put

$$(\phi_1(t)\eta_1+\phi_2(t)\theta_1) \text{ of (4), equal to } u_1t' \quad . \quad . \quad (a)$$

and

$$(\phi_1(t)\eta_2+\phi_2(t)\theta_2)=u_2t', \quad . \quad . \quad . \quad . \quad . \quad . \quad (b)$$

where (a) is the space covered by O′ along T during the time t' of the clock attached to the frame of origin O′, and (b) is the space covered by O′ along N during the time t' attached to the frame of origin O′, u_1 and u_2 being the average velocity of O′ in the said interval.

Therefore the Lorentz quantities $(x-ut)$ and $(x'+ut')$ become respectively

$$\{(x_1\eta_1+x_2\theta_1)-u_1t\} \quad \text{and} \quad \{(x_1'\eta_1+x_2'\theta_2)+u_1t'\},$$

t_1 being the time of the clock attached to the frame of fixed origin O.

As to the presence of the factor β, it is more rigorous to establish it as a fact following the experiment of Michelson and Morley than by way of a mathematical demonstration. This fact can also be expressed by the equation

$$\text{mod. N} = \frac{\text{mod. T}}{\sqrt{1-\frac{u_1^2}{c^2}}}$$

according to the notation here adopted.

If the velocity of the system is zero, we have

$$\text{mod. N}=\text{mod. T}=1.$$

As the value of u_1, constant with time, increases, T contracts, and as its value decreases, T expands. At the side of the contraction with the motion of O′ along the axis T must be considered the contraction along the axis N, which we indicate with

$$\beta_2 = \frac{1}{\sqrt{1-\frac{u_2^2}{c^2}}},$$

to distinguish it from the former β_1 *.

Comparing the transformation just obtained with that of Lorentz, and putting for brevity

$$\begin{cases} (x_1\eta_1+x_2\theta_1)=\mathrm{X}, & (x_1\eta_2+x_2\theta_2)=\mathrm{Y} \\ (x_1'\eta_1+x_2'\theta_1)=\mathrm{X}', & (x_1'\eta_2+x_2'\theta_2)=\mathrm{Y}', \end{cases}$$

Lorentz (L).

$$\begin{cases} x=\beta(x'+ut') & (1) \\ y=y' \ \ldots\ldots & (2) \\ z=z' \ \ldots\ldots & (3) \end{cases}$$

$$\begin{aligned} x' &= \beta(x-ut) \\ y' &= y \\ z' &= z \end{aligned}$$

Generalized (G).

$$\left.\begin{cases} \mathrm{X}=\beta_1(\mathrm{X}'+u_1t') & (1) \\ \mathrm{Y}=\beta_2(\mathrm{Y}'+u_2l') & (2) \\ \mathrm{Z}=\mathrm{Z}' \end{cases}\right\}\dagger$$

$$\begin{cases} \mathrm{X}'=\beta_1(\mathrm{X}-u_1t') & (3) \\ \mathrm{Y}'=\beta_2(\mathrm{Y}-u_2t) & (4) \\ \mathrm{Z}'=\mathrm{Z} \end{cases}$$

§ 3.

If a frame moves with any motion, the motion of the hands of the clock, which moves with the same motion of the frame, will be uniform only relatively to the frame with which it moves, because only relatively to the said frame will the centre of the clock be at rest. Therefore if a clock is placed on a planet, *e. g.*, Jupiter, the hands will have a uniform motion only relatively to the planet that carries it ; so that if the motion of the hands on Jupiter is compared with that of the hands of the same clock placed on the earth, the two motions will in reality be different. Consequently, if we wish to use a clock as

* In other words, to the appearance of motion under one form corresponds the disappearance of it under another, and, reciprocally, a fact comparable with that which we observe in the transformation of energy.

† Under this form the similarity between the more general expressions of the coordinates and those of Lorentz is visible. The transformation along the axis Z is considered further in the case of the motion of the origin in a space of three dimensions.

a measure of time it must be considered as belonging to the frame, viz., as being at rest relatively to it, or, what is the same, as moving with the same motion as the frame. For this reason in the above expression of the coordinates we have called t the time of the clock belonging to the frame of origin O and t' the time measured with the clock of the frame of origin O′.

By means of the equations G (1) and G (3), G (2), G (4), we can express t and t' in terms of X and X′ and Y and Y′: we obtain

$$\left\{\begin{array}{l} t'=\beta_1\left(t-\dfrac{u_1\mathrm{X}}{c^2}\right), \\ t=\beta\left(t'+\dfrac{u_1\mathrm{X}'}{c^2}\right), \end{array}\right\} \quad \text{and} \quad \left\{\begin{array}{l} t'=\beta_2\left(t-\dfrac{u_2\mathrm{Y}}{c^2}\right), \\ t=\beta_2\left(t'+\dfrac{u_2\mathrm{Y}'}{c^2}\right). \end{array}\right\} \qquad (6)$$

So we obtain so many couples of formulæ, each couple expressing t and t', as many are the dimensions of the space in which the origin moves. For a space of three dimensions we could obtain a set of three couples, each expressing t in terms of t' and t' in terms of t. And these values of time given by one of the components of the motion along one dimension are equal to those given along another dimension.

§ 4.

Case in which the origin describes a curve in space of three dimensions:

$$\mathrm{P}=\mathrm{O}+x_1\mathrm{I}_1+x_2\mathrm{I}_2+x_3\mathrm{I}_3. \quad . \quad . \quad . \quad . \quad (7)$$

Let TNB be unit vectors taken respectively along the tangent, normal and binormal to the curve, and let us assume that I_1, I_2, I_3 represent respectively their initial positions. Let O′ represent the moving origin, and y_1, y_2, y_3 its coordinates taken on $\mathrm{I}_1, \mathrm{I}_2, \mathrm{I}_3$; we have then

$$\frac{d\mathrm{O}'}{dt}=u\mathrm{T} \quad \text{and} \quad \mathrm{T}=\frac{dy_1}{dt}\mathrm{I}_1+\frac{dy_2}{dt}\mathrm{I}_2+\frac{dy_2}{dt}\mathrm{I}_3; \qquad (8)$$

moreover,

$$\mathrm{N}=\rho\frac{d\mathrm{T}}{ds} \quad \text{and} \quad \frac{d\mathrm{N}}{ds}=-\frac{1}{\rho}\mathrm{T}-\frac{1}{\rho_1}\mathrm{B}, \quad . \quad . \quad (9)$$

where ρ and ρ_1 are respectively the first and the second curvatures of the path of O′ ; we shall have then

$$\left.\begin{aligned} T&=i_1I_1+i_2I_2+i_3I_3,\\ N&=q_1I_1+q_2I_2+q_3I_3,\\ B&=t_1I_1+t_2I_2+t_3I_3, \end{aligned}\right\} \text{therefore} \left\{\begin{aligned} I_1&=g_1T+g_2N+g_3B,\\ I_2&=hT+hN+hB,\\ I_3&=m_1T+m_2N+m_3B, \end{aligned}\right\} \quad . \quad . \quad . \quad (10)$$

and substituting in (7) to I_1, I_2, I_3 their values given by (10), (7) becomes

$$P=O+p_1T+p_2N+p_3P,$$

where O is the initial position of the origin; thence the coordinates of P are derived with the same process followed in the case of space of two dimensions. The same process can be extended to a space of n dimensions, after giving the analytical properties of a hyperspace *.

XIV. *A Note on "Modification of Brillouin's Unified Statistics."* *By* D. S. Kothari, *Physics Department, University of Delhi* †.

In a paper in the February issue of this Magazine, Mr. Lindsay has attempted a generalization of the Fermi-Dirac statistics. He takes the distribution function to be

$$N_i=\frac{2\pi gV(2m)^{3/2}}{h^3}\frac{E_i^{1/2}dE_i}{a+e^{-\alpha+E_i/kT}}, \quad . \quad . \quad . \quad (1)$$

where a is permitted to vary in the neighbourhood of unity. Writing (1) in the form

$$N_i=\frac{2\pi gV(2m)^{3/2}}{(ha^{1/3})^3}\frac{E_i^{1/2}dE_i}{1+e^{-\alpha'+E_i/kT}}, \quad . \quad . \quad . \quad (2)$$

where $\alpha'=\alpha+\log a$; one at once notices that the modification introduced by Lindsay consists in *replacing the h occurring in the "usual formulæ" by $a^{1/3}h$.* Thus the results obtained by Lindsay (his equations (7), (9), (10), (16), (20), (25)) can be written down immediately.

Further, the "modified formulæ" in the *relativistic* statistics are also at once obtained by merely replacing h occurring in the usual formulæ ‡ by $a^{1/3}h$.

* See Tavani, "Motion and Hyperspace," Phil. Mag. April, 1921.

† Communicated by the Author.

‡ Kothari, Phil. Mag. xii. p. 674 (1931).

XV. *An Alternating Current Method for Collector Analysis of Discharge-tubes.* *By* R. H. Sloane *and* E. I. R. MacGregor, *Department of Physics, Queen's University, Belfast* *.

1. *Introduction.*

LANGMUIR'S method[1] of analyzing electric discharges from the current (i) voltage (V) characteristics of small auxiliary electrodes has been applied to a great number of discharge forms. It is now clear, however, that the discharge conditions which it requires can only be approximately realized in many instances, so that the range of exact application of the original theory is limited. An advance towards the analysis of a type of discharge in which one of the original postulates, that of the Maxwellian distribution of velocity amongst the electrons, fails, has, however, been made by Druyvestyn[2]. In a paper primarily concerned with the low voltage arc Druyvesteyn, deriving independently a result inherent in earlier work by Langmuir and Mott-Smith, has shown that the actual distribution function of the electron velocities (or energies) can be obtained from the second derivative of the probe characteristic for electrons in a retarding field. The relation deduced (which neglects secondary effects at the probe surface) is that

$$\rho\left\{\sqrt{\frac{2e}{m}(V_r-V_s)}\right\}=\frac{4}{Oe^2}(V_r-V_s)\frac{d^2i}{dV_s^2}, \quad . \quad \text{(i.)}$$

where $\rho\left\{\sqrt{\frac{2e}{m}(V_r-V_s)}\right\}$ represents the distribution function, m and e are the electronic constants, O is the collector area, and V_s and V_r the potentials of probe and space respectively. Previous determinations of this distribution function from the current-voltage characteristic have involved (*a*) a double graphical differentiation with its inevitable inaccuracies[3], (*b*) somewhat variable methods of obtaining the space potential. The principal object of the present investigation was to evolve a method of finding the second derivative of the electron current directly, and of automatically determining the space potential. The method described has proved to have

* Communicated by Prof. E. V. Appleton, F.R.S.

wider applications than were anticipated, and has been extended to include observation of the first derivative. The methods have the added advantage of being quite rapid in operation, a matter which will commend itself to those who have had experience in laborious reduction of observations in probe analysis.

2. *Theory.*

A current-voltage characteristic curve, free from discontinuities, may be represented by an equation of the form $i=f(\mathrm{V})$, where $f(\mathrm{V})$ is given by an infinite series in V. At any point on the characteristic curve given by a potential V superimpose an alternating potential $\mathrm{E}=\mathrm{A}\sin pt$. It is known [4] that the current i is now given by

$$\left.\begin{aligned} i=f(\mathrm{V})+\frac{\mathrm{A}^2}{4}f''(\mathrm{V})+\frac{\mathrm{A}^4}{64}f''''(\mathrm{V})+\ldots. \\ +\left\{\mathrm{A}f'(\mathrm{V})+\frac{\mathrm{A}^3}{8}f'''(\mathrm{V})+\ldots..\right\}\sin pt \\ -\left\{\frac{\mathrm{A}^2}{4}f''(\mathrm{V})+\frac{\mathrm{A}^4}{48}f''''(\mathrm{V})+\ldots\right\}\cos pt \\ -\left\{\frac{\mathrm{A}^3}{24}f'''(\mathrm{V})\ldots\ldots\ldots\ldots\right\}\sin 3pt \\ +\left\{\frac{\mathrm{A}^4}{192}f''''(\mathrm{V})\ldots\ldots\ldots\ldots\right\}\cos 4pt+\ldots \end{aligned}\right\} \quad \text{(ii.)}$$

where f', f'', f''', etc. are the first, second, third, etc. differential coefficients of the current with respect to voltage. The application of the alternating e.m.f. has thus given rise to new direct current terms, depending on the second, fourth, and higher order even derivatives and to an infinite number of new harmonic terms. If the voltage alternations are made sufficiently small $\Delta i=\mathrm{A}^2/4f''(\mathrm{V})$ nearly, where Δi is the change in the value of the direct current. As an approximation this formula has been used before to measure rectification efficiency in hard tubes. In this case the change in current produced by a given amplitude is measured for various rectifiers, *i. e.*, for different f'' (V). For any given rectifier Δi can also give a measure of the alternating amplitude *.

* This is the principle of the thermionic voltmeter, Moullin, Radio Freq. Measurements, Chap. IV.

In the present case, if A is kept constant and small, Δi gives a measure of the second derivative of the current-voltage characteristic at the point of operation. Thus as the operating point is moved along the curve, and at each point the potential is made to oscillate between $V \pm A/2$, (with A small), the rectified current for each value of the potential is proportional to the second derivative of the curve at that potential. The second derivative of a current-voltage curve can thus be recorded as the difference between currents registered with and without the alternating e.m.f. superposed. When A is small the alternating terms will also all vanish with the exception of the term $Af'(V) \sin pt$. The amplitude of the alternations then depends on the first derivative of the curve. We have used this principle to find the first derivative of certain characteristics. Our chief concern was, however, the determination of the second derivative of discharge-tube probe characteristics where, so far as we are aware, the method is novel.

3. *Experimental.*

The second derivative enters as a superposed second-order change in the collector current. To record it simultaneously with the ordinary i-V characteristic an additional galvanometer fed with a balancing current is inserted in series with a collector circuit of the usual type, as shown in fig. 1. R_1, R_2 are the galvanometer shunt resistances, R_4 is the potentiometer resistance providing the balancing current. This is fed through a high resistance R_3 to the galvanometer G_2. R_3 has a resistance of several thousand ohms to ensure that the adjustment of the balancing potentiometer has no effect on the shunting of G_2. The Pohl commutator K is designed so that putting the key over to the right brings the alternating e.m.f. into action without breaking the circuit, and thus obviates possible hysteresis from this cause *. The coupling to the oscillator is very weak, and thus the momentary shorting of the output coil produces a negligible effect on the oscillator. The A.C. is derived from an audio frequency (1000$\sim$) valve oscillator with a sinusoidal output. The amplitude used varied slightly

* For necessity for this see Emeléus, Brown, and Cowan, Phil. Mag., Jan. 1934.

for different characteristics, depending on the tube conditions. On the average it was from 0·01 to 0·1 volts peak.

The procedure is now as follows :—G_2 is short-circuited with the A.C. out of circuit. The steady current is then established by adjusting the Langmuir probe-circuit potentiometer (R_5). G_2 is then gradually put in circuit by increasing R_2, the spot being kept as nearly as possible at zero by adjustment of R_4, and when sufficiently sensitive to give a good deflexion when K is thrown over, the

Fig. 1.

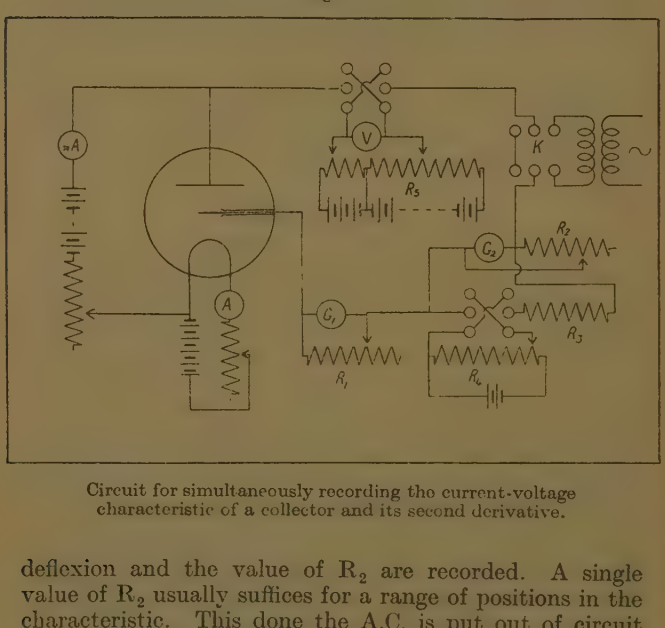

Circuit for simultaneously recording the current-voltage characteristic of a collector and its second derivative.

deflexion and the value of R_2 are recorded. A single value of R_2 usually suffices for a range of positions in the characteristic. This done the A.C. is put out of circuit again and the process repeated for each point on the curve. The method was tested on certain valve characteristics and proved quite easy in operation with two observers working simultaneously. As an example the second derivative of the current-voltage characteristic (for retarding voltages) of an " R " valve is shown in fig. 2 (A) with the accompanying characteristic (B).

In the application to discharges the method was used to find the second derivative of the collector characteristic in a low-voltage arc. The collector consisted of a molybdenum wire 4 mm. long, 0·1 mm. diameter, mounted in a low-voltage arc in mercury vapour at a pressure of 0·0008 mm., the arc current being 27·8 10^{-3} amp. As

Fig. 2.

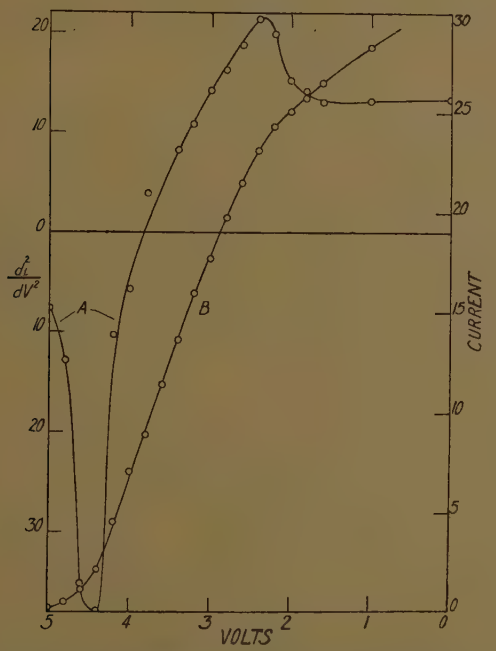

Current-retarding voltage curve (B) for an " R " valve, with its second derivative (A) as obtained automatically.

mentioned above the effect is a second-order one, and hence random current fluctuations which would be unnoticeable in an ordinary characteristic cannot be tolerated here; otherwise in certain regions of the characteristic they may completely mask the second derivative effect. On this account it was necessary to allow the tube to run for a longer time than is usually necessary for sufficiently

steady conditions to set in. A specimen second derivative curve (A) with the accompanying i-V characteristic (B) (including accelerated positive ions) is shown in fig. 3. The second derivative drops to zero where the curvature changes sign, *i. e.*, at the point of inflexion. The voltage at which this zero occurs can be determined with an accuracy of 0·005 volts at least, and so far as the present

Fig. 3.

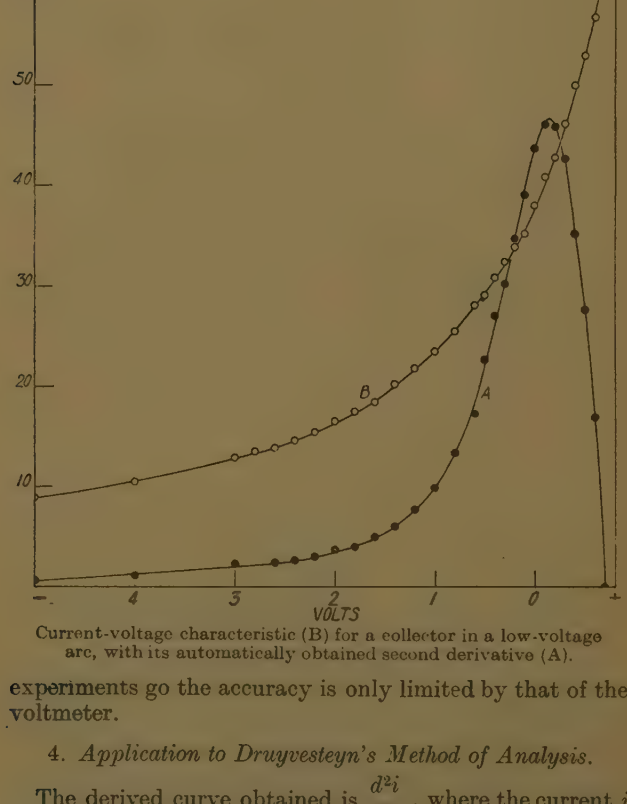

Current-voltage characteristic (B) for a collector in a low-voltage arc, with its automatically obtained second derivative (A).

experiments go the accuracy is only limited by that of the voltmeter.

4. *Application to Druyvesteyn's Method of Analysis.*

The derived curve obtained is $\frac{d^2i}{dV_g^2}$, where the current i is the resultant current and thus involves both the electron

and the positive ion currents. The electron distribution equation refers to the electron current only, and hence in calculating the distribution due allowance must be made for the effect of the positive ions. Since $i_r = i_e + i_p$, where the suffixes r, e, p denote resultant, electronic, and positive ion currents respectively,

$$\frac{d^2 i_r}{dV_s^2} = \frac{d^2 i}{dV_s^2} + \frac{d^2 i_p}{dV_s^2},$$

and hence

$$\rho_e(V) \propto \frac{d^2 i_r}{dV_s^2} - \frac{d^2 i_p}{dV_s^2}.$$

Hence if the positive ion distribution can be ascertained it can be allowed for.

If we assume that the positive ion curve follows the same law throughout the whole range of voltage, then the second derivative method itself can be used to find the correction for positive ions from the region of the characteristic at higher negative voltages, where the only current is the positive ion current. Thus, in a common case, if the positive ion characteristic is linear here the second derivative is recorded as zero, and hence the electron velocity distribution is determined by using $\frac{^2 i}{dV_s^2}$ as found directly. If the positive ion curve follows a parabolic law the second derivative has a constant value and produces an apparently uniform shift upwards of all the distribution values. This approximation usually suffices.

Having allowed for the positive ion current the zero of the velocity distribution, or what is practically equivalent, the space potential must be found. In order to locate the position of the space potential on an actual characteristic we must first consider the ideal Langmuir curve for a flat collector and treat the case of an actual characteristic as a deviation from this. The electron current for potentials negative to that of the space will follow a logarithmic law as a consequence of Boltzmann's theorem, *i. e.*, $i = K_1 e^{-cV}$ for $V < V_r$. At the space potential V_r the collector is receiving the random electron and positive ion currents, and $i = K_1$ for $V > V_r$. The logarithmic plot of electron current against potential thus shows a straight line until the space potential is reached, when the line abruptly bends over and becomes horizontal

(fig. 4). There is no doubt here as to the position of the space potential, which corresponds to the breakdown of the validity of Boltzmann's theorem. At the point of discontinuity all the terms with the exception of the constant in the logarithmic factor vanish simultaneously. In other words, the successive differential coefficients of

Fig. 4.

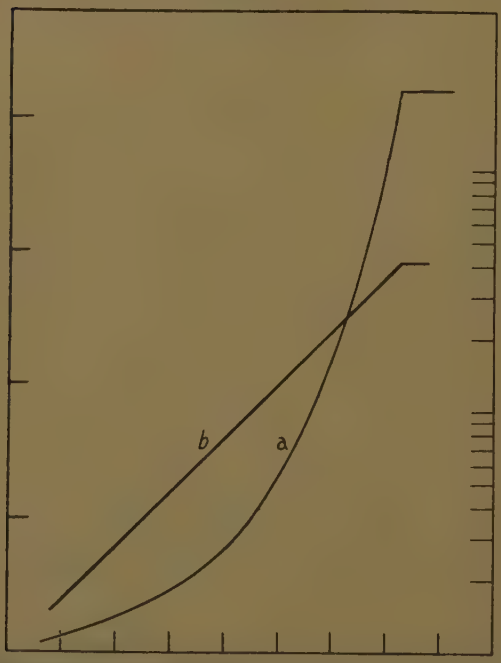

Ideal Langmuir curve for a flat collector (*a*) with current ordinate left, (*b*) with logarithm of current as ordinate, against voltage abscissa.

current with respect to voltage cease increasing and drop discontinuously to zero at the space potential.

In all actual cases in the neighbourhood of the space potential secondary effects such as reflexion tend to smooth out the discontinuity and prevent also a horizontal line being obtained, even with a flat collector. Consider as examples the following possibilities :—

(1) An approximately ideal case where Boltzmann's law holds reasonably well before the space potential region is reached. The form of the semi-logarithmic plot is shown in fig. 5. The mathematical results of the secondary effects may be represented by saying that whereas all the derivatives vanished simultaneously on the ideal curve they now vanish in succession at different voltages. The first derivative never actually falls to zero at all. Since the curve cannot readily be quantitatively corrected for the secondary effects, the location

Fig. 5.

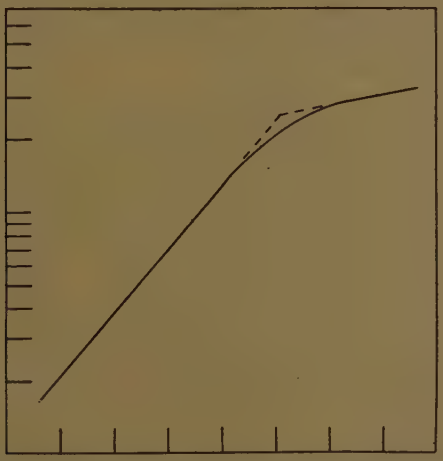

Voltage-logarithm of electron current to collector, showing slight departure from the ideal case in the region of the space potential.

of the space potential becomes a matter of compromise. We may take it, for example, as being given by the first break away from the semilogarithmic plot *. This will correspond theoretically to $\frac{d^2 i}{dV^2} = \infty$ becoming zero, or, in other words, to conditions where the Boltzmann relation first appears to break down. This gives a lower value of space potential than the actual one, since it is only the secondary effects which make the logarithmic plot first

* This has been the usual practice in this laboratory.

cease to be linear at this point. If, however, the point can be unequivocally determined from the curve, then in a series of characteristics for the purpose of comparison of space potential the error involved will not be important. On the other hand, if some aspect of probe theory is to be tested, then other methods will have to be found. The principal concern is, however, as a rule not the absolute values of temperature, concentration, etc., as how these vary with pressure, current density, or other tube parameters. The same relative point may then be taken without involving important errors. It must, however, be implicitly possible to determine this point accurately. In the case mentioned above (fig. 5) this has been difficult with the usual graphical method, as the break away is very gradual.

(2) The electron distribution is never truly Maxwellian, but the deviation is small. Druyvesteyn's method of analysis will have to be used. Here the space potential will provide the zero of the electron velocity distribution curve, and hence it is of the utmost importance that its value be obtained as accurately as possible. A method of defining the space potential in this case is to draw tangents to the semilogarithmic plot at the space potential bend and to take the intersection [(2)]; this point will thus depend on the average slope of the semilogarithmic plot or the average "electron temperature," and on the slope of the accelerating field curve, and will hence be essentially variable. The point may or may not coincide with the vanishing of the second derivative or the point of inflexion on the i-V characteristic. A coincidence will be fortuitous. In actual cases the position of the intersection with respect to the point of inflexion will depend on various factors, such as current density of the discharge or the type of collector used. As a rule the tangent intersection gives a point on the curve slightly positive to the potential for which the second derivative vanishes. This, however, is not necessarily the case. The two points are nearly always close together.

From the distribution equation (i.) it is seen that this distribution function will vanish when one of the two conditions is satisfied, namely, $V_r = V_s$ or $\dfrac{d^2i}{dV_s^2} = 0$. Assuming these do not occur at the same voltage we can

get no valid information at any point beyond that corresponding to the vanishing of the first. Suppose (*a*) the tangent intersection is positive to the point of inflexion. We have now a negative second derivative associated with a positive potential factor, giving a distribution as in fig. 6. In this case the distribution function is clearly meaningless to the left of A. However, the potential

Fig. 6.

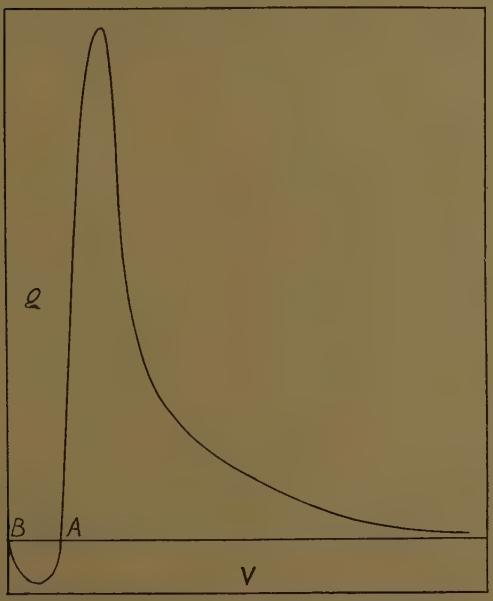

zero ($V_r = V_s$) is at B, and hence any voltage measurement ($V_r - V_s$) still has AB included in it. This anomaly clearly arises from the application of a correction for space potential without a corresponding one for curvature. The resulting uncertainty in ρ is greatest evidently for the slowest electrons. If, on the other hand, (*b*) the tangent intersection is negative to the point of inflexion, the distribution function will be as in fig. 7. The state of affairs would then be similar to the ideal case (1), with the

space potential slightly positive to the first break away from the logarithmic plot, but still negative to the vanishing point of $\frac{d^2i}{dV^2}$ *.

These examples suffice to show that since the absolute determination of the space potential from the characteristic is hardly possible in any actual case, the value will necessarily become one of definition, and that a reasonable

Fig. 7.

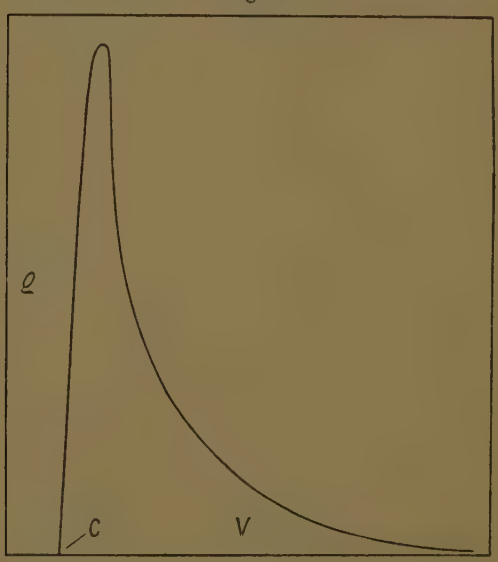

method of defining it is by the vanishing of $\frac{d^2i}{dV_s^2}$, to get rid of the anomaly of the double vanishing of $\rho(V)$. This definition will still be of little use unless the point of inflexion can be obtained accurately. It is here that the advantage of the alternating current method becomes evident, since with it, as mentioned before, the point can be obtained with practically any desired accuracy.

* A curve somewhat similar to fig. 6 would still be obtained if we proceeded to the left of C, fig. 7, but this would correspond in equation (i.) to an accelerating field for electrons.

The foregoing discussion may be summarized briefly as follows :—In order that distribution curves defined by equation (i.) may not be grossly erratic a standard method of space potential determination becomes a necessity ; location of the space potential from an actual characteristic is a matter of compromise, and the value obtained may lead to difficulties in the calculation of the distribution of velocities or energies among the electrons unless the space potential coincides with the point of inflexion of the curve ; this point may thus be conveniently taken as defining the position of the space potential.

Fig. 8.

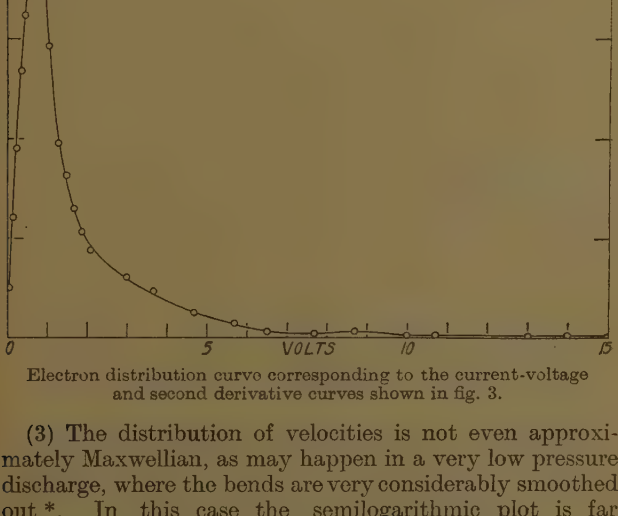

Electron distribution curve corresponding to the current-voltage and second derivative curves shown in fig. 3.

(3) The distribution of velocities is not even approximately Maxwellian, as may happen in a very low pressure discharge, where the bends are very considerably smoothed out *. In this case the semilogarithmic plot is far from straight and there seems no alternative in practice to taking the point of inflexion for the defined space potential. It must, however, be clearly emphasized that this method of definition as well as any other is still a method of compromise.

* As in the negative glow of a discharge in oxygen at low current density and less than 0·1 mm. pressure. (Unpublished work from this laboratory.)

In connexion with the space potential definition a small point arises if there is curvature of the positive ion graph, since then the vanishing of $\frac{d^2i_i}{dV_s^2}$ does not coincide with the vanishing of $\frac{d^2i_e}{dV_s^2}$. This effect is, however insignificant, since the positive ion curvature, if it exists at all, will be very small in comparison with that due to the electrons. Since, unless some means of accurately allowing for the secondary effects is evolved, an accurate value of slow group distribution is not possible, the method above appears to give the best compromise in the circumstances.

The distribution graph for the full i-V curve, (shown in part in fig. 3) is shown in fig. 8.

5. *Some Applications.*

Little has been mentioned about the first derivative method on account of the greater interest in the second derivative in connexion with Druyvesteyn's analysis. The first differential coefficient can be recorded on a calibrated rectifier, where the results obtained represent a considerable advance on the direct graphical method. The point of inflexion is now given by a maximum value of the first derivative, and can again be found with considerable accuracy. The method can similarly be applied to any i-V characteristic. This method of automatically finding the space potential would appear to give a quick and accurate method of field measurement by finding the space potentials of two points in the discharge.

As a special application the advice is an extremely delicate test of characteristic linearity. A standard procedure used in connexion with the positive ion curve in this work was to temporarily increase the superposed e.m.f., so that the alternations covered the whole range of the characteristic under test. Coupled with the square law of the rectifier this was able to bring up minute curvatures hardly detectable from the characteristic.

It is possible that in the application of these methods to other problems modifications of the circuits we have used could profitably be made. In the application in which we have been interested this has not been con-

sidered, as those employed have already been capable of greater accuracy in application than the steadiness of the discharge-tubes themselves allowed.

Summary.

An alternating current method is described which enables the second derivative of the current-voltage curve of an auxiliary electrode in a gaseous discharge to be obtained directly, provided the discharge conditions are sufficiently stable. This obviates the necessity for double graphical differentiation of the ordinary electron current-voltage curve when the second derivative is required for substitution in Druyvesteyn's distribution equation for electron speeds. The definition and determination of the space potential are discussed at length, and it is shown that the most reasonable point to take in this connexion is that at which the second derivative is zero. This point can be obtained by the present automatic method with considerable accuracy. Typical curves are shown to illustrate the application of the method to actual cases.

We desire to thank Professor E. V. Appleton, F.R.S., for much valuable criticism and advice, and Professor W. B. Morton for the provision of facilities. The problem was suggested to us by Dr. K. G. Emeléus.

References.

(1) Langmuir, Journ. Frank. Inst. cxcvi. p. 751 (1923).
(2) Druyvesteyn, *Zeits f. Physik*, lxiv. p. 781 (1930).
(3) Sloane and Emeléus, Physical Review, xliv. p. 333 (1933).
(4) Landale, Proc. Camb. Phil. Soc. xxv. p. 355 (1929).

XVI. *Notices respecting New Books.*

The Theory of Atomic Collisions. By N. F. Mott and H. S. W. Massey. (The International Series of Monographs on Physics.) [Pp. xv+283.] (Oxford, Clarendon Press; London, Oxford University Press, 1933. Price 17*s.* 6*d.* net.)

THIS book, the sixth volume of the International Series of Monographs on Physics, gives a very complete account of the application of classical and quantum mechanics to collisions

between atoms, electrons, and ions. The writers have each played an important part in the development of the theory of collisions, and this volume contains much published and unpublished work due to the authors and their collaborators. It is clearly indicated how their work and that of other investigators has progressed, so that now many types of collision process admit of quantitative treatment, while others can be explained qualitatively at least. While the book is primarily theoretical in outlook, experimental results are discussed in detail, and the comparisons of practical and theoretical work are an essential feature of the volume.

The early chapters of the book prepare the reader for the general theory of atomic collisions which is discussed in Chapter VIII. Some relevant wave mechanical theorems are given, and collisions, in which the internal state of the colliding particle is unchanged, are discussed. It is shown that only in the case of scattering by a Coulomb field is the wave mechanics in agreement with classical theory. A chapter on electron spin is followed by a discussion of collisions between two identical particles.

After the general treatment of Chapter VIII. several chapters are devoted to collisions of electrons with atoms. Elastic collisions are first discussed. The validity of Born's approximation when considering collisions of fast electrons, how it is necessary to take into account the distortion of the electron wave for medium velocity electrons, and exchange effects for slow electron impacts are all admirably presented. It is shown that the theory of ineleastic collisions of fast electrons with atoms gives results in accordance with experiment, but the treatment of inelastic collisions of slow electrons with atoms is more of a qualitative character.

A discussion of the collision of electrons with molecules follows, and some problems in chemical kinetics are indicated. Methods for calculating transition probabilities between two states, one of which is quantized, are discussed, and finally a relativistic treatment of the two-body problem is given, together with an account of the calculation of a nuclear field from anomalous α particle scattering.

This book will appeal to everyone interested in collision for, while the theorist will appreciate the mathematical methods and their development, the experimentalist will find the numerical results given in the book of considerable value.

FIG. 1.

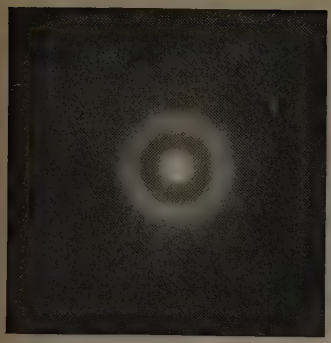

FIG. 2.

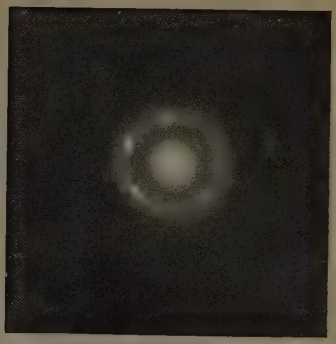

FIG. 3.

FIG. 4.

FIG. 5.

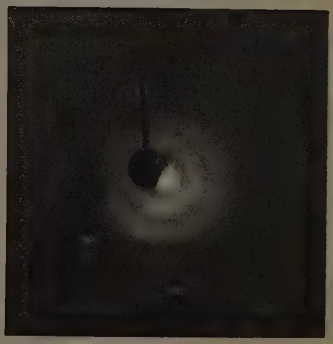

Fig. 1, benzene. Figs. 2, 3, 4, mixtures of benzene and ethyl phthalate in the ratios 2 : 1, 1 : 1, and 1 : 2 respectively. Fig. 5, ethyl phthalate.

FIG. 6.

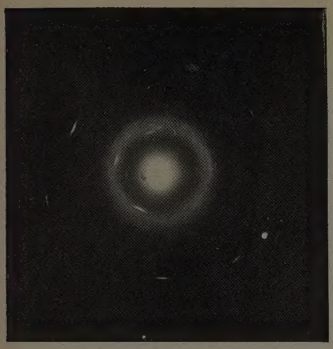

FIG. 7.

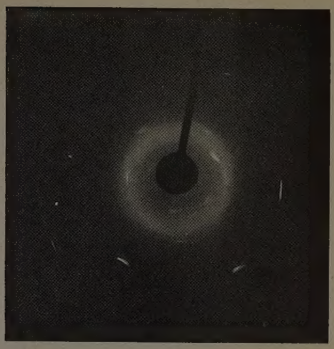

FIG. 8.

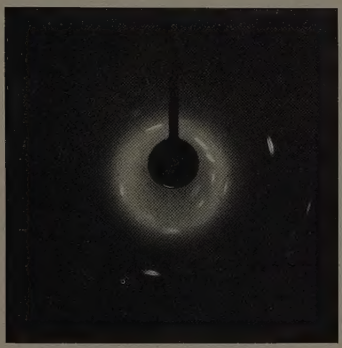

FIG. 9.

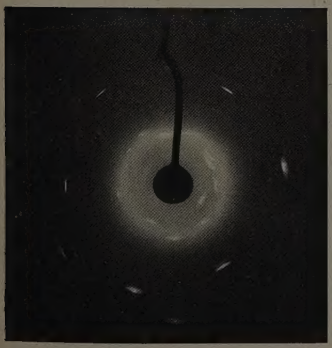

FIG. 10.

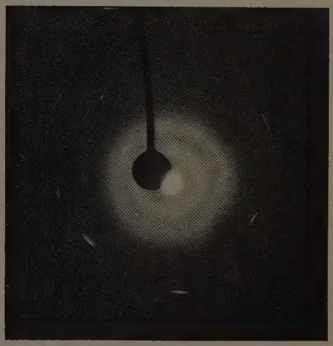

Fig. 6, pyridine. Figs. 7, 8, 9, mixtures of pyridine and ethyl phthalate in ratios 2 : 1, 1 : 1, and 1 : 2 respectively. Fig. 10, ethyl phthalate.

FIG. 11.

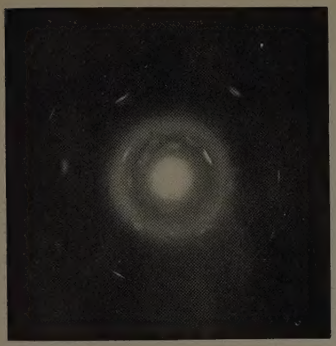

FIG. 12.

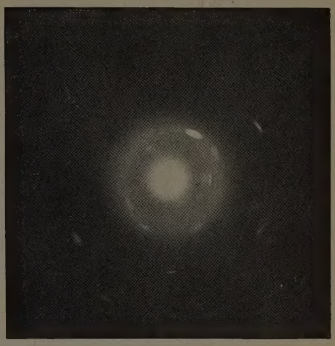

FIG. 13.

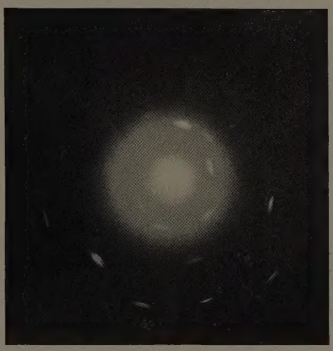

FIG. 14.

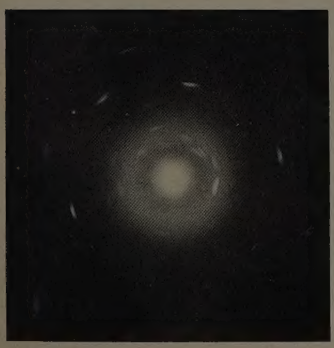

FIG. 15.

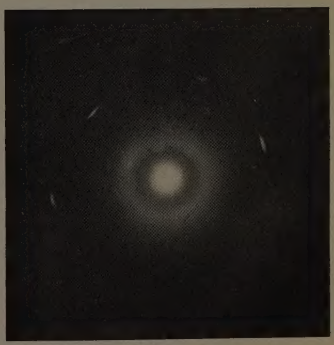

Fig. 11, acetic acid. Figs. 12, 13, 14, mixtures of acetic acid and *m*-xylene in ratios 2 : 1, 1 : 1, and 1 : 2 respectively. Fig. 15, *m*-xylene.